APPLICATION OF CHEMOMETRICS FOR QUALITY CONTROL OF *HIBISCUS SABDARIFFA* L.

By

Tasamaporn Sukwattanasinit

A Thesis Submitted in Partial Fulfillment of the Requirements for the Degree

DOCTOR OF PHILOSOPHY

Program of Pharmaceutical Chemistry and Natural Products

Graduate School

SILPAKORN UNIVERSITY

2008

APPLICATION OF CHEMOMETRICS FOR QUALITY CONTROL OF *HIBISCUS SABDARIFFA* L.

By

Tasamaporn Sukwattanasinit

A Thesis Submitted in Partial Fulfillment of the Requirements for the Degree

DOCTOR OF PHILOSOPHY

Program of Pharmaceutical Chemistry and Natural Products

Graduate School

SILPAKORN UNIVERSITY

2008

การประยุกต์ใช้คีโมเมตริกซ์ในการควบคุมคุณภาพสมุนไพรกระเจี๊ยบแดง

โดย
นางสาวทสมาพร สุขวัฒนาสินิทธิ์

วิทยานิพนธ์นี้เป็นส่วนหนึ่งของการศึกษาตามหลักสูตรปริญญาเภสัชศาสตรดุษฎีบัณฑิต
สาขาวิชาเภสัชเคมีและผลิตภัณฑ์ธรรมชาติ
บัณฑิตวิทยาลัย มหาวิทยาลัยศิลปากร
ปีการศึกษา 2551

The Graduate School, Silpakorn University has approved and accredited the Thesis title of “Application of Chemometrics for Quality Control of *Hibiscus Sabdariffa* L.” submitted by Tasamaporn Sukwattanasinit as a partial fulfillment of the requirements for the degree of Doctor of Philosophy, Program of Pharmaceutical Chemistry and Natural Products.

….....

(Assoc. Prof. Sirichai Chinatangkul,Ph.D.)

Dean of Graduate School

...../...../.....

The Thesis Advisors

1. Assoc. Prof. Uthai Sotanaphun, Ph.D.
2. Assoc. Prof. Jankana Burana-osot

The Thesis Examination Committee

..... Chairman

(Asst. Prof. Suchada Piriyaprasarth, Ph.D.)

...../...../.....

..... Member

(Assoc. Prof. Rapepol Bavovada, Ph.D.)

...../...../.....

..... Member

(Assoc. Prof. Manat Pongchaidecha, Ph.D.)

...../...../.....

..... Member

(Assoc. Prof. Uthai Sotanaphun, Ph.D.)

...../...../.....

..... Member

(Assoc. Prof. Jankana Burana-osot)

...../...../.....

45356901 : MAJOR : PHARMACEUTICAL CHEMISTRY AND NATURAL PRODUCTS
KEY WORDS : *HIBISCUS SABDARIFFA*/ ROSELLE/ QUALITY CONTROL/ CHEMOMETRICS/ ANTIOXIDANT/ ANTHOCYANINS
TASAMAPORN SUKWATTANASINIT : APPLICATION OF CHEMOMETRICS FOR QUALITY CONTROL OF *HIBISCUS SABDARIFFA* L.. THESIS ADVISORS : ASSOC. PROF. UTHAI SOTANAPHUN, Ph.D., ASSOC. PROF. JANKANA BURANA-OSOT. 187 pp.

The objectives of this research were to characterize the physical and chemical properties of dried roselle calyx, to establish the chemical fingerprints, and to determine radical scavenging activity as well as to build a model for prediction the activity.

The dried roselle calyx samples were obtained from various sources of Thailand (n = 35). The physical qualities were analyzed by general control method as described in Thai Herbal Pharmacopoeia. The modified pH-differential spectrophotometry was developed for analysis of total anthocyanins (TA) content. The method used methyl orange (MO) as an external standard and the correlation factor between concentration of TA and MO at the same absorbance value was applied to converse the concentration of MO to that of TA. The contents of total phenolic compounds (TP), organic acid and potassium were also analyzed. Chemometrics combined with High Performance Liquid Chromatography (HPLC), Ultraviolet-visible (UV-Vis) and Infrared (IR) spectroscopies were applied to study the chemical patterns. The radical scavenging activity was determined by DPPH assay. The prediction models were built from the data of HPLC and UV-Vis by partial least square (PLS) and uninformative variable elimination PLS (UVE-PLS) techniques.

The samples were classified based on their visual appearance into 2 major groups (the reddish group, n = 17 and the brownish group, n = 16). The other two samples had distinct small calyx. Between the reddish and the brownish, foreign matter, loss on drying, total ash and acid-insoluble ash were not different ($p > 0.05$), but ethanol-soluble and water-soluble extractives were higher in the first group ($p < 0.05$). The contents of TA, TP and acid were also higher in the first group ($p < 0.05$), while potassium content in both groups were not different ($p = 0.17$). The validation results of the modified pH-differential spectrophotometry showed that the method was accurate and precise. The TA contents analyzed by this method were not different from those of the HPLC method ($p = 0.71$). The HPLC chromatogram patterns of the reddish and the brownish were different. The standard HPLC fingerprint built from the data of the reddish could successfully discriminate the group of sample, whereas the UV-Vis and IR spectra patterns were unsuccessful in this point. The radical scavenging activity was higher in the reddish ($p < 0.05$). The best model with the lowest RMSEP value was the PLS model of HPLC chromatogram. The model used 10,641 x-variables and 3 PLS-factors. The RMSEP of model, $\pm$ 0.1910 what corresponded to 4.58%, was comparable to the error of laboratory analysis, $\pm$ 0.1869 what corresponded to 4.48%.

Program of Pharmaceutical Chemistry and Natural Products Graduate School, Silpakorn University Academic Year 2008
Student's signature…….
Thesis Advisors' signature 1. ..... 2. .....

45356901 : สาขาวิชาเภสัชเคมีและผลิตภัณฑ์ธรรมชาติ
คำสำคัญ : กระเจี๊ยบแดง/ ควบคุมคุณภาพ/ ฟิงเกอร์พรินท์/ คีโมเมตริกซ์/ ฤทธิ์ต้านอนุมูลอิสระ/ แอนโทไซยานิน

ทสมาพร สุขวัฒนาสินิทธิ์ : การประยุกต์ใช้คีโมเมตริกซ์ในการควบคุมคุณภาพสมุนไพรกระเจี๊ยบแดง. อาจารย์ที่ปรึกษาวิทยานิพนธ์ : รศ.ดร.อุทัย โสธนะพันธุ์ และ รศ.จันคนา บูรณะโอสถ. 187 หน้า.

งานวิจัยนี้มีวัตถุประสงค์เพื่อศึกษาลักษณะทางกายภาพ และทางเคมี สร้างฟิงเกอร์พรินท์ทางเคมี วิเคราะห์ฤทธิ์ต้านอนุมูลอิสระของกลีบเลี้ยงกระเจี๊ยบแดงแห้ง และสร้างโมเดลเพื่อทำนายฤทธิ์ดังกล่าว

การศึกษาทำในตัวอย่างกลีบเลี้ยงกระเจี๊ยบแดงแห้ง 35 ตัวอย่าง ที่สุ่มจากแหล่งต่างๆ ของประเทศไทย โดยศึกษาคุณสมบัติทางกายภาพด้วยวิธีของตำรามาตรฐานยาสมุนไพรไทย และพัฒนาวิธีวิเคราะห์ปริมาณแอนโทไซยานินรวมด้วยวิธีสเปกโทรโฟโตเมทรีแบบพีเอชดิเฟอเรนท์โดยใช้สารเมทิลออเรนจ์เป็นสารมาตรฐาน แล้วคำนวณปริมาณแอนโทไซยานินรวมจากค่าความสัมพันธ์ระหว่างความเข้มข้นของเมทิลออเรนจ์กับแอนโทไซยานินที่มีค่าการดูดกลืนแสงเท่ากัน รวมทั้งวิเคราะห์ปริมาณของฟีโนลิครวม กรดอินทรีย์ และโพแทสเซียม ในการศึกษารูปแบบขององค์ประกอบทางเคมีใช้คีโมเมตริกซ์ร่วมกับการวิเคราะห์ด้วยเทคนิคต่างๆ ได้แก่ เอชพีแอลซี ยูวี-วิสิเบิล และไออาร์ ส่วนการศึกษาฤทธิ์ต้านอนุมูลอิสระทำโดยวิธีดีพีพีเอช และสร้างโมเดลเพื่อทำนายฤทธิ์ด้วยเทคนิคพีแอลเอส และยูวีอีพีแอลเอส โดยใช้ข้อมูลจากเอชพีแอลซีโครมาโทแกรม และยูวี-วิสิเบิลสเปกตรัม

ผลการศึกษาพบว่า ตัวอย่างมีลักษณะภายนอกที่ต่างกัน และแบ่งเป็น 2 กลุ่มใหญ่ๆ คือ กลุ่มสีแดง (17 ตัวอย่าง) และกลุ่มสีน้ำตาล (16 ตัวอย่าง) และมีบางตัวอย่างที่มีขนาดกลีบเลี้ยงเล็ก (2 ตัวอย่าง) ปริมาณสารปนเปื้อน ความชื้น เถ้ารวม เถ้าที่ไม่ละลายในกรด ของกลุ่มสีแดง และกลุ่มสีน้ำตาลไม่ต่างกัน ($p > 0.05$) แต่ปริมาณสารสกัดด้วยเอทานอล และสารสกัดด้วยน้ำของกลุ่มสีแดงมากกว่ากลุ่มสีน้ำตาล ($p < 0.05$) ปริมาณสารแอนโทไซยานินรวม ฟีโนลิครวม และกรดอินทรีย์ ของกลุ่มสีแดงมากกว่ากลุ่มสีน้ำตาล ($p < 0.05$) ในขณะที่ปริมาณโพแทสเซียมของทั้งสองกลุ่มไม่แตกต่างกัน ($p = 0.17$) ผลการประเมินวิธีวิเคราะห์แอนโทไซยานินรวมที่พัฒนาขึ้นพบว่า วิธีนี้มีความถูกต้อง แม่นยำ และให้ผลการวิเคราะห์ไม่ต่างจากวิธีเอชพีแอลซี ($p = 0.71$) รูปแบบเอชพีแอลซีฟิงเกอร์พรินท์ของกลุ่มสีแดง และกลุ่มสีน้ำตาลมีความต่างกัน เมื่อนำฟิงเกอร์พรินท์มาตรฐานที่สร้างขึ้นจากข้อมูลของกลุ่มสีแดงไปทดสอบกับกลุ่มสีน้ำตาล พบว่าฟิงเกอร์พรินท์มาตรฐานดังกล่าวสามารถจำแนกความแตกต่างของกระเจี๊ยบทั้งสองกลุ่มได้ ในขณะที่รูปแบบสเปกตรัมยูวีวิสิเบิล และไออาร์ ไม่สามารถจำแนกความแตกต่างระหว่างกลุ่มได้ ในการทดสอบฤทธิ์ต้านอนุมูลอิสระพบว่า ฤทธิ์ของกระเจี๊ยบกลุ่มสีแดงมีมากกว่ากลุ่มสีน้ำตาล ($p < 0.05$) และพบว่าโมเดลที่สามารถใช้ทำนายฤทธิ์แล้วมีความแม่นยำที่สุด คือ โมเดลพีแอลเอสที่สร้างจากข้อมูลเอชพีแอลซี โดยโมเดลดังกล่าวประกอบด้วย ตัวแปรต้น 10,641 ตัวแปร และพีแอลเอสแฟคเตอร์ 3 แฟคเตอร์ มีความผิดพลาดเฉลี่ยอาร์เอมเอสอีพีในระดับที่น่าพอใจ คือ $\pm$ 0.1910 หรือคิดเป็น 4.58% เมื่อเทียบกับความผิดพลาดของการวิเคราะห์ทางห้องปฏิบัติซึ่งอยู่ที่ $\pm$ 0.1869 หรือคิดเป็น 4.48%

สาขาวิชาเภสัชเคมีและผลิตภัณฑ์ธรรมชาติ บัณฑิตวิทยาลัย มหาวิทยาลัยศิลปากร ปีการศึกษา 2551

ลายมือชื่อนักศึกษา .....

ลายมือชื่ออาจารย์ที่ปรึกษาวิทยานิพนธ์ 1. ..... 2. .....

ACKNOWLEDGEMENTS

I would like to express my eternal gratitude to my thesis advisor, Assoc. Prof. Dr. Uthai Sotanaphun for his constant, strong knowledge, inspiration and indefinite kindness. I also deeply thank my co-advisor, Assoc. Prof. Jankana Burana-osot for her valuable advice on the concept of quality control.

I also sincerely thank the members of thesis examination committee, Asst. Prof. Dr. Suchada Piriyaprasarth, Assoc. Prof. Dr. Manat Pongchaidecha and Assoc. Prof. Dr. Rapepol Bavovada, for their invaluable time and comment.

I am also grateful to Medicinal Plant Research Institute, Department of Medical Sciences, Ministry of Public Health, Thailand for partial financial support. I also thank the staffs at the Faculty of Pharmacy, Silpakorn University, Thailand for providing research facilities.

A special acknowledgement is extended to all my friends and colleagues, Dr. Yaowalak Amrumpai, Asst. Prof. Siripan Limsirichaikul, Asst. Prof. Wisit Tangkeangirisin, Ms. Arisarakorn Sirinamaratana, Ms. Arthittaya Jiaranaiselavong, Ms. Wilai Trakoon-osot, Mr. Wichai Santimaleeworakul, Mr. Chalermphon Wanawongthai, Mr. Surasit Lochid-amnuay, Mr. Lersak Prachuabaree, Ms. Patcharawan Tanamatayarat, Ms. Sasidhorn Sukphiboon and others for their profound sympathy, encouragement and many supports.

Finally, I would like to express my warm thanks to my parents and my family for their love.

CONTENTS

LIST OF TABLES

Table Page

Table Page

LIST OF FIGURES

CHAPTER I
INTRODUCTION

Hibiscus sabdariffa L. (Malvaceae), known in common as roselle or in Thai as Krachiap-Daeng [1], has been cultivated worldwide throughout the tropics such as West Africa, South Asia and South-East Asia [2]. In those regions, the red calyx of the plant has long history of traditional medicinal uses including treatment of hypercholesterolemia, urinary bladder stone [3], cough, hypertension and used as diuretic [1]. The clinical studies also revealed hypotensive activity [4,5], diuretic activity and genitourinary effect [1].

Recently, there has been wide interest in roselle. The demand of the herb in Germany and the United States has been considerably increasing in recent years [6]. In Thailand, as a result of the 10th National Economic and Social Development Plan (2548-2552 B.E.), roselle has been promoted in list of high competitive herb (product champion) [7]. Consumption of roselle also has been suggested for promoting health [8] because the herb possesses many beneficial pharmacological activities such as antimutagenic [9], hypocholesterolemic [10], hepatoprotective and free radical scavenging activities [11], while it has been regarded as non-toxic [12]. U.S. Food and Drug Administration (US FDA) has approved roselle for use as flavoring in alcoholic beverages [13]

With the worldwide expansion in the use of traditional medicine, safety, efficacy, and quality control of herbal medicine have become important concerns [14]. For roselle cultivated in Thailand, the emphasis has been on the pharmacological activities including diuretic [15], antimutagenic [9], chemopreventive [16], antioxidant [17], and hypochoresterolemic activities [10], with no scientific and regulation information concern over the chemical and quality control of the herb.

At the present, the quality control of traditional medicine is generally based on conventional practice or “marker approach”. The identification and quantitative determination of composition of traditional medicine has been performed by using one or two markers or pharmacologically active components found in the specimen. While the approach is simple, it cannot confer an overall quality assurance of an herbal product, because multiple constituents usually account in therapeutic effects. Moreover, the approach is suffered from limited number of available standards as well as lacking of a standard that is unique for a particular herb [18]. However the marker approach still has been applied for majority of the monographs of traditional medicine [19,20].

Because the marker approach failed to demonstrate the overall consistency and quality of herbal product, the concept of phytoequivalence has been recently developed, in Germany. As indicated by the phytoequivalence concept, to ensure the consistency and the quality of an herbal product, a detailed chemical profile of an herbal product is necessary to fit with that of clinically proven product. On a similar basis, the State Food and Drug Administration (SFDA) of China proposed to use fingerprints as a quality measurement of herbal extract or preparation [18]. In case of the identification of active compound(s) of the plant preparation and finished product is not possible, the World Health Organization (WHO) also suggested chromatographic fingerprint as a quality measurement [14]. The US FDA advocated qualitative and quantitative comparing of spectroscopic and/or chromatographic fingerprint of a botanical raw material, drug substance, or drug product against that of a reference sample or standard to ensure the identity, quality, as well as consistency from batch to batch [21]. The European Medicines Agency (EMEA) recommended chromatographic fingerprint for the determination of the stability of the herbal substance or herbal preparation [22].

A chemical fingerprint of a traditional medicine is a unique feature which could be a spectrum or a chromatogram, obtained by a defined procedure, to characterize the chemical composition of the traditional medicine [18]. As mentioned by Liang et al. [23], the fingerprint should be featured by fundamental attributions of “sameness” and “differences”, i.e. the identification of traditional medicine can be accurately done (“sameness”) even the amount of the characteristic components are not exactly the same for different samples of a particular traditional medicine (“differences”). In other word, the fingerprint should demonstrate both the “sameness” and “differences” among various samples. However, to get useful information from plentiful raw data such as all data points of the whole chromatogram or spectrum is a challenging task.

Chemometrics is the application of statistical, mathematical and logical techniques to retrieve chemical relevant information from the measured chemical data [24]. The application has been extensively applied in the field of quality control of herb such as evaluation of similarity between two chromatograms by Pearson’s correlation coefficient [25], prediction of pharmacological activity by chromatograms [26] and searching for optimum parameter to develop high performance liquid chromatography (HPLC) fingerprint [27].

The official method for quality control of roselle has been described in the European Pharmacopoeia: EUP 4.4. The described methods were based on the marker approach. The identification has been performed by thin layer chromatography (TLC) using

one marker, i.e., quinaldine red, to locate the positions of four chemical constituents of the herb. The quantitative determination of composition has been done by the coloring power test and the acid content assay. Other common tests, such as foreign matter, loss on drying and total ash, also have been declared [28].

Other criteria, obtained from the market survey of *Hibiscus sabdariffa*, cover the investigation of color, texture, aroma, free flow density, moisture, total ash, acid insoluble ash, impurity and microbial contamination. But there is no assay of any chemical in this specification [6].

In Thai Herbal Pharmacopoeia (THP) [20,29], there is no official method for quality control of roselle. To set our own criteria for quality control of roselle, based on conventional practice, and the chemicals found in various source of roselle including mucilages [30,31], organic acids [8], simple phenolic acids [17,32], flavonoids [30], anthocyanins [8,33], ascorbic acid, ß-carotene, lycopene [8], volatile compounds [34] and minerals [35], anthocyanins and phenolic acids seem to be rational markers because of their beneficial pharmacological activity [32,36,37,38,39]. Combining the assay of total anthocyanins and total phenolic acids with other general tests described in THP [20], the quality of roselle can be roughly investigated.

To obtain complete picture of the quality of roselle, chemical profile including HPLC chromatogram, diffuse reflectance infrared (DRIFT) spectrum and ultraviolet visible (UV-Vis) spectrum were employed along with chemometrics to construct and evaluate the chemical fingerprint of roselle. Moreover, as roselle is a potential source of antioxidant, the antioxidation activity was tested. The chemical profiles, as a representative of chemical components, were related to the antioxidation activity.

Therefore, the aims of this study were to characterize physical and chemical property of roselle from various sources of Thailand as the background information of roselle cultivated in Thailand and to establish the chemical fingerprints of roselle by using HPLC chromatogram, DRIFT spectrum and UV-Vis spectrum as well as to build the model for prediction of antioxidation activity by using these chemical profiles.

Goals and objectives

1 To characterize the physical and chemical properties of the roselle from various sources of Thailand.

2 To establish the chemical fingerprints of the roselle by using HPLC chromatogram, UV-Vis spectrum and DRIFT spectrum.

3 To determine antioxidation activity of the roselle and construct a model for prediction of antioxidation activity by using the chemical profiles including the HPLC chromatogram and the UV-Vis spectrum.

CHAPTER II
LITERATURE REVIEW

1 *Hibiscus sabdariffa* L.

1.1 Introduction

Hibiscus sabdariffa L., believed to be of African origin, has been cultivated worldwide throughout the tropics for its succulent fleshy, edible calyx, and a fairly strong fiber from the stem [2]. It has been generally known as Roselle, Indian sorrel, Jamaican sorrel, Red sorrel [2], Hibiscus, Jamaica sorrel, Karkade, Karkadi, Red tea, Rosella, Soborodo (Zobo drink), Sour tea [40] and Roselle of Rama [3].

In Thailand, the plant is named as Krachiap (central), Krachiap-daeng (central), Krachiap prieo (central) [41], Phak king kheng, Som keng, Khen (northern), Som taleng khreng (Tak) and Som-unu (Shan-Mae-Hong Son) [3].

Roselle has many medicinal, decorative, and culinary uses. In India, Africa and Mexico, all above-ground parts of the roselle are valued in traditional medicine [42]. However, most of the economic value, particularly as an ingredient in herbal teas, comes from the red calyx. In commerce the calyx is known by the names hibiscus and roselle [43]. Therefore the focus of this review is on the calyx of roselle or in short as roselle.

1.2 Morphological characters of *H. sabdariffa*

The plant is an erect annual herb of Malvaceae family that grows up to 4 m tall, with reddish cylindrical stem, nearly or quite glabrous. Stem is often woody at the base. Leaves are simple, alternate, having petiole. The lower leaves are often ovate but the upper leaves are 3-5 lobed or parted, the lobes are serrate or obtusely toothed. Petiole is 4-12 cm long. Flowers are solitary, axillary, nearly sessile, 5 to 7 cm in diameter consisting of epicalyx-segments 8-12, reddish, distinct, lanceolate to linear, adnate at base of the calyx. Calyx is 5-lobed, 1-2 cm long, usually becoming large and fleshy after anthesis, accrescent to 5 cm, thick, dark purple or red, cup-like, deeply parted, prominently 10-nerved and closely enveloping the capsule. The corolla consists of 5 petals, funnel-shaped, typically pale yellow with deep red blotches at the base and twice as long as calyx. Stamens are numerous, the filaments united into a staminal column; style single, 5-branched near summit, stigma capitate. Fruit is capsule, ovoid, pointed, 1-2 cm long, shorter than the calyx, having densely

sharp and stiff hairs, loculicidally dehiscent. Seed is reniform, 4-7 mm long, blackish brown, pilose [1,2,3,44]. The picture of roselle is shown in Figure 1.

Figure 1 Photograph of *H. sabdariffa* or roselle

1.3 Ethnomedical information of *H. sabdariffa*

Roselle is much used in the Tropics. After the petals drop from the flower, the remaining red calyx (the cup-like structures formed by the sepals) grows into seed-containing pods that look like flower buds [43]. And the so called “dried red roselle flower” is in fact the persistent calyx attached to the fruit [3]. The herb possesses refreshing and mildly stimulating activities. It is generally used as beverage, source of red food colorants as well as calming refreshment agent in mixed herbal tea and coffee [2]. In Thailand, roselle is used in folk remedy for the treatment of gastric ulcers, hypercholesterolemia, kidney stones, urinary bladder stones and strangury as well as for alleviation of thirst and as expectorant [3]. The details of ethnomedical uses of roselle in other countries and regions are listed in Table 1.

Table 1 Ethnomedical uses of *H. sabdariffa*

Country/ region	Ethnomedical uses	References
East Africa	Unripe fruit juice is taken orally with salt, pepper, asafetida and molasses as a remedy for biliousness	[1]
	The calyx infusion, called "Sudan tea", is taken to relieve coughs	[42]
Egypt	Decoction of hot water extract of the calyx is taken with sugar 3 times daily for high blood pressure	[1]
	Deep red tea from the calyces is popular used as a “refrigerant” i.e. a beverage that helps lower body temperature	[43]
	Hot water extract of the entire plant is taken orally for heart and nerve diseases, as a laxative, to reduce weight, as a diuretic, to activate and neutralize hepatic secretion, to activate gastric secretion, as a digestive, for arteriosclerosis, as a diaphoretic, to give a euphoric impression and as an intestinal antiseptic	[1]
Europe	Dried calyces and epicalyces are used primarily as a caffeine-free beverage tea	[43]
German-speaking countries	Medicinal tea usually combined with lemon balm leaf (*Melissa officinalis*, Lamiaceae) and St. John’s wort herb (*Hypericum perforatum*, Clusiaceae) is used for nervous restlessness and difficulty falling asleep	[43]
Guatemala	Roselle "ade" is a favorite remedy for the aftereffects of drunkenness	[42]
	Hot water extract of dried calyx is taken orally as a diuretic and for renal inflammation	[1]
Iran	Sour hibiscus tea is a traditional treatment for hypertension	[43]
North Africa	Calyx preparations are used to treat cough, sore throat, and genital problems	[43]
Senegal	Roselle extract is used for lowering blood pressure	[42]

Table 1 Ethnomedical uses of *H. sabdariffa* (continued)

Country/ region	Ethnomedical uses	References
Sudan	Hot water extract of flowers is taken orally as a blood purifier	[1]
	Hot water extract of the dried flowers is taken orally for coughs	[1]
	Deep red tea from the calyces is popular used as a "refrigerant" i.e. a beverage that helps lower body temperature	[43]
Thailand	Fruit is used for alleviation of thirst, gastric ulcers, hypercholesterolemia	[3]
	Flower is used for treatment of kidney stones, urinary bladder stones and strangury and used as an antihypercholesterolemic and expectorant	[3]
	Not specified part was used for decreasing of body temperature, alleviation of thirst, health promotion, fatigue, biliary diseases, disorders of urination, cough, as an antihypertensive, antihypercholesterolemic, expectorant, blood tonic, element tonic, antidiabetic and vasodilator	[3]
	Decoction of dried calyx is taken orally for high blood pressure	[1]
Not specified	Not specified part was used as antiseptic, aphrodisiac, astringent, bilious, cancer, cataplasm, cholagogue, choleretic, coffee, debility, demulcent, digestive, diuretic, dyspepsia, dysuria, emollient, fever, hangover, heart, hypertension, laxative, nerves, refrigerant, resolvent, scurvy, sedative, strangury, tea and tonic	[45]

1.4 Clinical study, pharmacological activity and toxicity of *H. sabdariffa*

The majority of clinical studies of roselle are on blood pressure lowering effect. The efficacy of ethnomedical use of the herb for lowering blood pressure has been clinically confirmed [4,5,46]. The researches in animal models suggest potential health benefits of roselle such as cholesterol-lowering effect [10,47], antioxidation [36,48,49] and anticarcinogenic action [9,50]. The applications of the roselle extract in the preparation of a medicament for countering oxidization of low density lipoproteins, reducing cholesterol or triglyceride in plasma or inhibiting atherosclerosis have also been patented [51]. Other pharmacological activity and toxicity tests of roselle are listed in Table 2.

Table 2 Clinical study, pharmacological activity and toxicity of *H. sabdariffa*

Activity	Plant used	Model of study	Results	References
Acid phosphatase inhibition	Dried calyx Egypt/ in ration/ 10.0% of diet	*In vivo*, rats were fed cholic acid vs. cholesterol-loaded animals	Weak activity	[47]
Acidifying activity	Dried fruit juice Thailand/ decoction/ 24.0 g/day	Clinic, oral, male adult	Inactive	[52]
Alkaline phosphatase inhibition	Dried calyx Egypt/ in ration/ 10.0% of diet	*In vivo*, rats were fed cholic acid vs. cholesterol-loaded animals	Weak activity	[47]
Alpha amylase inhibition	Dried flowers Thailand/ 50% methanol extract	*In vitro*, porcine pancreatic alpha amylase inhibitory assay	High inhibitory activity	[53]
Analgesic activity	Commercial sample of calyx Saudi Arabia/ water extract/ 500.0 mg/kg	*In vivo*, intragastric, mouse vs. hot plate method	Active	[54]

Table 2 Clinical study, pharmacological activity and toxicity of *H. sabdariffa* (continued)

Activity	Plant used	Model of study	Results	References
Antibacterial activity	Beverage containing roselle calyx	Not stated	Bactericidal against *Escherichia coli, Bacillus subtilis, Salmonella typhosa* and *Klebsiella pneumoniae*	[3]
	Roselle infusion/ 6 g, 4 times per day, for 7 days	Clinic, oral, 33 female with significant bacteriuria	Inactive/ fail to reduce lower urinary tract infection compared to the group receiving an antibiotic	[3]
Antichistosomal activity	Dried sepals Sudan/ water extract/ 100.0 ppm	*In vitro*, *Schistosoma mansoni*	Active	[55]
Anticlastogenic activity	Dried fruit Nigeria/ water extract/ 50, 100, 150 mg/kg for 7 days	*In vivo*, micronucleus assay, male Swiss albino mice given with IP sodium arsenite 2.5 mg/kg	Active	[56]
Antiedema	Flowers Japan/ methanol extract/ 2.0 mg/ear	*In vitro*, external, mouse vs. 12-o-tetradecanoylphorbol-13-acetate (TPA)-induced ear inflammation	Active/ inhibition ratio (IR) = 17	[57]

Table 2 Clinical study, pharmacological activity and toxicity of *H. sabdariffa* (continued)

Activity	Plant used	Model of study	Results	References
Antihepatotoxic activity	Dried flowers Taiwan/ methanol extract/ 0.1 mg/ml	Rat, hepatocytes vs. *tert*-butylhydro-peroxide cytotoxicity	Active	[11]
Antihyperlipidemia	Dried calyx Egypt/ in ration/ 5.0% of diet	*In vivo*, rats were fed cholic acid vs. cholesterol-loaded animals	Active	[47]
	Polysaccharides from fruits/ dose not stated	*In vivo*, rats were induced hyperlipidemia	Active/ significant decrease in cholesterol and triglyceride levels	[58]
	Dried calyx/ dried water extract/ 500 and 1000 mg/kg for 6 weeks	*In vivo*, hypercholesterolemic male Sprague-Dawley rat	Active/ significant decrease in cholesterol, triglyceride and LDL levels	[10]
Antihypertriglyceridemia	Dried calyx Egypt/ in ration/ 5.0% of diet	*In vivo*, rats were fed cholic acid vs. cholesterol-loaded animals	Active	[47]
Anti-inflammation	Commercial sample of calyx Saudi Arabia/ water extract/ 500.0 mg/kg	*In vivo*, intragastric, rat vs. carrageenan – induced pedal edema	Inactive	[54]

Table 2 Clinical study, pharmacological activity and toxicity of *H. sabdariffa* (continued)

Activity	Plant used	Model of study	Results	References
Anti-inflammation (continued)	Dried fruits Thailand/ Decoction/ 3.0 g/person (expressed as dry weight of plant)	Clinic, oral, 50 adult with kidney stone were treated with extract 3 times a day for 7 days to 1 year	Active/ the extract showed anti-inflammatory action after operation	[59]
Antioxidation	Calyx/ water extract/ dose not stated	*In vitro*, linoleic acid model system	Active	[60]
		In vitro, liposome model system	Active	[60]
	Part not stated/ dose not stated	*In vitro*, linoleic acid model system	Active	[61]
	Protocatechuic acid isolated from roselle/ 0.2 and 0.5 mmol/kg	*In vivo*, gavage, male Sprague-Dawley rat with lipopolysaccharide-induced hepatic damage	Active	[36]
	Dried flower/ extract contain 2.5% anthocyanins, 1.7% polyphenolic acid and 1.43% flavonoids	*In vivo*, oral, male Wistar rats with reversible cirrhosis induced by IP CCl_4	Active	[49]

Table 2 Clinical study, pharmacological activity and toxicity of *H. sabdariffa* (continued)

Activity	Plant used	Model of study	Results	References
Antipyresis	Commercial sample of calyx Saudi Arabia/ water extract/ 500.0 mg/kg	*In vivo*, intragastric, rat vs. yeast induced pyrexia	Active	[54]
Antitoxic activity	Dried flower heads, 1.0 g/liter	*In vitro*, broth culture, *Aspergillus flavus*	Active/ the production of aflatoxin was inhibited	[62]
Antitumor- promoting activity	Fresh flowers Thailand/ methanol extract/ 200.0 mg/ml	Cells-RAJI vs. EBV activation induced by HPA (40 ng/ml)	Inactive	[63]
Antiviral activity	Dried flowers/ water extract/ 10.0%	*In vitro*, cell culture, Herpes virus type2, Vaccinia virus	Active	[64]
		In vitro, cell culture, Influenza virus A2 (manheim 57), PoliovirusII	Inactive	[64]
Chemoprevention	Dried flower Thailand/ dried 80% ethanol extract/ 1.0 g/kg	*In vivo*, oral gavage, Male F344 rat in which aberrant crypt focus (ACF) formation was induced	Active/ inhibit the ACF formation at the initiation state but stimulate the ACF formation at post- initiation state	[9]
Choleretic activity	Flowers France/ water extract/ dose not stated	Clinic, oral, adult	Active	[46]

Table 2 Clinical study, pharmacological activity and toxicity of *H. sabdariffa* (continued)

Activity	Plant used	Model of study	Results	References
Creatinine level decreasing activity	Dried fruit juice Thailand/ decoction/ 24.0 g/day	Clinic, oral, male adult	Active	[52]
Cytotoxic activity	Flowers Egypt/ 70% ethanol extract/ dose not stated	*In vitro*, cell culture, ca-Ehrlich-Ascites cells	Active/ greatest effect only after 24 hours exposure	[65]
	Dried flowers/ water extract/ 10.0%	*In vitro*, cell culture, HELA cells	Weak activity	[64]
Estrogenic effect	Dried calyx Sudan/ water extract/ 500.0 mg/kg	*In vivo*, IP, female rats (immature)	Active/ result significant at $p < 0.001$ level	[66]
Glutamate- oxaloacetate-transaminase inhibition	Dried calyx Egypt/ in ration/ 10.0% of diet	*In vivo*, rats were fed cholic acid vs. cholesterol-loaded animals	Active	[47]
Glutamate- pyruvate-transaminase inhibition	Dried calyx Egypt/ in ration/ 10.0% of diet	*In vivo*, rats were fed cholic acid vs. cholesterol-loaded animals	Weak activity	[47]
Diuretic activity	Dried calyx Guatemala/ decoction/ 1.0 g/kg	*In vivo*, nasogastric, rat	Strong activity	[67]

Table 2 Clinical study, pharmacological activity and toxicity of *H. sabdariffa* (continued)

Activity	Plant used	Model of study	Results	References
Diuretic activity (continued)	Dried calyx/ boiling water (3 g in 300 ml)/ 3 times per day for 7 days to 1 year	Clinic, oral, 50 human	Active	[3]
	Flowers France/ water extract/ dose not stated	Clinic, oral, adult	Active	[46]
Genitourinary effect (unspecified)	Dried fruit juice Thailand/ decoction/ 24.0 g/day	Clinic, oral, male adult	Active/ decreased urinary levels of sodium, potassium, and phosphate demonstrated	[52]
			Equivocal/ decreased levels of uric acid and calcium in urine	[52]
Hypotensive activity	Dried calyx China/ 95% ethanol extract/ 200 mg/kg	*In vivo*, IV, dog	Weak activity/ blood pressure drop was from 137 to 68 mmHg with a duration of 6-12 minutes	[68]
	Dried calyx Sudan/ water extract/ 25.0 mg/animal	*In vivo*, IV, cat (animals anesthetized with alpha-chloralose)	Active/ effect blocked by atropine	[69]

Table 2 Clinical study, pharmacological activity and toxicity of *H. sabdariffa* (continued)

Activity	Plant used	Model of study	Results	References
Hypotensive activity (continued)	Water extract/ dose not stated	*In vivo*, IV, dog	Weak activity	[70]
	Flowers France/ water extract/ dose not stated	Clinic, oral, adult	Active	[46]
	Sour tea Iran/ decoction prepared with 2 spoonfuls of tea in 1 glass of boiled water and boiled for 20-30 min	Clinic, oral, 31 patients of moderate essential hypertension	Active	[4]
	Dried calyx Mexico/ infusion prepared with 10 g of dried calyx on 0.5 l of water/ once a day for 4 weeks	Clinic, oral, 39 Mexican patients of mild to moderate hypertension	Active	[5]
Intestinal motility inhibition	Dried calyx Sudan/ water extract/ 5.0%	*In vivo*, dog (oral-cecal transit time assayed by first detection of phthalylsulphasalazine in blood)	Active	[71]

Table 2 Clinical study, pharmacological activity and toxicity of *H. sabdariffa* (continued)

Activity	Plant used	Model of study	Results	References
Intestinal motility inhibition (continued)	Dried calyx Sudan/ water extract/ 5.0%	*In vivo*, rat (oral-cecal transit time assayed by transit of graphite-agar suspension)	Active	[71]
Laxative activity	Flowers France/ water extract/ dose not stated	Clinic, oral, adult	Active	[46]
	Dried flowers Nigeria/ decoction/ 0.8 g/kg	*In vivo*, intragastric, rat	Equivocal	[72]
Miscellaneous effect: used as a refreshing, mildly stimulating beverage	Hot water extract/ dose not stated	Clinic, oral, adult	Active	[73]
Mutagenic activity	Dried fruits Japan/ 50.0 μg/plate	*In vitro*, agar plate, *Salmonella typhimurium TA100*	Active/ metabolic activation was not required for activity	[74]
		In vitro, agar plate, *Salmonella typhimurium TA98*	Active/ metabolic activation required to obtain positive results	[74]
	Calyx/ water extract/ dose not stated	*In vitro*, *Salmonella typhimurium TA100*	Inactive/ either with or without S9 mix	[60]

Table 2 Clinical study, pharmacological activity and toxicity of *H. sabdariffa* (continued)

Activity	Plant used	Model of study	Results	References
Mutagenic activity (continued)	Calyx/ water extract/ dose not stated	*In vitro*, *Salmonella typhimurium TA98*	Inactive/ either with or without S9 mix	[60]
Pigment (coloring agent) use	Dried flowers Japan/ water extract/ variable concentration	-	Suitable for food color use, biological activity reported has been patented	[75]
Radical scavenging activity	Dried flowers Taiwan/ methanol extract	_	Active/ ED50 = 0.017 mg/ml	[11]
Reverse transcriptase inhibition	Dried calyx Egypt/ water extract	Virus HIV-1	Inactive/ IC50 = 320.0 μg/ml	[76]
	Dried calyx Egypt/ methanol extract	Virus HIV-1	Inactive/ IC50 = 1.0 mg/ml	[76]
Smooth muscle relaxation	Dried calyx Sudan/ water extract/ 2.0%	*In vitro*, rabbit ileum	Active/ effect not influenced by phentolamine, propanolol, haloperidol and guanethidine	[71]
	Dried petals Nigeria/ hot water extract	*In vitro*, rat aorta vs. ACH-induced contractions	Active/ IC50 = 0.53 mg/ml	[77]
		In vitro, rat aorta vs. de-endotheliazed muscle strips	Active/ IC50 = 2.53 mg/ml	[77]

Table 2 Clinical study, pharmacological activity and toxicity of *H. sabdariffa* (continued)

Activity	Plant used	Model of study	Results	References
Spasmogenic activity	Dried calyx Sudan/ water extract/ 0.4 mg/ml	*In vitro*, frog muscle (rectus abdominus)	Active/ effect slightly antagonized by tubocurarine	[69]
	Dried calyx Sudan/ water extract/ 1.0 mg/ml	*In vitro*, rabbit uterus (estrogenic induced)	Active/ effect blocked by indomethacin and hydrocortisone, but not by atropine or cyproheptadine	[69]
	Dried calyx Sudan/ water extract/ 0.16%	*In vitro*, rabbit ileum	Active/ effect blocked by atropine	[71]
Spasmolytic activity	Dried calyx Sudan/ water extract/ 0.4 mg/ml	*In vitro*, frog muscle (rectus abdominus) vs. ACH-induced contractions	Active/ effect antagonized by tubocurarine	[69]
		In vitro, rat uterus (estrogenic) vs. rhythmic contractions	Active/ effect not antagonized by propanolol or ranitidine	[69]
	Dried petals Nigeria/ water extract/ 0.6 mg/ml	*In vitro*, rat aorta vs. norepinephrine-induced contractions	Active	[78]
		In vitro, rat aorta vs. K^+-induced contractions	Inactive	[78]

Table 2 Clinical study, pharmacological activity and toxicity of *H. sabdariffa* (continued)

Activity	Plant used	Model of study	Results	References
Spasmolytic activity (continued)	Dried calyx Sudan/ water extract/ 5.0 mg/ml	*In vitro*, guinea pig tracheal chain vs. ACH-induced contractions	Active	[69]
		In vitro, guinea pig tracheal chain vs. histamine – induced contractions	Active	[69]
		In vitro, guinea pig tracheal chain vs. serotonin – induced contractions	Active	[69]
		In vitro, rabbit aorta vs. norepinephrine– induced contractions	Active/ effect not antagonized by atropine, propanolol or ranitidine	[69]
	Dried calyx Sudan/ water extract/ 10.0 mg/ml	*In vitro*, rat diaphragm vs. electrically induced contractions	Active/ physostigmine and suxamethonium enhanced the effect	[69]
Toxicity assessment (acute effect)	Dried calyx China/ hot water extract	*In vivo*, gastric intubations, rabbit	LD50 129.1 g/kg	[68]
	Dried calyx/ 30% concentration of hot water extract	*In vivo*, intraperitoneal, mice	LD50 0.4-0.6 ml	[3]

Table 2 Clinical study, pharmacological activity and toxicity of *H. sabdariffa* (continued)

Activity	Plant used	Model of study	Results	References
Toxicity assessment (acute effect) (continued)	Dried calyx Nigeria/ water: methanol extract (1: 4)/ 0, 1, 3, 5,10 and 15 dose of 250 mg/kg	*In vivo*, oral, Wistar albino rats	Aspatate aminotransferase (AST) and alanine aminotransferase (ALT) were significantly increased ($p < 0.05$) for in which two specific tests, the coloring power test and the acid content assay, as well as other common tests have been declared. in which two specific tests, the coloring power test and the acid content assay, as well as other common tests have been declared. all treatment group	[79]

Table 2 Clinical study, pharmacological activity and toxicity of *H. sabdariffa* (continued)

Activity	Plant used	Model of study	Results	References
Toxicity assessment (acute effect) (continued)	Dried calyx Nigeria/ water: methanol extract (1: 4)/ 0, 1, 3, 5,10 and 15 dose of 250 mg/kg	*In vivo*, oral, Wistar albino rats	Alkaline phosphatase and lactate dehydrogenase were not affected ($p > 0.05$)	[79]
			Not any histopathological features of livers and hearts were observed for all treatment group	
Toxicity assessment (subchronic effect)	Dried calyx Nigeria/ dried hot water extract/ 1.15, 2.30 and 4.60 g/kg for12 weeks	*In vivo*, oral, rats	Not any change in the absolute and relative testicular weight ($p > 0.05$)	[80]
			Significant decrease in the epididymal sperm counts in the 4.60 g/kg group ($p < 0.05$)	

Table 2 Clinical study, pharmacological activity and toxicity of *H. sabdariffa* (continued)

Activity	Plant used	Model of study	Results	References
Toxicity assessment (subchronic effect) (continued)	Dried calyx Nigeria/ dried hot water extract/ 1.15, 2.30 and 4.60 g/kg for12 weeks	*In vivo*, oral, rats	Distortion of tubules and a disruption of epithelial organization were observed in 1.15 g/kg group	[79]
			Hyperplasia of testis with thickening of the basement membrane were observed in 2.30 g/kg group	
			Disintegration of sperm cells were observed in 4.60 g/kg group	
Tyrosinase inhibition	Dried part not specified/ type extract not stated/ 500.0 μg/ml	*In vitro*, cell culture, melanoma-B16	Inactive	[81]
Uric acid decreasing activity	Dried fruit juice Thailand/ decoction/ 24.0 g/day	Clinic, oral, male adult	Inactive	[52]
Uricosuric activity	Dried calyx Guatemala/ decoction/ 1.0 g/kg	*In vivo*, nasogastric, rat	Active	[67]

Table 2 Clinical study, pharmacological activity and toxicity of *H. sabdariffa* (continued)

Activity	Plant used	Model of study	Results	References
Uterine relaxation	Water extract/ dose not stated	*In vitro*, female rat, unspecified condition	Active	[70]
Xanthine oxidase inhibition	Dried flowers Taiwan/ 95% ethanol extract	_	Active/ IC50 = 0.742 mg/ml	[11]

1.5 Chemical constituents of *H. sabdariffa*

Nutritionists have found roselle calyx sold in Central American markets to be high in calcium, niacin, riboflavin and iron [42]. Apart from common nutrients, there are several groups of chemical compound found in roselle such as anthocyanins, phenolic acids, organic acid, mucilage and resin. The chemical constituents of roselle are listed in Table 3 and the structures are shown in Figure 2.

Table 3 Chemical constituents of *H. sabdariffa*

Compounds	Plant parts	References
Alkane to C_4: Alcohol		
Ethanol	Fruit	[82]
Isoamyl-alcohol (3-methyl-1-butanol)	Fruit	[82]
Isopropyl-alcohol	Fruit	[82]
Methanol	Fruit	[82]
3-methyl-1-butanol	Fruit	[82]

Table 3 Chemical constituents of *H. sabdariffa* (continued)

Compounds	Plant parts	References
Alkane to C_4: Organic acid		
Acetic acid	Fruit	[82]
Aspartic acid	Flower	[3]
Butyric acid (butanoic acid)	Fruit	[82]
Citric acid	Calyx, Flower, Fruit	[3,82,83]
Formic acid	Fruit	[82]
Glycolic acid	Flower	[82]
Malic acid	Flower, Fruit	[3,82]
Oxalic acid	Calyx, Flower, Fruit	[3,82,83]
Propionic acid (propanoic acid)	Fruit	[82]
Tartaric acid	Calyx, Flower, Fruit	[3,83]
Benzenoids		
Anisaldehyde	Fruit	[82]
Benzaldehyde	Fruit	[82]
Benzyl-alcohol	Fruit	[82]
Gallic acid	Fruit	[3]
Protocatechuic acid	Flower	[82]
Carbohydrates		
L-arabinose	Fruit	[3]
Carbohydrates	Flower	[82]
Cellulose	Fruit	[3]
Fiber	Flower	[82]
Fructose	Calyx	[83]
D-galactose	Fruit	[3]
Galactose	Flower	[3]
D-glucose	Fruit	[3]
Glucose	Calyx	[83]
Mucilage	Calyx	[82]
Pectin	Calyx, Flower, Fruit	[3,82]
Polysaccharides	Calyx, Fruit	[58,83]
L-rhamnose	Fruit	[3]
Sucrose	Calyx	[82]
D-xylose	Fruit	[3]

Table 3 Chemical constituents of *H. sabdariffa* (continued)

Compounds	Plant parts	References
Carotenoid		
β-carotene	Flower	[82]
Flavonoids: Anthocyanins		
Anthocyanins	Calyx, Fruit	[3,82]
Chrysanthemin (cyanidin-3-glucoside)	Flower	[3]
Cyanidin-3(2(G)-glycosyl)-rutinoside	Flower	[3]
Cyanidin-3,5-diglucoside	Flower	[3]
Cyanidin-3-β-D-glucoside	Flower	[3]
Cyanidin-3-sambubioside	Calyx, Flower	[3,82]
Cyanin (cyanidin-3,5-diglucoside)	Flower	[3]
Delphinidin	Calyx,Flower	[3,82]
Delphinidin-3-glucoside	Calyx	[82]
Delphinidin-3-monoglucoside	Flower	[3]
Delphinidin-3-*O*-β-D-glucoside	Flower	[3]
Delphinidin-3-sambubioside	Flower, Calyx	[3,82]
Delphinin	Flower	[82]
Hibiscin (delphinidin glycoside)	Flower	[3,82]
Malvin (malvidin-3,5-glucoside)	Flower	[3]
Myrtillin (delphinidin-3-glucoside)	Flower	[3]
Flavonoids: Anthoxanthins		
Anthoxanthin	Flower	[3]
Gossypetin	Flower, Fruit	[3]
Gossypetin-3-glucoside	Flower	[82]
Gossypetin-3-*O*-β-D-glucoside	Flower	[3]
Gossypetin-7-glucoside	Flower	[3]
Gossypetin-8-glucoside	Flower	[3]
Gossypin (gossypetin-8-*O*-glucoside)	Flower	[3]
Gossypitrin (gossypetin-7-*O*-glucoside)	Flower	[3]
Gossytrin (gossypetin-3-*O*-glucoside)	Flower	[3]
Hibiscetin	Flower	[3,82]
Hibiscitrin (hibiscetin-3-*O*-β-D-glucopyranoside)	Flower	[3]
Quercetin	Flower, Fruit	[1,3]
Sabdaretin	Flower	[82]

Table 3 Chemical constituents of *H. sabdariffa* (continued)

Compounds	Plant parts	References
Lipids		
Caprylic acid	Fruit	[82]
Fat	Flower	[82]
Oleic acid	Fruit	[3]
Pelargonic acid	Fruit	[82]
Stearic acid	Fruit	[3]
Waxes	Flower	[3]
Minerals		
Aluminum	Flower	[82]
Calcium	Flower	[82]
Calcium oxalate	Fruit	[82]
Chromium	Flower	[82]
Cobalt	Flower	[82]
Iron	Flower	[82]
Magnesium	Flower	[82]
Manganese	Flower	[82]
Phosphorus	Flower	[82]
Potassium	Flower	[82]
Selenium	Flower	[82]
Silicon	Flower	[82]
Sodium	Flower	[82]
Tin	Flower	[82]
Zinc	Flower	[82]
Miscellaneous lactones		
Hibiscic acid	Flower	[3,82]
Hibiscus acid	Flower	[3]
Monoterpenes		
Alpha-terpinyl-acetate	Fruit	[82]
Proteins		
Protein	Flower	[82]
Steroids		
β-sitosterol	Flower, Fruit	[3]
Tannins		
Tannic acid	Fruit	[3]

Table 3 Chemical constituents of *H. sabdariffa* (continued)

Compounds	Plant parts	References
Vitamins		
Ascorbic acid	Flower, Fruit	[82]
Niacin	Flower	[82]
Thiamine	Flower	[82]
Miscellaneous and undefined group		
Ash	Flower	[82]
Galacturonic acid	Flower	[3]
Glucides (carbohydrates)	Fruit	[3]
Gossypetic	Flower, Fruit	[1]
Heterosides	Flower	[3]
Resin	Calyx, Flower	[3,82]
Sabdaretrin	Flower	[3]
Utalonic acid	Flower	[82]
Water	Flower	[82]

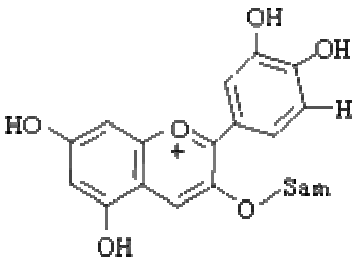

Cyanidin-3-sambubioside

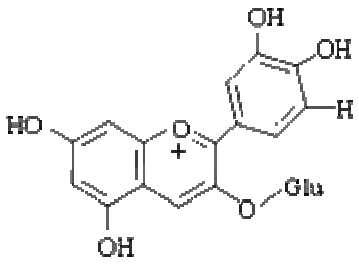

Cyanidin-3-glucoside or Chrysanthemin

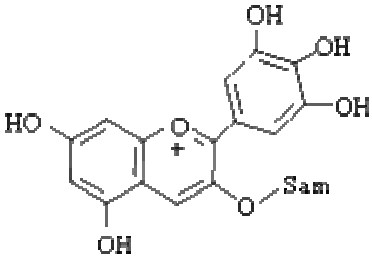

Delphinidin-3-sambubioside

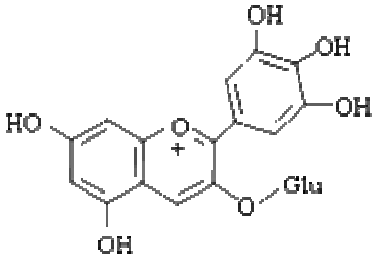

Delphinidin-3-glucoside

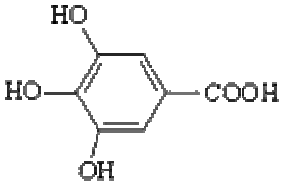

Gallic acid

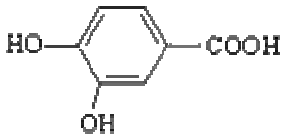

Protocatechuic acid

Figure 2 Chemical constituents of *H. sabdariffa*

1.6 Commercial value of *H. sabdariffa*

The possibility of health promoting and natural colorant uses has generated interest in roselle. The herb is attracting the attention of food and beverage as well as pharmaceutical manufacturers who feel it may have exploitable possibilities as a natural food product and as a colorant to replace some synthetic dyes [42]. Most of the roselle economic value, particularly as an ingredient in herbal teas, comes from the calyx [43].

Because of the rapid withering of the roselle, it would not be an economical product to export fresh over long distances. The calyx is either frozen or dried in the sun or artificially for out-of-season supply, marketing or export. In Mexico, the dried calyx is packed for sale in imprinted, plastic bags while it is pressed into solid cakes or balls

for retailing in Africa. In Senegal, the dried calyx is squeezed into great balls for shipment to Europe [42].

According to the market survey of dried calyx of roselle, the primary import markets for the roselle are the United States and Germany. In recent years, the demand of roselle has been considerably increasing. The United States imported over 5 thousand metric tons, while Germany imported nearly 43 thousand metric tons of plant and plant part in 1997 for making herbal teas, medicines and perfumes, an increase of 74% and 32%, respectively from 1994 levels [6].

The main supply of roselle comes from Thailand, Sudan, China, and Mexico. Sudanese roselle, formerly the primary source of roselle sold in herbal teas in the United States, is considered by many in the herb trade as the preferred product. Due to the US trade embargo on agricultural goods from Sudan, the majority of roselle in the United States now comes from China and Thailand [43].

In Thailand, the production of dried calyx is about 250-650 MTs per year, and approximately 70% of the yield has been exported [84]. As a result of the 10th National Economic and Social Development Plan (2548-2552 B.E.), roselle has been promoted as a list of high competitive herb (product champion) [85].

1.7 Quality control of *H. sabdariffa*

The official method for quality control of roselle has been described in the European Pharmacopoeia: EUP 4.4. in which two specific tests, the coloring power test and the acid content assay, as well as other common tests have been declared [28].

Other criteria, obtained from the "Market Survey: *Hibiscus sabdariffa*", cover the investigation of color, texture, aroma, free flow density, moisture, total ash, acid insoluble ash, impurity and microbial contamination. But there is no assay of any chemical in this specification (Table 4). The survey also stated that roselle has very different qualities depending on where it is grown. The most desirable product is from Thailand and Sudan, but roselle from these two countries is also very different [6].

In Thai Herbal Pharmacopoeia (THP) [20,29], there is no official method for quality control of roselle. For roselle grown up in Thailand, most of the study was on the pharmacological activities with no attention given to the chemical and quality control of the herb.

Table 4 Common guidelines and specifications for dried *H. sabdariffa*

Guidelines	**Specifications**
Description	*Hibiscus sabdariffa*
Packaging	Item must be packed in 50 lb. poly (or less) lined boxes or multi-walled sacks (adequately protecting product for shipment) with clear markings indicating the item contained. Shipment must be accompanied by packing list clearly indicating the consignment, weight and country of origin.
Raw ingredient sample:	
(a)Visual	Purple-red color.
(b)Aroma	Floral, berry-like aroma. Free from objectionable off odors.
(c)Texture	Lump free, free flowing particles
Prepared sample:	
(a)Visual	Clear, deep red solution with some background purple hues. Blue hues are undesirable.
(b)Aroma	Slight berry aroma.
(c)Flavor	A well balanced, tart and astringent flavor. Some cranberry notes as well as a slight drying effect. Not excessively tart, acidic or bitter. Should be free of off-flavors and other undesirable spice/botanical notes.
Testing Parameters:	
Test Units:	*Specifications*
(a) Free Flow Density	G/CC Minimum 0.45, Maximum 0.60
(b) Moisture	12%
(c) Total Ash	10%
(d) Acid Insoluble Ash	1.5%
(e) Sieve Analysis	Thru US#20 95.0%
5 Min Rotate	Thru US#60 5.0%
(f) Insect Fragments each	400
(g) Whole Insects (field/storage) each	25/5
(h) *Salmonella*	negative
(i) Coliform	2 of 5 over 10 CFU, 0 of 5 over 100 CFU
(j) *E. coli* (MPN)	2 of 5 over 3 CFU, 0 of 5 over 20 CFU
(k) *E. coli* (Film)	0 of 5 over 10 CFU
(l) *S. Aureus*	1 of 5 over 100 CFU, 0 of 5 over 1000 CFU
(m) Standard Plate Count	0 of 5 over 1,000,000 CFU
(n) Yeast/Mold	0 of 5 over 10,000 CFU

Source: [6]

1.8 Conclusions

Roselle is a potential herb for used as health promoting food product and natural colorants as well as exporting as raw materials to make herbal tea and medicines. With the worldwide expansion in the use, safety, efficacy, and quality control of herbal medicine have become important concerns. For roselle cultivated in Thailand, there is no scientific and regulation information concerning over the chemical and quality control of the herb. Therefore, as the background information of roselle grown up in Thailand, the study

about physical and chemical property of roselle from various sources of Thailand is needed. And the method used to determine the quality of herb is also in great requirement.

2 Anthocyanins

Anthocyanins (from the Greek anthos = a flower, and kyanos = dark blue), a group of flavonoids, are water soluble and vacuolar pigments responsible for a great range of colors from scarlet to blue. They are found mainly in the flowers and fruits of higher plants. The skeleton structure is C6-C3-C-6 (phenyl-2-benzopyrilium structure) or anthocyanidins (Figure 3). The anthocyanidins or aglycones structure consist of an aromatic ring [A] bonded to a heterocyclic ring [C] that contains oxygen, which is also bonded by a carbon–carbon bond to a third aromatic ring [B] [86,87].

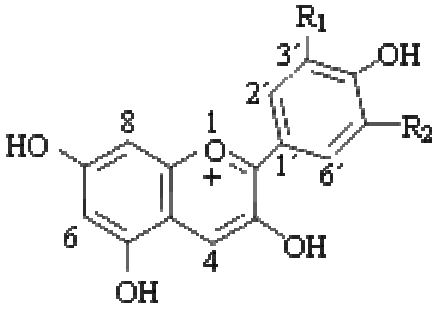

Figure 3 Chemical structure of anthocyanidins

Anthocyanins show high diversity in nature, produced by the number of hydroxylated groups on anthocyanidins skeleton, the nature and the number of bonded sugars to the aglycone structure, as well as the aliphatic or aromatic carboxylates bonded to the sugar in the molecule and the position of these bonds. Up to now there are reports of more than 500 anthocyanins and 23 anthocyanidins of which only six, as listed in Table 5, are the most common in vascular plants [86].

Table 5 Structures of common anthocyanidins (refer to Figure 3)

Antocyanidins	**R_1**	**R_2**
Cyanidin	OH	H
Delphinidin	OH	OH
Malvidin	OCH_3	OCH_3
Pelargonidin	H	H
Peonidin	OCH_3	H
Petunidin	OCH_3	OH

2.1 Anthocyanins as marker for good manufacturing practices, natural food colorants and nutraceutical uses

In production area, anthocyanins have several important functions i.e. as markers for good manufacturing practices and as natural food colorants as well as for nutraceutical uses. Humans are fascinated by color, and the consumers associates the color with safety, quality, and as indicator of good processing. As a large number of natural products are colored by anthocyanins, analysis of anthocyanins based on the fact that each fruit has a characteristic anthocyanin pattern, has been undertaken to detect adulteration in the product. In this respect, the HPLC combined with multivariate statistical methods is suggested [87].

Due to safety concern, the synthetic colorants used extensively in foods, medicines and cosmetics to achieve a better visual appearance are diminished. Currently, only 7 synthetic pigments can be used in food under U.S. FDA regulations. Consequently, the study of natural colorants is an extensive and active area of investigation [88]. Among the most utilized vegetable colorants in the food industry, carotenoids and anthocyanins are included [86]. The potential of various food plants as commercial sources of anthocyanins are such as cranberry, blueberry, red cabbage, bilberries, grapes as well as roselle calyx [89]. However, in the United States, extracts of grape are the only anthocyanins source approved by the FDA as a food colorant [87].

Anthocyanins also have nutraceutical properties. According to the review by Castañeda-Ovando et al. [86], several studies suggested that the anthocyanins content and their corresponding antioxidant activity contribute to the protective effect of fruits and vegetables against degenerative and chronic diseases. Both anthocyanidins and anthocyanins showed a higher antioxidant activity than vitamins C and E. Moreover, a linear correlation between the values of the antioxidant capacity and the anthocyanins content in

blackberries, red raspberries, black raspberries and strawberries was also stated in the report. There are several reports focused on the effect of anthocyanins in cancer treatments.

Although the importance of natural pigments is known, there are limited reports on the use of plants or fruits for anthocyanin extraction in the industrial scale. The causes might be the effectiveness of extraction and recovery, the marketability of resulting extracts and the practical suitability for food and pharmaceutical products. Another important factor is the stability and intensity of coloration provided by anthocyanins [86].

2.2 Analysis of anthocyanins

Anthocyanins are polar molecules, thus the most common solvents used for the extractions are aqueous mixtures of ethanol, methanol or acetone. At a neutral or alkaline solution, anthocyanins are not stable; thus the most common methods are those which use acidified methanol or ethanol as extractants. The low pH of extract facilitates the formation of the flavylium ion, but some hydrolysis may occur during storage. Consequently, the use of weak acids such as citric acid or acetic acid is recommended for the extraction of complex anthocyanins. In aqueous acetone, the anthocyanin molecules undergo significant structural modification, a phenomenon that did not occur in acidified methanol. Thus aqueous acetone is not an appropriate solvent for extraction [86,87].

The extraction methods are not selective for anthocyanins, other compounds, such as sugars, organic acids and pectins are co-extracted. For identification purpose, it is necessary to isolate the anthocyanins of interest. In the purification process, Solid Phase Extraction (SPE) by C_{18} or Sephadex cartridges, Liquid-Liquid Extraction (LLE), ion-exchange resins such as Amberlite CG-50 was commonly employed. Separation methods involve basic chromatography; paper chromatography and Thin Layer Chromatography (TLC), to the use of modern chromatographic techniques like Counter Current Chromatography (CCC), Medium Pressure Liquid Chromatography (MPLC), Capillary Electrophoresis (CE) and the High Performance Liquid Chromatography (HPLC). While the most common method is HPLC with UV-Vis or photodiode array (PDA) detectors [86,87,90].

In the quality evaluation of crude, the identification of anthocyanins has a critical role in taxonomic and adulteration studies. Spectral data in the UV-Vis region provide the simplest means of identification [91]. The HPLC with PDA has been also used in the anthocyanins identification, but the difficulty to obtain reference compounds and the spectral similarities of the anthocyanins represent an important drawback. Thus, Mass Spectrometry (MS) and Nuclear Magnetic Resonance (NMR) of ^{1}H and ^{13}C have become the preferred techniques for anthocyanins identification [86]. Identification of anthocyanins by

Infrared Spectroscopy (IR), florescence and excited fluorescence spectra, and Gas Liquid Chromatography (GLC) have been also reported [91]. In some case, the classical hydrolysis and chemical tests of hydrolyzed product are important to verify the structure, particularly in complex molecules [87].

Up to now several methods have been applied for the quantitative determination of anthocyanins in plant extracts. There are TLC densitometry [92], FTIR [93], Capillary Zone Electrophoresis (CZE) [94], HPLC [8,92,95,96], and spectrophotometry [33,92,95,97]. The most prominent ones are the last two methods. HPLC is superior in separation, identification and quantification of individual anthocyanins while spectrophotometry is simple, rapid, inexpensive and suitable for the analysis of total anthocyanin content [98].

The most common method used for the separation of anthocyanins is reversed-phase LC but there is no single standard procedure. UV diode-array absorbance detection (DAD) is usually used to collect on-line spectra. Single wavelength detectors, between 520 and 546 nm can selectively monitor anthocyanins separation. The gradient elution, using methanol or acetonitrile as an organic modifier, and low pH (pH < 2) of mobile phase is the most effective system for separation [99].

In the case of laboratories which do not have access to HPLC, the pH-differential spectrophotometric method is a good alternative one because the result of analysis by this method shows high correlation with that of HPLC method. Moreover the method has been verified by AOAC's strict validation guidelines [100].

The pH-differential spectrophotometric method is based on reversible structural transformations of anthocyanin pigments with a change in pH manifested. At pH 1.0, the red colored oxonium or flavylium cation form predominates and at pH 4.5 the colorless hemiketal or carbinol pseudobase form is dominance (Figure 4). Therefore, the method permits accurate and rapid measurement of the total anthocyanins, even in the presence of polymerized degraded pigments and other interfering compounds [101].

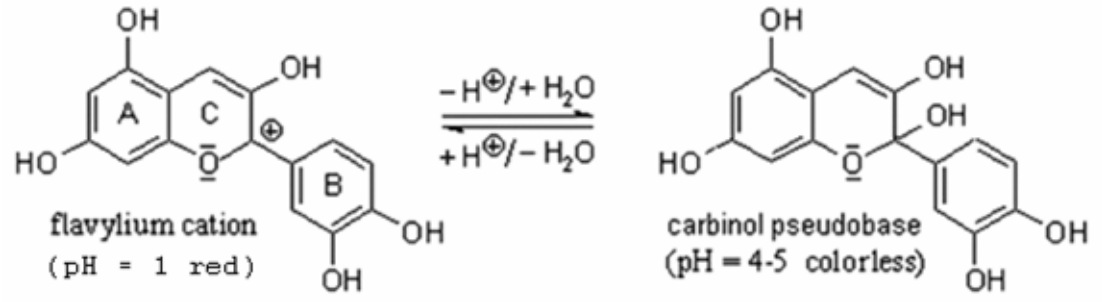

Figure 4 Predominant structural form of anthocyanins present at pH 1.0 and pH 4.5

2.3 Conclusions

The most common method for analysis of anthocyanins is HPLC and spectrophotometric method. While the HPLC is superior in separation and analysis of individual anthocyanin, the spectrophotometric is considered as a simple, rapid, inexpensive and suitable for the analysis of total anthocyanin content.

3 Approach for quality control of herbal medicine

High chemical complexity of herbal medicine makes quality control through chemical analysis difficult. The current approach for authentication and quantitative quality control of herbal medicine can be categorized into the “component-based” and “pattern-based” approaches [18] or as the “compound-oriented” and “pattern-oriented” approach [102]. Component-based or compound-oriented approach targets specific components with some known chemical properties as an individual component while pattern-based or pattern-oriented approach targets all detectable components as an overall feature or as an image.

3.1 Component-based or compound-oriented approach

The component-based approach includes the marker approach and the multi-component or multi-compound approach which is a natural extension of the marker approach [18,102].

3.1.1 Marker approach

At the present, practice for authentication and quantitative quality control of herbal medicine is based extensively on the marker approach. If active component(s) is known, such active component(s) is most logical to use as the target for identification and quantitative quality control of herbal medicine. When active component(s) is not known, an analytical marker(s) substance which should be specific for the particular

botanical could be chosen for analytical purpose, although it should only serve for internal batch control [103]. In some case only one marker is recommended, such as chlorogenic acid is recommended for the identification and quantitative quality control of Flos Lonicerae (content ≥ 1.5%) and Flos Chrysanthemi (content ≥ 0.2%) [102]. But in some situation more than one marker are used such as in the case of formulated Chinese medicine Qingfu Guanjie Shu (capsule) which 4 markers, namely sinomenine, paeoniflorin, paeonol and curcumin are used [104]. Based on this approach, the present of selected marker(s), usually few compared with several compounds of herb, can be used to ensure the authentication. And the content of them can also be used to ensure that the concentrations and ratios of components in herb are present at reproducible levels. In this way, the marker approach gives a very few chemical information for both authentication and quantitative quality control of herbal medicine.

While the marker approach is simple, it is suffered from limited number of available standards as well as lacking of a standard that is unique for a particular herb. The example is chlorogenic acid which presents in both Flos Lonicerae and Flos Chrysanthemi and thus this single marker cannot be used to differentiate between these two species [102]. Moreover, as described above, it cannot give a complete picture of an herbal product, because multiple constituents usually account in therapeutic effects [18]. The synergy and other interactions of phytomedicine have been reviewed by Williamson [105].

3.1.2 Multi-components or multi-compounds approach

Because the marker approach fails to demonstrate the overall consistency and quality of herbal medicine, the extended of marker approach, multi-component or multi-compound approach, has been developed. To represent the sample, this approach uses relatively high numbers of components or even all identified compounds, in the other name chemical profile of the sample [18]. In an example shown by Zeng et al, to control the quality of a ginkgo leaf product, the determination of total flavonol glycosides (i.e. quercetin, isorhamnetin and kaempferol) and total terpene lactones (i.e. bilobalide, and ginkgolides A, B and C) were used. The authors also stated that the multi-compound approach uses multiple compounds with known chemical properties and does not need chemical markers in quality assessment. The success has been obviously seen in the chromatograms that have overlapping peaks; with sophisticated instrumental and/or chemical methods that take advantage of spectra or other chemical properties at very close retention time, such as HPLC-DAD and HPLC-MS, and chemometric deconvolution and resolution, several compounds can be identified [102].

3.2 Pattern-based or pattern-oriented approach

As pointed by Nielsen, the drawbacks of component-based approach, both the marker and the multi-component approach, are difficulties originated from selection for an optimal set of integration parameters for chromatograms obtained from analysis of complex sample, subjective peak selection to include in the analysis and a large amount of data are discarded [106]. Fundamentally, irrelevant information should be removed and relevant chemical information should be extracted as much as possible, during data treatment. But in many real cases, it is hard to define correctly what information is relevant and what should be discarded, especially when the noisy data or complex data are analyzed.

The phytoequivalence concept was developed, recently, in Germany. According to this concept, a detailed chemical profile of an herbal product is necessary to fit with that of clinically proven product to ensure consistency and quality of herbal product. On a similar basis, the State Food and Drug Administration (SFDA) of China proposed to use fingerprints for quality measurement of an herbal extract or preparation [18]. A chemical fingerprint of a traditional medicine is a unique feature which could be a spectrum or a chromatogram, obtained by a defined procedure, to characterize the chemical composition of the traditional medicine [18]. As mentioned by Liang et al. [23], the fingerprint should demonstrate both the “sameness” and “differences” among various samples. In accordance with this definition, the chemical fingerprint may be analyzed by two approaches; the multi-component approach as described above and the pattern-based approach [18]. However, the pattern-based approach is more useful than the component-based approach in most cases [102]. The pattern approach was recommended as a potential and reliable approach for the quality control of herbal medicine. This approach can be called in the other name as “all-information based approach” [18]. According to Mok and Chau [18], SFDA of China adopted the fingerprints based on all-information based approach in the regulation of Traditional Chinese Medicine (TCM) injection products. The pattern-based approach includes single pattern approach or fingerprint analysis and multi-pattern approach [18,102].

3.2.1 Single pattern approach or fingerprint analysis

The basic concept of the pattern approach is to evaluate the whole pattern or all data acquired from analytical instrument such as the entire chromatographic profile or the full spectrum as a chemical feature. The data may be obtained from one-, two- or higher dimensional chromatographic and/or spectral instruments. Although the relationship between the pattern and the chemical compositions of the sample may be

unclear, under the same experimental condition, the pattern of a chromatogram or a spectrum is solely contributed by the chemical components presented in the extract [18,102].

As mentioned by Zeng et al, the single pattern approach or fingerprint analysis focuses on only one type of pattern (e.g. chemical fingerprints of chromatograms and spectra) for the quality control of herbal medicine. There may be more than one fingerprint; those fingerprints may be obtained from different instruments/detectors as long as the fingerprints show only chemical characters [102]. Whereas only one chemical fingerprint obtained from only one instrument with one detector has been classified as the single pattern approach by Mok and Chau. If combined chemical fingerprints or combined instruments/detectors are used for assessment of quality, it will be classified as multi-pattern approach [18]. For example, a fingerprint obtained from HPLC/MS/MS is classified as it is based on single pattern approach and multi-pattern approach by Zeng et al and Mok and Chau, respectively.

3.2.2 Multi-patterns approach

According to Zeng et al, the multi-pattern approach assesses the quality of herbal medicine by multiple patterns. For example, both chromatographic fingerprints and biological activity profiles are used for the quality control of herbal medicine. This approach serves for the discovery of bioactive ingredients, assessment of medical effects, correlation between chemical fingerprints and pharmacological indices, and quality control [102]. For example, as cited by Zeng et al, Wang *et al*. found 32 potential bioactive components of *Radix Angelicae Sinensis* (Danggui) in rabbit plasma and over ten are new compounds [102]. But, as indicated by Mok and Chau, the multi-pattern approach does not limit to quality assessment that combines different kinds of pattern, such as chemical and biological patterns. The combined chemical fingerprints are also classified as multi-pattern approach [18].

3.2.3 Fingerprint application

In case of the identification of an active principle of the plant preparation and finished product is not possible, the World Health Organization (WHO) suggests chromatographic fingerprint as a quality measurement [14]. The U.S. Food and Drug Administration (FDA) suggests qualitative and quantitative comparing of spectroscopic and/or chromatographic fingerprint of a botanical raw material, drug substance, or drug product against that of a reference sample or standard to ensure the identity, quality, as well as consistency from batch to batch [21]. The European Medicines Agency (EMEA) suggests

chromatographic fingerprint for the determination of the stability of the herbal substance or herbal preparation [22].

3.3 Conclusions

Currently, two main approaches, component-based and pattern-based approaches, are applied for authentication and quantitative quality assessment of herbal medicine. Marker approach and multi-component approach are classified as component-based approach, while single pattern approach and multi-pattern approach are classified as pattern-based approach. Their pros and cons under the purpose for quality control of herbal medicine have been stated. For simple and rapid development of quality control method, the marker approach can be used as a basis, but the pattern approach is highly recommended for intensive quality control.

4 Chemometrics tools for quality control of herbal medicine

4.1 Introduction to chemometrics

Chemometrics has been developed for almost 40 years as a subdiscipline in chemistry. The word “chemometrics” was coined in the 1970s. As defined by Massart et al., “chemometrics is a chemical discipline that uses mathematics, statistics, and formal logic to

(i) design or select optimal experimental procedures,

(ii) to provide maximum relevant chemical information by analyzing chemical data, and

(iii) to obtain knowledge about chemical systems” [107].

According to Brereton [108], an interesting difference between chemometrics and traditional computational or theoretical chemistry is that theoretical chemistry rarely come across matrices that are not square and need to be inverted (*via* the pseudoinverse). The distinction between chemometrics and quantitative structure-activity relationships (QSAR) is that a critical phase of handling and preparing instrumental data prior to or (in some case simultaneously with) pattern recognition algorithms is usually presented in the chemometrics, while such phase is absent in many other areas of science. The borderlines with computational chemistry are such as chemometrics does not involve structure representation or database algorithms and it is not part of quantum chemistry. In general, there could not be well differentiated the chemometrics from the application of computational

algorithms to handle analytical data, such as Neural Networks, Genetic Algorithms, Support Vector Machines and Machine Learning.

The chemometrics has been evolved continuously; the earliest applications were based on a simple analytical chemical dataset, for example deconvolution of peaks from cluster of two or three peaks of HPLC chromatogram. In 1990s, the applications of chemometrics were on problems with intermediate complexity and the size of problem is much larger than those in 1980s. As an example by Brereton [108], the chromatographic pattern recognition of pharmaceuticals that deals with a series about 50 chromatograms and each chromatogram contain about 20 peaks, most peaks are common to several of the chromatograms and there are quite well identified features that allow the ability to distinguish two groups according to their origins. But, current developments are on very complex problem solving. The example is chromatographic data in biological applications such as metabolomics or proteomics. The dataset may consist of a thousand chromatograms and each chromatogram consists of several hundred detectable peaks. This could result that we may be dealing with 1,000 chromatograms of around 500 peaks each (total 500,000 detectable peaks and many peaks are unique to a small number of chromatograms) and thus more complicated problem.

In the beginning, chemometrics was based around laboratory and process instrumental analytical chemistry e.g. using partial least squares (PLS) to calibrate the UV-Vis spectrum of a mixture to determine the concentrations of each constituent. Although it is not very glamorous, this area is still the majority of reports on the use of chemometrics, especially in the experimental design and the interpretation of multivariate spectroscopic data. In the 1970s and 1980s, food chemistry was one of the main early growth areas especially in the use of NIR and food analysis. Process chemistry joined in the 1980s, with the establishment of several research centers. An important involvement was pharmaceutical chemistry. This major growth caused substantial growth in the applications of HPLC and NIR to pharmaceuticals, food and process analysis as well as other main principles. Over the last few years, the applications have substantially diversified. The most remark extension is the biological and medical area, with the enormous development of chemical analysis instruments such as gas chromatography-mass spectrometry (GC-MS), nuclear magnetic resonance (NMR), optical spectroscopy and pyrolysis, and the tradition of computationally oriented biologists. Other important development areas are chemical engineering (far beyond the original process analytics), forensics (the use of chemical and spectroscopic information to determine origins of specimens), multivariate image analysis (especially of pharmaceutical tablets), and material sciences (including thermal analysis) [108].

4.2 Application of chemometrics to quality control of herbal medicine

4.2.1 Experimental design

Although the experiments in chemistry are performed relatively rapid, and if necessary, it can be repeated under slightly different conditions, most real world experiments are expensive, and some need days or months to achieve the goals e.g. to optimize the parameters of chromatographic separation [109]. Experimental design is a strategic plan to collect empirical knowledge, i.e. knowledge based on the analysis of experimental data and not on theoretical models. The purpose of experimental design is to generate experimental data with an important amount of structured variation, that enable analyst to find out which design variables (X) have an influence on the response variables (Y), in order to understand the interactions between the design variables and thus determine the optimum conditions, by performing a minimum number of experiments [110]. Various experimental designs e.g. face-centered cube designs [111], full factorial designs [112] were applied to optimize the extraction parameters (e.g. extraction time and temperature). Optimization of parameters of chromatographic separation and capillary electrophoresis (CE) (e.g. flow rate, temperature, gradient solvent system, and detector) by sequential uniform designs [113], uniform designs [27], simplex designs, as well as full factorial designs were also reported [114].

Full factorial designs combine all defined levels of all design variables. For instance, a full factorial design investigating 3 design variables (X_s) where X_1 is a 2-level continuous variable, X_2 is a 3-level continuous variable and X_3 is a 4-level category variable will include 2 x 3 x 4 = 24 experiments. This designs are perfectly balanced, i.e. each level of each design variable is studied an equal number of times in combination with each level of each other design variable, and include enough experiments to allow use of a model with all interactions. Thus, they are a logical choice if variables interactions are of interest. For screening purpose, 2-level full factorial designs can be used very effectively. However the pitfalls are that they only provide an approximation within the experimental range, quadratic terms are not included into account and if all possible interaction terms are taken into account no error can be estimated. For optimization, full factorial designs with 3-level (or more) continuous variables can be used since the number of levels is compatible with a quadratic model.

4.2.2 Chromatographic fingerprint analysis

Because chromatographic fingerprint becomes one of the most powerful tools for quality control of herbal medicine, both construction or obtaining and

analysis of chromatographic fingerprint become an important aspect. However, the complexity of herbal medicine i.e. many peaks are detected in chromatographic fingerprint and the nature of variation of chromatographic instruments and experimental conditions occurred in each run cause the difficulty in both the establishment and the analysis of chromatographic fingerprints. As a result, extracting most relevant information from chromatographic data is an important step for representing and interpreting chromatographic fingerprint.

4.2.2.1 Information theory

As described above that chromatographic fingerprint usually shows complex pattern. According to Gong et al. (2003), performance of obtained fingerprint is closely dependent on the chromatographic separation degrees and concentration distribution of all chemical components in that herbal medicine. To evaluate the performance of a chromatographic fingerprint, two main approaches, local and global approaches were applied. Local approaches are the approaches that consider parameters of each detected peak e.g. signal intensity, retention time, peak area and/or peak height as well as other criteria, but not contemplate on the whole chromatographic curve, while the global approaches are on the contrary. In order to calculate the information content of a chromatogram correctly, the identification of non-overlapping peaks and estimation of the noise and/or error level of a chromatographic fingerprint is necessary in the local approach. However, in practice, those tasks are quite crucial. To solve the problems, information theory, based on the global approach was applied [115]. The authors proposed the simple method to calculate the information content (ϕ) of a chromatographic fingerprint as shown in the following;

$$\phi = -\sum\left(\frac{x_i}{\sum x_i}\log\left(\frac{x_i}{\sum x_i}\right)\right),$$

where x_i and $\sum x_i$ is the real chromatographic response of the chemical components involved in the chromatogram under study and its summation, respectively [23,115]. In theory, if and only if x_i with unchangeable variance is characterized by normal distribution can its information content (ϕ) reach its maximum i.e. the maximum information content will be achieved with fingerprint with all of peaks just completely separated. Further separation cannot provide any more information and becomes unnecessary. But, if there are overlapped peaks or incompletely separated peaks, such peaks will show non-Gaussian normal

distribution character and therefore a loss of information. The advantage of this method is that it considers the whole chromatogram feature (global) not the individual peak parameters i.e. retention time, peak intensity, peak width, peak area and/or peak height of each identified peak (local). Thus it is unnecessary to identify the chromatographic peaks at first and the noise might have a small influence on the calculation of the information content [23,115].

4.2.2.2 Chromatographic fingerprint alignment

Between each time of chromatographic analysis, deterioration of instruments and variation in experimental conditions always occurs, thus pre-processing of chromatographic data particularly correction for chromatographic shift is an important step for obtaining chemical relevant information. SpecAlign is a free software developed by Wong [116] used for alignment of mass spectra or chromatographic profile. According to Wong, the short brief of SpecAlign program is a developed heuristic algorithm that has a computational complexity of $O(ds)$, where d is the number of spectral data points and s is the number of spectra. "The algorithm is based on the insertion and deletion of data points to shift regions in each spectrum, m, to align with the corresponding region in a reference spectrum, r, as marked by reference points, P_{im} and P_{jr} where i and j are points between 0 and d.

By default, the algorithm makes use of an average spectrum (comprising all spectra to be aligned) as a reference, although a user-specified spectrum may be used. Reference points typically consist of automatically selected peaks, but may also consist of manually selected peaks or points within each spectrum. The algorithm proceeds as follows for each spectrum, m, to be aligned to the reference spectrum, r:

(1) For each j in P_{jr} find the closest matching P_{im}. If no match is found within a window of a size, w, specified by the user, then moves to the next point $j + 1$.

(2) If P_{im} is found but not aligned to P_{jr} , find the minima between, P_{im} and $P_{(i-1)m}$, $\min_{-1}$ and, P_{im} and $P_{(i+1)m}$, $\min_{+1}$ where insertions or deletions are to be made for alignment of P_{im} to P_{jr} .

(3) If $P_{im} > P_{jr}$ (for the value of the x-axis), then points are to be deleted from the $\min_{-1}$ and points to be inserted at $\min_{+1}$. If $P_{im} < P_{jr}$ then the reverse applies.

(4) Where points are inserted, the y-axis value for the inserted point is estimated by a least squares quadratic polynomial fit to its adjacent w points".

4.2.2.3 Principal components analysis (PCA)

In chromatographic fingerprints, disturbances are due to two main causes; disturbances introduced by the instruments or experimental conditions and disturbances introduced by unexpected changes of the analyzed samples [117]. Correction of disturbances introduced by the instruments, such as chromatographic shift, has been described above. For the detection of disturbances introduced by unexpected changes of the samples, chromatographic data of each sample should be investigated. However, analysis of high dimensional vectors or complex feature such as chromatographic fingerprint of herbal medicine is not an easy task due to human visual limitation. Generally, transforming the high dimensional vector into a low dimensional space could greatly enhance comparative analysis and detection of unexpected changes of the samples. However, it is important that such low dimensional feature generated from mathematical transformation should retain the critical information of the original fingerprint. Among those techniques utilized to extract useful information from high dimensional data, principal component analysis (PCA) is a popular one.

PCA is a mathematical procedure for resolving sets of data into orthogonal components whose linear combinations approximate the original data to any desired degree of accuracy. The principle of PCA is to find the directions in space along which the distance between data points is the largest or the other word to find the linear combinations of the initial variables that contribute most to making the samples different from each other. The directions, or combinations of original variables, are called principal components (PCs) or latent variables (LVs) or factors. The PCs are computed iteratively, in such a way that the first PC carries the most information. Then the second PC is calculated, in the same way i.e. to carry most information, from the residual information (i.e. not taken into account by the previous PC) and so on. This process can go on until as many PCs have been computed as there are variables in the data. Then the PCs form a new set of coordinate axes. By this way, the variation in the data can be described by minimum latent variables which allow easy in comparing between the samples. In matrix representation, the model with a given number of components is written as:

$$X = TP^T + E ,$$

where X(n, k) represents the data matrix with n samples and k variables, T(n, a) is the scores matrix with n samples and a PCs, P^T(a, k) denotes the transposed loading matrix with a PCs and k variables, and E(n, k) is the error matrix with n samples and k variables. The new

coordinate system has two advantages over the original set of axes. First, each PC are orthogonal to each other thus there is no multicollinerity. Second, they are ranked so that each one carries more information than any of the following ones [110,118]. In the Unscrambler software [110], computation of PCA is based on non-linear iterative partial least square (NIPALS) algorithm. The algorithm extracts one factor at a time. Each factor is obtained iteratively by repeated regressions of X on scores $\hat{t}$ to obtain improved $\hat{p}$ and of X on these $\hat{p}$ to obtain improved $\hat{t}$.

For example, as shown in Figure 5, each sample (°) is explained by two variables, variable 1 and variable 2. The PCs is calculated in such a way that PC 1 explains the most variation in the samples and PC 2 will then carry the most remaining information. Each PC is the linear combination between variable 1 and variable 2. How the variable 1 and variable 2 are weighted in each PC is expressed by loadings. Each sample coordinate referenced to the new axes (PC 1 and PC 2) is call scores. In case of there are many variables e.g. chromatographic data at each retention time and thus many PCs may be calculated, the scores of only first two or three PCs may be used to compare between samples, since the first coming PCs are the most significance.

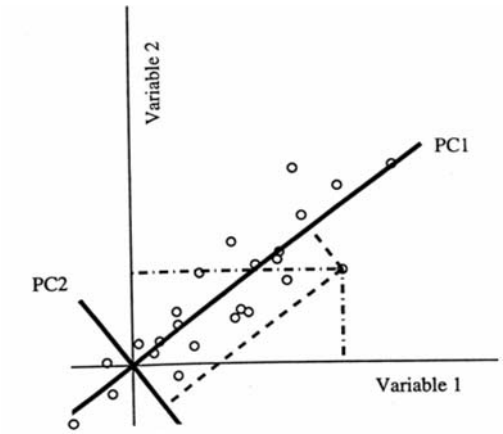

Figure 5 Samples plot (°) referenced to original variable (variable 1 and variable 2) (– · –) and referenced to PCs (PC1 and PC2) (– –) axis
Source: [119]

4.2.2.4 Similarity index and application of bootstrapping

As described above that quality control of herbal medicine by pattern approach consider whole fingerprint as a feature. Thus, the intuitive evaluation method is to compare the similarities or differences between fingerprints' shape. The most commonly used standards for evaluation of similarity of the multivariate systems are correlation coefficient and congruence coefficient [23]. Here only correlation coefficient will be described due to the simplicity and intuitiveness.

During the establishment of standard fingerprint (SF), similarity between a tentative standard fingerprint and a testing fingerprint (TF) was evaluated by the correlation coefficient (c). The correlation coefficient between two chromatograms, x and y; $x = (x_1, \ldots, x_T)'$ and $y = (y_1, \ldots, y_T)'$ can be expressed by

$$c(\mathrm{x},\mathrm{y}) = \frac{\sum_{i=1}^{T}(x_i - \bar{x})(y_i - \bar{y})}{\sqrt{\sum_{i=1}^{T}(x_i - \bar{x})^2}\sqrt{\sum_{i=1}^{T}(y_i - \bar{y})^2}},$$

where x_i and y_i are the absorbance measured at retention time t_i of chromatograms x and y, $\bar{x}$ and $\bar{y}$ are the mean absorbance of chromatograms x and y, and T is the number of retention time.

However, by the use of the statistic $c(w_s, w_m)$; where w_s is SF and w_m is TF, a critical value (c-value) or a lower bound is needed to accept or reject the testing fingerprint. Fang et al [25] employed bootstrap method to estimate the distribution of $c(w_s, w_m)$ and corresponding critical value (c-value).

Let G_0 and G_1 denote the fingerprint group of the standard specimen and an arbitrary fingerprint, respectively. $f_0(\cdot)$ and $f_1(\cdot)$ represent the probability density function (p.d.f.) of G_0 and G_1. Assume that $w_1, \ldots, w_{m-1}$ are fingerprints from G_0 while w_m is from G_1. The hypotheses for fingerprint examination are: $H_0: f_0(\cdot) = f_1(\cdot)$ against $H_1: f_0(\cdot) \neq f_1(\cdot)$. The null hypothesis is accepted or w_m is qualified if $c(w_s, w_m)$ is more than c-value, otherwise unqualified. To determine the c-value, an estimation of the distribution of $c(w_s, w_m)$ under H_0 is necessary. The bootstrap method was used to estimate the distribution of $c(w_s, w_m)$ and the corresponding critical value (c-value) for the given type I error (α error) rate. Let $w_1^1, \ldots, w_m^1$ denote the first bootstrap sample of $w_1, \ldots, w_m$. Treat the sample $w_1^1, \ldots, w_m^1$ to be the replacement of $w_1, \ldots, w_m$. Calculate $c(w_s^1, w_m^1)$ and note it as

c_1, where w_s^1 is the SF calculated from the first bootstrap sample while w_m^1 is the TF from the first bootstrap sample. Recursively, generate B bootstrap samples, then calculate c_1, …, c_B. The distribution obtained by bootstrap method is defined by

$$F_{\mathrm{BOOT}}^{(B)}(x) = \frac{1}{B}\sum_{i=1}^{B} I\{c_i < x\},$$

where $I\{A$ is the indicator function of the set A. Sort c_1, …, c_B as $c_{(1)}$, …, $c_{(B)}$ in ascending order. For a given type I error rate α, the value $c_{([B\alpha])}$ is an estimate of the critical value for testing H_0, where [Bα] is the integer part of Bα.

By determination of correlation coefficient between the standard fingerprint and new testing fingerprint and using critical value as a cut off criteria, fault sample can be detected. The sample will be rejected if the correlation coefficient is less than critical value [25].

4.2.3 Multivariate calibration and prediction

Calibration is the process of constructing a mathematical model to relate the output of an instrument, predictor or X-matrix, to the property of interest, response or Y-matrix. Generally, the predictor(s) is obtained from cheap, easy-to-perform measurements, while the response(s) is obtained from the more expensive or time-consuming one(s) e.g. measurement of UV-Vis spectrum to predict concentration of particular substances. The methods attempting to fit a model to observed data (X and Y) in order to quantify the relationship between them are called in generic term as regression. Univariate regression uses a single predictor, which is often insufficient to precisely model a property of complex system, while multivariate regression uses several predictors simultaneously, thus modeling the property of interest with more accuracy [110,119].

According to Kramer [118], there are 5 steps for developing and applying the model successfully. First, collect the best data you can. Then, construct the model (calibration) and test the obtained model carefully (validation). Next, use the model carefully (prediction). The last, improve the model as necessary. These 5 steps are run in cycle i.e. when it is necessary to improve the model then new data will be collected first and so on the other steps will follow. Here, each step will be described in details [110,118].

The first step, collect the data, is the most time-consuming of the five steps. In this step many factors such as number of samples in the training set and

accuracy of response (Y) values for those samples, number of samples for the validation set (if any) and accuracy of response (Y) values for those samples, and noise level in the X-data must be compromised. Differentiating between acceptable and unacceptable data is the key for development of a good model.

Calibration is the step where the collected data are interpreted. Among the five steps, calibration is the easiest one since it involves moving data into the computers, selecting some options and waiting only few seconds or minute for the results. By computer, the response variable (Y) is calibrated against the independent variables (X) using data of the training samples. Thus, the data of the training set or calibration set, which contain measurement values of both predictors (X) and response (Y) of known samples should contain all expected components and span the Y-ranges of interest. Among all multivariate calibration methods, partial least square (PLS), the most widely applied technique [107], and uninformative variable elimination PLS (UVE-PLS) will be described in details, in the next section.

Usually, a calibration model is made to do predictions in the future. It is desirable to have the models that can work for a broad range of variables. However, this is not usually the case. Validation is the step where the obtained models are checked to discover any weakness or limitations of them i.e. how well they can be applied to explain new samples, before applying them to the real operating. The model, calculated from the data of the training set, will be used to predict the response (Y) of validation samples from their measured predictor data (X). Then the predicted values are compared to the expected values. The error between those values is an indicative of the error that could expect when the calibration model are applied to predict new unknown samples. Two major approaches are applied for validation; test set validation and cross validation. Test set validation is the most objective method because the test samples do not influence the calibration model. However if there are small sample set ($n < 50$), it is not practical to use this method. Cross validation is a more efficient way of utilizing the samples if the sample set is small or moderate [110]. The major advantage of cross validation is that it allows for significance testing which will be described in UVE-PLS section.

Once the model is constructed and properly validated, it can be used to do predictions for new samples. Prediction is the process of using an existing calibration model to predict response values for new samples. The process involves feeding measured predictors values (X) of new samples into a model to obtain computed (predicted) response values (Y) of those unknown samples.

Finally, as long as the model is used, it is necessary to have program of validation. In general, as instrument aged, sample and process change, gradually deterioration in the performance of initial calibration model is usually observed. Regular updating the model can prevent this deterioration. However, if there is a significant change in the application, new model might be made from scratch.

4.2.3.1 Partial least square (PLS)

Partial least square (PLS) or projection to latent structures or PLS-regression (PLSR) is a generalization of multiple linear regression (MLR). Unlike MLR, PLS can be used to analyze data with strongly collinear, noisy and numerous X-variables [120]. Same as described in the PCA, PLS also finds a few new variables called LVs. But instead of using only X-matrix to find the LVs as in the PCA method, the PLS method models both the X- and Y-matrix simultaneously to find those latent variables in X that will best predict the latent variables in Y. In matrix representation, the PLS model with a given number of components is written as:

$$X = TP^T + E ,$$

and $$y = Tq + f ,$$

where X(n, k) represents the predictor matrix, vector y(n, 1) is a response variable, T(n, a) is the score matrix, P^T(a, k) denotes the transposed loading matrix, q (a, 1) is a loading vector, E(n, k) and f(n, 1) are the residuals matrix.

In the Unscrambler [110], the centered data of both X and y are used for computation of PLS factors. For each factor $a = 1,..., A_{max}$, the computation steps are as follows;

(i) by using the variability remaining in y, the loading weights (w_a) are computed using least square (LS) and the local "model"

$$\hat{w}_a = c\, X_{a-1}^T y_{a-1} ,$$

when c is the scaling factor that makes the length of the final $\hat{w}_a$ equal to 1, i.e.

$$c = (y_{a-1}^T X_{a-1}\, X_{a-1}^T y_{a-1})^{-0.5} ;$$

(ii) estimate the scores $\hat{t}_a$ using the local "model"

$$X_{a-1} = t_a \hat{w}_a^t + E ;$$

(iii) estimate the loading (q_a) using the local "model"

$$q_a = y_{a-1}^T \hat{t}_a / \hat{t}_a^T \hat{t}_a ;$$

(iv) create new X and y residuals by subtracting the estimated effect of this factor:

$$\hat{E} = X_{a-1} - \hat{t}_a \hat{p}_a^t ,$$

$$\hat{f} = y_{a-1} - \hat{t}_a \hat{q}_a ,$$

when $$\hat{p}_a = X_{a-1}^T \hat{t}_a / \hat{t}_a^T \hat{t}_a .$$

Replace the former X_{a-1} and y_{a-1} by the new residuals $\hat{E}$ and $\hat{f}$ and increase a by 1 to calculate next factors.

The PLS loadings express how each of the X- and Y-variables is related to the model component summarized by the T-scores. P-loadings express how much each X-variable contributes to a specific model component, and can be used exactly the same way as PCA loadings. Directions determined by the projections of the X-variables are used to interpret the meaning of the location of a projected data point on a T-score plot in terms of variations in X. Q-loadings express the direct relationship between the Y-variables and the T-scores. Thus, the directions determined by the projections of the Y-variables (by means of the Q-loadings) can be used to interpret the meaning of the location of a projected data point on a T-score plot in terms of sample variation in Y. Loading weights (W) are specific to PLS. Variables with large loading weight values are important for the prediction of Y.

4.2.3.2 Uninformative variable elimination PLS (UVE-PLS)

Uninformative variable elimination PLS (UVE-PLS) relies on the principle of the PLS method. The idea of UVE-PLS is to reduce the number of original variable before calculating for LVs by removing original variables that are considered as unimportant. The main steps of UVE-PLS can be summarized as follows [26]:

(i) find the optimal complexity of the PLS model using the cross-validation procedure;

(ii) simulate a matrix R(n, r) with r artificial variables as columns (where $r > 300$), with numbers drawn from a normal distribution and multiplied by a small constant 10^{-10};

(iii) augment the original data X(n, p) with matrix R to form XR(n, $p + r$);

(iv) construct n PLS models for the augmented data matrix with leave-one-out cross-validation, and store n vectors of regression coefficients, b, in a matrix B of a size (n, $p + r$);

(v) for every regression coefficient, define its stability coefficient as the ratio of the column mean and the column standard deviation of B;

(vi) define a cut-off value to distinguish between informative and uninformative variables as the absolute value of the maximal stability of the regression coefficients describing artificial variables;

(vii) remove from the original data matrix X all the variables for which the absolute value of the stability coefficient is below the cut-off value;

(viii) construct a final PLS model for the data containing informative variables only.

In the Unscrambler [110], during cross validation process, a number of sub-models are created and B-coefficients of each sub-model are calculated. For each variable, the difference between the B-coefficient in a sub-model (B_i) and that in the total model (B_{tot}) can be computed. The Unscrambler takes the sum of the squares of the differences in all sub-models to get an expression of the variance of the B_i estimate for a variable. With a t-test the significance of the estimate of B_i is calculated. Under ideal conditions, the resulting regression coefficients can be presented with uncertainty limits that correspond to 2 standard deviations (SD). Variables with uncertainty limits that do not cross the zero line are significant variables. Usually, when X-variables with no significant contribution to the prediction of Y are removed before construction a new model, the new model will fit as well as the original and validate better.

4.3 Conclusions

Chemometrics is a chemical discipline that applies mathematics, statistics, and formal logics to obtain most relevant chemical information from large recorded data. Nowadays, chemomerics is widely applied to the fields of food, pharmaceutical product, industrial processing and medical study. In the quality control of herbal medicine which is considered as a study of complex system, chemometrics is helpful in several steps. Some chemometrics tools commonly applied to the quality control of herbal medicine including the design of experiment, the alignment of chromatographic data, the reduction of data dimension

by PCA, the comparison between two fingerprints by using similarity index as well as the multivariate calibration by PLS and UVE-PLS method have been described in this chapter.

CHAPTER III
MATERIALS AND METHODS

1 Plant materials

Thirty-five samples of roselle from different locations throughout Thailand were purchased from local markets in the years 2003 and 2004, and identified by Asssociate Prof. Dr. Uthai Sotanaphun. The voucher specimens (US-03 001 to US-03 022 and US-04 001 to US-04 013) are deposited at the Herbarium of the Department of Pharmacognosy, Silpakorn University, Thailand.

Most of samples were received as dried raw material, while other eight fresh samples, i.e. the sample number 4, 5, 6, 8, 10, 13, 14 and 15, were dried by hot air oven (Heraeus UT5050E; Kleinostheim, Germany) at temperature between 45 to 55 °C. Foreign matter was removed and quantified according to the method described in 3.1. Then, the samples were cut into small particle with cutting mill (RetschGmbH SK1; Haan, Germany) and sieved. Finally, roselle powder which size less than 250 µm was kept in screw cap glass bottles, protected from light and placed in desiccators at 4°C, before use.

2 Preparation of standard anthocyanins

2.1 Isolation of standard anthocyanins

Fresh calyx of roselle (3.03 kg) was blended with hot water (2,000 ml). The extract was centrifuged at 7,000 rpm for 30 minutes (Kubota centrifuge model 6500; Tokyo, Japan). The clear red supernatant was subjected to an Amberlite XAD-16 resin (180 g) (Fluka; Buchs, SG, Schweiz) and washed with an excessive amount of water until the water was clear and had no taste. The adsorbed material was eluted from the resin by 0.1% hydrochloric acid in methanol until the eluent was colorless. The eluate was combined, dried under reduced pressure at 40°C (Rotarvapor Büchi R-134; Flawil, Switzerland) and redissolved in a small amount of 0.1% hydrochloric acid in methanol. After keeping at 4°C in a dark place, for 2 days, a red precipitate (407.7 mg) was collected. The precipitate was further purified by a Sephadex® LH-20 (Sigma; MO, USA) column (Ø 2.7 x 62 cm) eluted with ethanol. The elution fractions were collected depending on the color observation and monitored by the TLC method described in 4.2. Two pure anthocyanins, compound I (57.9 mg) and compound II (12.6 mg), were obtained (Scheme 1).

Both compound I and compound II were used as TLC marker in the study of TLC fingerprint. However, compound II had been isolated in a very low amount (12.6 mg); consequently it could not be considered as a practical standard. Therefore only compound I was further used in the validation of HPLC fingerprint (see section 4.3.5.1) and the development of method for analysis of total anthocyanins (see section 5.1).

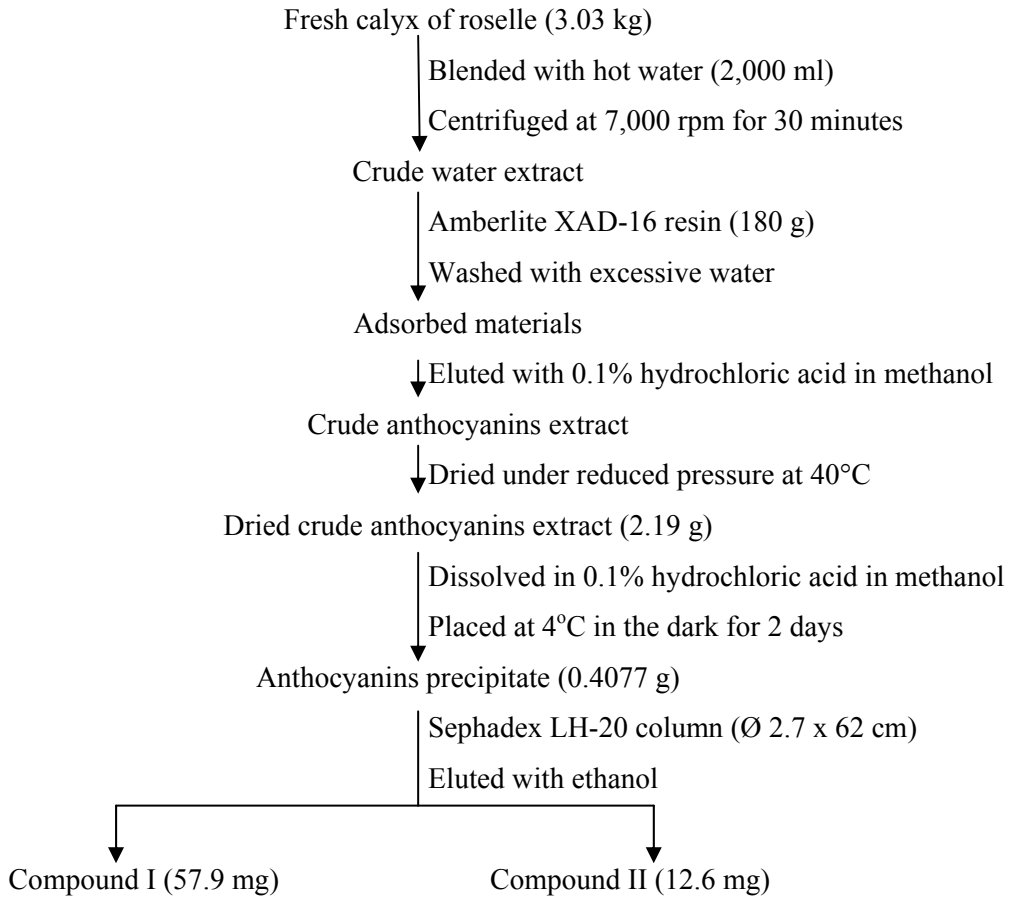

Scheme 1 Isolation of standard anthocyanins

2.2 Identification of the isolated compounds

Identification of the isolated compounds was performed by comparing their ^{1}H NMR data (300 MHz) (Bruker 300 Ultrashield; Karlsruhe, Germany) with the previously reported data of delphinidin-3-sambubioside and cyanidin-3-sambubioside, [121].

2.3 Purity assay of the isolated compounds

As described above, isolated in a very few amount, compound II could not be considered as a practical standard. Therefore only compound I was assayed for its purity. The HPLC method modified from de Ancos [96] was used. Compound I (2.40 mg) was dissolved in the mixture of 4% phosphoric acid and 100% acetonitrile (94: 6) (1.8 ml) and filtered through Puradisc™ syringe membrane filter (nylon, pore size 0.45 μm) (Whatman; Middlesex, England) before injected. The purity was calculated as the mean from six injections. The chromatographic condition was as follows.

HPLC system:	Agilent 1100 series pump, a solvent degasser, an auto sampler, a photodiode-array detector (DAD), and a Chemstation for LC software A10.02 (Agilent; CA, USA)
Column:	Bondclone C18 (300 x 3.9 mm, 10μm particle size) (Phenomenex; CA, USA)
Guard column:	ODS guard column (3.0 x 4 mm) (Phenomenex; CA, USA)
Mobile phase:	(A) 4% phosphoric acid (B) 100% acetonitrile
Program:	0-10 min isocratic elution with 6% (B) 10-55 min linear gradient to 20% (B) 56-60 min isocratic elution with 6% (B)
Flow rate:	1 ml/min
Temperature:	room temperature
Detection:	254 nm
Injection:	5 μl

3 General quality control methods

Analytical grade chemicals and distilled water were used in all experiments of general quality control methods.

3.1 Foreign matter [29]

Dried whole calyx (100 g) was spread in a thin layer. Foreign matter was detected by inspecting with the unaided eye and with the use of a 6x lens, and separated.

The percentage of foreign matter was calculated with reference to the original air-dried substance.

3.2 **Loss on drying** [29]

Roselle powder was thoroughly mixed. The accurately weighed powder (2 g) was sampling to a tarred glass-stoppered, shallow weighing bottle that has been dried for 30 minutes at 105^{o}C. After replacing the stopper, all contents and bottle were weighed. The bottle was gently sidewise shaken to make the test specimen distributed as evenly as practicable to a dept of about 5 mm generally, and not over 10 mm. The loaded bottle was dried in the drying oven (Heraeus UT5050E; Kleinostheim, Germany), previously set the temperature at 105^{o}C. The stopper was removed and left also in the oven. Upon opening the oven chamber, the bottle was closed promptly and allowed to come to room temperature in desiccators before weighing. The test specimen was dried until the difference between two consecutive weights is not more than 0.0010 g. If the difference is more than 0.0010 g, the specimen was dried for another 1 hour. The percentage of loss weight was calculated with reference to the air-dried substance.

3.3 **Total ash** [29]

Total ash was analyzed by Scientific and Technological Equipment Centre, Silpakorn University, Nakorn Pathom, Thailand.

Generally, roselle powder (2 to 4 g) was accurately weighed to a suitable tarred crucible (usually of platinum or silica), previously ignited by furnace (Carbolite CSF 1100; Derbyshire, UK), cooled and weighed. The sample was incinerated by gradually increasing the temperature, not exceeding 450^{o}C, until free from carbon. Then it was allowed to room temperature and weighed.

If a carbon-free ash cannot be obtained in this way, the crucible was cooled and the residue was moistened with about 2 ml of water or a saturated solution of ammonium nitrate. Then, it was firstly dried on a water-bath and on a hot plate and finally incinerated to constant weight. The percentage of total ash was calculated with reference to the air-dried substance.

3.4 **Acid insoluble ash** [29]

Acid insoluble ash was analyzed by Scientific and Technological Equipment Centre, Silpakorn University, Nakorn Pathom, Thailand.

The total ash obtained from the method described in 3.3 was boiled for 5 minutes with 25 ml of dilute hydrochloric acid. The insoluble matter was collected on an ashless filter paper, washed with hot water until the filtrate was neutral, and ignited at about 500^{o}C (Carbolite CSF 1100; Derbyshire, UK). The percentage of acid-insoluble ash was calculated with reference to the air-dried substance.

3.5 **Water-soluble extractive** [29]

Roselle powder (5 g), accurately weighed, was macerated with 100.0 ml of distilled water in a closed flask for 24 hours, shaken frequently during the first 6 hours and then allowed to stand for 18 hours. The filtrate (20.0 ml) was evaporated to dryness in a tarred, flat-bottomed, shallow dish and it was further dried at 105^{o}C (Heraeus UT5050E; Kleinostheim, Germany) to constant weight. The percentage of water-soluble extractive was calculated with reference to the air-dried substance.

3.6 **Ethanol-soluble extractive** [29]

The method described in 3.5 was used, but the solvent was changed to absolute ethanol (Carlo Erba; Milano, Italy). Precaution against loss of ethanol during filtering was aware.

3.7 **Data analysis**

Overall general quality control parameters were calculated as mean $\pm$ SD. Analytical data that considered as outliers and extremes of each parameter by boxplot were excluded before calculation of mean and SD.

A boxplot is a kind of graph showing the distribution of the data (Figure 6). The upper and lower edges of the box represent the third (Q_3) and the first quartile (Q_1), respectively. And a line located across this box shows the second quartile (Q_2) or the median value. The box length or the interquartile range (IQR) is the range between Q_3 and Q_1. The upper and lower bars show the maximum and minimum limits of values that justified as normal values. These bars are calculated from $Q_3 + 1.5(IQR)$ and $Q_1 - 1.5(IQR)$, respectively. Cases with values between 1.5 and 3 box lengths from the upper or lower edge of the box are outliers. And cases with values more than 3 box lengths from the upper edge or less than 3 box lengths from the lower edge of the box are extremes.

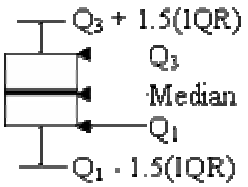

Figure 6 Boxplot of data: Q_1 = the first quartile, Q_2 = the second quartile or the median, $Q_3$the third quartile, IQR = the interquartile range

4 Qualitative control methods

Analytical grade chemicals and distilled water were used in all qualitative control methods.

4.1 Chemical identification

4.1.1 Sample solution and test solution preparation

The sample extract was prepared by macerating roselle powder (300 mg) with water (8 ml) for 15 minutes and filtering (Solution A).

The beet root extract was prepared by macerating fresh beet root (10.2 g) with water (10 ml) for 30 minutes and filtering. The obtained extract (0.5 ml) was diluted with water (9.5 ml) to make the final solution (Solution B).

All other synthetic red dyes solution namely Ponceau 4R, Carmoisine, Amaranth and Erythrosine prepared in water as a solution of 1% w/v (0.5 ml) was diluted with water (9.5 ml) to make the final solution (Solution C).

4.1.2 Procedures

4.1.2.1 **Test A** [87,122]

The solution A, B and C (0.2 ml) was separately added with 2 M hydrochloric acid (0.2 ml) and heated at 100^{o}C for 5 minutes. The red color of solution A should be stable. If the red color vanishes, it may be betacyanin response.

4.1.2.2 **Test B** [87,122]

The solution A, B and C (0.2 ml) was separately added with 2 M sodium hydroxide dropwise. The red color of solution A should change to blue-green and slowly fade. If the color changes to yellow, it may be betacyanins response.

4.1.2.3 Test C

The solution A, B and C (0.2 ml) was separately added with 2 M sodium hydroxide dropwise. The red color of solution A should change to blue-green and the color should be reversed if 2 M hydrochloric acid was added dropwise, immediately.

4.1.2.4 Test D [87]

The solution A, B and C (0.2 ml) was separately added with aluminium chloride test solution (4 drops). The red color of solution A should shift to violet or the spectra should display a bathochromic change and the color should be reversed if 2 M hydrochloric acid was added.

4.1.2.5 Test E

The solution A, B and C (0.2 ml) was separately added with lead acetate test solution (4 drops). In solution A, blue precipitate and clear supernatant should be obtained.

4.1.2.6 Test F [122]

The solution A, B and C (0.2 ml) was separately added with ferric chloride test solution (4 drops). The red color of solution A should change to dark green.

4.2 Thin-layer chromatography (TLC) fingerprint

The TLC method was modified from European Pharmacopoeia 2001 [28]. Analytical grade chemicals and distilled water were used in all experiments of TLC. Ethyl acetate (Ajax Finechem; Mt. Wellington, New Zealand), 2-propanol (Merck; Darmstadt, Germany) and formic acid (Carlo Erba; Milano, Italy) were used.

4.2.1 Sample solution and standard solution preparation

The sample solution was prepared by macerating roselle powder (1 g) with 0.1% conc. hydrochloric acid in methanol (10 ml), shaking frequently for 15 minutes and filtering.

The standard cyanidin-3-sambubioside (Cy-3-sam) solution (A) was prepared by dissolving Cy-3-sam (0.9 mg), isolated in laboratory in 0.1% conc. hydrochloric acid in methanol (3 ml).

The standard delphinidin-3-sambubioside (Dp-3-sam) solution (B) was prepared by dissolving Dp-3-sam (1.8 mg), isolated in laboratory in 0.1% conc. hydrochloric acid in methanol (10 ml).

The standard quinaldine red solution (C) was prepared by dissolving quinaldine red (Merck; Darmstadt, Germany) (2.5 mg) in 0.1% conc. hydrochloric acid in methanol (10 ml).

4.2.2 Procedures

The chromatographic condition is as follows,

Technique:	one way, ascending, single development
Adsorbent:	silica gel 60 F_{254}, precoated on aluminium sheet (Merck; Darmstadt, Germany)
Mobile phase:	ethyl acetate: 2-propanol: water: formic acid (6 : 2 : 2 : 1 v/v/v/v)
Development:	over a path of 10 cm
Temperature:	25-30 ^{o}C
Application:	20 µl, as bands
Drying:	in air
Detection:	a) daylight b) spraying with dilute sulfuric acid and heating at 100^{o}C, examined under daylight

4.3 High performance liquid chromatography (HPLC) fingerprint

Acetonitrile (HPLC grade) (Carlo Erba; Milano, Italy), phosphoric acid (AR) (BDH; Poole, UK), methanol (AR) (Ajax Finechem; Mt. Wellington, New Zealand) and Nanopure® water 18.3 mΩ were used in all experiments of HPLC.

4.3.1 Sample preparation

The sample solution was prepared by macerating roselle powder (2 g) with 50% methanol (10 ml) and sonicating for 15 minutes in ultrasonic bath (Elma® transsonic 890/H; Singen, Germany). The extract was filtered through Puradisc™ syringe membrane filter (nylon, pore size 0.45 µm) (Whatman; Middlesex, England) before injected.

4.3.2 Optimization of HPLC condition

The HPLC condition for constructing the fingerprint of roselle was modified from de Ancos [96]. The experiments were carried on HPLC system consisted of Agilent 1100 series pump, a solvent degasser, an auto sampler, a photodiode-array detector (DAD) and a Chemstation for LC software version A10.02 (Agilent; CA, USA). Two solvents, 4% phosphoric acid (*A*) and 100% acetonitrile (*B*) were programmed as two steps; step I: an isocratic elution at 6% (*B*) and step II: a linear gradient elution to 20% (*B*). To optimize the solvent program, a full factorial experimental design was applied. It involved two factors;

(i) the duration used for an isocratic elution and

(ii) the duration used for a linear gradient elution.

The chromatograms of each experiment were recorded at five wavelengths i.e. 254, 280, 316, 365 and 520 nm. The factors and corresponding levels were shown in Table 6. The information (ϕ) obtained from each chromatogram was calculated by following formula,

$$\phi = -\sum\left(\frac{x_i}{\sum x_i}\log\left(\frac{x_i}{\sum x_i}\right)\right),$$

where x_i and $\sum x_i$ is the real chromatographic response of the chemical components involved in the chromatogram under study and its summation, respectively [23]. The program that gives the maximum information was used for constructing the fingerprint of roselle.

Table 6 Factors and levels for optimization of the solvent program of HPLC

Factors	**Levels**		
	1	2	3
i: duration used for an isocratic elution (min)	15	20	25
ii: duration used for a gradient elution (min)	40	45	50

4.3.3 Procedures

Based on the data from the HPLC optimization, the HPLC chromatograms of roselle were obtained by the followings.

HPLC system:	Agilent 1100 series pump, a solvent degasser, an auto sampler, a photodiode-array detector (DAD) and a Chemstation for LC software A10.02 (Agilent; CA, USA)
Column:	Bondclone C18 (300 x 3.9 mm, 10µm particle size) (Phenomenex; CA, USA)
Guard column:	ODS guard column (3.0 x 4 mm) (Phenomenex; CA, USA)
Mobile phase:	(A) 4% phosphoric acid (B) 100% acetonitrile
Program:	0-20 min isocratic elution with 6% (B) 20-70 min linear gradient to 20% (B) 71 minlinear gradient to 6% (B)
Flow rate:	1 ml/min
Temperature:	room temperature
Detection:	254 nm
Injection:	5 µl

4.3.4 Data analysis

The chromatograms were corrected for their retention time shift by Spec Align program [116]. Natural clustering of samples was surveyed by principal component analysis (PCA) using the Unscrambler version 9.5 software program [110]. Outlier samples were detected by the bootstrapping method using Resampling Stats for Excel version W3.20 [123].

During the establishment of standard fingerprint (SF), similarity between a tentative standard fingerprint and a testing fingerprint (TF) was evaluated by the correlation coefficient (*c*). The bootstrap method was used to estimate the distribution of the correlation coefficient and the corresponding critical value (*c*-value). This critical value (*c*-value) or the lower bound value of correlation coefficient was used as a criterion to accept or reject the testing fingerprint. If the correlation coefficient between the tentative standard fingerprint and the testing fingerprint is less than critical value, that testing fingerprint would

be classified as an outlier (see the details of method in Chapter I, section 4.2.2.4). After all outliers were eliminated, the HPLC fingerprint was calculated from the remained data by Excel 2003. The median data at each retention time were the HPLC fingerprint of roselle.

4.3.5 Validation of HPLC fingerprint of *H. sabdariffa*

4.3.5.1 Identification of chromatographic peaks

The identification of the peaks was carried out using the delphinidin-3-sambubioside isolated in our laboratory.

4.3.5.2 Injection precision

The injection precision was determined by replicate injection of the same sample solution for six times in a day. The relative standard deviation (%RSD) of retention time and peak area of delphinidin-3-sambubioside were calculated.

4.4 Ultraviolet-visible (UV-Vis) fingerprint

4.4.1 Sample preparation

The sample extract was prepared by macerating roselle powder (1 g) with 50% methanol (5 ml) and sonicating for 15 minutes in ultrasonic bath (Elma® transsonic 890/H; Singen, Germany). The extract (0.2 ml) was diluted with 50% methanol (0.8 ml). The obtained solution (0.3 ml) was further diluted with 50% methanol (4.9 ml) to make the final solution.

4.4.2 Procedures

The final solution was scanned for its UV-Vis absorption spectrum in the wavelength of 190 to 1100 nm (UV-Vis spectrophotometer Agilent 8453 model G 11C3A; CA, USA), using 50% methanol as the blank.

4.4.3 Data analysis

The UV-Vis spectrum in the region of 250 to 650 nm was surveyed by principal component analysis (PCA) using the Unscrambler version 9.5 software program [110]. Outlier samples were detected by the bootstrapping method using Resampling Stats for Excel version W3.20 [123]. The UV-Vis fingerprint was the median data at each wavelength calculated by Excel 2003.

4.5 Infrared (IR) fingerprint

4.5.1 Procedures

Roselle powder which size less than 250 μm was grinded with potassium bromide (KBr) powder and filled in microcup DRIFT accessory. The IR spectrum was recorded in Kubelka-Munk (KM) unit between 4000 and 400 cm^{-1} using an IR spectrophotometer (Magna-IR™ spectrometer 750; Nicolet) equipped with a KBr beamsplitter and a deuterated triglycine sulfate (DTGS) detector. The resolution was set at 4 cm^{-1} and the number of scans per sample was 32. Background spectra of pure KBr were recorded before analysis of samples.

4.5.2 Data analysis

Spectrum was baseline corrected before analysis. Principal component analysis (PCA) was performed using the Unscrambler version 9.5 software program [110].

5 Quantitative control analysis

5.1 Development of method for analysis of total anthocyanins in *H. sabdariffa*

5.1.1 HPLC for analysis of total anthocyanins in *H. sabdariffa*

5.1.1.1 Sample preparation

Dried roselle powder (100 mg) was macerated with 0.1% hydrochloric acid in 75% methanol (10 ml) at room temperature in a dark place for 24 hours, and then filtered through Puradisc™ syringe membrane filter (nylon, pore size 0.45 μm) (Whatman; Middlesex, England) before injected.

5.1.1.2 Standard solution preparation and calibration curve

The standard delphinidin-3-sambubioside was prepared in 0.1% hydrochloric acid in 75% methanol in the concentration range of 24.97 - 299.62 μg/ml, and filtered through Puradisc™ syringe membrane filter (nylon, pore size 0.45 μm) (Whatman; Middlesex, England) before injected.

The calibration curve was plotted between the concentrations of delphinidin-3-sambubioside and the correspondence area under curve (AUC).

5.1.1.3 Procedures

The HPLC method modified from de Ancos [96] was used with some verification. The chromatographic condition is as follows.

HPLC system:	Agilent 1100 series pump, a solvent degasser, an auto sampler, a photodiode-array detector (DAD), and a Chemstation for LC software A10.02 (Agilent; CA, USA)
Column:	Bondclone C18 (300 x 3.9 mm, 10µm particle size) (Phenomenex; CA, USA)
Guard column:	ODS guard column (3.0 x 4 mm) (Phenomenex; CA, USA)
Mobile phase:	(A) 4% phosphoric acid (B) 100% acetonitrile
Program:	0-10 min isocratic elution with 6% (B) 10-55 min linear gradient to 20% (B) 56-60 min isocratic elution with 20% (B)
Flow rate:	1 ml/min
Temperature:	room temperature
Detection:	520 nm
Injection:	10 µl

By reference to the calibration curve of delphinidin-3-sambubioside, total anthocyanin content in the sample was calculated as percentage of delphinidin-3-sambubioside based on the dried weight.

5.1.2 pH-differential spectrophotometry

5.1.2.1 Condition for extraction of anthocyanins

In order to find the most suitable solvent for extraction of anthocyanins from dried calyx of roselle, preliminary study was performed with aqueous-methanolic solvents (0 to 100% methanol), and acidic aqueous-methanolic solvents (0.1% hydrochloric acid in 50 to 100% methanol). Roselle powder (50 mg) was macerated with 5 ml of each solvent, at room temperature, in a dark place for 24 hours and filtered. The extract was analyzed by the method described in 5.1.2.3. The higher of calculated absorbance value indicated that the more amounts of anthocyanins were extracted. The solvent that gave the highest calculated absorbance value was selected for the further examination, the determination of appropriate herb to solvent ratio. Various herb to solvent ratios (1:50, 1:100,

1:150, 1:200, 1:250 and 1:300) were investigated. The calculated absorbance value was transformed to extractive content of total anthocyanins, based on the calibration curve of standard anthocyanin. The maximum herb to solvent ratios can be detected by gradually increasing herb to solvent ratio until additional solvent had no or less effect on the percent extractive content.

5.1.2.2 Standard solution preparation and calibration curve

The standard anthocyanin, delphinidin-3-sambubioside, was prepared in the concentration range of 12 - 93 μg/ml in 0.1% hydrochloric acid in 75% methanol. The standard series, at each concentration, were examined as described in 5.1.2.3. The calibration curve was plotted between the final concentrations of the standard anthocyanin and the correspondence calculated absorbance values.

5.1.2.3 Procedures [101]

Two portions of the extract (0.5 ml) were taken for analysis. The first portion was mixed with buffer pH 1.0 (2.5 ml) and the other was mixed with buffer pH 4.5 (2.5 ml). After 15 minutes but not over 60 minutes, absorbance at 520 nm (A_{520}) and at 700 nm (A_{700}) (Hitachi U-2000 spectrophotometer; Tokyo, Japan) of each extract was measured against a blank cell filled with distilled water. The absorbance of the sample extract (A) was calculated as follows,

$$A = (A_{520} - A_{700})_{\text{pH 1.0}} - (A_{520} - A_{700})_{\text{pH 4.5.}}$$

5.1.2.4 Sample analysis

Based on the data obtained from the condition for extraction of anthocyanins (section 5.1.2.1), dried roselle powder (160 mg) was macerated with 25 ml of 0.1% hydrochloric acid in 75% methanol at room temperature, in a dark place for 24 hours and filtered.

The extract was analyzed by the method described in 5.1.2.3. By reference to the standard anthocyanin calibration curve, the content of total anthocyanins in the sample was calculated as percentage of delphinidin-3-sambubioside based on the dried weight.

5.1.3 Modified pH-differential spectrophotometry

5.1.3.1 Determination of a correlation factor between delphinidin-3-sambubioside and methyl orange

The standard delphinidin-3-sambubioside and the standard methyl orange (Merck;Darmstadt, Germany) were prepared in 0.1% hydrochloric acid in 75% methanol in the concentration range of 12 - 93 μg/ml and 6 - 46 μg/ml, respectively. Both series dilutions were analyzed for calculated absorbance values by the method described in 5.1.2.3. Then a relative concentration or a correlation factor between them that possessed a same absorbance value was calculated from their calibration curves.

5.1.3.2 Procedures

In routine work, the modified pH-differential spectrophotometry method was performed by using methyl orange as a standard. The series dilution of methyl orange prepared in the concentration range of 6 - 46 μg/ml were analyzed for calculated absorbance values by the method described in 5.1.2.3. Then the concentration of methyl orange was transformed to the concentration of delphinidin-3-sambubioside by their correlation factor, previously calculated in 5.1.3.1, and a calibration curve of delphinidin-3-sambubioside was constructed. The sample extract was analyzed by the same method as that of methyl orange. By reference to the simulated calibration curve of delphinidin-3-sambubioside, the content of total anthocyanins in the sample was calculated as percentage of delphinidin-3-sambubioside based on the dried weight.

5.1.4 Validation of modified pH-differential spectrophotometry [124]

5.1.4.1 Linearity

Linearity of the standard anthocyanin and standard methyl orange was determined over a 3-days period. The slope and other statistical parameters of the calibration curves were calculated by linear regression.

5.1.4.2 Repeatability and intermediate precision

Repeatability was evaluated in 3 determinations on the same day for 3 samples, while the intermediate precision was assessed for 3 consecutive days. The data were expressed as the relative standard deviation (%RSD)

5.1.4.3 Limit of detection (LOD) and limit of quantitation (LOQ)

Limit of detection (LOD) and limit of quantitation (LOQ) were calculated based on the standard deviation of y-intercept (δ) and the slope (s) of the calibration curve by using the formulae 3.3 δ/s and 10 δ/s, respectively.

5.1.4.4 Accuracy

Total anthocyanin contents determined by the modified pH-differential spectrophotometry were compared with those of the HPLC method. Paired t-test was used for analysing of significance of difference.

5.2 Analysis of total phenolic compounds

5.2.1 Condition for extraction of total phenolic compounds

In order to find the most suitable solvent for extraction of phenolic compounds from roselle, preliminary study was performed with aqueous-methanolic solvents (0-100% methanol), and acidic aqueous-methanolic solvents (0.1% hydrochloric in 50-100% methanol). Dried roselle powder (100 mg) was macerated with 10 ml of each solvent at room temperature for 24 hours and filtered.

The extract was analyzed by the method described in 5.2.3. The absorbance values of extracts prepared from each solvent were compared. The higher of absorbance value indicated that the more amounts of phenolic compounds were extracted. The solvent that gave the highest absorbance value was selected for the further examination. To determine the appropriate herb to solvent ratio, various herb to solvent ratios (1:50, 1:100, 1:150, 1:200, 1:250 and 1:300) were investigated. Then the absorbance values of each extract were transformed to extractive contents of total phenolics, based on the calibration curve of standard gallic acid. The maximum herb to solvent ratio could be detected by increasing herb to solvent ratio until addition solvent had no effect on the extractive content.

5.2.2 Standard solution preparation and calibration curve

Standard gallic acid (Fluka; Buchs, SG, Schweiz) and standard protocatechuic acid (Fluka; Buchs, SG, Schweiz) were prepared in 50% methanol at the concentration range of 40 - 255 µg/ml and 45 - 180 µg/ml, respectively. The series dilutions of both were analyzed by the method described in 5.2.3.

A standard calibration curve of each standard was plotted between the final concentrations and the correspondence absorbance values.

5.2.3 **Procedures** [125]

Sample extract (0.2 ml) was mixed with distilled water (3.55 ml) and Folin-Ciocalteau's reagent (0.25 ml) (Fluka; Buchs, SG, Schweiz). After 1 minute and before 8 minutes, 20% sodium carbonate solution (1 ml) was added, mixed and the time was adjusted to zero. After 90 minutes, the absorbance of the reactant was recorded at 750 nm (Hitachi U-2000 spectrophotometer; Tokyo, Japan) against a blank cell filled with the same reactant, without sample.

5.2.4 **Sample analysis**

Based on the data obtained from the condition for extraction of total phenolic compound, dried roselle powder (160 mg) was macerated with 50% methanol (25 ml) at room temperature for 24 hours and filtered.

The sample extract was analyzed by the method described in 5.2.3. By reference to the calibration curve of gallic acid and the calibration curve of protocatechuic acid, the content of total phenolic compounds in roselle was calculated as percentage of gallic acid (gallic acid equivalence, GAE) and percentage of protocatechuic acid, based on the dried weight, respectively.

5.2.5 **Method validation** [124]

Linearity, repeatability, intermediate precision, limit of detection (LOD) and limit of quantitation (LOQ) were determined by the method described in 5.1.4.

5.3 **Analysis of total acid content**

Total acid content was determined by titration method modified from European Pharmacopoeia 4.4 [28]. The dried roselle powder (1.0000 g) was added with carbon dioxide free water (100.0 ml) and stirred for 15 minutes. After filtered, the filtrate (50.0 ml) was added with carbon dioxide free water (100.0 ml). The solution was titrated with 0.1 M sodium hydroxide until pH 7.0, and, determined the end-point potentiometrically. The percentage of acid content was expressed as citric acid ($C_6H_8O_7$) with reference to the dried weight.

Each ml of 0.1 M sodium hydroxide is equivalent to 6.4 mg of citric acid.

5.4 Analysis of potassium content [126]

The potassium content was analyzed by Scientific and Technological Equipment Centre, Silpakorn University, Nakhon Pathom, Thailand.

A sufficient amount of total ash obtained from the determination of total ash (described in 3.3) was digested with 6 M hydrochloric acid. Then, the potassium content in the acid solution was measured by Inductively Coupled Plasma Emission Spectrophotometer (Varian Liberty 220; Australia) using potassium oxide, K_2O RS as standard. The percentage of potassium content was calculated with reference to the dried weight.

6 Radical scavenging activity

6.1 Determination of radical scavenging activity

6.1.1 Standard solution preparation and calibration curve

Ascorbic acid was prepared in 50% methanol at the concentration range of 3.98 - 19.91 μg/ml. The standard series, at each concentration, were analyzed by the method described in 6.1.2.

The calibration curve was plotted between the final concentrations of ascorbic acid and the correspondence percentage of radical scavenging activity.

6.1.2 Procedures

The radical scavenging activity was determined by the DPPH method [127] with some modification. The reaction in 50% methanol was consisted of 2,2-diphenyl-1-picryl-hydrazyl (DPPH) (Fluka; Buchs, SG, Schweiz) solution (0.4 ml) in the last concentration of 78 μM or 0.0031% w/v and test solution (0.4 ml). After 90 minutes of the reaction, the absorbance at 520 nm was measured (Hitachi U-2000 spectrophotometer; Tokyo, Japan). The radical scavenging activity was calculated as follows,

$$\% \text{ radical scavenging activity} = [(A_{control} - A_{sample})/ A_{control}\ ] \times 100$$

when $A_{control}$ is the absorbance of DPPH in 50% methanolic solution without test solution, and A_{sample} is absorbance of DPPH in 50% methanolic solution in the presence of the test solution.

6.1.3 Sample analysis

Roselle powder (100 mg) was macerated with 50% methanol (50 ml) in a dark place for 24 hours and filtered. The extract (0.5 ml) was further diluted with 50% methanol (3 ml) to give test solution. The solution was analyzed as that described in 6.1.2. By comparing the activity of test solution with that of ascorbic acid solution, the radical scavenging activity of sample was calculated as percentage of ascorbic acid equivalence antioxidant capacity (AEAC) reference to the air-dried substance.

6.2 Prediction of radical scavenging activity

6.2.1 Source of data

The radical scavenging activity data, analyzed by the DPPH method, of 35 roselle samples were obtained by the method describe in section 6.1. The data of HPLC chromatogram and UV-Vis spectrum of each sample were obtained by the method described in the section 4.3 and 4.4, respectively. The samples were randomly divided into a calibration set (about 60% of samples) for building a model, and a prediction set (about 40% of samples) for validating a model. For ensuring that the calibration samples span the range of radical scavenging activity, the samples which possess the minimum and the maximum value of radical scavenging activity were manually selected to the calibration set.

6.2.2 Data preprocessing

The HPLC chromatograms were corrected for their retention time shift by Spec Align program [116]. No pre-treatments were applied to the UV-Vis spectrum data because of no sign of baseline shift.

6.2.3 Data analysis

The chemometric analysis was performed using the Unscrambler version 9.5 software program [110]. The corrected HPLC chromatograms and the UV-Vis spectrum in the region of 250 to 650 nm were surveyed by principal component analysis (PCA) before model construction.

Multivariate calibration models relating the HPLC chromatograms and UV-Vis spectral data with the radical scavenging activity data were developed from the calibration set using partial least square regression (PLS1). In calibration process, all samples of the calibration set were used to construct the model. Root mean squared error of calibration (RMSEC) was calculated as follows,

$$\text{RMSEC} = \sqrt{\frac{\sum_1^N (\hat{y}_{cal} - y_{ref})^2}{N}}$$

when $\hat{y}_{cal}$ is the fitted value of radical scavenging activity on the model, y_{ref} is the measured value of radical scavenging activity, and N is the number of calibration sample.

The optimum number of PLS factor was determined by leave one out cross validation (LOOCV) using the minimum residual variance. The model was validated by two methods i.e. leave one out cross validation (LOOCV) and prediction set or test set validation.

The LOOCV used the same set of data to calibrate and validate the model. In validation process, one sample was left out from the calibration set and the model was constructed from the remaining data points. Then, the value of the left-out samples was predicted and the prediction residuals were computed as root mean squared error of cross validation (RMSECV). The RMSECV was calculated as follows,

$$\text{RMSECV} = \sqrt{\frac{\sum_1^N (\hat{y}_{LOOCV} - y_{ref})^2}{N}}$$

when $\hat{y}_{LOOCV}$ is the predicted value of radical scavenging activity of the submodel, y_{ref} is the measured value of radical scavenging activity, and N is the number of calibration sample.

The prediction set or test set validation used an external test set in the validation process. The values of the prediction set or test set were predicted and the prediction residuals were computed as root mean squared error of prediction (RMSEP). The method used to calculate of RMSEP was the same as described in RMSECV, but the external test samples were used. The predicted values and the measured values of the test set were also compared. And paired t-test was used for analyze of significance of difference between them.

Robustness comparison between models was done by using the RMSEP value. The distribution of the RMSEP values of each model was simulated by using bootstrap technique. The corresponding 95% confidence intervals were used for robustness comparison between models.

7 Overall chemical quality of *H. sabdariffa* in Thailand

Overall results of quantitative anaysis, i.e. total anthocyanins content, total phenolic compound, total acid content and potassium content, as well as the radical

scavenging activity of roselle samples cultivated in Thailand were summarized as mean $\pm$ SD. Analytical data that considered as outliers and extremes of each parameter by boxplot were excluded before calculation.

CHAPTER IV
RESULTS AND DISCUSSIONS

1 Plant materials

The fresh roselle samples (n = 8), after separating from the seed pods, were dried. The drying ratio, the ratio between fresh weight to dry weight, was 8.51 calculated as the median of 8 fresh samples.

All samples (n = 35) were divided into 3 groups namely the reddish group (n = 17), the brownish group (n = 16) and the small calyx group (n =2), according to their characteristics (Table 7). The reddish sample was classed as a higher grade material while the brownish sample was a lower grade one which is often found after inefficient drying and storage under inappropriate condition [128,129,130]. The small calyx sample was a rarely found, distinctive one and not generally used for consuming. The sources and the details of the samples were listed in Table 7.

2 Preparation of standard anthocyanins

2.1 Isolation of delphinidin-3-sambubioside (Dp-3-sam)

Compound I (delphinidin-3-sambubioside, 0.0579 g), the major anthocyanin of roselle and Compound II (cyanidin-3-sambubioside, 0.0126 g) were isolated from aqueous extract of fresh roselle. The procedure could be divided into 4 steps. Firstly, to avoid clogging of the adsorbent column, the water extract was centrifuged to remove plant lees and high molecular weight polymers. Then, by adsorption on XAD-16 polystyrene resin, anthocyanins and other phenolic compounds were separated from other hydrophilic substances. Co-extracted substances such as mucilage, pectin, plant acid, salt and sugar were easily removed. The next step, the mixture of anthocyanins and phenolic compounds were eluted from the resin by acidic methanol, and anthocyanins were crystallized. Finally, the anthocyanins were purified by using a Sephadex® LH-20 gel filtration chromatography. Two pure anthocyanins, Compound I (hRf = 24) and Compound II at (hRf = 32) were obtained (Figure. 7).

Table 7 Years of receiving, sources and characteristics of *H. sabdariffa* samples

Sample number	Year	Source	Characteristic
01	2004	Uttaradit	Brown
02	2004	Saraburi	Red
03	2004	Ratchaburi	Red
04	2003	Sa Kaeo[a]	Small calyx
05	2004	Chiang Mai[a]	Small calyx
06	2004	Ang Thong[a]	Red
07	2004	Chai Nat	Red
08	2003	Suphan Buri[a]	Red
09	2004	Saraburi-Lop Buri	Red
10	2003	Nakhon Pathom[a]	Red
11	2004	Ratchaburi	Red
12	2003	Songkhla	Red
13	2003	Nakhon Pathom[a]	Red
14	2003	Nakhon Pathom[a]	Red
15	2003	Chon Buri[a]	Red
16	2004	Khon Kaen	Red
17	2004	Lop Buri	Red
18	2004	Nakhon Sawan	Red
19	2004	Ranong	Red
20	2003	Chiang Mai	Brown
21	2003	Chiang Mai	Brown
22	2003	Chiang Mai	Brown
23	2003	Chiang Mai	Brown
24	2003	Uttaradit	Brown
25	2003	Chiang Mai	Brown
26	2003	Chiang Rai	Brown
27	2003	Chiang Mai	Brown
28	2003	Chiang Mai	Brown
29	2003	Chiang Mai	Brown
30	2003	Chiang Mai	Brown
31	2003	Chiang Mai	Brown
32	2003	Chiang Mai	Brown
33	2003	Chiang Mai	Brown
34	2003	Lamphun	Brown
35	2004	Khon Kaen	Red

[a] The samples were received as fresh materials

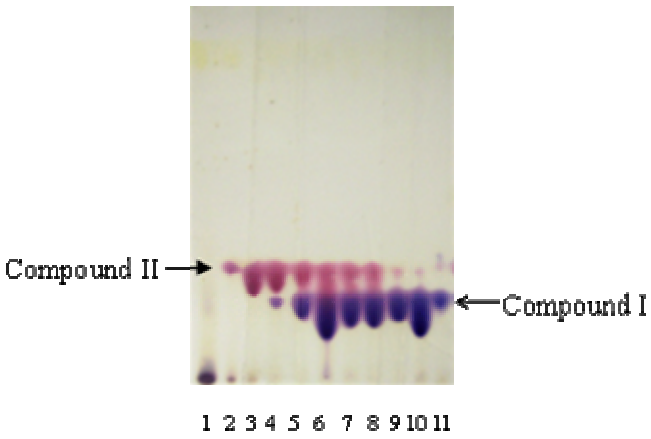

Figure 7 Thin-layer chromatograms of fractions from Sephadex® LH-20 gel filtration chromatography: stationary phase = silica gel 60 F_{254}, mobile phase = ethyl acetate : 2-propanol : water : formic acid (6 : 2 : 2 : 1), detection under daylight, 1 to 11 = the fraction obtained from Sephadex® LH-20 gel filtration chromatography

2.2 Identification and purity of the isolated compounds

Compound I and Compound II were identified by comparing their ^{1}H NMR data with data previously reported [121]. The ^{1}H NMR data of Compound I was very similar to that of delphinidin-3-sambubioside (Dp-3-sam) (Figure 8), the most prevalent anthocyanin found in roselle. Assignments of ^{1}H chemical shifts were shown in Table 8. Some differences could be observed owing to the difference in solvent and radiofrequency used in the studies. However, the ^{1}H NMR signals of Compound I at 8.88, 6.87 and 6.66 ppm were clearly those of H4, H6 and H8, respectively. The two symmetry protons, H2′ and H6′, displayed a 2H signal at 7.78 ppm, while two anomeric protons of sambubiose showed two doublet signals at 5.43 and 4.66 ppm. These data supported that Compound I was delphinidin-3-sambubioside.

^{1}H NMR data of Compound II was very similar to that of cyanidin-3-sambubioside (Cy-3-sam) (Figure 8), the second most prevalent anthocyanin found in roselle. Assignments of ^{1}H chemical shifts were shown in Table 8. The ^{1}H NMR signals of Compound II at 8.91, 6.88 and 6.66 ppm were those of H4, H6 and H8, respectively. On the basis of chemical shifts and coupling-patterns the singlet signal at 8.05 ppm was assigned to H2'. Two doublet signals at 7.05 and 8.24 ppm were assigned to H5' and H6', respectively.

The purity of the isolated delphinidin-3-sambubioside analyzed by HPLC method was 97.44 ± 1.88%.

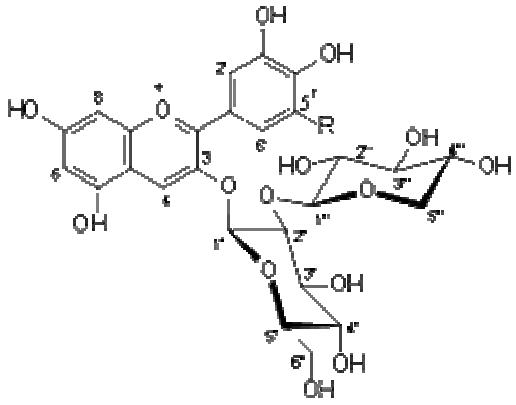

Figure 8 Chemical structure of delphinidin-3-sambubioside (Compound I) (R = OH) and cyanidin-3-sambubioside (Compound II) (R = H)

3 General quality control methods

The general quality control methods including foreign matter, loss on drying, total ash, acid insoluble ash, water-soluble extractive and ethanol-soluble extractive of each sample were shown in Table 9.

As described in section 1 that the samples were divided into three groups, thus the general quality control methods of each group were summarized separately as mean $\pm$ SD (Table 10). Analytical data that considered as outliers and extremes of each general quality control method by boxplot were excluded before calculation. The outliers and extremes in each group were shown with “a” mark, the outliers and extremes of the reddish combined with the brownish (n = 33) were shown with “b” mark and those of all samples (n = 35) were shown with “c” mark, in Table 9. Due to amount of some samples was very low, the foreign matter could be analyzed only one time in these samples, and SD could not be calculated. These foreign matter values were shown with “d” mark in Table 9. Total ash and acid insoluble ash were determined in duplicate, but the SD data could not acquire from analyzer. These were shown with “e” mark in Table 9.

Comparison between the reddish and the brownish groups, all of their general quality control methods except for water extractive value and ethanol extractive value, were not different ($p > 0.05$). Both the water extractive value and the ethanol extractive value of the reddish group were higher than those of the brownish group (Table 10). This result might be due to conversion of extractable red monomeric anthocyanins to non-extractable brown polymeric anthocyains in the latter group. The assumption was based on the report that monomeric anthocynins could be degraded by light and storage temperature, and a new brown polymer with a larger molecular weight was formed [128,130]. Although the solubility

of this brown polymer neither in water nor in ethanol had been reported [130], the larger in molecular weight generally causes the less water solubility. Moreover, the extraction results of this current study also showed that both water extract and ethanol extract of the brownish roselle samples were likely to be clear with a colorless or a pale brown color. But those of the reddish roselle samples were likely to be dark red. Therefore, the conversion of monomeric anthocyanins to brown polymeric anthocyains might reduce extractable substances in water and in ethanol. Because the number of samples of the small calyx group was too low, the comparison among all three groups could not be performed.

Table 8 ^{1}H NMR data of Compound I and Compound II comparing with ^{1}H NMR data of delphinidin-3- sambubioside (Dp-3-sam) and cyanidin-3-sambubioside (Cy-3-sam)

	Compound I[a]	**Dp-3-sam**[b]	**Compound II**[a]	**Cy-3-sam**[b]
	***δ* (ppm) *J* (Hz)**	***δ* (ppm) *J* (Hz)**	***δ* (ppm) *J* (Hz)**	***δ* (ppm) *J* (Hz)**
Aglycone	Delphinidin		Cyanidin	
H_4	8.88 s	8.88 s	8.91 s	8.96 s
H_6	6.87 s	6.84 d (1.6)	6.88 s	6.90 d (1.6)
H_8	6.66 s	6.65 d (1.9)	6.66 s	6.68 d (1.9)
$H_{2'}$	7.78 s	7.74 s	8.05 s	8.05 d (2.27)
$H_{5'}$	-	-	7.05 d (8.4)	7.03 d (8.7)
$H_{6'}$	7.78 s	7.74 s	8.24 d (8.1)	8.26 dd (2.3; 8.7)
Sugar 1	*β*-D-glucopyranosyl		*β*-D-glucopyranosyl	
$H_{1''}$	5.43 d (7.5)	5.47 d (7.8)	5.38 d (6.9)	5.41 d (7.8)
$H_{2''}$	4.00 t (8.2)	4.04 dd (7.8; 8.4)	3.90 m	3.98 dd (7.8; 9.0)
$H_{3''}$	3.77 m	3.85 dd (8.4; 9.6)	3.75 m	3.80 dd (9.0; 9.6)
$H_{4''}$	3.56 m	3.60 t (9.6)	3.56 m	3.55 t (9.6)
$H_{5''}$	3.56 m	3.66 dd (5.4; 9.6)	3.56 m	3.60 dd (5.4; 9.6)
$H_{6(a)''}$	3.77 m	3.83 dd (5.4; 12.0)	3.75 m	3.78 dd (5.4; 12.0)
$H_{6(b)''}$	3.92 d (11.4)	3.99 d (10.2)	3.90 m	3.94 d (11.0)
Sugar 2	*β*-D-xylopyranosyl		*β*-D-xylopyranosyl	
$H_{1'''}$	4.66 d (7.5)	4.75 d (7.8)	4.70 (overlap with CD_3OD)	4.77 (d 7.8)
$H_{2'''}$	3.21 t (8.2)	3.26 dd (7.8; 9.0)	3.90 m	3.24 dd (7.8; 9.0)
$H_{3'''}$	3.31 m	3.36 t (9.0)	3.75 m	3.33 t (9.0)
$H_{4'''}$	3.40 m	3.43 m	3.40 m	3.42 m
$H_{5(a)'''}$	3.56 m	3.66 dd (5.4; 11.4)	3.56 m	3.60 dd (5.4; 12.0)
$H_{5(b)'''}$	2.96 t (10.8)	3.04 dd (10.8; 11.4)	3.05 t (11.0)	3.02 d (11.6; 12.0)

[a] *δ* in ppm and *J* (parentheses) in Hz, 300 MHz, CD_3OD : $CDCl_3$,

[b] ^{1}H NMR data previously reported [121], *δ* in ppm and *J* (parentheses) in Hz,

s = singlet, d = doublet, dd = double doublet and m = multiplet

Table 9 General quality control methods of each roselle sample (mean ± SD)

Sample number	Foreign matter (% w/w)	Loss on drying (% w/w)	Total ash[e] (% w/w)	Acid insoluble ash[e] (% w/w)	Water extractive (% w/w)	Ethanol extractive (% w/w)
01	0.32 ± 0.12	11.06 ± 0.04	7.10	0.74	50.11 ± 0.32[a]	13.26 ± 0.22[a]
02	1.29 ± 0.32	10.99 ± 0.00	7.30	0.73	51.51 ± 0.01	13.69 ± 0.07
03	1.05 ± 0.67	13.02 ± 0.03	8.70	1.04	46.66 ± 0.33	8.48 ± 0.01
04	1.57 ± 0.56	10.37 ± 0.03	7.20	0.32	49.08 ± 0.02	23.80 ± 0.13[c]
05	1.59 ± 0.60	9.61 ± 0.02	8.40	0.35	54.97 ± 0.24	13.73 ± 0.06
06	1.56 ± 0.49	11.71 ± 0.03	6.90	0.78	51.76 ± 0.55	11.06 ± 0.12
07	2.68 ± 1.28	12.00 ± 0.03	10.50	0.37	47.72 ± 0.26	9.76 ± 0.02
08	0.23 ± 0.11	11.27 ± 0.04	6.30	0.45	50.60 ± 0.17	10.43 ± 0.18
09	0.65 ± 0.16	12.63 ± 0.02	8.30	0.62	46.51 ± 0.19	12.69 ± 0.04
10	1.61 ± 0.63	10.80 ± 0.00	7.70	0.41	51.65 ± 0.22	17.20 ± 0.12[a]
11	1.31 ± 0.22	9.83 ± 0.03	8.90	0.37	50.28 ± 0.61	14.64 ± 0.09
12	1.29 ± 0.73	12.54 ± 0.09	10.30	1.81[a, b, c]	48.72 ± 0.61	7.29 ± 0.05
13	0.75 ± 0.41	13.62 ± 0.07[b, c]	7.60	0.32	48.44 ± 0.17	12.89 ± 0.08
14	1.69[d].	8.15 ± 0.01[b, c]	9.70	1.07	48.39 ± 0.19	4.15 ± 0.03[a]
15	2.81 ± 0.64	10.95 ± 0.08	7.90	0.20	55.58 ± 0.42	10.90 ± 0.09
16	2.00 ± 0.84	10.18 ± 0.04	9.10	0.50	52.13 ± 0.08	9.70 ± 0.04
17	1.21 ± 0.24	10.71 ± 0.09	8.70	0.40	50.59 ± 0.03	11.45 ± 0.04
18	0.94 ± 0.24	10.90 ± 0.08	9.20	0.37	53.24 ± 0.54	7.54 ± 0.16
19	2.05 ± 1.18	10.44 ± 0.11	8.70	0.31	54.22 ± 0.54	11.75 ± 0.07
20	1.73[d]	11.48 ± 0.04	7.90	0.86	46.20 ± 0.03	6.90 ± 0.09
21	1.03[d]	11.15 ± 0.05	8.10	0.99	46.21 ± 0.03	5.28 ± 0.03
22	1.92 ± 0.28	11.09 ± 0.05	8.50	0.87	41.96 ± 0.03[a]	6.60 ± 0.00
23	2.20 ± 0.13	11.58 ± 0.03	11.00	0.44	45.81 ± 0.05	5.61 ± 0.03
24	1.16 ± 0.27	10.25 ± 0.05	7.30	0.37	45.90 ± 0.42	9.29 ± 0.12[a]
25	6.28 ± 0.43[a, b, c]	10.99 ± 0.02	6.60	0.68	45.52 ± 0.16	10.34 ± 0.03[a]
26	0.75 ± 0.25	10.92 ± 0.01	7.80	0.37	45.82 ± 0.24	19.76 ± 0.05[a, b, c]
27	1.65[d]	12.29 ± 0.00	7.30	1.02	46.46 ± 0.39	6.87 ± 0.13
28	1.82[d]	10.91 ± 0.04	7.90	0.98	45.77 ± 0.19	6.54 ± 0.04
29	1.77[d]	10.72 ± 0.01	7.90	0.98	44.54 ± 0.19[a]	6.13 ± 0.11
30	0.54[d]	12.17 ± 0.03	8.30	1.11	46.80 ± 0.10	5.96 ± 0.02
31	1.07 ± 0.44	11.19 ± 0.01	10.70	0.41	41.74 ± 0.25[a]	6.96 ± 0.06
32	0.96 ± 0.28	11.84 ± 0.00	9.10	0.41	43.04 ± 0.22[a]	8.48 ± 0.13[a]
33	1.79[d]	11.18 ± 0.02	10.30	0.48	47.54 ± 0.17[a]	6.37 ± 0.10
34	0.79[d]	11.71 ± 0.05	10.30	0.44	46.81 ± 0.02	6.64 ± 0.09
35	0.86 ± 0.28	9.73 ± 0.08	10.60	0.96	45.99 ± 0.14	10.44 ± 0.03

[a] The outliers and extremes of each group

[b] The outliers and extremes of the reddish combined with the brownish groups (n = 33)

[c] The outliers and extremes of all samples (n = 35)

[d] SD not determined

[e] SD could not be acquired

Table 10 General quality control methods of roselle samples in each group (mean ± SD)

General quality control method	Reddish (n = 17)	Brownish (n = 16)	Small calyx (n = 2)	Reddish and Brownish (n = 33)	All samples (n = 35)
Foreign matter (% w/w)	1.41 ± 0.69	1.30 ± 0.57	1.58 ± 0.01	1.36 ± 0.63	1.37 ± 0.61
Loss on drying (% w/w)	11.15 ± 1.36	11.28 ± 0.53	9.99 ± 0.54	11.17 ± 0.73	11.16 ± 0.83
Total ash (% w/w)	8.61 ± 1.24	8.51 ± 1.37	7.80 ± 0.85	8.56 ± 1.29	8.52 ± 1.27
Acid insoluble ash (% w/w)	0.56 ± 0.28	0.70 ± 0.28	0.34 ± 0.02	0.63 ± 0.28	0.61 ± 0.28
Water extractive (% w/w)	50.23 ± 2.77[a]	46.13 ± 0.45[a]	52.02 ± 4.16	48.01 ± 3.36	48.24 ± 3.47
Ethanol extractive (% w/w)	10.85 ± 2.13[a]	6.35 ± 0.55[a]	18.76 ±7.12	9.23 ± 3.13	9.36 ± 3.18

[a] Mean values between the reddish and the brownish groups are significantly different ($p < 0.05$)

4 Qualitative quality control

4.1 Chemical identification

The chemical identification of roselle was based on its chemical constituents including anthocyanins and phenolic compound. The results of the chemical test of roselle extract were shown in Figure 9. For identification purpose, the extract of beet root contained the other class of natural red pigment, betalains, was also tested and compared. The results of chemical test of some synthetic red dyes were also shown (Table 11).

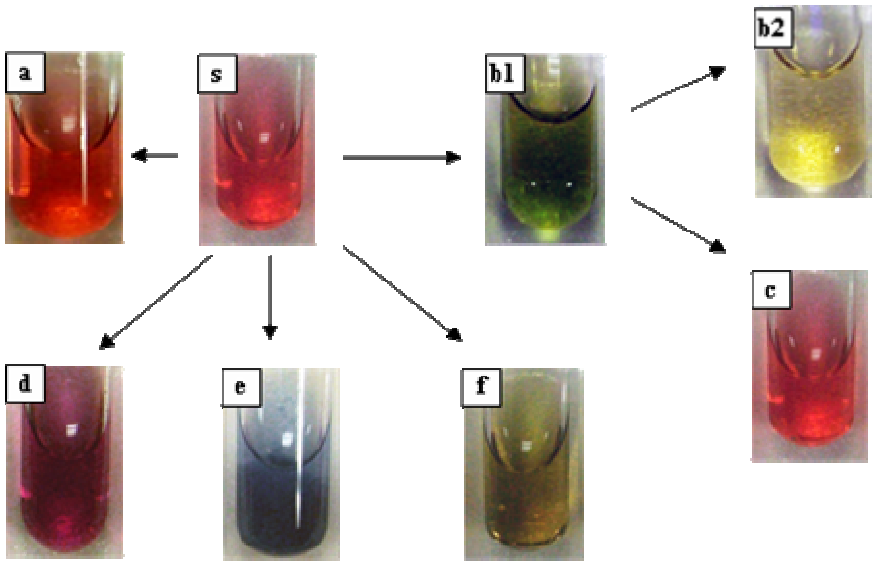

Figure 9 Chemical reactions of the roselle: **a)** the extract after heated with 2M hydrochloric acid, **b1)** the extract after added 2M sodium hydroxide, **b2)** the fade of the extract after leaving solution b1 to stand, **c)** the extract after added 2M sodium hydroxide and immediately added 2M hydrochloric acid, **d)** the extract after added aluminium chloride test solution, **e)** the extract after added lead acetate test solution and **f)** the extract after added ferric chloride test solution, **s)** the roselle extract used as control

The extract of roselle and beet root could be differentiated by the stability to acid hydrolysis and the color at basic pH of their main pigment (Table 11: test 1 and 2). The anthocyanins are much more stable to acid hydrolysis than the betalains thus after heated with 2M hydrochloric acid, the extract of roselle was still red while that of beet root was nearly colorless. At basic pH, the color of anthocyanins was blue-green while that of betalains was yellow [87].

The extract of roselle was differentiated from the other synthetic dyes in this study by the color at basic pH, the reaction with lead acetate and ferric chloride. At basic pH, the extract of roselle was blue-green while those of the synthetic dyes showed distinct color tones i.e. brown red to purple (Table 11: test 2). With lead acetate, the extract of roselle gave blue precipitate, while the synthetic dyes gave red to violet precipitate (Table 11: test 5). With ferric chloride, the extract of roselle changed to dark green, while some synthetic dyes, Amaranth and Ponceau 4R, did not change. The other dyes gave red to brown red precipitate (Table 11: test 6).

In conclusions, from a variety of tests, the inclusive identification of roselle could be accomplished by using only four selected combination tests i.e. heating with acid, color in basic pH, reaction with lead acetate and reaction with ferric chloride (Table 11: test 1, 2, 5 and 6).

Table 11 Chemical reaction of roselle extract, beet root extract and some synthetic dyes

Reaction	Roselle	Beet root	Amaranth	Carmoisine	Erythrosine	Ponceau 4R
Negative control						
Heat with 2M HCl (1)						
NaOH (2)						
$AlCl_3$ (3)	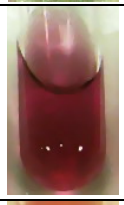					
$AlCl_3$ + HCl (4)						
Lead acetate (5)						
Ferric chloride (6)						

4.2 Thin-layer chromatography (TLC) fingerprint

Two mainly chemical constituents of roselle are delphinidin-3-sambubioside and cyanidin-3-sambubioside. However, they are not commercially available. A task and high expenditure was needed to purify these standard anthocyanins. In European Pharmacopoeia 2001 [28], the quinaldine red has been used as an Rf indicator for TLC of roselle. In this study, the pigment was also used. To enhance separation degree and to reduce spot diffusion, the mobile phase was changed from acetic acid : water : butanol (15 : 30 : 60 v/v/v) to ethyl acetate : 2-propanol : water : formic acid (6 : 2 : 2 : 1 v/v/v/v). In addition, pure compounds of the two main anthocyanins, isolated in our laboratory, were also spotted on TLC to identify the relative Rf to quinaldine red. The pure delphinidin-3-sambubioside was rapidly degraded after removal the plate from the chamber. In routine identification, only quinaldine red was suggested to be TLC position marker.

The TLC fingerprints of 35 samples of roselle were shown in Figure 10. Some samples possessed a very pale spot under daylight owing to the very less content of the color constituent, anthocyanins. The majority of these samples were the members of the brownish group e.g. sample number 26, 30, 31, 32. Atypical samples, sample number 4-5also showed pale spots of anthocyanins. Comparing between the reddish samples and the brownish samples, the red spots of anthocyanins were normally more intense in the former cases. These results were consistent with the contents of total anthocyanins in roselle that the contents of total anthocyanins in the reddish samples were generally higher than those in the brownish samples (Table 33 and Table 34). Thus the red color of roselle might signify the content of anthocyanins in itself.

Normally, the chromatograms obtained with roselle samples showed two pink spots of delphinidin-3-sambubioside and cyanidin-3-sambubioside with relative Rf value of 0.29-0.44 and 0.40-0.54 to the quinaldine red (solution C), respectively. Several spots of higher and lower hRf values may be found. After spraying the plate with dilute sulfuric acid and heating at 100°C until colors had fully developed; more several spots of different colors situating above and below those of due to delphinidin-3-sambubioside and cyanidin-3-sambubioside were shown (Table 12); see also Figure 10. Apart from two red spots of delphinidin-3-sambubioside and cyanidin-3-sambubioside, it was hard to definitely specify that which spots were common to all roselle samples. Therefore, only the possibility to found other spots as listed in Table 12 was reported. In other words, the TLC chromatogram of common roselle should contain at least two red spots of delphinidin-3-sambubioside and cyanidin-3-sambubioside with relative Rf value of 0.29-0.44 and 0.40-0.54

to that of quinaldine red. Other spots as listed in Table 12 may be found but it was not crucial to found all spots in the TLC chromatogram of roselle.

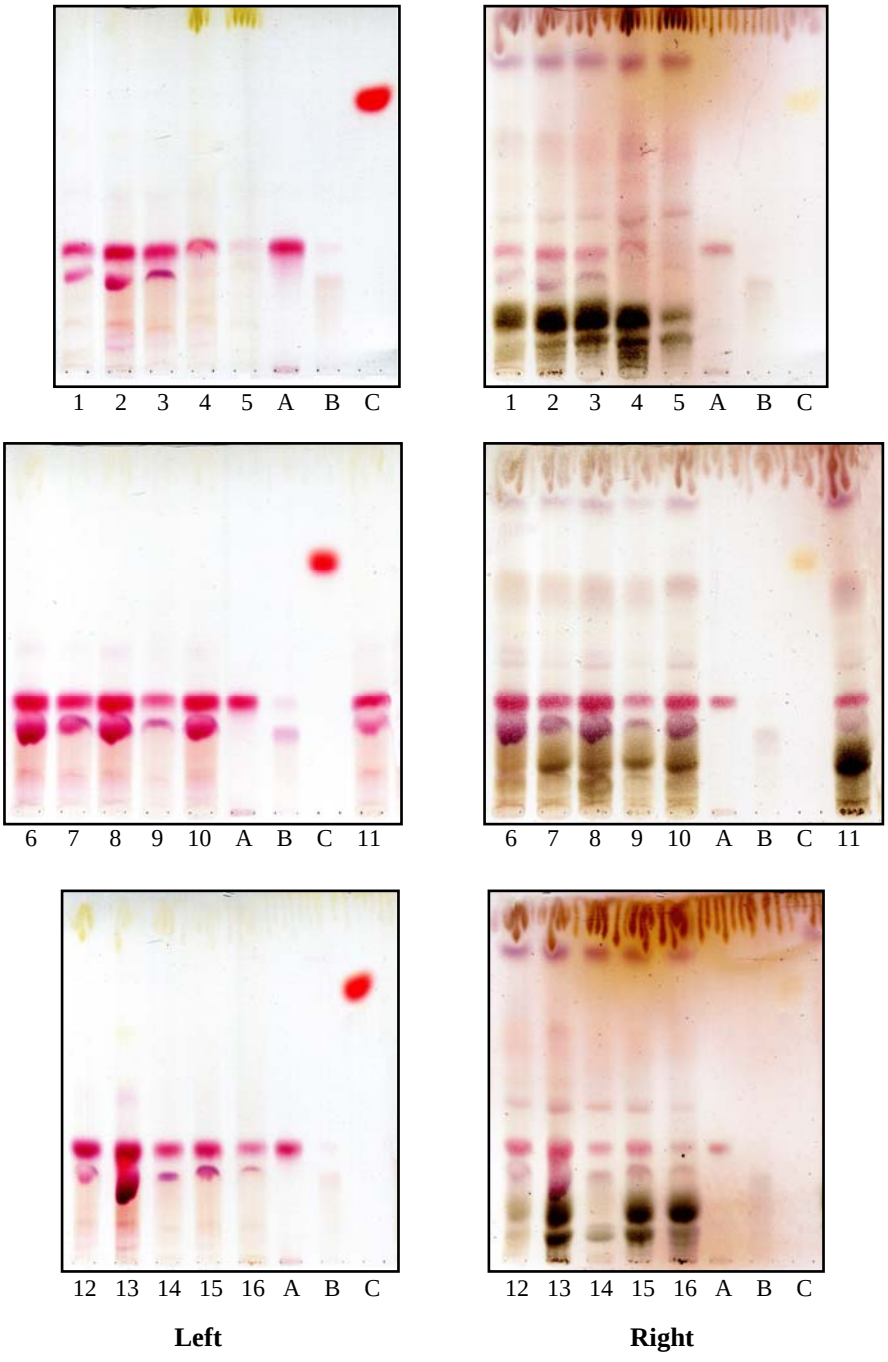

Figure 10 Thin-layer chromatograms of roselle prepared with 0.1% conc. hydrochloric acid in methanol: **left)** detection under daylight and, **right)** sprayed with diluted sulfuric acid and heated, stationary phase = silica gel 60 F_{254}, mobile phase = ethyl acetate : 2-propanol : water : formic acid (6 : 2 : 2 : 1), 1-35 = sample number, A = cyanidin-3-sambubioside, B = delphinidin-3-sambubioside, C = quinaldine red

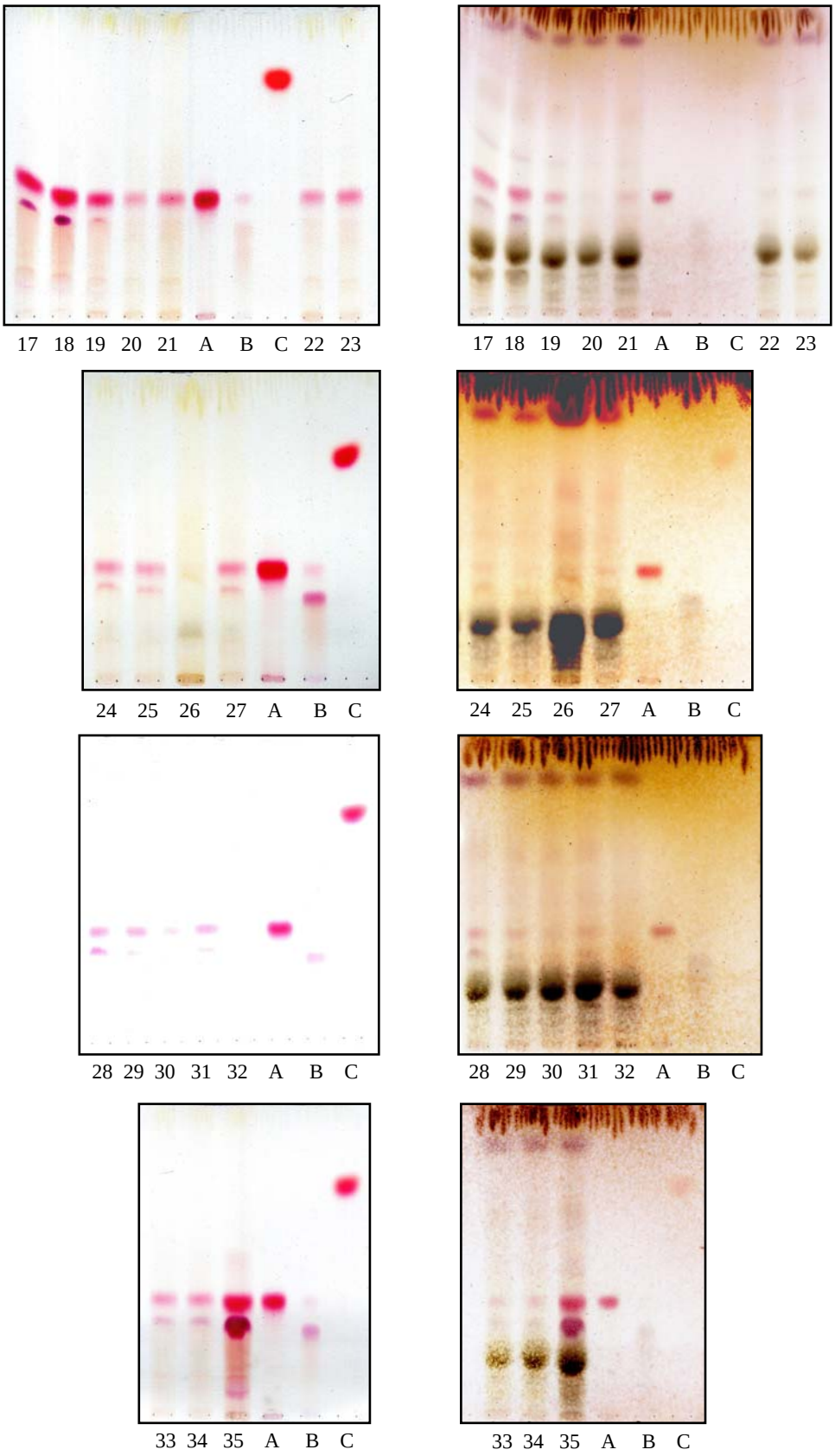

Figure 10 Thin-layer chromatograms of roselle… (cont.)

Table 12 hRf values of components in the roselle extract prepared from 0.1% conc. hydrochloric acid in methanol

Spot	hR_f	RR_f [a]	Sample		Quinaldine	
			Detection under daylight	Spray with dil.H_2SO_4	Detection under daylight	Spray with dil.H_2SO_4
1	3 - 9	0.04 - 0.12	Pink	_	_	_
2	6 - 13	0.08 - 0.18	_	Dark brown	_	_
3	7 - 13	0.10 – 0.18	Pink			
4	10 - 17	0.14 – 0.23	Pale orange	_		
5	13 - 20	0.19 – 0.28	_	Dark brown		
6 [b]	*21 - 32*	*0.29 - 0.44*	*Pink*	*Violet*	_	_
7 [c]	*29 - 39*	*0.40 - 0.54*	*Pink*	*Pink*	_	_
8	39 - 51	0.54 - 0.70	_	Pale violet	_	_
9	44 - 50	0.61 - 0.69	Pale pink	_	_	_
10	60 - 68	0.83 - 0.94	_	Pale violet	_	_
	68 - 77	*1.00*	_	_	*Red*	*Pale orange*
11	83 - 92	1.14 - 1.27	_	Violet	_	_
12	93 - 99	1.28 - 1.37	Pale yellow	Brown		

[a] RR_f (Relative R_f value) = the R_f value referenced to Rf value of quinaldine red

[b] Spot 6 = delphinidin-3-sambubioside

[c] Spot 7 = cyanidin-3-sambubioside

4.3 High performance liquid chromatography (HPLC) fingerprint

4.3.1 Sample preparation

Preliminary experiment was carried out to find a suitable solvent for the extraction of chemical components from roselle. Boiling water and 50% methanol were tested. The HPLC chromatograms of the water extract and 50% methanol extract seem to be not much difference (Figure 11), but the preparation of water extract was more difficult because of its high viscosity. Therefore 50% methanol was selected as the extractive solvent for sample preparation. Various herb to solvent ratios (w/v), 1 : 50, 1 : 25 and 1 : 5, were further examined (Figure 12). Due to appropriate of signal response, the herb to solvent ratio of 1 : 5 was selected. As above information, 50% methanol at the herb to solvent of 1 : 5 (w/v) was selected as the solvent for the extraction of chemical components from roselle.

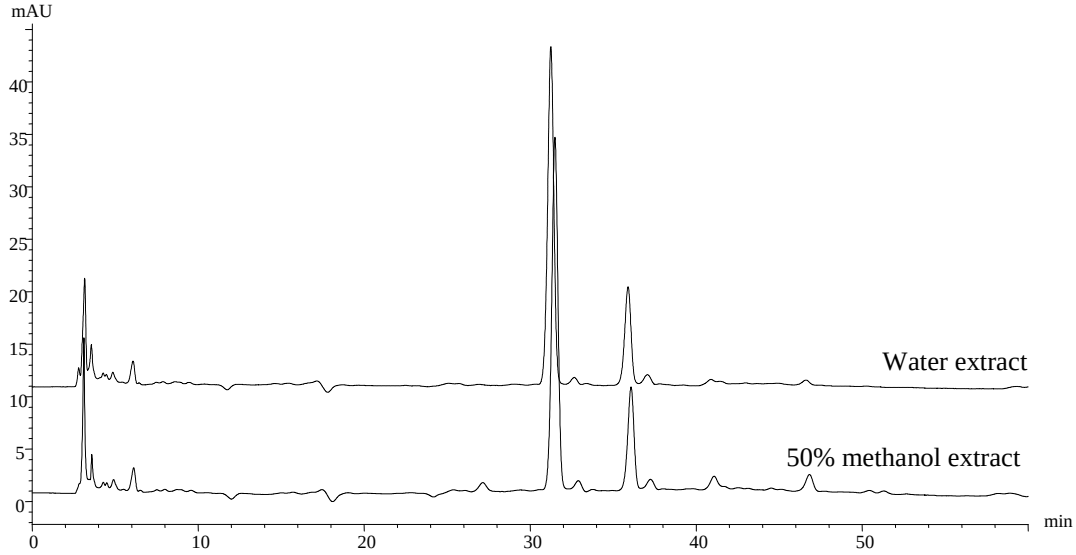

Figure 11 HPLC chromatograms of roselle extract prepared from 50% methanol (—) and water (- -): *solvent A = 4% phosphoric acid, solvent B = 100% acetonitrile,* solvent program = 0-10 min isocratic elution with 6% *B*, 10-55 min linear gradient to 20% *B*, 56-60 min isocratic elution with 6% *B*, detection at 254 nm

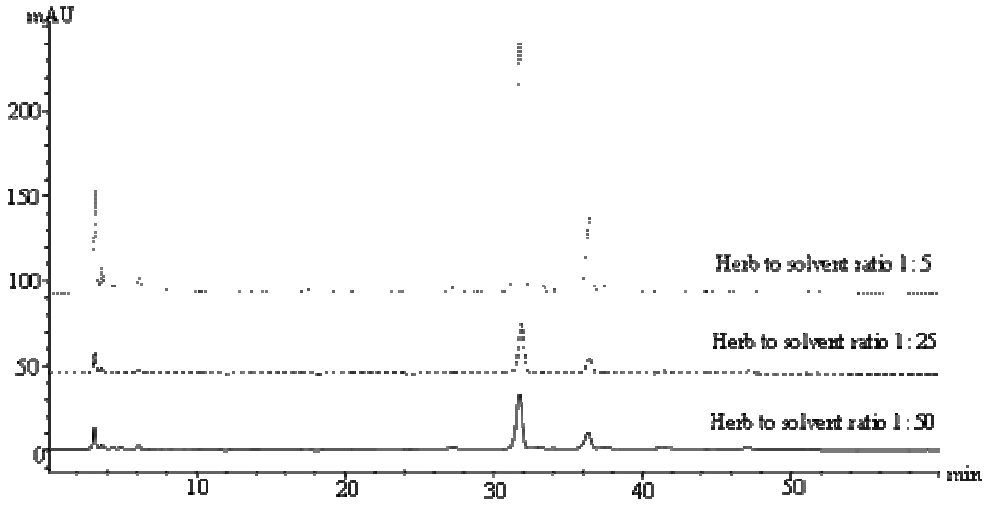

Figure 12 HPLC chromatograms of roselle extracted prepared from 50% methanol at various herb to solvent ratios (w/v), 1 : 50 (—), 1 : 25 (⁻ ⁻) and 1 : 5 (·····)*: solvent A = 4% phosphoric acid, solvent B = 100% acetonitrile,* solvent program = 0-10 min isocratic elution with 6% *B*, 10-55 min linear gradient to 20% *B*, 56-60 min isocratic elution with 6% *B*, detection at 254 nm

4.3.2 Optimization of HPLC condition

The solvent program of HPLC was optimized by a full factorial experiment design. Two factors, the durations of an isocratic and a gradient elution, were investigated. Each factor was varied with three levels as listed in Table 6. As a result, eight of different solvent programs were tested (Table 13). To check the precision of the method, the center condition (the solvent program using 20 min of isocratic elution and 45 min of gradient elution), was performed for five times. Five detection wavelengths in the UV and visible region, 254, 280, 316, 365 and 520 nm were investigated. The wavelength at 254 nm is generally absorbed by almost chromophore. Based on the presence of phenolic compounds and anthocyanins found in roselle [30,33,129], the other four detection wavelengths were also investigated. The wavelength at 280 nm is the representative of hydroxybenzoates and flavan-3-ols such as gallic acid and catechin. The wavelength at 316 nm is the maximum absorption of hydroxycinnamates such as caffeic acid, whereas flavonols such as rutin absorbs at 365 nm. And anthocyanins such as delphinidin have a visible absorption peak at 520 nm [129]. The information calculated by information theory [115] of each HPLC chromatogram was shown in Table 13. The highest information (3.60) was obtained from the chromatogram recorded at 365 nm of the Run no. 5 of which the durations used for an isocratic elution and a linear gradient elution were 20 and 50 minutes, respectively. However the signals at 365 nm were very low thus the other wavelengths were considered for instead. The chromatogram detected at 254 nm of the Run no. 5 and also Run no.3 gave the second highest information (3.49). In this study the solvent program of the Run no. 5 was selected. Thus the optimize HPLC condition for constructing the HPLC fingerprint of roselle was the solvent program of the Run no. 5 and the detection at 254 nm. The chromatograms detected at 254 nm of the full factorial experiment were shown in Figure 13.

Table 13 Information of the HPLC chromatograms obtained from full factorial experiment

Run no.	Factor		Information				
	i [a]	***ii*** [b]	**254 nm**	**280 nm**	**316 nm**	**365 nm**	**520 nm**
1	15	45	3.45	3.31	3.34	3.53	2.80
2	20	45	3.45	3.32	3.35	3.55	2.81
3	25	45	3.49	3.35	3.37	3.57	2.84
4	20	40	3.43	3.30	3.34	3.53	2.77
5	20	50	3.49	3.36	3.38	3.60	2.86
6	25	40	3.45	3.32	3.34	3.53	2.80
7	25	50	3.48	3.35	3.36	3.59	2.88
8	15	40	3.45	3.31	3.35	3.53	2.76
9	20	45	3.42	3.30	3.31	3.52	2.83
10	20	45	3.43	3.30	3.32	3.54	2.83
11	15	50	3.46	3.32	3.34	3.56	2.84
12	20	45	3.42	3.30	3.31	3.52	2.82
13	20	45	3.45	3.32	3.33	3.55	2.83

[a] Duration used for an isocratic elution (min)

[b] Duration used for a gradient elution (min)

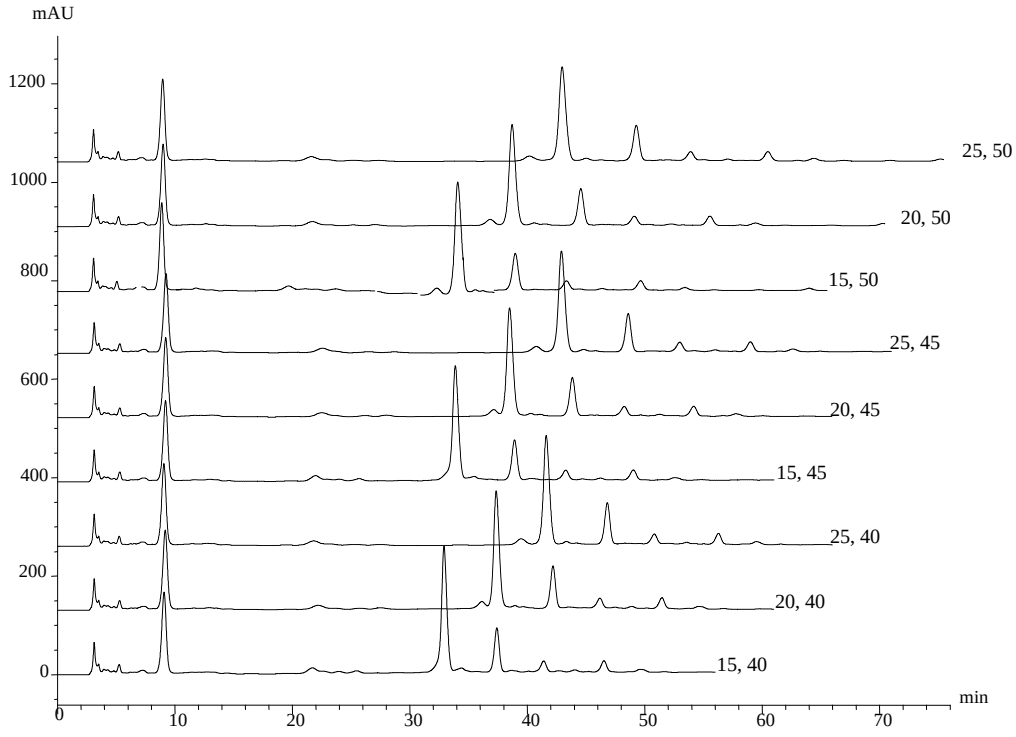

Figure 13 HPLC chromatograms of roselle extracted prepared from 50% methanol determined by various solvent programs: *solvent A = 4% phosphoric acid, solvent B = 100% acetonitrile*, full factorial experimental design : factor *i* (the first number) = duration used for an isocratic elution at 6% *B* (levels of *i* = 15, 20 and 25 min), factor *ii* (the last number) = duration used for a gradient elution to 20% *B* (levels of *ii* 40, 45 and 50 min), detection at 254 nm

4.3.3 Establishment of HPLC fingerprint of *H. sabdariffa*

HPLC is often used to establish the chromatographic fingerprint for various kinds of Traditional Chinese Medicine (TCM) [131] [132]. In this study, the HPLC fingerprint of roselle was established. Raw chromatograms of all samples were corrected for the time shift. After the correction (Figure 14), the data were surveyed by principal component analysis (PCA). The PCA was implemented on the data matrix of the HPLC chromatograms. Each row represents the chromatogram of each sample. Thus the size of data matrix was 35 x 10641, while 35 was the number of sample and 10641 was the number of response collected at each retention time. The PCA score plot (Figure 15a) revealed that the HPLC chromatograms of samples were clearly divided into 3 clusters; A, B and C according to the predefined groups; the reddish, the brownish and the small calyx

group, respectively. However the PCA score of the sample number 1 which was the member of the brownish group was more close to those of the small calyx group.

On the PC1 axis, the reddish samples were seemed to be located from the origin and widely scattered towards the positive end while the brownish samples were located more tightly at the negative end. On the PC2 axis, the majority of samples from the reddish group were scattered on the negative side while those from the brownish group were on the opposite side. From the PCA score pattern, it could be expected that the HPLC chromatograms of each group had their own characteristics.

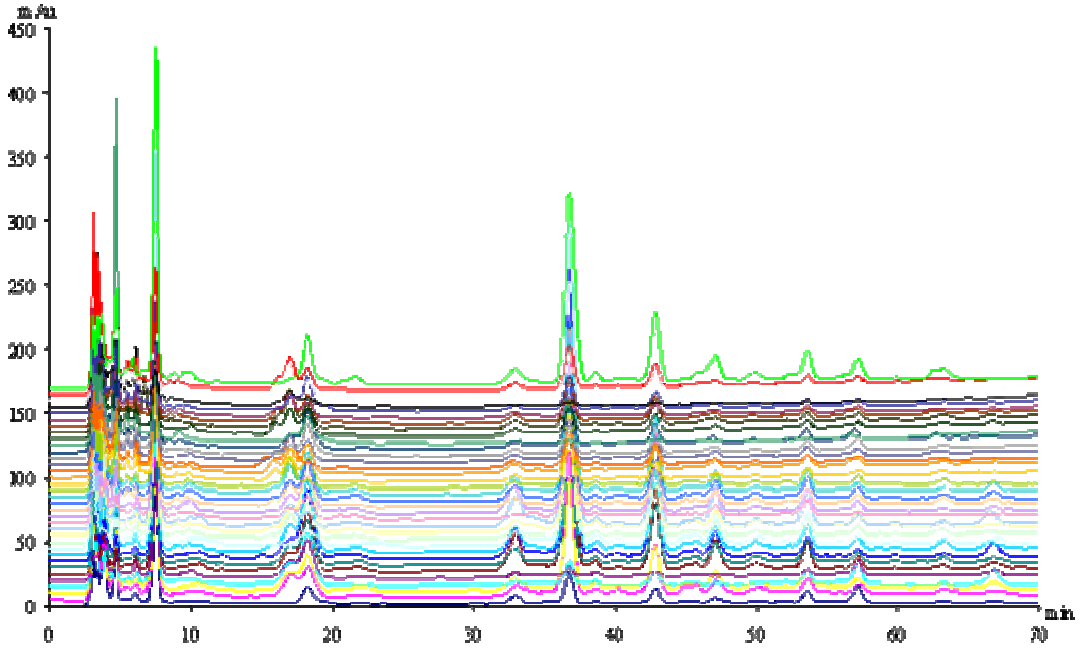

Figure 14 HPLC chromatograms after correction for the time shift of roselle extract (n = 35) prepared from 50% methanol: *solvent A = 4% phosphoric acid, solvent B = 100% acetonitrile*, solvent program = 0-20 min isocratic elution with 6% *B*, 20-70 min linear gradient to 20% *B*, 71 min linear gradient to 6% *B*, detection at 254 nm

The PCA score plot (Figure 15a) and the loading plot of PC1 (Figure 15b blue line) show that the chromatograms of the reddish samples (Figure 16a) tended to have more intensity at around 7.47, 36.71 and 42.75 minutes than those of the brownish samples (Figure 16b). While the PCA score plot (Figure 15a) and the loading plot of PC2 (Figure 15b red line) indicated that at around 3 to 7 minutes, the chromatograms of the brownish samples (Figure 16b) tended to have higher intensity than those of the reddish samples (Figure 16a)

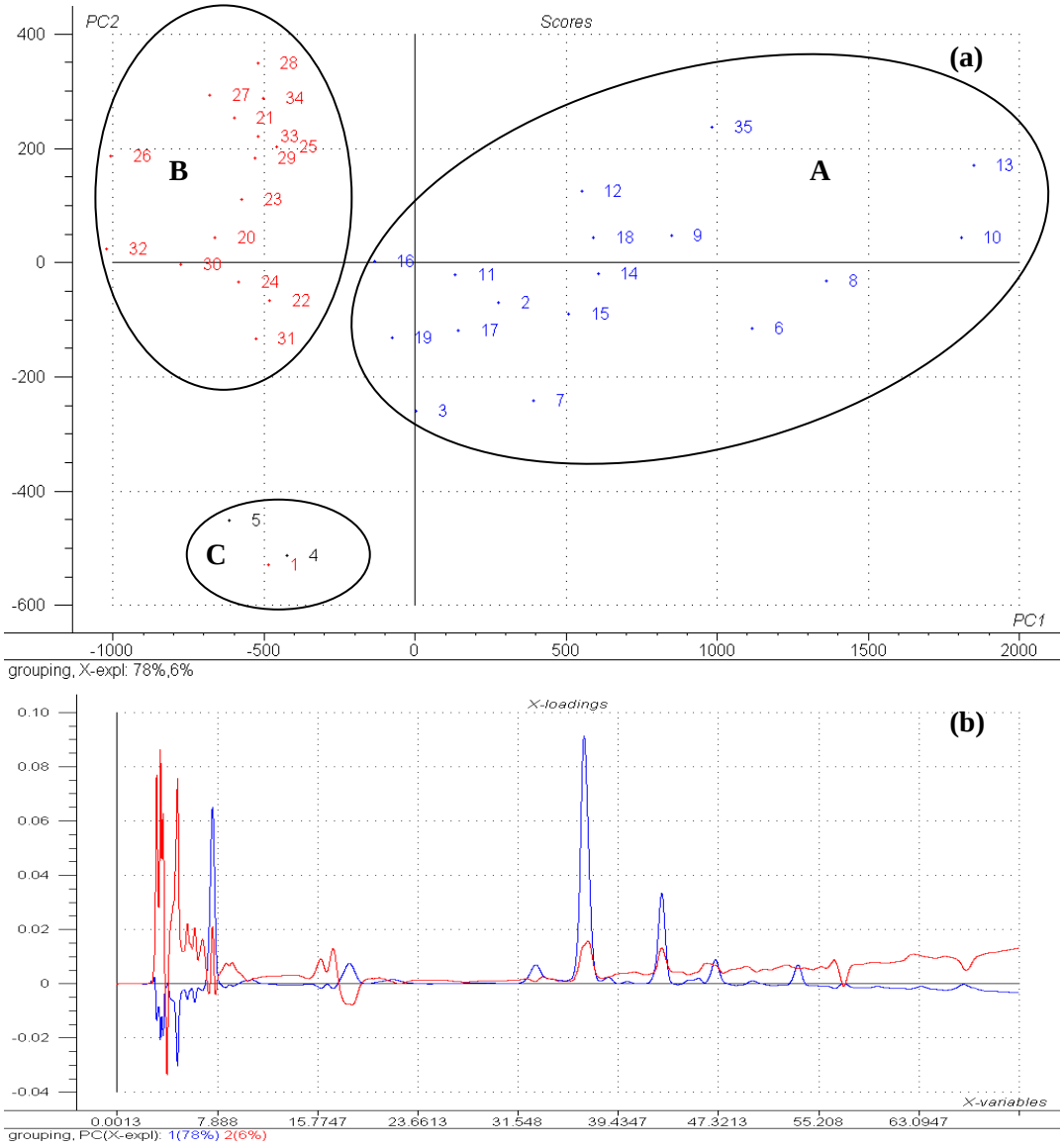

Figure 15 PCA of HPLC chromatogram of roselle extract (n = 35) prepared from 50% methanol: **a)** score plot of PC1 (78% X-variance explained) and PC2 (6% X-variance explained), the blue markers = the reddish samples, the red markers = the brownish samples, the green markers = the small calyx samples, 01-35 = sample number, A = cluster of the reddish samples, B = cluster of the brownish samples, C = cluster of the small calyx samples, **b)** loading plot of x-variables, blue line = PC 1, red line = PC2

As previously mentioned in the section 1, the reddish sample was classified as a higher grade material while the brownish sample and the small calyx sample were a lower grade material and a distinctively found one, respectively. Therefore to ensure that the proposed fingerprint was a representative chromatogram of the desired characteristics, the fingerprint of roselle was constructed from only the HPLC chromatograms of the reddish group (n = 17) (Figure 16a). The rest samples, the brownish and the small calyx (n = 18), were used as test set.

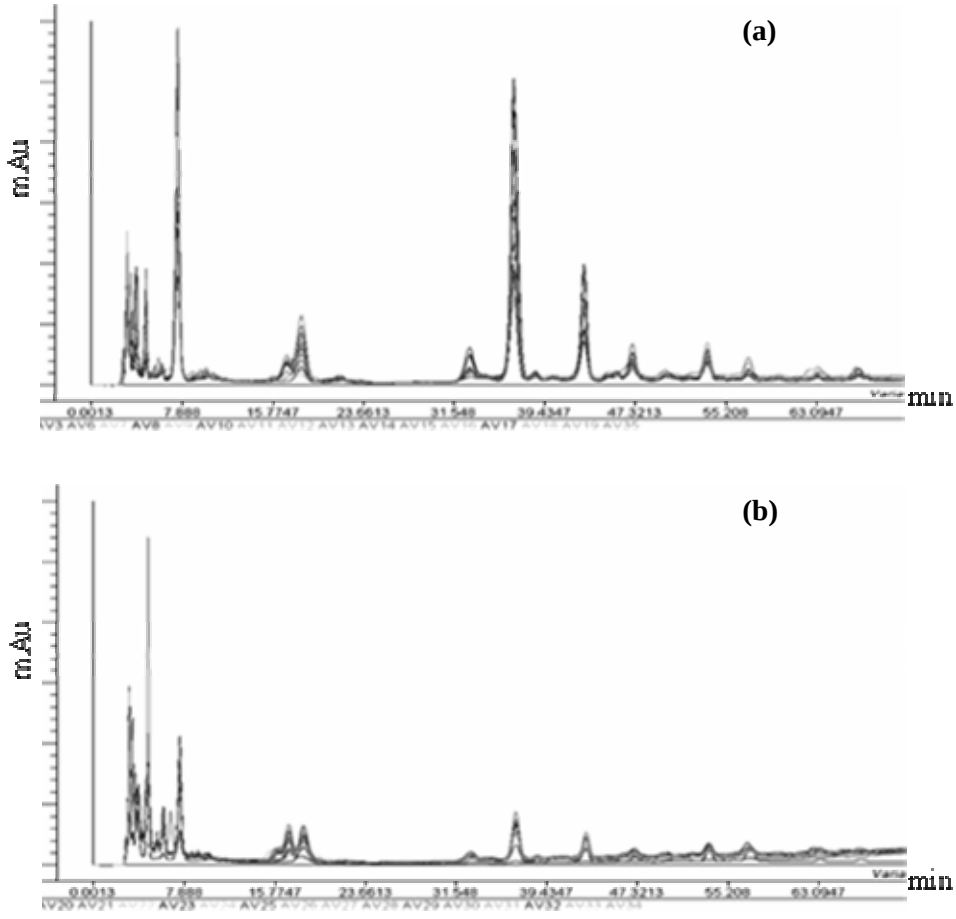

Figure 16 HPLC chromatograms of roselle extract prepared from 50% methanol: **a)** the reddish samples (n = 17), **b)** the brownish samples (n =16), *solvent A = 4% phosphoric acid, solvent B = 100% acetonitrile*, solvent program = 0-20 min isocratic elution with 6% *B*, 20-70 min linear gradient to 20% *B*, 71 min linear gradient to 6% *B*, detection at 254 nm

During the establishment of HPLC fingerprint of roselle, seventeen chromatograms of the reddish roselle (Figure 16a) were denoted by X = (x_1, …, x_{17}) where x_k was a T-dimensional column vector representing each chromatogram, and T was the number of retention time. The distribution of $c(w_s, w_m)$ and corresponding *c*-value for the type I error rate at 0.05 had been estimated from 5000 bootstrap samples, where w_s was a tentative HPLC fingerprint calculated as the median of chromatograms x_1 to x_{16} and x_{17} was the a testing chromatogram, w_m. For enhancing the estimation accuracy, ten rounds of such bootstrap were repeated, the corresponding lower bounds, $c_{(250),}$ were 0.9146, 0.9128, 0.9140, 0.9133, 0.9121, 0.9137, 0.9156, 0.9127, 0.9128 and 0.9129 while the mean of those values was equal to 0.9134. The tentative standard fingerprint (Figure 17), the median of x_1 to x_{17}, and the lower bound, 0.9134, had been applied for testing original 17 chromatograms of the reddish roselle. All of the correlation coefficients between the tentative standard fingerprint and each chromatogram were more than 0.9134 (Table 14). Thus all of the reddish samples were qualified. On the contrary, when the same criteria were applied to test the brownish and the small calyx samples, all of those samples were classified as unqualified samples (Table 14). Thus the HPLC fingerprint of roselle and the corresponding critical value set in this study had provided not only the criteria for identification but also the criteria for classification between the high quality and the low quality materials.

The characteristic peaks of HPLC fingerprint of roselle were shown in Table 15 (see also Figure 17). The peak number 3, at the retention time of 36.49 ± 0.95 min had been identified as delphinidin-3-samubioside, the most prevalent anthocyanin found in roselle. The two major peaks of the reddish roselle at the retention time of 36.49 ± 0.95 min and 42.57 ± 0.83 min had the area around 6617.17 ± 2693.84 and 2524.26 ± 880.77, respectively.

Comparing between the common pattern of HPLC chromatograms of the reddish roselle (n = 17) and those of the brownish roselle (n = 16), the peak areas of all 7 peaks of the reddish roselle were higher than those of the brownish roselle (Table 15). However, the relative peak area of peak number 1, based on the peak area of delphinidin-3-samubioside (peak number 3), of the reddish group (0.67 ± 0.16) was lower than that of brownish group (2.48 ± 2.29).

For future testing new unknown sample, the similarity between the established HPLC fingerprint (Figure 17) and a new testing chromatogram will be computed. If the correlation coefficient between those two chromatograms was more than the critical value, 0.9134, the new testing chromatogram will be accepted otherwise it will be rejected.

4.3.4 Validation of HPLC fingerprint of *H. sabdariffa*

The identification of the peaks in sample solution was carried out using delphinidin-3-sambubioside isolated in our laboratory. The highest peak in the chromatogram at the retention time of 36.49 ± 0.95 minute (Figure 17) was due to delphinidin-3-sambubioside. The precision calculated as %RSD of retention time and peak areas of delphinidin-3-sambubioside from six injections of one sample solution were 1.21% and 2.72%, respectively.

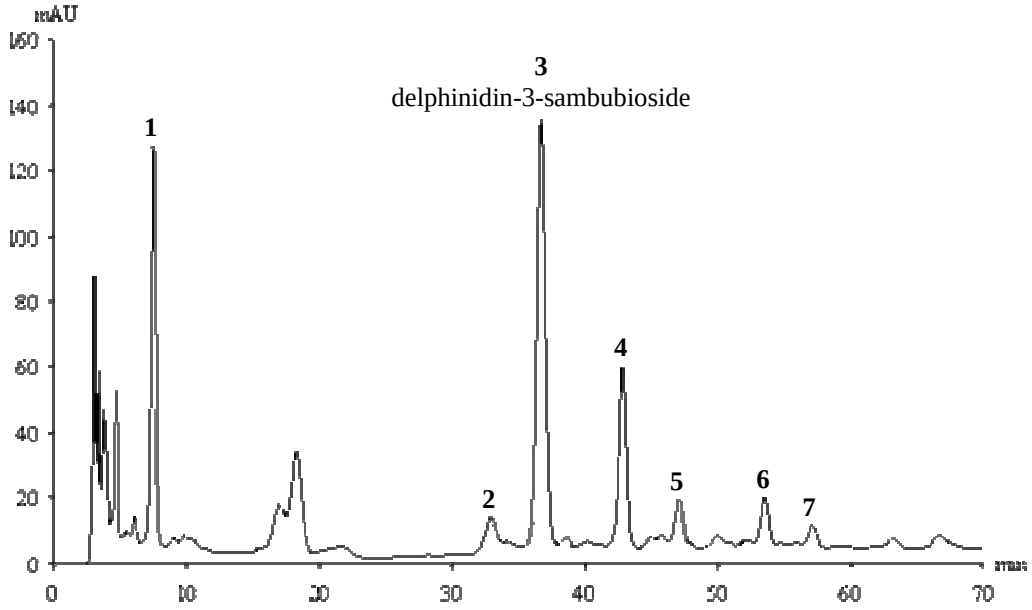

Figure 17 HPLC fingerprint of roselle extract (n = 17) prepared from 50% methanol: *solvent A = 4% phosphoric acid, solvent B = 100% acetonitrile,* solvent program = 0-20 min isocratic elution with 6% *B,* 20-70 min linear gradient to 20% *B,* 71 min linear gradient to 6% *B,* detection at 254 nm

Table 14 Correlation coefficients between the HPLC fingerprint of roselle (refer to Figure 17) and HPLC chromatogram of each sample (refer to Figure 16)

Sample number	Predefined group	Correlation coefficient[a]	Quality classification
01	Brown	0.7681	Unqualified
02	Red	0.9848	Qualified
03	Red	0.9339	Qualified
04	Small calyx	0.7088	Unqualified
05	Small calyx	0.6543	Unqualified
06	Red	0.9753	Qualified
07	Red	0.9907	Qualified
08	Red	0.9657	Qualified
09	Red	0.9918	Qualified
10	Red	0.9444	Qualified
11	Red	0.9473	Qualified
12	Red	0.9638	Qualified
13	Red	0.9516	Qualified
14	Red	0.9762	Qualified
15	Red	0.9777	Qualified
16	Red	0.9166	Qualified
17	Red	0.9463	Qualified
18	Red	0.9918	Qualified
19	Red	0.9318	Qualified
20	Brown	0.6667	Unqualified
21	Brown	0.6762	Unqualified
22	Brown	0.7658	Unqualified
23	Brown	0.7121	Unqualified
24	Brown	0.6993	Unqualified
25	Brown	0.7286	Unqualified
26	Brown	0.3658	Unqualified
27	Brown	0.6224	Unqualified
28	Brown	0.6924	Unqualified
29	Brown	0.7263	Unqualified
30	Brown	0.5796	Unqualified
31	Brown	0.7515	Unqualified
32	Brown	0.3915	Unqualified
33	Brown	0.7146	Unqualified
34	Brown	0.7161	Unqualified
35	Red	0.9376	Qualified

[a] Correlation coefficient between the standard HPLC fingerprint of roselle and HPLC chromatogram of each sample (critical correlation coefficient = 0.9134)

Table 15 The retention time, peak area and relative peak area of 7 characteristic peaks of HPLC fingerprint common pattern of roselle

Peak number	Retention time (min)	AUC			Relative retention time	Relative AUC		
		Reddish (n = 17)	Brownish (n = 16)	Small calyx (n = 2)		Reddish (n = 17)	Brownish (n = 16)	Small calyx (n = 2)
1	7.28 ± 0.49	4147.22 ± 1421.73	2238.56 ± 626.12	3070.36 ± 597.81	0.20 ± 0.01	0.67 ± 0.16	2.48 ± 2.29	5.70 ± 2.39
2	32.41 ± 1.65	1020.26 ± 527.99	263.02 ± 140.99	198.09 ± 22.74	0.89 ± 0.02	0.16 ± 0.05	0.22 ± 0.09	0.40 ± 0.27
3[a]	36.49 ± 0.95	6617.17 ± 2693.84	1135.46 ± 515.90	615.05 ± 362.27	1.00 ± 0.00	1.00 ± 0.00	1.00 ± 0.00	1.00 ± 0.00
4	42.57 ± 0.83	2524.26 ± 880.77	552.70 ± 258.95	370.19 ± 298.37	1.17 ± 0.01	0.39 ± 0.07	0.49 ± 0.05	0.55 ± 0.16
5	46.72 ± 0.99	969.23 ± 355.97	250.42 ± 156.29	105.08 ± 16.11	1.28 ± 0.01	0.15 ± 0.04	0.21 ± 0.09	0.22 ± 0.15
6	53.17 ± 0.95	947.76 ± 322.79	346.23 ± 172.20	389.01 ± 233.08	1.46 ± 0.01	0.16 ± 0.05	0.31 ± 0.09	0.63 ± 0.01
7	56.65 ± 1.04	519.21 ± 249.74	342.88 ± 207.80	704.51 ± 276.41	1.55 ± 0.01	0.09 ± 0.05	0.33 ± 0.19	1.23 ± 0.27

[a] Peak of delphinidine-3-sambubioside

4.4 Ultraviolet-visible (UV-Vis) fingerprint

The UV-Vis spectrums of roselle extract prepared from 50% methanol were shown in Figure 18. Only the wavelengths in the region of 250 to 650 nm were selected for constructing the UV-Vis fingerprint of roselle since the absorbance values between 190 and 250 nm were too high and on the contrary, they were too low at wavelengths beyond 650 nm. Due to the presence of hydroxybenzoates and flavan-3-ols, hydroxycinnamates, flavonols as well as anthocyanins in roselle, the maxima absorption peaks of each compound at 280, 316, 365 and 520 nm, respectively were used as the representatives for quantitative analysis of these compounds in roselle [129]. In this study, the maxima absorption peaks of roselle, the wavelengths around 284, 324 and 531 nm, were little shifted from those of the hydroxybenzoates and flavan-3-ols, hydroxycinnamates, and anthocyanins, respectively (Figure 18). But, the maxima absorption peak around 365 nm that was due to flavonols structure was not detected in this study.

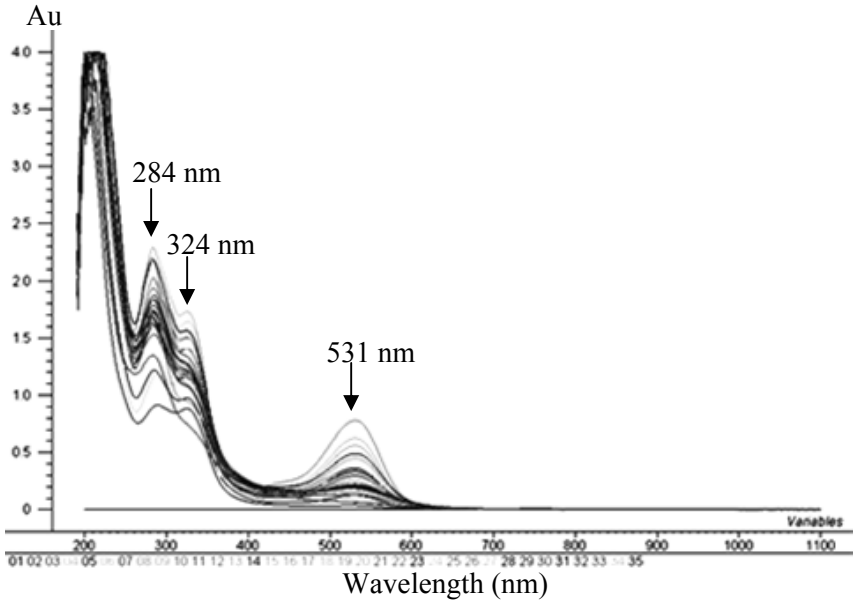

Figure 18 UV-visible spectra in the region of 190 to 1100 nm of roselle extract (n = 35) prepared from 50% methanol

The data was surveyed for any natural clustering by the PCA. The PCA was implemented on the data matrix of the UV-Vis spectrum. Each row represents the spectrum of each sample. Thus the size of data matrix was 35 x 401, while 35 was the number of sample and 401 was the number of absorbance value collected at each wavelength. The PCA score plot of the spectrum in the region of 250 to 650 nm showed the coarse clusters (Figure 19a). However those clusters could not be definitely separated. On the PC1 axis, the reddish samples were seemed to be located from the origin and scattered more towards the positive end while the brownish samples were located from the origin and scattered more towards the negative end. On the PC2 axis, the samples from the reddish group were scattered more towards the negative end while the samples from the brownish group were on the opposite site (Figure 19a).

The PCA score plot (Figure 19a) and the loading plot of PC1 (Figure 19b blue line) showed that the UV-Vis spectrum of the reddish samples (Figure 20a) tended to have more intensity around 450 to 600 nm than those of the brownish samples (Figure 20b). While the PCA score plot (Figure 19a) and the loading plot of PC2 (Figure 19b red line) indicated that in the region of 360 to 445 nm, the spectrum of the reddish samples (Figure 20a) tended to have less intensity than those of the brownish samples (Figure 20b).

The sample outliers were excluded by bootstrapping method. During the establishment of UV-Vis fingerprint of roselle, seventeen spectrums of the reddish roselle (Figure 20a) were denoted by $X = (x_1, \ldots, x_{17})$ where x_k was a T-dimensional column vector representing each spectrum, and T was the number of wavelength. The distribution of $c(w_s, w_m)$ and corresponding *c*-value for the type I error rate at 0.05 were estimated from 5000 bootstrap samples, where w_s was a tentative standard fingerprint calculated as the median of spectrum x_1 to x_{16} and x_{17} was the a testing spectrum, w_m. For enhancing the estimation accuracy, ten rounds of such bootstrap were repeated, the corresponding lower bounds, $c_{(250)}$, were 0.9784, 0.9790, 0.9805, 0.9785, 0.9802, 0.9800, 0.9821, 0.9821, 0.9794 and 0.9795 while the mean of those values was 0.9800. The tentative UV-Vis fingerprint, the median of spectrum of the reddish group (n = 17), and this lower bound, 0.9800, had been applied for testing original 17 spectrums of the reddish roselle. One outlier (sample10), of which correlation coefficient was 0.9746, was detected and excluded. The bootstrap was performed again with the remaining sample (n = 16). Ten round of corresponding lower bounds, $c_{(250)}$, were 0.9912, 0.9915, 0.9915, 0.9912, 0.9914, 0.9912, 0.9913, 0.9912, 0.9913 and 0.9912 while the mean was 0.9913. New tentative UV-Vis fingerprint (Figure 21), the median of spectrum of the reddish group after exclusion of sample10 (n = 16), and the new lower bound, 0.9913, were applied for testing the remained reddish roselle. All of the correlation

coefficients between the new tentative fingerprint and each spectrum were more than 0.9913 (Table 16). Thus all of the reddish samples were qualified.

To examine whether the obtained UV-Vis fingerprint (Figure 21) and the corresponding lower bound, 0.9913, could be applied to distinguish the unqualified (brownish and small calyx samples) from the qualified samples or not, the fingerprint were tested with the unqualified samples. By these criteria, almost all of the brownish samples (75%) were misclassified as a qualified reddish sample (Table 16). In this situation the established UV-Vis fingerprint(Figure 21) and the corresponding critical value of correlation coefficient, 0.9913, could not be regarded as a good fingerprint of roselle.

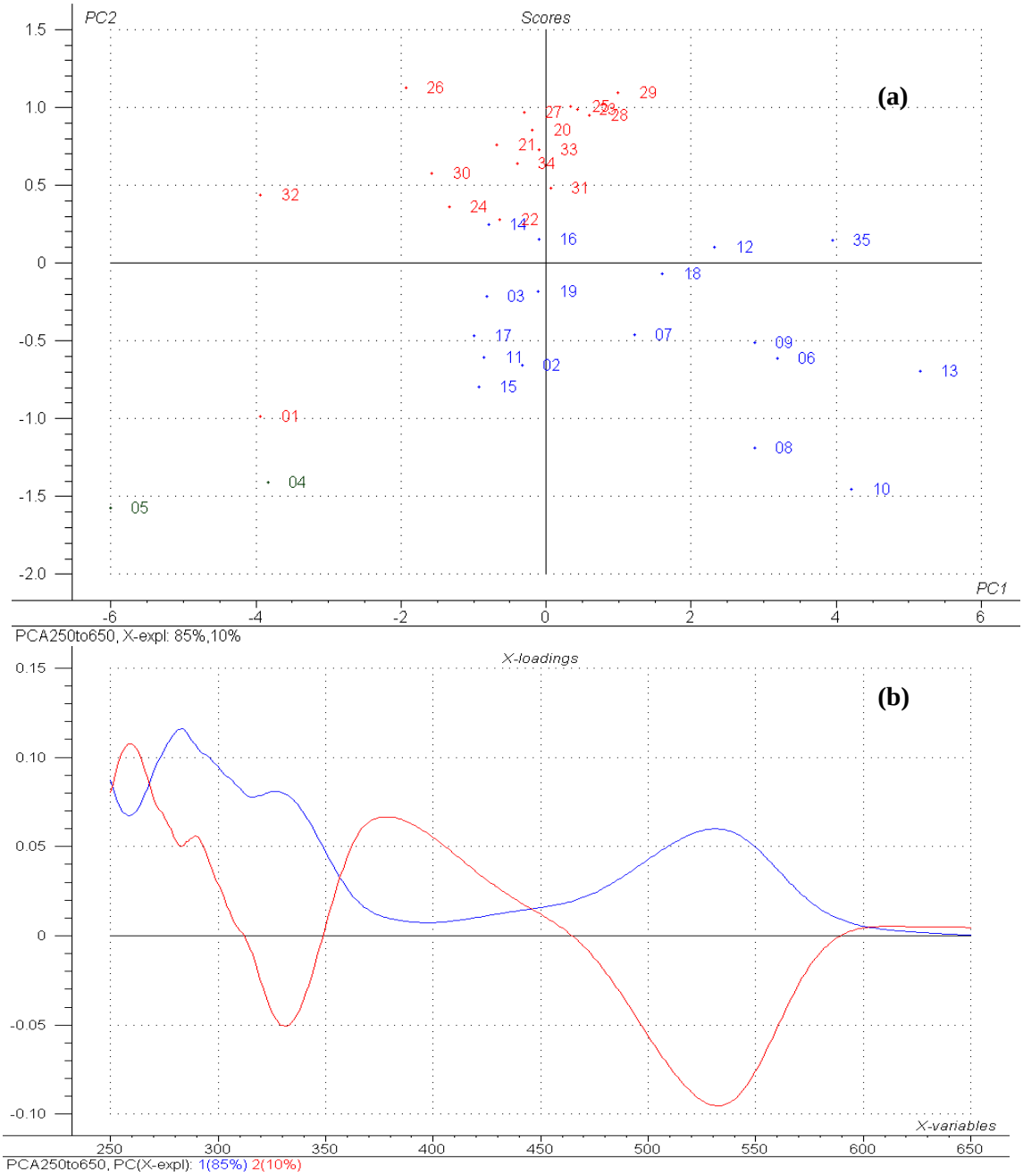

Figure 19 PCA of UV-visible spectra in the region of 250 to 650 nm of roselle extract (n = 35) prepared from 50% methanol: **a)** score plot of PC1 (85% X-variance explained) and PC2 (10% X-variance explained), blue markers = the reddish samples, red markers = the brownish samples, green markers = the small calyx samples, 01-35 = sample number **b)** loading plot of x-variables, blue line = PC 1, red line = PC2

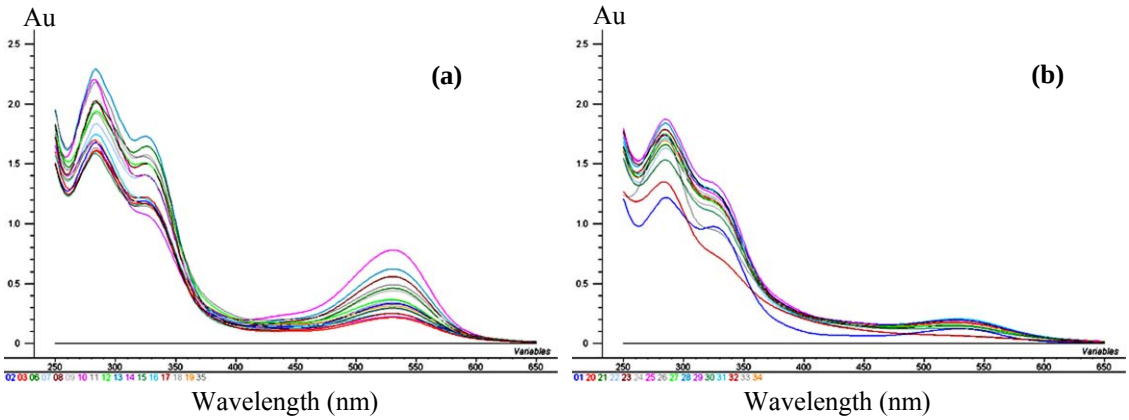

Figure 20 UV-Vis spectra in the region of 250 to 650 nm of roselle extract prepared from 50% methanol: **a)** the reddish samples (n = 17) and **b)** the brownish samples (n =16)

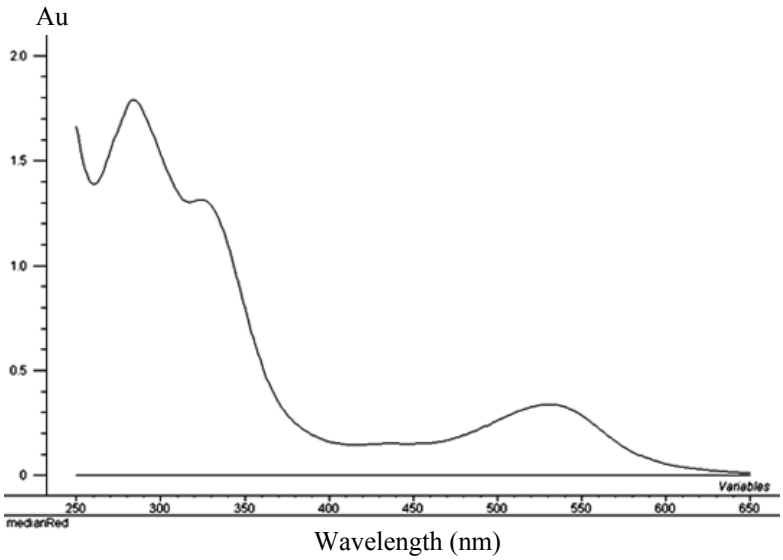

Figure 21 Median of UV-Vis spectra in the region of 250 to 650 nm of the reddish roselle extract after exclusion of outlier sample (n = 16)

Table 16 Correlation coefficients between UV-Vis fingerprint of roselle and UV-Vis spectrum of each sample

Sample number	Predefined group	Correlation coefficient[a]	Quality classification
01	Brown	0.9952	Qualified[b]
02	Red	0.9997	Qualified
03	Red	0.9983	Qualified
04	Small calyx	0.9773	Unqualified
05	Small calyx	0.9804	Unqualified
06	Red	0.9961	Qualified
07	Red	0.9993	Qualified
08	Red	0.9934	Qualified
09	Red	0.9976	Qualified
10	Red	0.9771	Unqualified[c]
11	Red	0.9998	Qualified
12	Red	0.9991	Qualified
13	Red	0.9943	Qualified
14	Red	0.9943	Qualified
15	Red	0.9998	Qualified
16	Red	0.9981	Qualified
17	Red	0.9996	Qualified
19	Red	0.9986	Qualified
20	Brown	0.9923	Qualified[b]
21	Brown	0.9914	Qualified[b]
22	Brown	0.9955	Qualified[b]
23	Brown	0.9930	Qualified[b]
24	Brown	0.9921	Qualified[b]
25	Brown	0.9918	Qualified[b]
26	Brown	0.9759	Unqualified
27	Brown	0.9906	Unqualified
28	Brown	0.9939	Qualified[b]
29	Brown	0.9938	Qualified[b]
30	Brown	0.9890	Unqualified
31	Brown	0.9957	Qualified[b]
32	Brown	0.9733	Unqualified
33	Brown	0.9937	Qualified[b]
34	Brown	0.9935	Qualified[b]
35	Red	0.9992	Qualified

[a] Correlation coefficient between UV-Vis fingerprint of roselle and UV-Vis spectrum of each sample (critical correlation coefficient = 0.9913)
[b] Misclassified samples
[c] Outlier sample

4.5 Infrared (IR) fingerprint

The diffuse reflectance infrared Fourier transform (DRIFT) spectra presented in Kubelka-Munk unit between 4000 to 400 cm^{-1} of each sample was shown in Figure 22. The region above 2000 cm^{-1} were excluded because of large disturbance from –OH absorption of moisture and antisymmetric C=O stretching of carbon dioxide in the environment with the band around 3400 cm^{-1} and 2349 cm^{-1}, respectively. Thus, the spectrum in the region of 2000 to 600 cm^{-1} was surveyed for constructing the IR fingerprint.

The spectra in the range of 2000 to 600 cm^{-1} (Figure 23) were analyzed by PCA. The PCA was implemented on the data matrix of the DRIFT spectrum. Each row represented the spectrum of each sample. Thus the size of data matrix was 35 x 727, while 35 was the number of sample and 727 was the number of response in Kubelka-Munk unit collected at each wavelength. The PCA score plot of baseline corrected spectra (Figure 24a) showed that in the selected region, the IR spectra of the reddish samples were not different from those of the brownish samples. The IR region (2000 to 600 cm^{-1}) which could not differentiate the groups of roselle sample should not be a good fingerprint of roselle as previously mentioned in the section 1 that the reddish samples were classified as a higher grade material while the brownish samples and the small calyx samples were a lower grade material and a distinctively found one, respectively. Thus, for classifying of materials, subranges of wavenumber were examined.

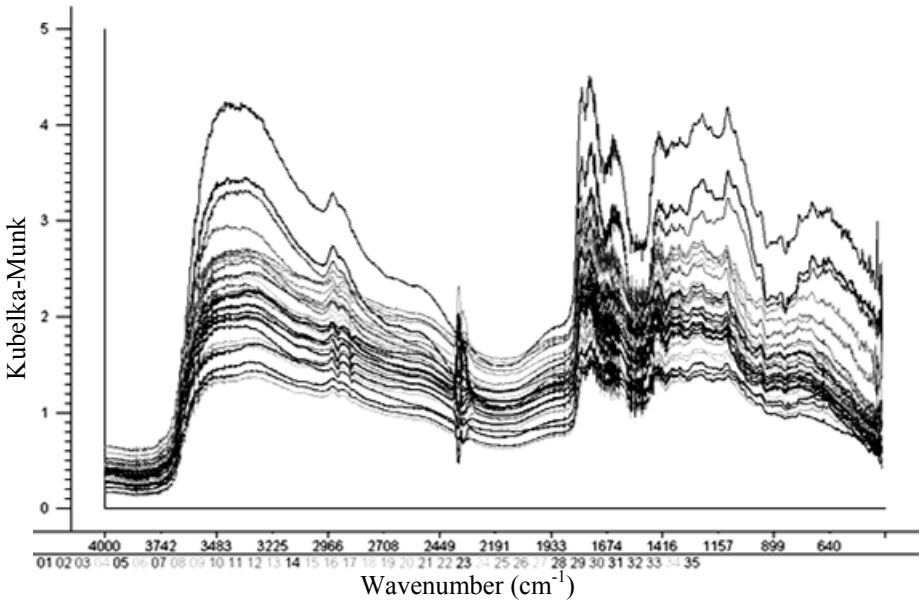

Figure 22 DRIFT spectra in the region of 4000 to 400 cm^{-1} of roselle powder (n = 35)

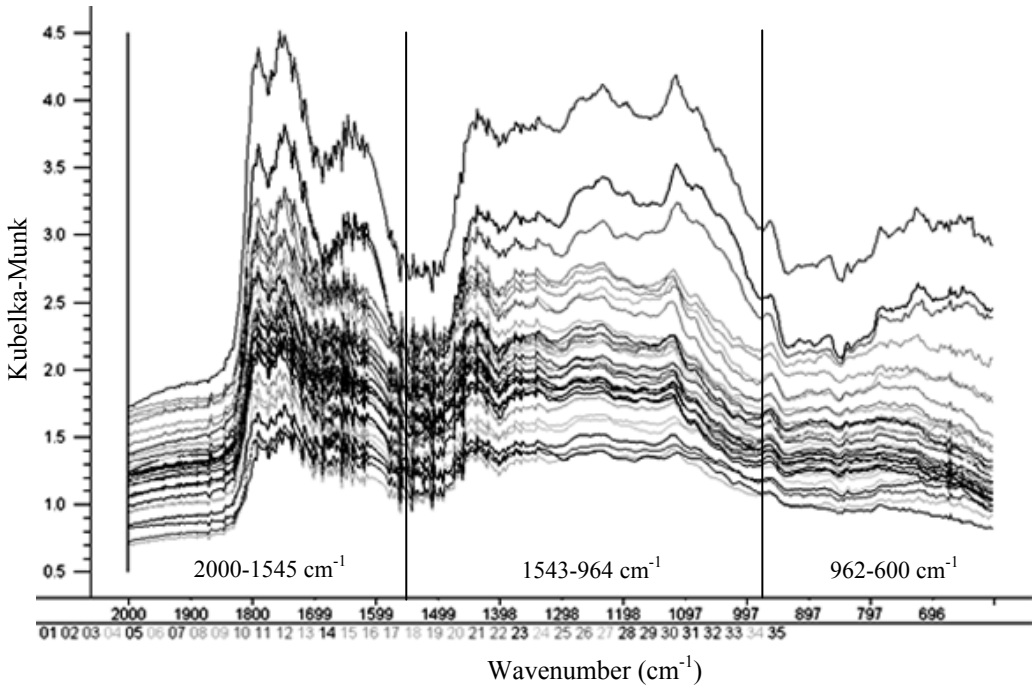

Figure 23 DRIFT spectra in the region of 2000 to 600 cm^{-1} of roselle powder (n = 35)

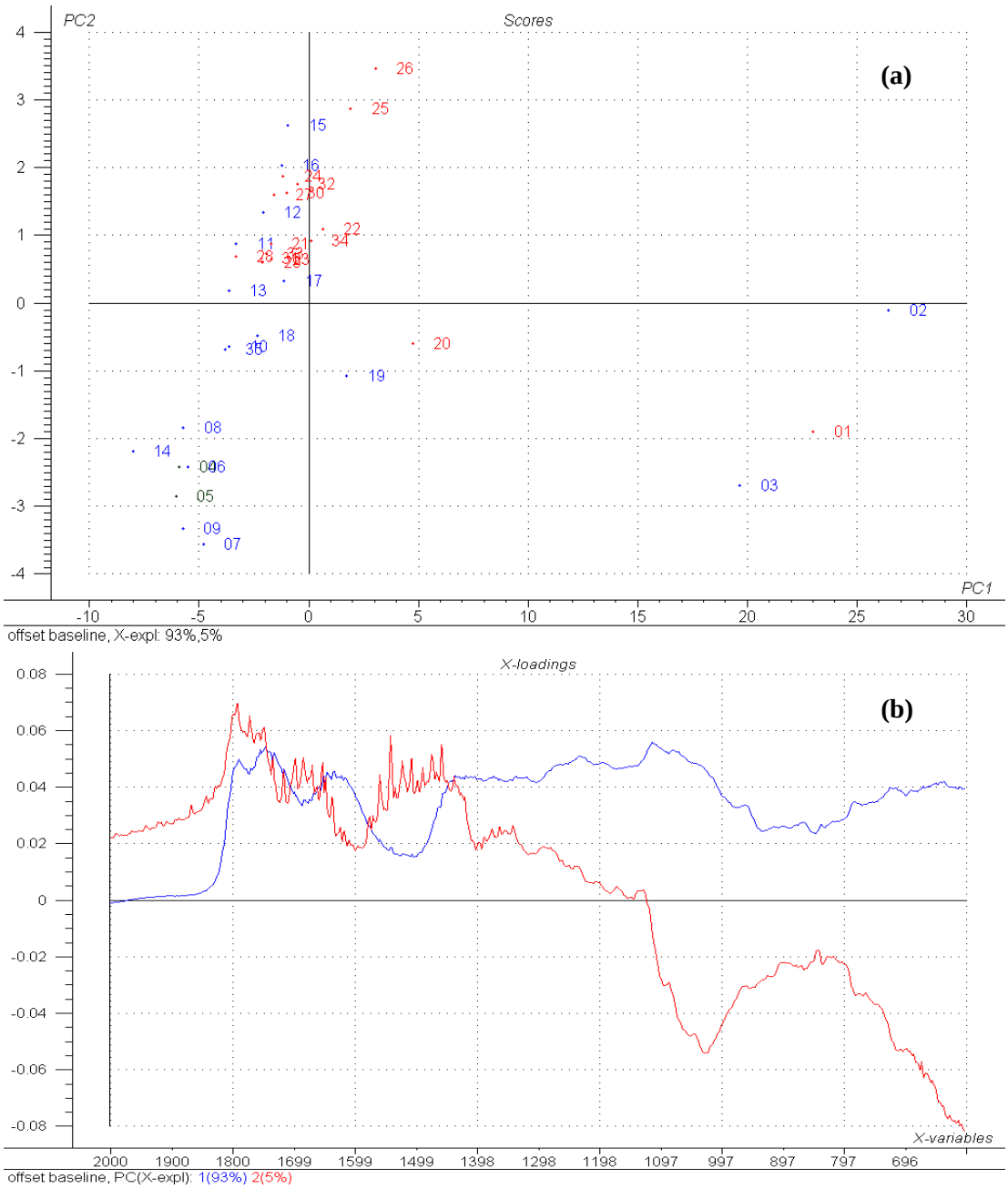

Figure 24 PCA of the DRIFT spectra in the region of 2000 to 600 cm^{-1} of roselle powder (n = 35): **a)** score plot of PC1 (93% X-variance explained) and PC2 (5% X-variance explained), blue markers = the reddish samples, red markers = the brownish samples, green markers = the small calyx samples, 01-35 = sample number, **b)** loading plot of x-variables, blue line = PC 1, red line = PC2

Among the tested ranges (2000 to1545 cm^{-1}, 1543 to 964 cm^{-1} and 962 to 600 cm^{-1}) the last region (962 to 600 cm^{-1}) seemed to be the best area for classification of roselle. The baseline corrected spectra (Figure 25) were analyzed by PCA. The PCA score plot of spectra in this region exhibited coarse clusters of the reddish, the brownish and the small calyx samples (Figure 26a). The samples from brownish group were located more towards the positive end of PC1 while the samples from reddish group were widely scattered more towards the negative end of PC1. While the positions on the PC2 axis of both group seemed to be not different. Like the score plot of UV-Vis spectra, the score plot of DRIFTspectra showed some overlapping. Sample number 1, 2 and 3 had their own characteristics and they were located more towards the positive end of PC2 while the rest samples were located around the origin of PC2. The PCA score plot (Figure 26a) and the loading plot of PC1 (Figure 26b) showed that the DRIFT spectrum of the reddish samples (Figure 27a) tended to have less intensity than those of the brownish samples (Figure 27b).Since the clusters of the reddish and the brownish roselle partly coverd on each other, the representative DRIFT fingerprint could not be established here.

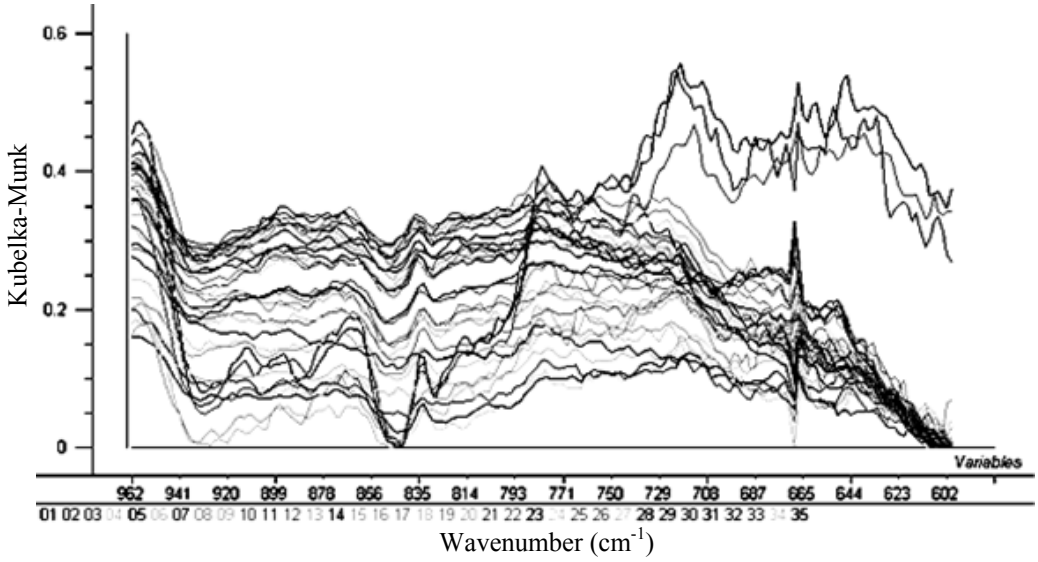

Figure 25 DRIFT spectra after baseline correction in the region of 962 to 600 cm^{-1} of roselle powder (n = 35)

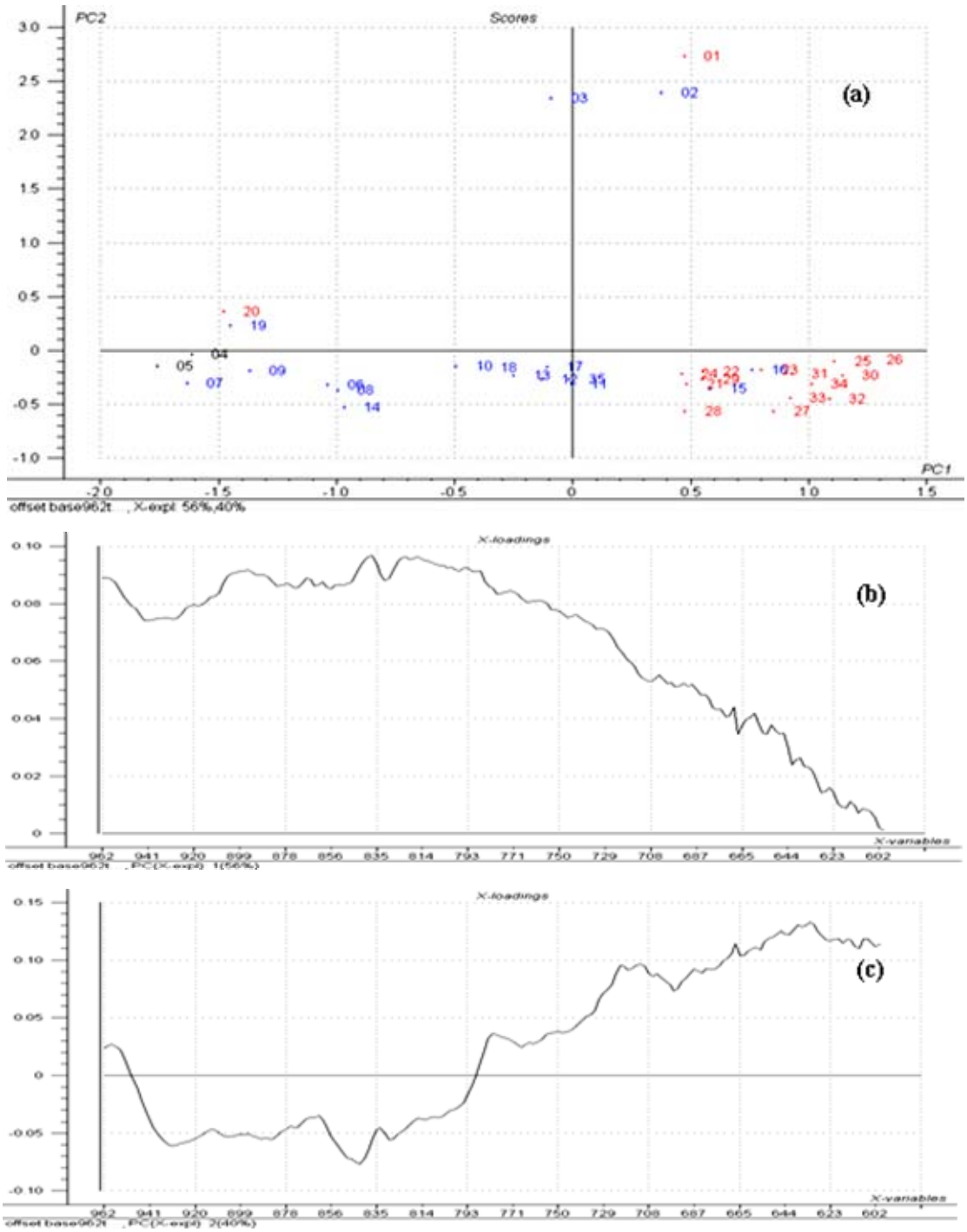

Figure 26 PCA of the DRIFT spectr in the region of 962 to 600 cm^{-1} of roselle powder (n = 35): **a)** score plot of PC1 (56% X-variance explained) and PC2 (40% X-variance explained), blue markers = the reddish samples, red markers = the brownish samples, green markers = the small calyx samples, 01-35 = sample number, **b)** loading plot of x-variables of PC 1, **c)** loading plot of x-variables of PC2

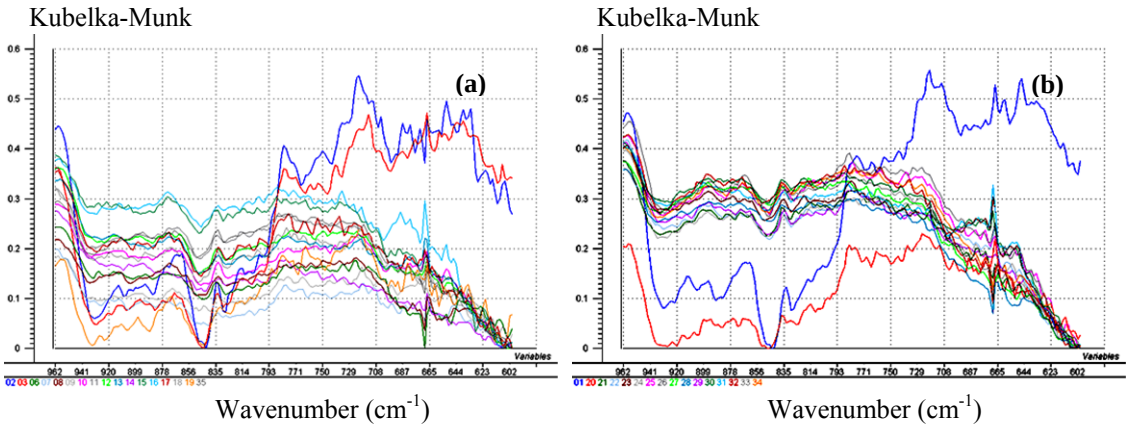

Figure 27 DRIFT spectra in the region of 962 to 600 cm^{-1} of roselle powder (n = 35): **a)** the reddish samples (n = 17) and **b)** the brownish samples (n =16)

5 Quantitative control methods

5.1 Development of method for analysis of total anthocyanins in *H. sabdariffa*

5.1.1 pH-differential spectrophotometry

5.1.1.1 Sample preparation

To find a suitable condition for the extraction of anthocyanins from roselle, the most appropriate solvent and the optimize herb to solvent ratio (w/v) were surveyed. Because anthocyanins are water soluble and it can also be extracted with polar organic solvents, a variety of solvents based on an aqueous-methanolic system (0 to 100% methanol), and an acidified aqueous-methanolic system (0.1% hydrochloric acid in 50 to 100% methanol) were tested while the herb to solvent ratio was fixed at 1:100 (w/v). The result (Figure 28) showed that, the calculated absorbance value of 0.1% hydrochloric acid in 75% methanol extract (0.821) was the highest and significantly different from those of the other extract ($p < 0.05$), except for 0.1% hydrochloric acid in 100% methanol extract. Although the absorbance of 0.1% hydrochloric acid in 75% methanol extract was not different from that of 0.1% hydrochloric acid in 100% methanol extract, the absorbance of the former was obviously higher than that of the latter. Thus the most appropriate solvent was 0.1% hydrochloric acid in 75% methanol.

Then the optimize herb to solvent ratio of the selected solvent, 0.1% hydrochloric acid in 75% methanol, was investigated on the varied herb to solvent ratios, the ratios from 1 : 50 to 1 : 300 (w/v). The calculated absorbance value was transformed to extractive content of total anthocyanins, based on the calibration curve of standard anthocyanin or delphinidin-3-sambubioside. The result (Figure 29) showed that,

when the herb to solvent ratio was increased from 1 : 100 to 1 : 50, the extractive total anthocyanin content was decreased from 1.03 to 0.87%; therefore the maximum herb to solvent ratio was seemed to be 1 : 100. In other words, to achieve the exhaustive extraction, the minimum volume of the solvent was 100 ml per 1 g of plant material. Additional solvent did not increase extractive capability. At the herb to solvent ratios from 1 : 100 through 1 : 300, extractive contents of total anthocyanins were not different ($p > 0.05$). However the solvent to sample ratio was adjusted to 100 : 0.64 (v/w) in order that the extracts of all samples could be analyzed in an appropriate range of absorbance values. Thus the sample was prepared by the method described in Chapter III, Materials and Methods, under section 5.1.2.4.

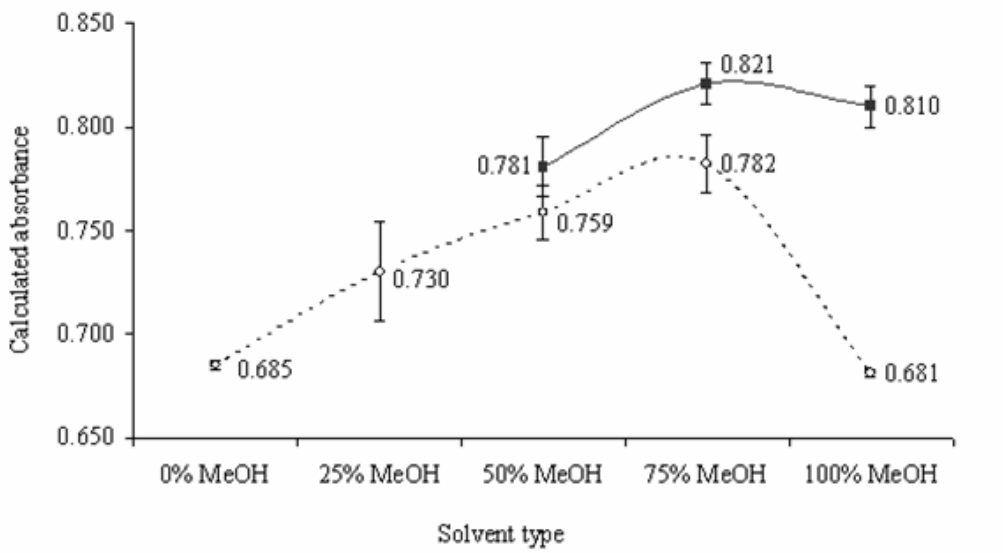

Figure 28 Calculated absorbance values (mean and SD, n = 6) of extracts prepared from an aqueous-methanolic system (0, 25, 50, 75 and 100% methanol) (○), and an acidified aqueous-methanolic system (0.1% hydrochloric acid in 50, 75 and 100% methanol) (●)

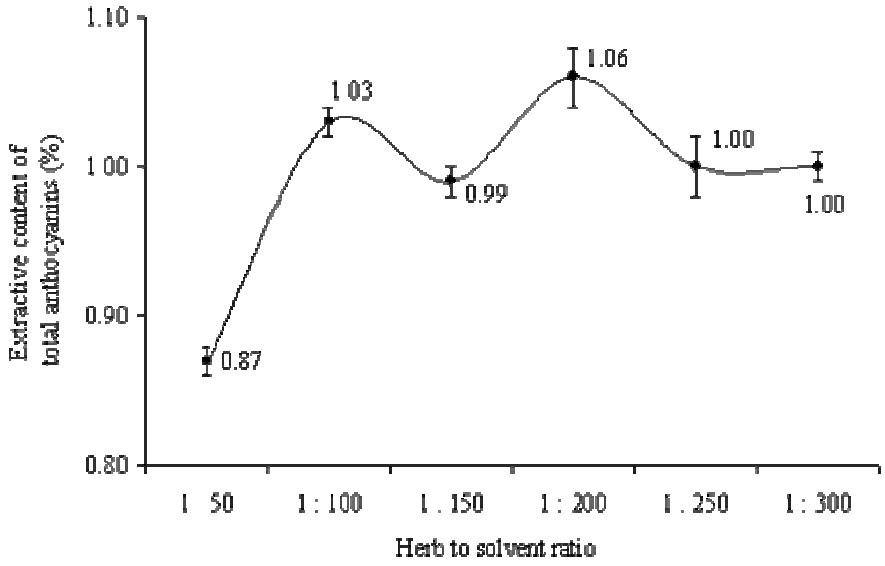

Figure 29 Extractive content of total anthocyanins[a] (mean and SD, n = 6) of extracts prepared from 0.1% hydrochloric acid in 75% methanol at the herb to solvent ratio of 1 : 50, 1 : 100, 1 : 150, 1 : 200, 1 : 250 and 1 : 300 (w/v)

[a] The calculated value was based on the calibration curve of delphinidin-3-sambubioside

5.1.1.2 Sample analysis

The roselle samples were analyzed by the pH-differential spectrophotometric method. Based on the calibration curve of delphinidin-3-sambubioside (Figure 30), the percentages of total anthocyanins content in 35 samples of roselle were calculated. The result was shown in Table 17 (Method 1). Comparing between the results of this original pH-differential spectrophotometry (Method I in Table 17) and those of modified pH-differential spectrophotometry (Method II in Table 17), the results of these two method were significantly different (paired samples test, $p < 0.05$). Method 1 gave higher results than Method II. However, the differences were very few i.e. the average difference was only 0.0029 (paired samples test, $p < 0.05$). Comparing this difference with the variation originated from analytical method itself, the SD, this statistical significant different seemed to be meaningless.

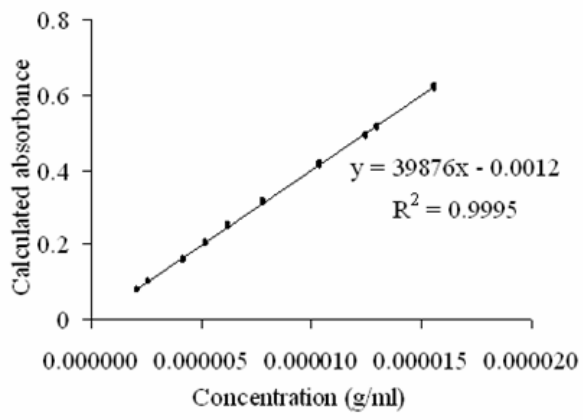

Figure 30 Calibration curve of delphinidin-3-sambubioside (Dp-3-sam) analyzed by the pH- differential spectrophotometric method

Table 17 Comparison between total anthocyanin content (% w/w calculated as Dp-3-sam based on dried weight) in roselle (mean ± SD) determined by the pH-differential spectrophotometric method (Method 1) and the modified pH-differential spectrophotometric method (Method 2)

Sample number	Total anthocyanins (%)		Sample number	Total anthocyanins (%)	
	Method 1[a]	Method 2[b]		Method 1[a]	Method 2[b]
01	0.51 ± 0.01	0.51 ± 0.01	19	1.24 ± 0.01	1.24 ± 0.01
02	1.38 ± 0.01	1.38 ± 0.01	20	0.49 ± 0.00	0.49 ± 0.00
03	1.30 ± 0.02	1.29 ± 0.02	21	0.51 ± 0.01	0.51 ± 0.01
04	0.33 ± 0.00	0.32 ± 0.00	22	0.67 ± 0.00	0.67 ± 0.00
05	0.11 ± 0.00	0.11 ± 0.00	23	0.66 ± 0.00	0.66 ± 0.00
06	2.17 ± 0.02	2.16 ± 0.02	24	0.45 ± 0.01	0.45 ± 0.01
07	1.79 ± 0.01	1.78 ± 0.01	25	0.58 ± 0.01	0.58 ± 0.01
08	2.56 ± 0.01	2.55 ± 0.01	26	0.05 ± 0.00	0.05 ± 0.00
09	1.97 ± 0.01	1.97 ± 0.01	27	0.47 ± 0.02	0.47 ± 0.02
10	2.96 ± 0.02	2.95 ± 0.02	28	0.69 ± 0.01	0.68 ± 0.01
11	1.33 ± 0.01	1.32 ± 0.01	29	0.67 ± 0.00	0.67 ± 0.00
12	1.77 ± 0.02	1.77 ± 0.02	30	0.37 ± 0.00	0.37 ± 0.00
13	2.65 ± 0.01	2.64 ± 0.01	31	0.65 ± 0.01	0.65 ± 0.01
14	1.86 ± 0.01	1.86 ± 0.01	32	0.06 ± 0.00	0.06 ± 0.00
15	1.59 ± 0.01	1.59 ± 0.01	33	0.62 ± 0.00	0.62 ± 0.00
16	1.04 ± 0.01	1.04 ± 0.01	34	0.63 ± 0.00	0.63 ± 0.00
17	1.22 ± 0.02	1.22 ± 0.02	35	2.03 ± 0.02	2.03 ± 0.02
18	1.84 ± 0.01	1.83 ± 0.01			

[a] Calculation was based on a calibration curve of delphinidin-3-sambubioside

[b] Calculation was based on a simulation calibration curve of delphinidin-3-sambubioside

5.1.2 Modified pH-differential spectrophotometry

5.1.2.1 Determination of a correlation factor between delphinidin-3-sambubioside and methyl orange

Because a task and high expenditure was needed to obtain standard anthocyanin, it was not quite practicable to use anthocyanin as a routine standard. Modified pH-differential spectrophotometry was developed to solve the problem. Methyl orange is a commonly used pH indicator. At pH 1.0, it appears as red while turning yellow at pH 4.5. This color changing property was quite similar to that of delphinidin-3-sambubioside. Therefore methyl orange was tested to be used as a routine standard for quantitative determination of total anthocyanins. The idea of this alternative method has been used in the official monograph of European Pharmacopoeia 2001 [19] for the quantitative analysis of some herbal markers.

A relative concentration between methyl orange and delphinidin-3-sambubioside that possessed the same absorbance value was setup from their calibration curve as follows,

$$A_{\text{del-3-sam}} = 39876\, C_{\text{del-3-sam}} - 0.0012,$$

$$A_{\text{methyl orange}} = 101192\, C_{\text{methyl orange}} + 0.0067,$$

where

$A_{\text{del-3-sam}}$ is a calculated absorbance of delphinidin-3-sambubioside,

$C_{\text{del-3-sam}}$ is a concentration of delphinidin-3-sambubioside (g/ml),

$A_{\text{methyl orange}}$ is a calculated absorbance of methyl orange, and

$C_{\text{methyl orange}}$ is a concentration of methyl orange (g/ml).

If

$$A_{\text{del-3-sam}} = A_{\text{methyl orange}},$$

then

$$39876\, C_{\text{del-3-sam}} - 0.0012 = 101192\, C_{\text{methyl orange}} + 0.0067$$

$$C_{\text{del-3-sam}} = 2.5377\, C_{\text{methyl orange}} + 1.98\times10^{-7}.$$

The relative concentration equation between delphinidin-3-sambubioside and methyl orange demonstrated that in two solutions that possess the same absorbance value, the concentration of the solution of delphinidin-3-sambubioside will be about 2.5377 times of the concentration of the solution of methyl orange. This relative

concentration or correlation factor will be used for transforming between the concentrations of delphinidin-3-sambubioside and methyl orange at the same absorbance value.

5.1.2.2 Sample analysis

The roselle samples were analyzed by the modified pH-differential spectrophotometric method. A simulated calibration curve of delphinidin-3-sambubioside (Figure 31b) was constructed from a calibration curve of methyl orange (Fig 31a) *via* the correlation factor described in 5.1.2.1. Based on the simulated calibration curve of delphinidin-3-sambubioside, the total anthocyanins content in 35 samples of roselle were calculated. The results were shown in Table 17 (Method 2).

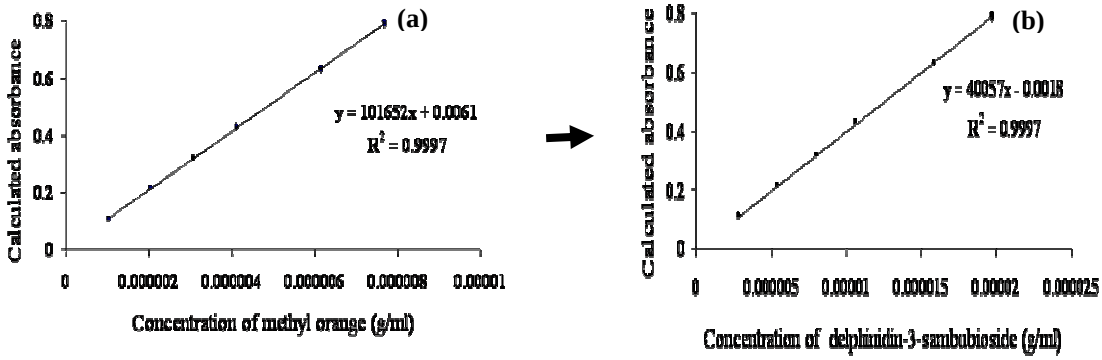

Figure 31 Calibration curve analyzed by the modified pH- differential spectrophotometric method: **a)** calibration curve of methyl orange and **b)** simulated calibration curve of delphinidin-3-sambubioside

5.1.3 Validation of modified pH-differential spectrophotometry

The modified pH-differential spectrophotometric method for quantitative determination of total anthocyanins of roselle was validated according to ICH guidelines [124]. Linearity of Dp-3-sam and methyl orange assessed in the range of 2.6 - 15.6 µg/ml and 1.0 - 7.7 µg/ml, respectively, showed good linearity. The regression lines were y = 39862x – 0.0004, r^2 = 0.9994 and y = 101652x + 0.0061, r^2 = 0.9997, respectively. The simulated calibration curve also showed good linearity over the range of 2.8 - 19.7 µg/ml. The regression lines was y = 40057x – 0.0018, r^2 = 0.9997 (Table 18).

Repeatability studied in 3 replicates of 3 samples which contained different amount of total anthocyanins showed low RSD (< 6%). Intermediate precision analyzed in 3 samples in 3 consecutive days also showed low RSD (< 5%) (Table 18). The repeatability and the intermediate precision of the pH-differential spectrophotometric

method (Method 1) and the modified pH-differential spectrophotometric method (Method 2) were not very much different. They were considered as a good reliability based on the guidance for industry that suggested the precision determined at each concentration level of bioanalytical method should not exceed 15% [133]. The overall precision evaluated results indicated that the modified method was precise for the determination of anthocyanin content in roselle.

Limit of detection (LOD) and limit of quantitation (LOQ) calculated by using the formulae 3.3δ/s and 10δ/s, respectively of the modified method was 0.28 and 0.85 μg/ml, respectively. While LOD and LOQ of original method were 0.06 and 0.19 μg/ml, respectively (Table 18).

Specificity of the method was assured by the basis of the pH-differential method that was specially designed for the determination of total monomeric anthocyanin content in plant materials [101], [134]. Moreover, the results from the modified pH-differential spectrophotometric method were also compared with those from the independent, the HPLC method. HPLC chromatogram of roselle revealed two major and a minor anthocyanins identified as Dp-3-sam, cyanidin-3-sambubioside (Cy-3-sam) and delphinidin-3-glucoside (Dp-3-glu), respectively (Figure 32). The identification was performed by comparing their retention times with that of the standard Dp-3-sam and those previously reported [116]. Total anthocyanin content was calculated based on total peak area of anthocyanins against the calibration curve of Dp-3-sam ($y = 24439688x - 115.6817$, $r^2 = 0.9998$) (Figure 33). The results of the developed method were not different from those of the HPLC method (paired t-test, $p = 0.71$) (Table 19).

All of the validation studies of the modified method reveal acceptable results compared with the original method (Table 18). Moreover, amounts of total anthocyanins in 35 roselle samples determined by the modified method and the original method were nearly the same (Table 17 and Figure 34). Therefore, the simple, specific, precise, and accurate spectrophotometric method suggested in this study could be used as a routine method for the analysis of total anthocyanin content in roselle.

Table 18 Validation parameters of the pH-differential spectrophotometric method (Method 1) and the modified pH-differential spectrophotometric method (Method 2)

Parameters	**Method 1**			**Method 2**		
Range (µg/ml)	2.6-15.6			2.8-19.7		
Slope	39862			40057		
Intercept	-0.0004			-0.0018		
r^2	0.9994			0.9997		
Limit of detection (LOD (µg/ml))	0.06			0.28		
Limit of quantitation (LOQ (µg/ml))	0.19			0.85		
	Day 1	Day 2	Day 3	Day 1	Day 2	Day 3
Precision (%RSD)						
Repeatability						
Sample 01 (n = 3)	2.87	0.56	0.80	2.79	0.56	0.78
Sample 05 (n = 3)	5.75	4.45	0.80	5.93	4.42	0.79
Sample 10 (n = 3)	0.53	0.95	0.53	0.55	0.96	0.53
Intermediate precision (3 days)						
Sample 01	1.98			1.91		
Sample 05	4.53			4.60		
Sample 10	1.25			1.75		

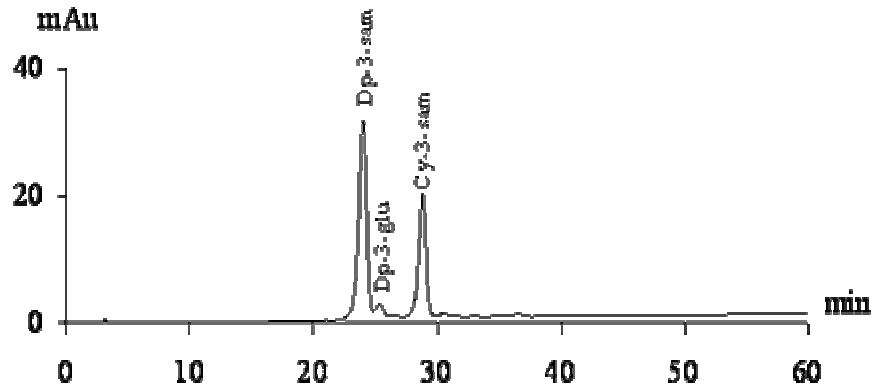

Figure 32 HPLC chromatogram of roselle extract prepared from 0.1% hydrochloric acid in 75% methanol: Dp-3-sam = delphinidin-3-sambubioside, Dp-3-glu = delphinidin-3-glucoside, Cy-3-sam = cyanidin-3-sambubioside, *solvent A = 4% phosphoric acid, solvent B = 100% acetonitrile*, solvent program = 0-10 min isocratic elution with 6% *B*, 10-55 min linear gradient to 20% *B*, 56-60 min isocratic elution with 20% *B*, detection at 520 nm

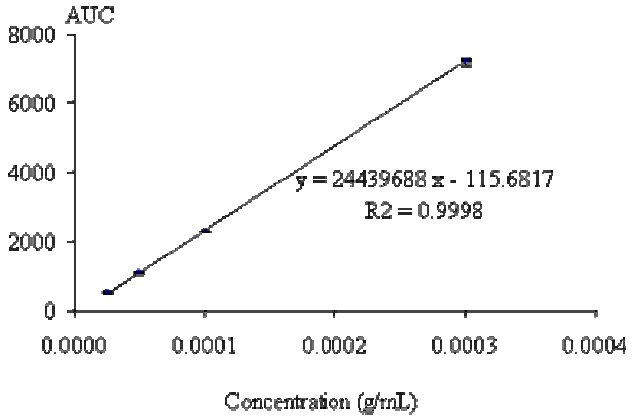

Figure 33 Calibration curve of delphinidin-3-sambubioside analyzed by the HPLC method: *solvent A = 4% phosphoric acid, solvent B = 100% acetonitrile*, solvent program = 0-10 min isocratic elution with 6% *B*, 10-55 min linear gradient to 20% *B*, 56-60 min isocratic elution with 20% *B*, detection at 520 nm

Table 19 Comparison between total anthocyanin content (% w/w calculated as Dp-3-sam based on dried weight) determined by the modified pH-differential spectrophotometric method and the HPLC method (mean ± SD for three replicates)

Sample number	Modified pH-differential spectrophotometric method	HPLC method
01	0.49 ± 0.00	0.47 ± 0.02
03	1.30 ± 0.01	1.28 ± 0.06
04	0.30 ± 0.00	0.25 ± 0.00
10	2.85 ± 0.01	2.92 ± 0.00
19	1.19 ± 0.02	1.14 ± 0.06
30	0.29 ± 0.00	0.26 ± 0.00
35	2.00 ± 0.02	2.05 ± 0.02

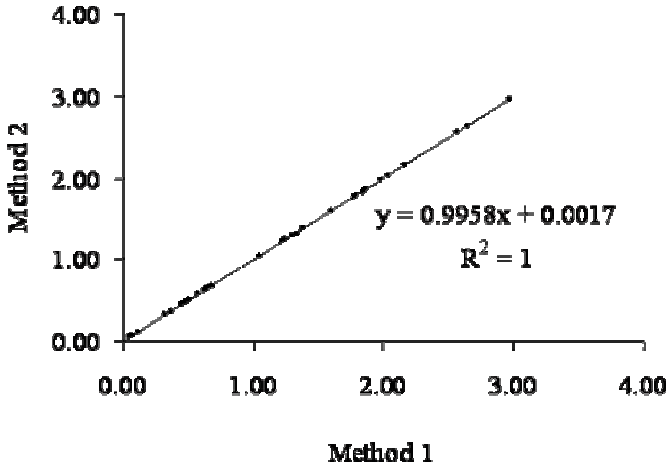

Figure 34 Comparison between total anthocyanin content (% w/w calculated as Dp-3-sam based on dried weight) in roselle determined by the pH-differential spectrophotometric method (Method 1) and the modified pH-differential spectrophotometric method (Method 2)

5.2 Analysis of total phenolic compounds

5.2.1 Sample preparation

To find a suitable condition for the extraction of phenolic compounds from roselle, the most suitable solvent and the optimize herb to solvent ratio (w/v) were surveyed. A variety of solvents based on an aqueous-methanolic system (0 to 100% methanol), and an acidified aqueous-methanolic system (0.1% hydrochloric acid in 50 to 100% methanol) were tested while the herb to solvent ratio was fixed at 1:100 (w/v). The result (Figure 35) showed that, the absorbance value of the 50% methanol extract (0.950) was the highest. Although the absorbance of 50% methanol extract was not different from those of 25% methanol extract and 0.1% hydrochloric acid in 50% methanol extract, it was obviously higher. Thus the most suitable solvent was 50% methanol.

Then the optimize herb to solvent ratio (w/v) of the selected solvent, 50% methanol, was investigated on the varied herb to solvent ratios, the ratios from 1 : 50 to 1 : 300 (w/v). The absorbance value was transformed to extractive content of total phenolic compounds, based on the calibration curve of standard gallic acid. The result (Figure 36) showed that, when the herb to solvent ratio was increased from 1 : 300 through 1 : 250, 1 : 200 and 1 : 150, the extractive content of total phenolic compounds had not much changed. The extractive contents of total phenolic compounds at those ratios were not different ($p > 0.05$). But further increasing of herb to solvent ratio from 1 : 150 to 1 : 100 and 1 : 50 caused

the extractive content of total phenolic compounds to gradually decrease from 2.42 to 2.29 and 2.01, respectively ($p < 0.05$). Therefore the maximum herb to solvent ratio was seemed to be 1 : 150. The appropriate herb to solvent ratios were the ratios beginning from 1 : 150 through 1 : 300. According to these results, the sample was prepared by the method described in Chapter III, Materials and Methods, under section 5.2.4.

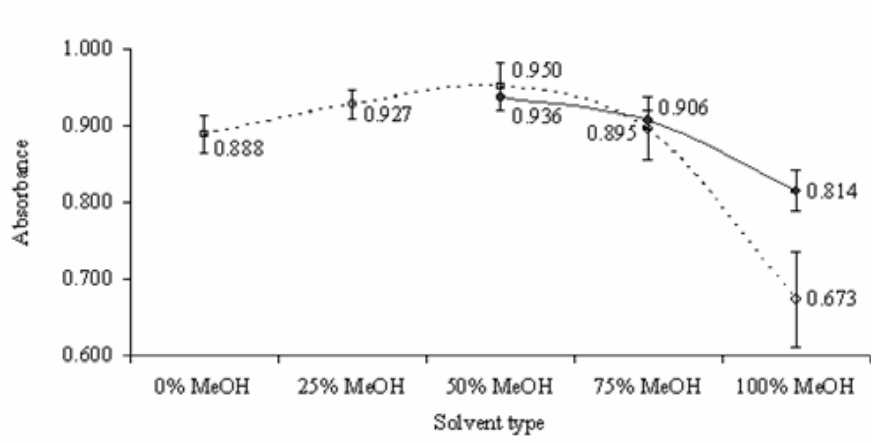

Figure 35 Absorbance values (mean and SD, n = 6) of extracts prepared from an aqueous-methanolic system (0, 25, 50, 75 and 100% methanol) (○), and an acidified aqueous-methanolic system (0.1% hydrochloric acid in 50, 75 and 100% methanol) (●)

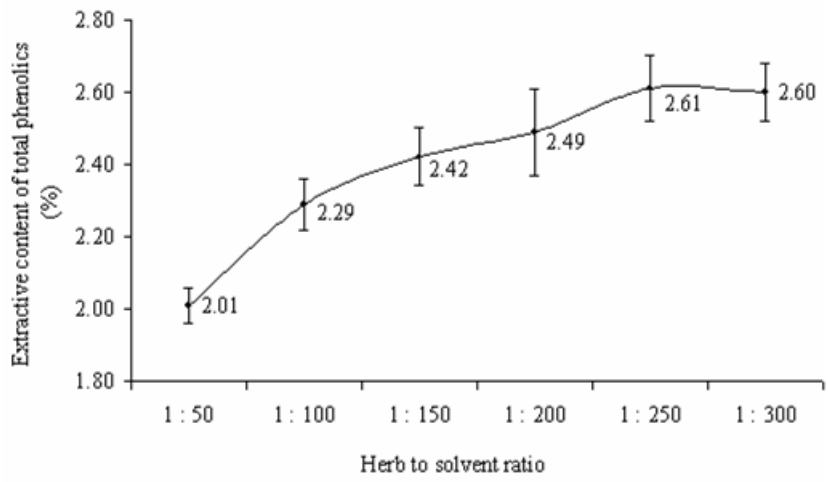

Figure 36 Percent extractive content of total phenolic compounds[a] (mean and SD, n = 6) of roselle extracts prepared from 50% methanol at herb to solvent ratio of 1 : 50, 1 : 100, 1 : 150, 1 : 200, 1 : 250 and 1 : 300 (w/v)

[a] The calculated value was based on the calibration curve of gallic acid

5.2.2 Sample analysis

The content of total phenolic compounds in 35 roselle samples analyzed by the Folin-Ciocalteau's method modified from Waterman [125] were shown in Table 20. Two commercial standards were used as references. Gallic acid, the commonly found phenolic compound, has been generally applied as a standard [135,136,137]. So the gallic acid equivalence (GAE) could be compared with other reports. However, gallic acid has not been reported in roselle. Thus protocatechuic acid, the phenolic compound found in this herb, was also used as an analytical standard. By reference to the calibration curve of gallic acid and the calibration curve of protocatechuic acid, the content of total phenolic compounds was calculated as GAE and protocatechuic acid equivalence (% w/w based on the dried weight), respectively.

Table 20 Content of total phenolic compounds calculated as gallic acid equivalent (GAE) and protocatechuic acid equivalent (% w/w based on the dried weight) in roselle (mean ± SD)

Sample number	Total phenolic compounds (% w/w)		Sample number	Total phenolic compounds (% w/w)	
	Gallic acid equivalence	Protocatechuic equivalence		Gallic acid equivalence	Protocatechuic equivalence
01	1.84 ± 0.03	1.58 ± 0.07	19	2.52 ± 0.01	2.25 ± 0.01
02	2.64 ± 0.02	2.27 ±0.02	20	2.36 ± 0.04	2.10 ± 0.03
03	2.79 ± 0.02	2.40 ± 0.02	21	2.53 ± 0.01	2.24 ± 0.01
04	1.79 ± 0.01	1.53 ± 0.01	22	2.39 ± 0.02	2.13 ± 0.02
05	1.33 ± 0.02	1.13 ± 0.07	23	2.55 ± 0.04	2.26 ± 0.03
06	3.39 ± 0.02	2.92 ± 0.02	24	2.09 ± 0.03	1.86 ± 0.02
07	3.07 ± 0.02	2.63 ± 0.02	25	2.46 ± 0.02	2.18 ± 0.01
08	3.46 ± 0.01	2.97 ± 0.01	26	1.61 ± 0.02	1.45 ± 0.02
09	3.22 ± 0.03	2.80 ± 0.02	27	2.39 ± 0.01	2.06 ± 0.01
10	3.57 ± 0.04	3.09 ± 0.07	28	2.59 ± 0.04	2.23 ± 0.03
11	2.52 ± 0.02	2.20 ± 0.01	29	2.64 ± 0.01	2.27 ± 0.01
12	3.16 ± 0.01	2.75 ± 0.01	30	2.19 ± 0.01	1.90 ± 0.01
13	3.58 ± 0.01	3.10 ± 0.01	31	2.39 ± 0.01	2.07 ± 0.01
14	2.65 ± 0.02	2.30 ± 0.02	32	1.51 ± 0.01	1.32 ± 0.01
15	2.67 ± 0.02	2.33 ± 0.01	33	2.32 ± 0.02	2.01 ± 0.01
16	2.56 ± 0.03	2.24 ± 0.03	34	2.42 ± 0.04	2.09 ± 0.03
17	2.53 ± 0.01	2.26 ± 0.01	35	3.43 ± 0.02	2.95 ± 0.02
18	3.11 ± 0.02	2.76 ± 0.02			

5.2.3 Method validation

The Folin-Ciocalteau's method was used with some verification. The summary of verification results were shown in Table 21. Linearity of gallic acid and protocatechic acid assessed in the range of 1.57 - 10.20 μg/ml and 1.82 - 7.26 μg/ml, respectively, showed good linearity. The regression lines were y = 105977x + 0.0165, r^2 = 0.9993 and y = 128217x – 0.0361, r^2 = 0.9992, respectively (see also Figure 37). Repeatability studied in 6 replicates of 3 samples which contained different amount of total anthocyanins show low RSD (< 3%). Intermediate precision analyzed in 3 samples in 3 consecutive days also show low RSD (< 6%). LOD and LOQ calculated by using the formulae 3.3δ/s and 10δ/s, respectively, of the GAE method was 0.17 and 0.52 μg/ml, respectively while those of the protocatechuic acid equivalent method was 0.82 and 2.49 μg/ml, respectively.

Table 21 Validation parameters of the Folin-Ciocalteau's method using gallic acid and protocatechuic acid as standards

Parameters	**Gallic acid equivalence**			**Protocatechuic acid equivalence**		
Range (μg/ml)	1.57-10.20			1.82-7.26		
Slope	105977			128217		
Intercept	0.0165			-0.0361		
r^2	0.9993			0.9992		
Limit of detection (LOD (μg/ml))	0.17			0.82		
Limit of quantitation (LOQ (μg/ml))	0.52			2.49		
	Day 1	Day 2	Day 3	Day 1	Day 2	Day 3
Precision (%RSD)						
Repeatability						
Sample 01 (n = 6)	1.69	1.14	0.81	1.72	2.05	0.91
Sample 05 (n = 6)	1.56	1.66	0.80	1.62	1.89	0.91
Sample 10 (n = 6)	1.26	1.22	0.53	0.60	0.79	0.99
Intermediate precision (3 days)						
Sample 01	1.24			4.69		
Sample 05	1.72			5.98		
Sample 10	0.75			2.20		

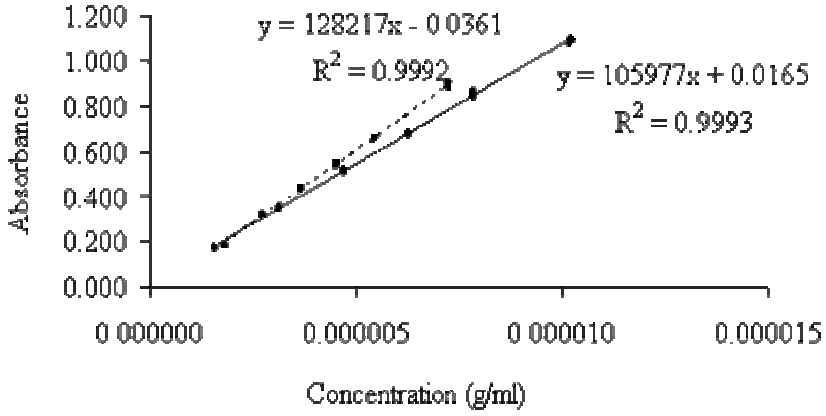

Figure 37 Calibration curve analyzed by Folin-Ciocalteau's method of gallic acid (■) and protocatechuic acid (♦)

5.3 Analysis of acid content

The acid content was determined by using the method described in European Pharmacopoeia (2001) [28]. The acid content calculated as citric acid (% w/w based on the dried weight) of 35 roselle samples was shown in Table 22.

Table 22 Acid content calculated as citric acid (% w/w based on the dried weight) in roselle (mean ± SD)

Sample number	Acid content (% w/w)	Sample number	Acid content (% w/w)
01	16.04 ± 0.02	19	15.32 ± 0.06
02	15.78 ± 0.07	20	12.18 ± 0.17
03	12.20 ± 0.09	21	10.80 ± 0.02
04	20.10 ± 0.02	22	11.09 ± 0.04
05	16.31 ± 0.24	23	11.12 ± 0.05
06	14.33 ± 0.05	24	13.74 ± 0.04
07	13.67 ± 0.18	25	13.21 ± 0.04
08	14.96 ± 0.06	26	15.76 ± 0.06
09	13.74 ± 0.06	27	11.96 ± 0.04
10	17.20 ± 0.03	28	11.75 ± 0.06
11	15.26 ± 0.04	29	11.39 ± 0.08
12	15.40 ± 0.09	30	11.69 ± 0.08
13	15.11 ± 0.10	31	11.47 ± 0.04
14	7.93 ± 0.06	32	14.60 ± 0.02
15	14.32 ± 0.02	33	12.25 ± 0.06
16	13.74 ± 0.02	34	11.95 ± 0.05
17	14.02 ± 0.18	35	13.56 ± 0.15
18	12.42 ± 0.10		

5.4 Analysis of potassium content

The potassium content (% w/w based on the dried weight) analyzed by Inductively Coupled Plasma Emission Spectrophotometer (Varian Liberty 220; Australia) was shown in Table 23.

Table 23 Potassium content (% w/w based on the dried weight) in roselle

Sample number	Potassium[a] (% w/w)	Sample number	Potassium[a] (% w/w)
01	1.77	19	2.60
02	1.49	20	1.59
03	1.81	21	1.59
04	1.48	22	1.59
05	1.93	23	2.72
06	1.50	24	2.03
07	2.45	25	1.49
08	2.06	26	1.86
09	1.90	27	1.32
10	2.05	28	1.40
11	1.75	29	1.39
12	3.13	30	1.32
13	2.02	31	2.24
14	2.17	32	2.54
15	1.96	33	2.62
16	2.22	34	2.44
17	2.32	35	2.67
18	2.33		

[a] SD could not be acquired

6 Radical scavenging activity

6.1 Determination of radical scavenging activity

Recently, there has been wide interested in an antioxidant activity of roselle [10,17,129,138,139,140]. Some studies [17,139,140] used lipid peroxidation assays, and some [129] used free radical scavenging assays. While lipid peroxidation should be the first line of tests to establish the potential antioxidant action [141], the DPPH assay, the assay that measure the scavenging ability of antioxidants towards the stable radical 2,2-diphenyl-1-picryl-hydrazyl (DPPH) has been recommended as a valid and easy assay to evaluate scavenging activity [142]. For quality control purpose, the DPPH assay was selected as the method to measure the scavenging ability of roselle.

The DPPH method was modified from Leong [127]. The activity of roselle samples were compared with that of ascorbic acid, a water soluble antioxidant. By calculation against the calibration curve of ascorbic acid (Figure 38), the result was expressed

as the percentage of ascorbic acid equivalence antioxidant capacity (AEAC) reference to the air-dried substance (Table 24). The precision of the DPPH method calculated as %RSD obtained from six replicate measurements of the three roselle samples were less than 5%.

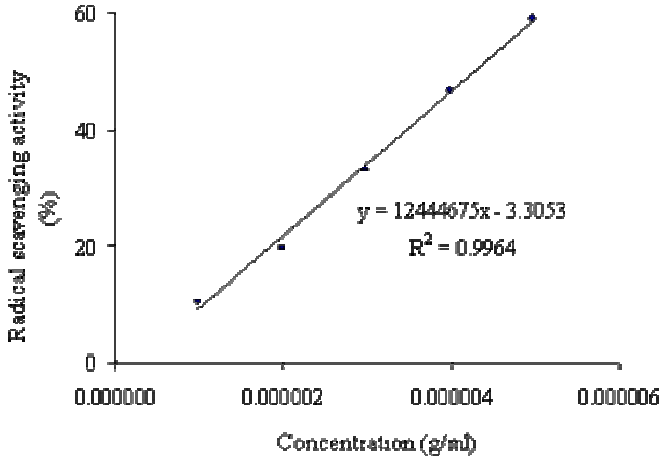

Figure 38 Calibration curve of radical scavenging activity of ascorbic acid analyzed by DPPH method

Table 24 Radical scavenging activity (% w/w equivalence to ascorbic acid) in roselle (mean ± SD)

Sample number	Radical scavenging activity (% w/w equivalence to ascorbic acid)	Sample number	Radical scavenging activity (% w/w equivalence to ascorbic acid)
01	2.67 ± 0.14	19	3.76 ± 0.06
02	4.01 ± 0.17	20	3.32 ± 0.07
03	4.15 ± 0.14	21	3.59 ± 0.11
04	2.36 ± 0.11	22	3.69 ± 0.07
05	1.92 ± 0.16	23	3.71 ± 0.06
06	5.06 ± 0.16	24	3.29 ± 0.21
07	4.69 ± 0.15	25	3.81 ± 0.08
08	5.43 ± 0.13	26	2.68 ± 0.11
09	4.95 ± 0.15	27	3.55 ± 0.12
10	5.80 ± 0.20	28	4.04 ± 0.12
11	4.23 ± 0.15	29	4.16 ± 0.11
12	4.90 ± 0.15	30	3.51 ± 0.07
13	5.74 ± 0.19	31	3.98 ± 0.07
14	4.51 ± 0.18	32	2.84 ± 0.05
15	4.24 ± 0.14	33	3.79 ± 0.08
16	4.02 ± 0.10	34	3.88 ± 0.06
17	4.10 ± 0.12	35	5.55 ± 0.06
18	4.31 ± 0.11		

6.2 Prediction of radical scavenging activity

To save the cost and time for the DPPH assay, a simultaneous method for the determination of scavenging activity and the identification of roselle was developed. The radical scavenging activity would be predicted based on the HPLC chromatogram and the UV-Vis spectral data of the sample, which were also used for identification of plant by fingerprint concept as described in 4.3.3 and 4.4.

Corrected HPLC chromatograms (reproduced as Figure 39) or UV-Vis spectra in the region of 250 to 650 nm (Figure 40) of 35 samples were surveyed by PCA. The PCA score plots of the HPLC chromatograms (reproduced as Figure 41) and the UV-Vis spectra (reproduced as Figure 42) revealed that both the HPLC chromatograms and the UV-Vis spectra of the sample number 1, 4 and 5 were located separately from the others. From the PCA score pattern, it could be expected that the sample number 1, 4 and 5 had their specific characteristics that were different from those of the others. Thus the samples number 1, 4 and 5 were justified as outliers and excluded before model calculation.

The remained samples (n = 32) were divided into the calibration set and the prediction set by random selection. To ensure that the calibration model cover the range of predicted variable, the radical scavenging activity, two samples that possessed the maximum and the minimum value of radical scavenging activity were manually selected to the calibration set. The calibration set and the prediction set contained 60% (n = 19) and 40% (n = 13) of samples, respectively. The descriptive statistics (mean, standard deviation and range) of the radical scavenging activity of both set had been shown in Table 25. The distribution of the radical scavenging activity of the calibration set was wider than that of prediction set.

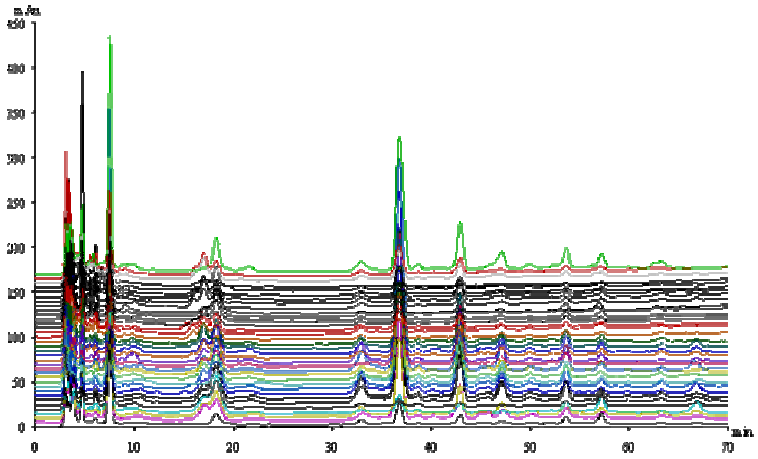

Figure 39 HPLC chromatograms after correction for the time shift of roselle extract prepared from 50% methanol (n = 35): *solvent A = 4% phosphoric acid, solvent B = 100% acetonitrile*, solvent program = 0-20 min isocratic elution with 6% *B*, 20-70 min linear gradient to 20% *B*, 71 min linear gradient to 6% *B*, detection at 254 nm

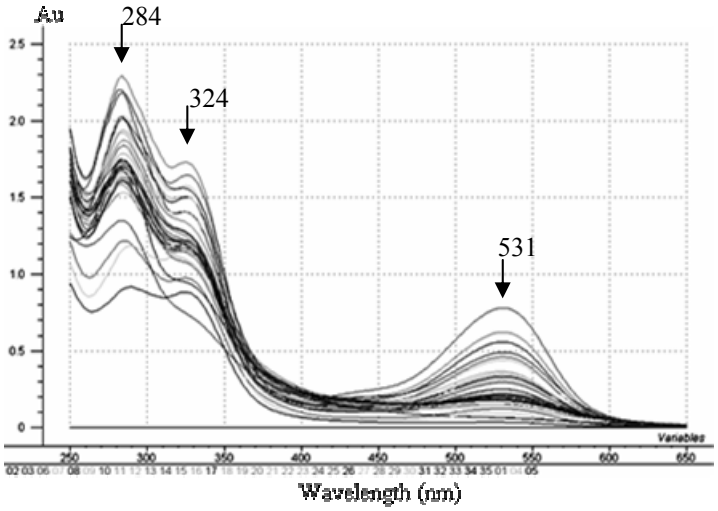

Figure 40 UV-visible spectra in the region of 250 to 650 nm of roselle extract prepared from 50% methanol (n = 35)

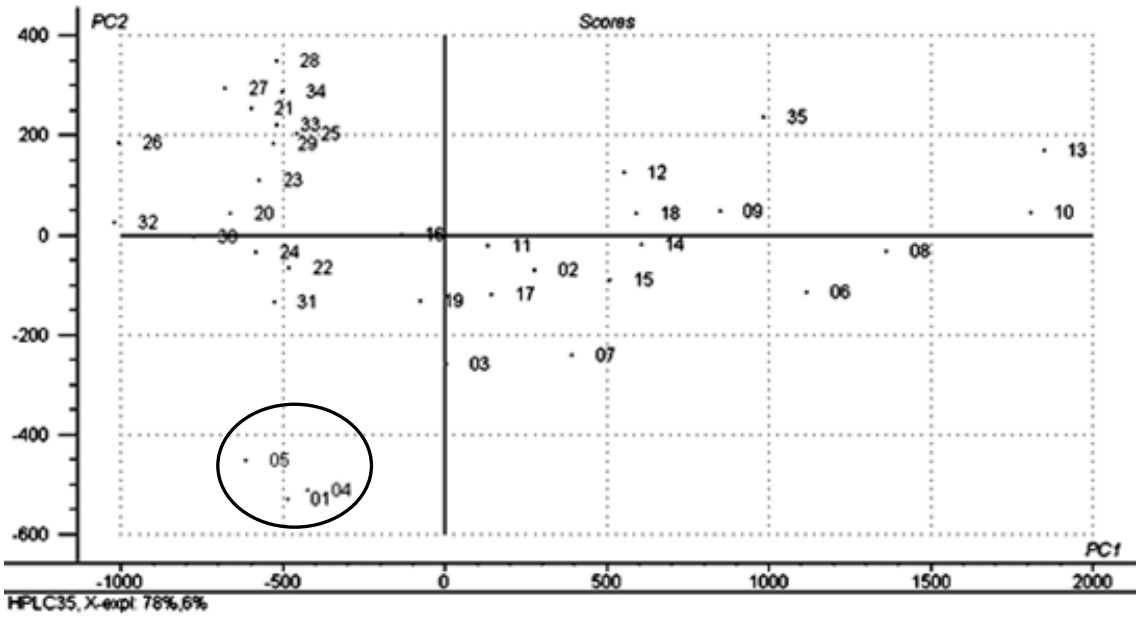

Figure 41 PCA score plot of HPLC chromatograms of roselle extract (n = 35) prepared from 50% methanol: PC1 (78% X-variance explained) and PC2 (6% X-variance explained), 01-35 = sample number

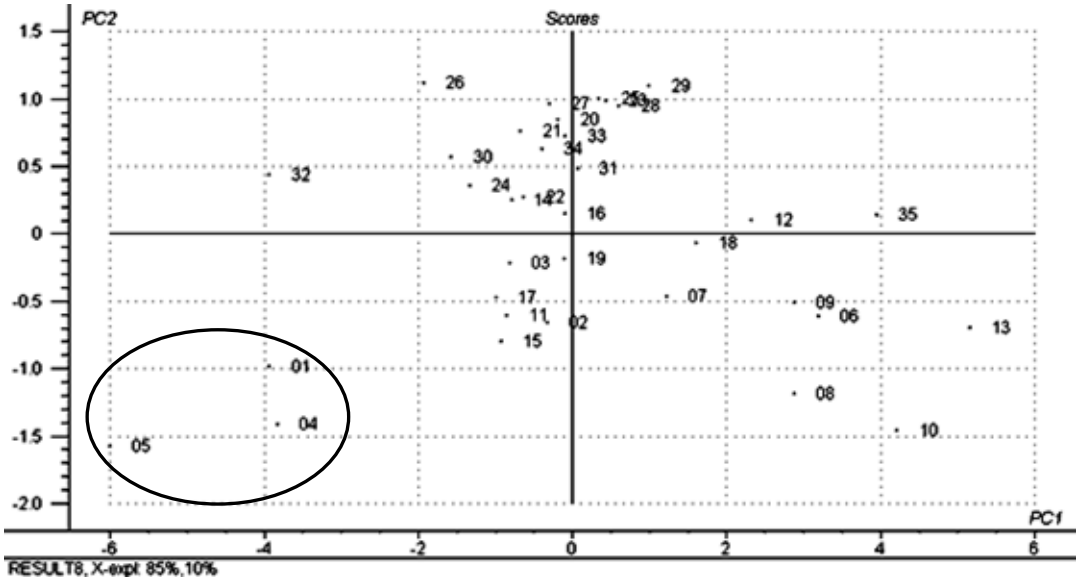

Figure 42 PCA score plot of UV-Vis spectra in the region of 250 to 650 nm of roselle extract (n = 35) prepared from 50% methanol: PC1 (85% X-variance explained) and PC2 (10% X-variance explained), 01-35 = sample number

Table 25 Descriptive statistics of the radical scavenging activity of the calibration set and the prediction set

	Calibration set (n = 19)	Prediction set (n = 13)	All (n = 32)
Mean	4.25	4.05	4.17
Standard deviation	0.91	0.53	0.78
Minimum	2.68	3.51	2.68
Maximum	5.80	5.43	5.80

6.2.1 Prediction by HPLC chromatogram

After the correction of retention time shifts, the corrected HPLC chromatograms (x-variables) were related with the corresponding radical scavenging activity (y-variable) by PLS1. The PLS1 was performed on the calibration set (n = 19), thus the size of X-matrix was 19 x 10641, while 19 was the number of sample and 10641 was the number of response collected at each retention time. And the size of Y-matrix was 19 x 1, while 19 was the number of sample and 1 was the number of predicted variable, the radical scavenging activity of sample. The chromatograms of the calibration set were shown in Figure 43.

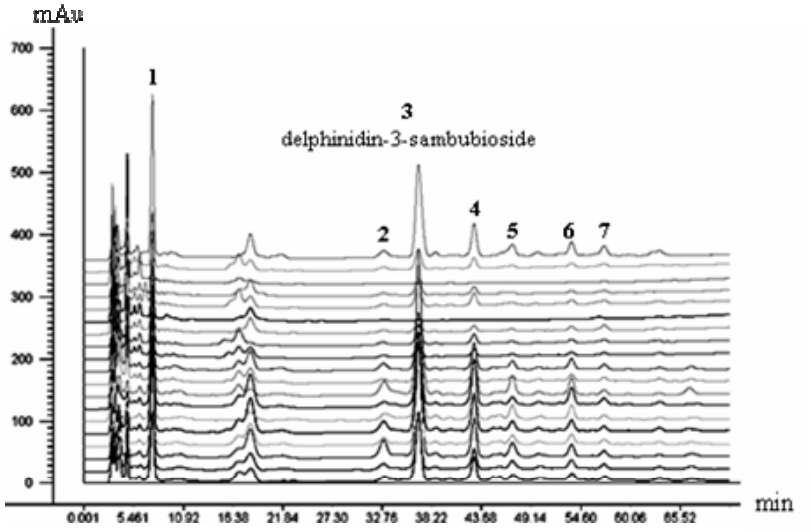

Figure 43 HPLC chromatograms of calibration set of roselle extract prepared from 50% methanol (n = 19): *solvent A = 4% phosphoric acid, solvent B = 100% acetonitrile*, solvent program = 0-20 min isocratic elution with 6% *B*, 20-70 min linear gradient to 20% *B*, 71 min linear gradient to 6% *B*, detection at 254 nm

The PLS1 model built from all x-variables contained 3 PLS factors determined by leave one out cross validation (LOOCV) using the minimum residual validation variance (Figure 44). The regression coefficients of each variable were shown in Figure 45. The model was validated by two methods i.e. leave one out cross validation (LOOCV) and prediction set or test set validation. The validation results by the LOOCV were demonstrated as a root mean square error of cross validation (RMSECV) and a correlation coefficient between predicted and measured y (R of LOOCV) while those of prediction set or test set validation were shown as a root mean square error of prediction (RMSEP) and a correlation coefficient between predicted and measured y (R of prediction set) The validation results of PLS1 model were summarized in Table 26.

Comparing among three types of error i.e. the root mean square error of calibration (RMSEC), RMSECV and RMSEP, the results was RMSEC < RMSEP < RMSECV (Table 26). This finding was against the normal finding that the prediction error of cross validation should be less than that of test set. The problem might be due to the high cross validation errors of the sample number 26, 24 and 28. In these samples the LOOCV errors showed the most three highest distinction from the corresponding calibration errors (Figure 46). If these samples were excluded from the LOOCV, the RMSECV would be 0.1811, and the RMSEC < RMSECV < RMSEP.

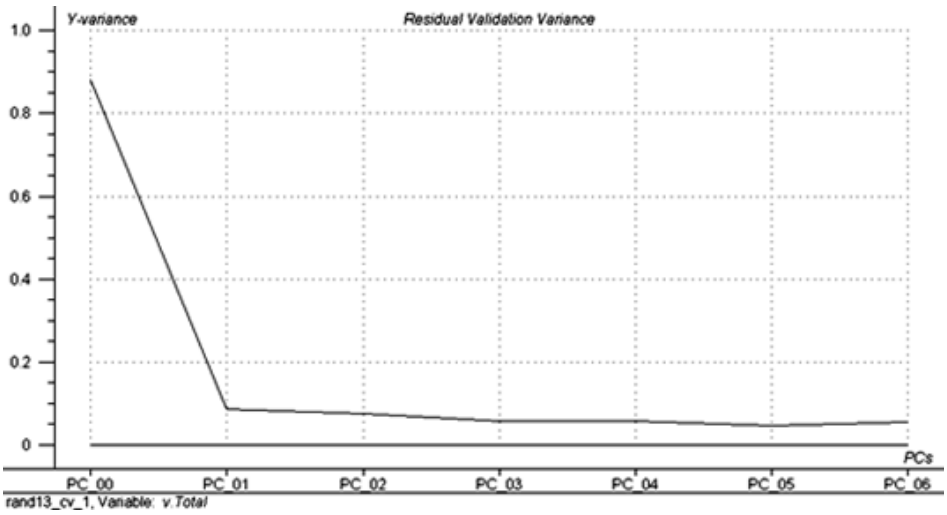

Figure 44 Residual variance of leave one out cross validation plotted as a function of PLS-factors of the PLS1 model built with all x-variables of HPLC chromatogram (optimum number of PC = 3)

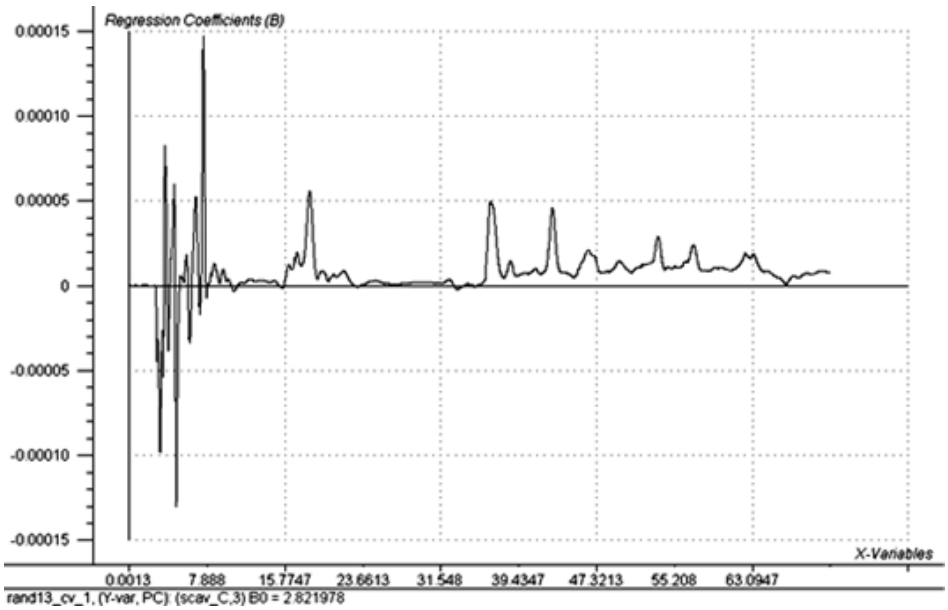

Figure 45 Regression coefficients of each variable of the PLS1 model built with all x-variables of HPLC chromatogram (number of PC = 3, explained y calibration variance = 97.45%, offset = 2.821978)

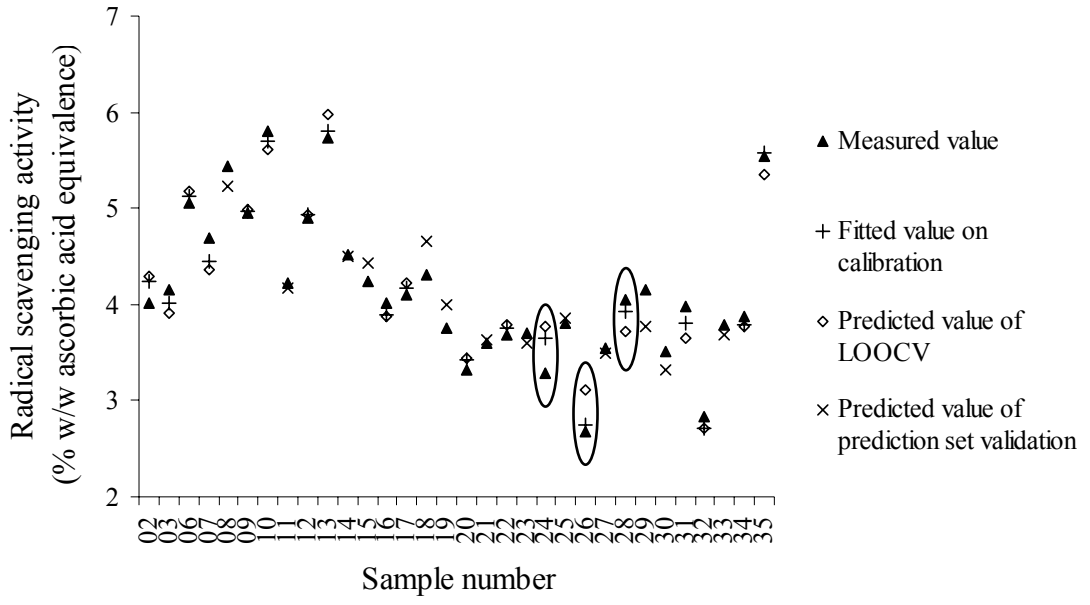

Figure 46 Comparison of measured value, fitted value on calibration, predicted value of leave one out cross validation (LOOCV) and predicted value of prediction set validation of the PLS1 model built with all x-variables of HPLC chromatogram (number of PC = 3, explained y calibration variance = 97.45%)

By using the uncertainty test function [110], some uninformative variables were identified and excluded. New model was constructed from the remaining variables. The new model, the uninformative variables elimination PLS1 model (UVE-PLS1), contained only 2 PLS factors (Figure 47). Compared with the original PLS1 model, the number of PLS factor used in the UVE-PLS1 model was less (Table 26). Therefore, the UVE-PLS1 model was simpler than the original PLS1 model. The retained variables (2954 variables) (Figure 48) were the signals at around the retention time of 8.22 - 8.59 min, 20.37 - 20.83 min, 24.71 - 25.09 min, which were corresponding to those of unidentified substances. The other region of retained variables was the region at around the retention time of 36.16 - 64.45 min. This region was seemed to be selected from the peak number 3 which was the peak of delphinidin-3-sambubioside (retention time = 36.49 min), peak number 4 (retention time = 42.57 min), peak number 5 (retention time = 46.72 min), peak number 6 (retention time = 53.17 min) and the peak number 7 (retention time = 56.65 min) (see also Table 15). The regression coefficients and robustness of UVE-PLS1 model were shown in Figure 48 and summarized in Table 26, respectively.

From the validation results of the PLS1 and the UVE PLS1 models (Table 26), the RMSECV values were conflicting with the RMSEP values i.e. the validation results of LOOCV were unrelated with those of test set validation. In details, the RMSECV of UVE-PLS1 model seemed to be less than that of PLS1 model but the RMSEP of UVE-PLS1 model seemed to be more than that of PLS1 model. The inconsistent results might be due to the method employed for the detection of uninformative variables, the uncertainty test function. For finding uninformative variables, the uncertainty test function exploited only the data of calibration samples but not those of prediction samples. Therefore, this variable elimination method could enhance only the validation result of LOOCV, RMSECV, but could not improve the validation result of independent prediction set, RMSEP.

The predicted values along with deviation as well as the measured values of radical scavenging activity of each prediction sample were shown in Table 27 (see also Figure 46). The predicted values of both PLS1 and UVE-PLS1 models were not different from the measured value (paired t-test, $p > 0.05$).

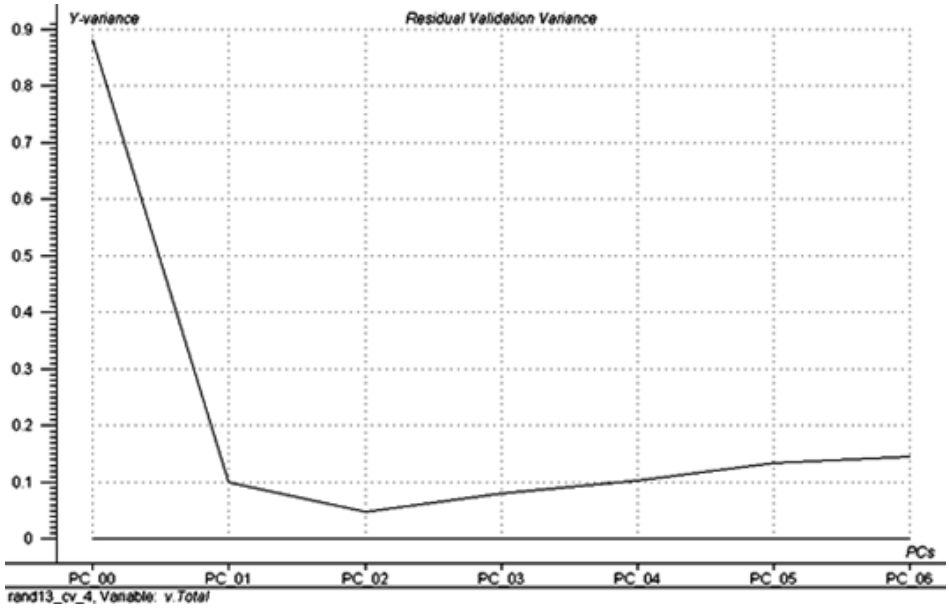

Figure 47 Residual variance of leave one out cross validation plotted as a function of PLS-factors of uninformative variable elimination PLS1 (UVE-PLS1) model built with x-variables of HPLC chromatogram (optimum number of PC = 2)

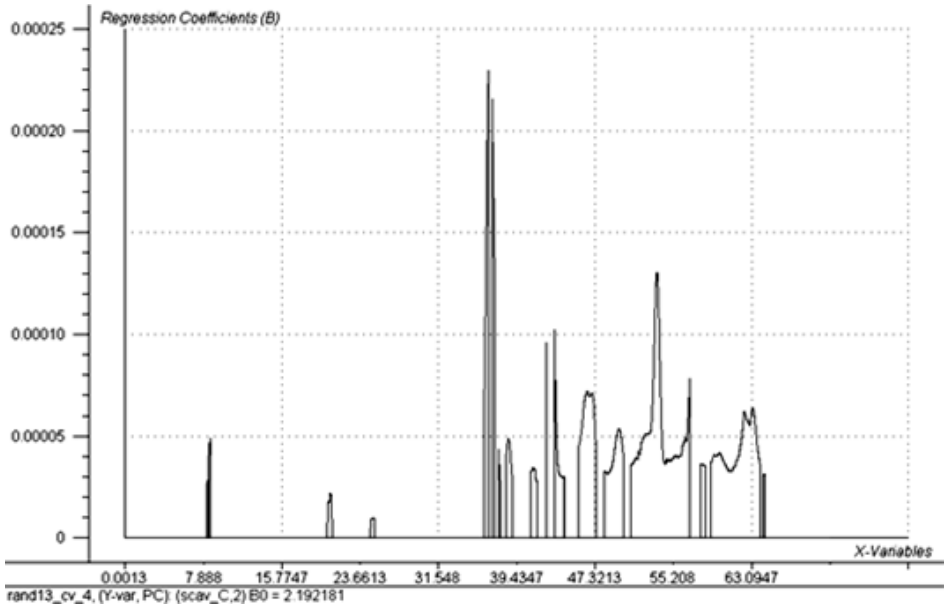

Figure 48 Regression coefficients of each variables of the model built with uninformative variable elimination PLS1 of HPLC chromatogram (number of PC = 2, explained y calibration variance = 94.57%, offset = 2.192181)

In the Unscrambler [110], the prediction by PLS gives not only the predicted values but also the deviations of them. This deviation is calculated as a function of the global model error, the sample leverage, and the sample residual X-variance. A large deviation implies that the sample used for prediction is dissimilar to the samples used to build the calibration model. Hence, the predicted value with large deviation cannot be relied on. There has been no criterion to judge that how much deviation is considered as a large yet. In this study, some predicted values were associated with quite large deviations when compared with general error of the laboratory analysis, the DPPH method. For example, the deviations of the predicted values of sample number 8 from both PLS1 and UVE-PLS1 models were about three times of average error of DPPH method. Consequently, the predicted values of these samples might be in suspicion.

Table 26 Summarize of model parameters and validation results of model using for prediction of radical scavenging activity by HPLC chromatogram

Model	Variables	PLS-factor[a]	RMSEC[b]	R (Calibration)[c]	RMSECV[d]	R (LOOCV)[e]	RMSEP[f]	R (Prediction set)[g]
PLS1_HPLC	10641	3	0.1420	0.9872	0.2388	0.9633	0.1910	0.9326
UVE-PLS1_HPLC	2954	2	0.1903	0.9768	0.2187	0.9693	0.2193	0.9276

[a] Number of optimum PLS-factors in model determined by leave one out cross validation (LOOCV)

[b] Root mean square error of calibration

[c] Correlation between measured value and predicted value of calibration

[d] Root mean square error of leave one out cross validation (LOOCV)

[e] Correlation between measured value and predicted value during leave one out cross validation (LOOCV)

[f] Root mean square error of prediction

[g] Correlation between measured value and predicted value of prediction

Table 27 The measured values (mean ± SD), predicted values and deviation of predicted values of radical scavenging activity (% w/w equivalence to ascorbic acid) predicted by HPLC chromatogram of the prediction set

Sample number	Measured value	PLS1		UVE-PLS1	
		Predicted	Deviation	Predicted	Deviation
08	5.43 ± 0.13	5.22	0.30	5.37	0.32
11	4.23 ± 0.15	4.17	0.17	4.30	0.14
14	4.51 ± 0.18	4.51	0.20	4.76	0.32
15	4.24 ± 0.14	4.42	0.23	4.54	0.14
18	4.31 ± 0.11	4.66	0.12	4.62	0.13
19	3.76 ± 0.06	4.00	0.16	3.92	0.14
21	3.59 ± 0.11	3.63	0.16	3.93	0.19
23	3.71 ± 0.06	3.60	0.11	3.69	0.11
25	3.81 ± 0.08	3.86	0.18	3.98	0.20
27	3.55 ± 0.12	3.49	0.17	3.76	0.16
29	4.16 ± 0.11	3.78	0.12	3.85	0.15
30	3.51 ± 0.07	3.32	0.13	3.29	0.11
33	3.79 ± 0.08	3.69	0.15	3.72	0.13

The areas under curve (AUC) of 7 characteristic HPLC peaks of roselle (see also Figure 43 and Table 15) were also investigated to predict of radical scavenging activity. The PLS1 model built from all AUCs of each 7 characteristic peak contained only 1 PLS factor determined by LOOCV using the minimum residual validation variance value (Figure 49). The regression coefficients of each variable were shown in Figure 50. And the robustness of the PLS1 model was summarized in Table 28.

By using the uncertainty test function [110], an uninformative variable, the AUC of peak number 7, was identified and excluded. New model was constructed from the remained 6 variables. The new model also contained only 1 PLS factor. The regression coefficients and robustness of UVE-PLS1 model were shown in Figure 51 and summarized in Table 28, respectively.

The validation results, both the RMSECV and the RMSEP, of models built from AUCs by PLS1 and UVE-PLS1 method were seemed to be not different (Table 28). The reason that why uninformative variable elimination could not improve any of validation result, compared to the original PLS method, might be due to the X-data i.e. the AUCs used in the model building. In contrast to numerous raw HPLC data points, the AUCs

were only a few numbers of integrated parts of them, thus some data reduction or elimination of redundant variables had occurred in this integration step. When the uninformative variable elimination was applied on the integration data, the AUCs, only few redundant X-variables were eliminated. Therefore, based on X-variables resembling the AUCs data used in this study, the UVE-PLS1 could not improve any of validation, compared to the original PLS1 method.

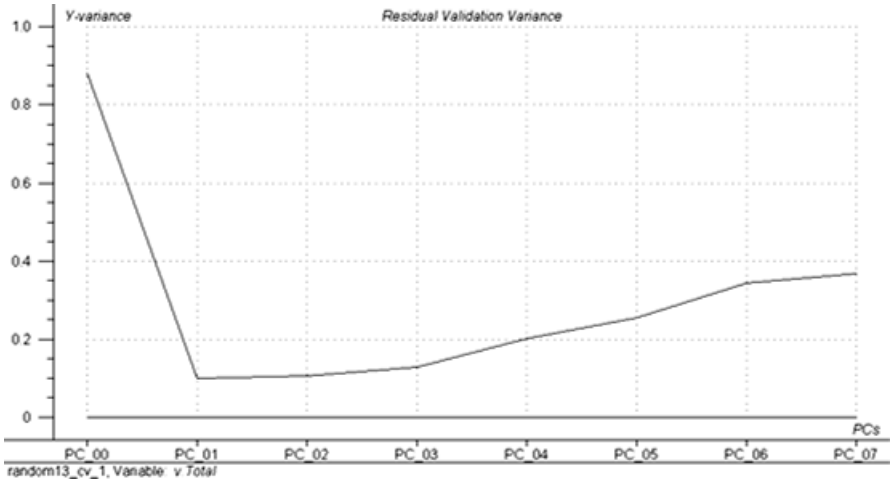

Figure 49 Residual variance of leave one out cross validation plotted as a function of PLS-factors of the PLS1 model built with all areas under curve (AUCs) of each 7 characteristic peak of HPLC chromatogram of roselle (optimum number of PC = 1)

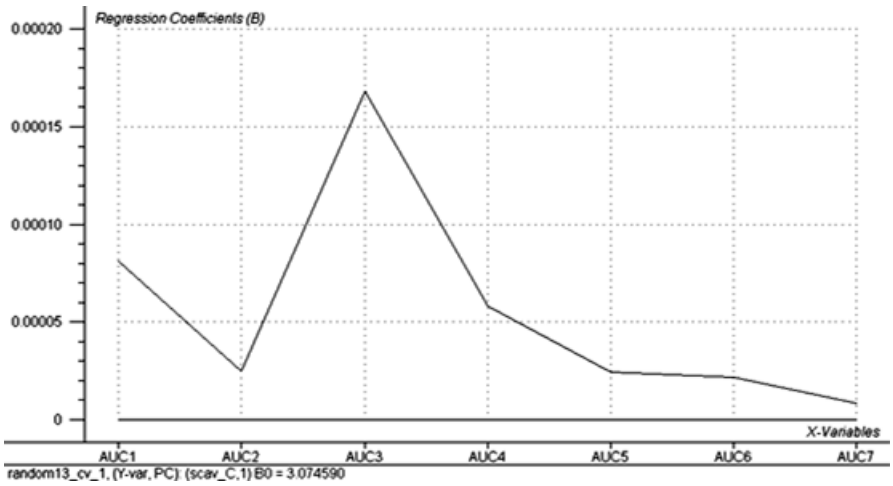

Figure 50 Regression coefficients of each variable of the PLS1 model built with all areas under curve (AUCs) of each 7 characteristic peak of HPLC chromatogram of roselle (number of PC = 1, explained y calibration variance = 89.97%, offset = 3.074590)

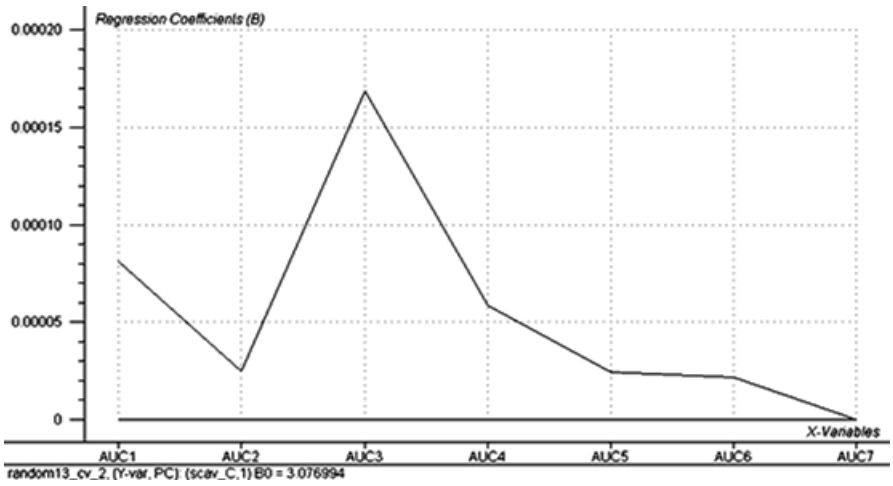

Figure 51 Regression coefficients of each variables of the model built with uninformative variable elimination PLS1 of areas under curve (AUCs) of HPLC chromatogram of roselle (number of PC = 1, explained y calibration variance = 89.92%, offset = 3.076994)

Another atypical result was that the RMSEP obtained from each model of both PLS1 and UVE-PLS1 models were less than the RMSEC and the RMSECV obtained from those corresponding models (Table 28). These findings were against the normal findings that the prediction errors arranged in order of magnitude from the smallest to the largest error should be RMSEC < RMSECV < RMSEP instead of RMSEP < RMSEC < RMSECV, as found in this study. The unexpected results might be the consequences of some unique calibration samples.

As shown in Figure 52, the calibration samples which were symbolized as pink markers covered the y-range of prediction samples which were symbolized as brown markers. The target line is an ideal line where the predicted y values were equal to their measured y values. In general, indicated by the distance between the sample coordinate and the target line, the predicted y values of the prediction samples were closest to the measured values while the predicted y values from the LOOCV were furthest from those measured values. When examined in details, three calibration samples, the sample number 2, 28 and 31, obviously seemed to be the source of high calibration error i.e. high RMSEC. The measured y values of these three samples were roughly the same (4.01, 4.04 and 3.98% w/w ascorbic acid equivalence, respectively) while the fitted y values were apparently different (4.45, 3.67 and 3.50% w/w ascorbic acid equivalence, respectively) (Figure 53). The raw AUCs data of these three samples were plotted, compared with the AUCs of sample number 16 which was better fitted to the regression line (Figure 54). There

was no indication of anomalous AUCs. Because the confirmations of all X and y values had not been made, the roots of problem were still unclear.

After exclusion of those three samples, a new PLS1 model was built from the remained samples (n = 16). The new PLS1 model also contained 1 PLS factor similar to the optimum PLS factor of the original PLS1 and UVE-PLS1 model. The regression coefficients of each variable were shown in Figure 55. And the robustness of the model was summarized in Table 28. From the validation results, the new PLS1 model could lessen RMSEC and also improve the correlation coefficient between the measured and predicted value during calibration stage (R of calibration). However, the RMSEP of new model indicated that it was not as good as the original PLS1 model (Table 28).

All three models were applied to predict of radical scavenging activity of external test samples (n = 13). The predicted values along with deviation as well as the measured values of radical scavenging activity of each prediction sample were shown in Table 29. The predicted y values from all three models using AUCs as the predictors, i.e. original PLS1, UVE-PLS1, and PLS1 model after exclusion of three suspect calibration samples, were not difference from the measured value (paired t-test, $p > 0.05$). Again, some predicted values were associated with quite large deviations when compared with the standard deviations of the measured values. Consequently, the predicted values of these samples might be in suspicion.

Table 28 Summarize of model parameters and validation results of model using for prediction of radical scavenging activity by the areas under curve (AUCs) of characteristic peaks of HPLC chromatogram of roselle

Model	Variables	PLS-factor[a]	RMSEC[b]	R (Calibration)[c]	RMSECV[d]	R (LOOCV)[e]	RMSEP[f]	R (Prediction set)[g]
PLS1_AUC	7	1	0.2816	0.9485	0.3172	0.9344	0.2520	0.9243
UVE-PLS1_AUC	6	1	0.2823	0.9483	0.3178	0.9342	0.2521	0.9245
PLS1_AUC (n = 16)	7	1	0.2366	0.9693	0.2797	0.9572	0.2816	0.9243

[a] Number of optimum PLS-factors in model determined by leave one out cross validation (LOOCV)

[b] Root mean square error of calibration

[c] Correlation between measured value and predicted value of calibration

[d] Root mean square error of leave one out cross validation (LOOCV)

[e] Correlation between measured value and predicted value during leave one out cross validation (LOOCV)

[f] Root mean square error of prediction

[g] Correlation between measured value and predicted value of prediction

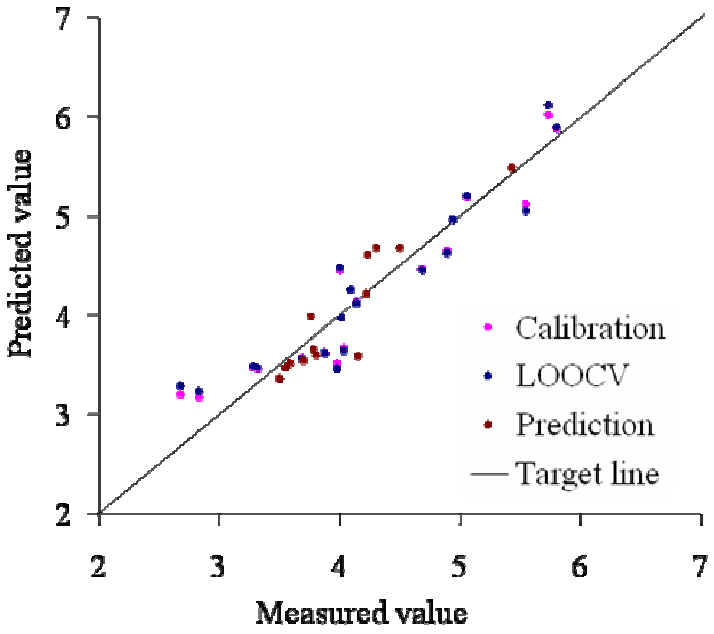

Figure 52 Predicted y values and measured y values plot of calibration and prediction samples by PLS1 model built with all areas under curve (AUCs) of each 7 characteristic peak of HPLC chromatogram of roselle (number of PC = 1, explained y calibration variance = 89.97%)

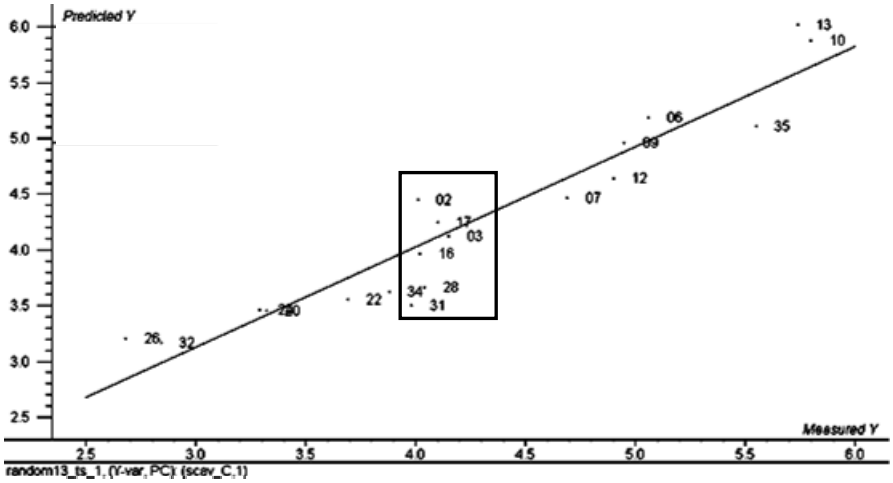

Figure 53 Predicted y values and measured y values plot of calibration samples by PLS1 model built with all areas under curve (AUCs) of each 7 characteristic peak of HPLC chromatogram of roselle (number of PC = 1, explained y calibration variance = 89.97%)

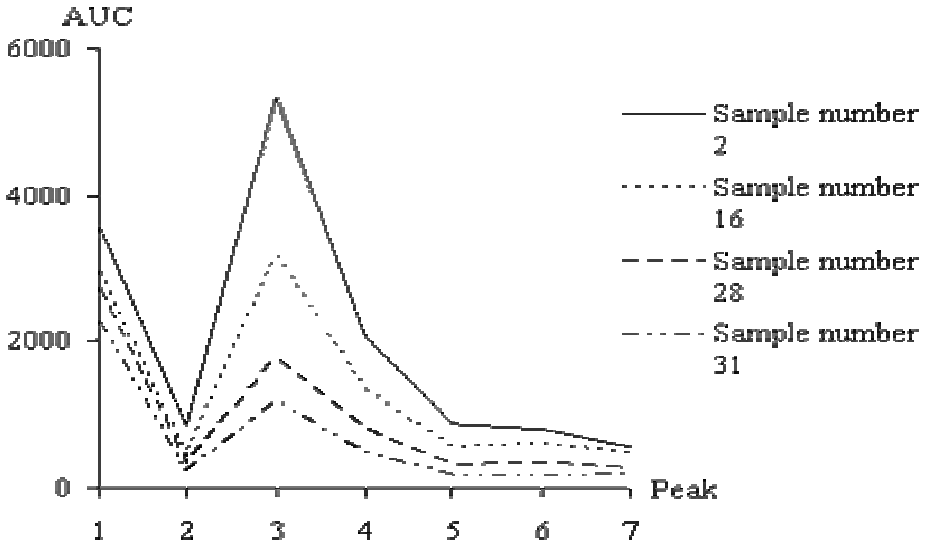

Figure 54 Raw areas under curve (AUCs) data of each 7 characteristic peak of HPLC chromatograms of roselle samples number 2, 28 and 31 compared with sample number 16

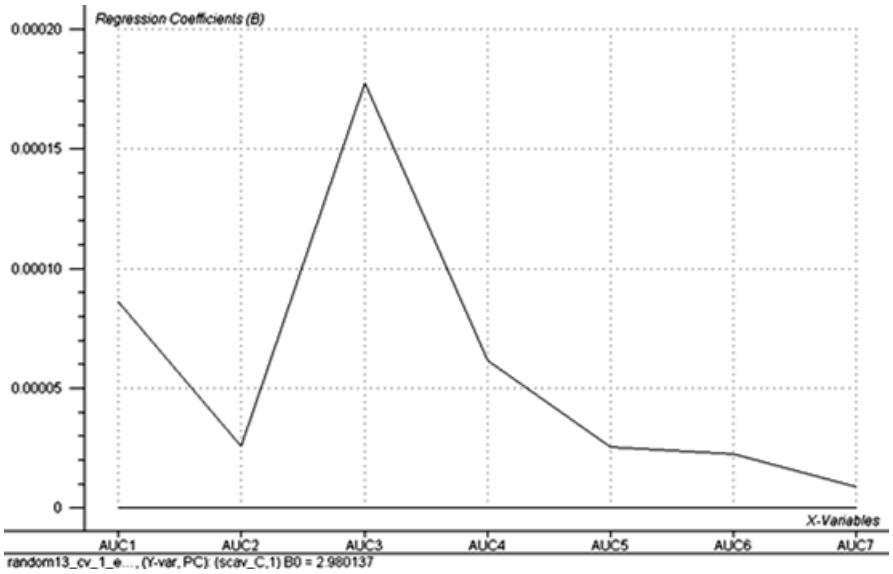

Figure 55 Regression coefficients of each variables of the model built with all areas under curve (AUCs) of each 7 characteristic peak of HPLC chromatogram of roselle after exclusion of samples number 2, 28 and 31 (number of PC = 1, explained y calibration variance = 93.96%, offset = 2.980137)

Table 29 The measured values (mean ± SD), predicted values and deviation of predicted values of radical scavenging activity (% w/w equivalence to ascorbic acid) predicted by the areas under curve (AUCs) of characteristic peaks of HPLC chromatogram of the prediction set

Sample number	Measured value	PLS1		UVE-PLS1		PLS1 (n = 16)	
		Predicted	Deviation	Predicted	Deviation	Predicted	Deviation
08	5.43 ± 0.13	5.48	0.81	5.48	0.82	5.52	0.66
11	4.23 ± 0.15	4.22	0.15	4.22	0.15	4.18	0.13
14	4.51 ± 0.18	4.67	0.59	4.68	0.59	4.67	0.48
15	4.24 ± 0.14	4.61	0.45	4.61	0.47	4.60	0.37
18	4.31 ± 0.11	4.68	0.17	4.68	0.17	4.67	0.15
19	3.76 ± 0.06	3.99	0.13	3.99	0.13	3.94	0.12
21	3.59 ± 0.11	3.51	0.13	3.51	0.13	3.44	0.12
23	3.71 ± 0.06	3.54	0.12	3.54	0.12	3.47	0.11
25	3.81 ± 0.08	3.60	0.28	3.60	0.29	3.53	0.25
27	3.55 ± 0.12	3.46	0.13	3.46	0.13	3.39	0.12
29	4.16 ± 0.11	3.58	0.12	3.58	0.12	3.51	0.12
30	3.51 ± 0.07	3.35	0.13	3.35	0.13	3.27	0.12
33	3.79 ± 0.08	3.64	0.23	3.64	0.20	3.58	0.20

6.2.2 Prediction by UV-Vis spectrum

Although the UV-Vis spectrophotometric technique could not be regarded as an effective technique for constructing the fingerprint of roselle as described in section 4.4, it has major advantages over the HPLC technique in simple, rapid and inexpensive one. Thus, in this section, the UV-Vis spectrum was explored to predict the total radical scavenging activity of roselle samples.

The samples used in both calibration and prediction set were the same as those for the prediction by HPLC chromatogram (see also Table 25). The UV-Vis spectrums (x-variables) in the range of 250 to 650 nm were related with the corresponding radical scavenging activity (y-variable) by PLS1. The PLS1 was performed on the calibration set (n = 19), thus the size of X-matrix was 19 x 401, while 19 was the number of sample and 401 was the absorbance collected at each wavelength. And the size of Y-matrix was 19 x 1, while 19 was the number of sample and 1 was the number of predicted variable, the radical scavenging activity of sample. The UV-Vis spectra of calibration set were shown in Figure 56.

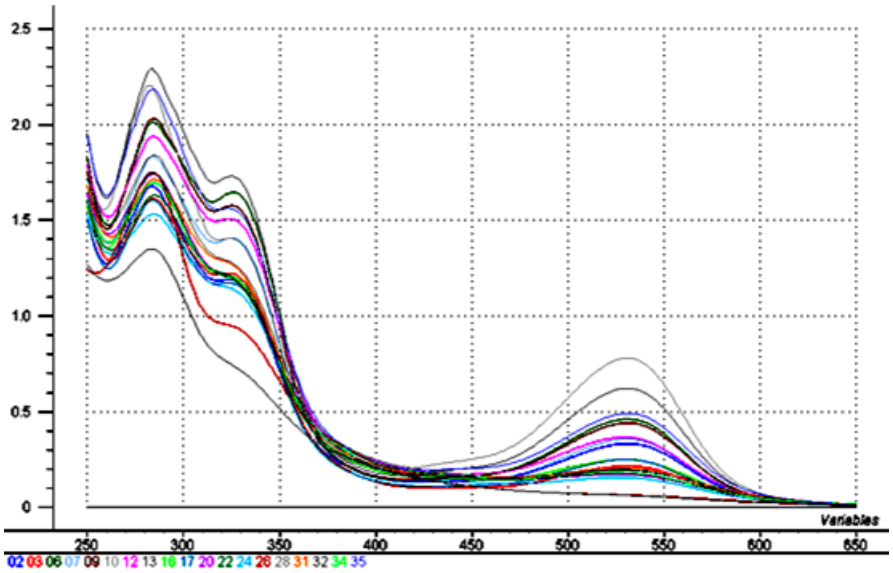

Figure 56 UV-Vis spectra of calibration set of roselle (n = 19)

The PLS1 model built from all x-variables contained 2 PLS factors determined by LOOCV using the minimum residual validation variance value (Figure 57). The regression coefficients of each variable were shown in Figure 58. And the robustness of the model was summarized in Table 30. Comparing among three types of error i.e. RMSEC, RMSECV and RMSEP, the result was RMSEC < RMSECV < RMSEP (Table 30). This finding was similar to normal finding that the RMSEC should be less than RMSECV and RMSEP, respectively.

By using the uncertainty test function [110], some uninformative variables had been excluded. New model, the UVE-PLS model, was constructed from the remained variables. The UVE-PLS1 model contained 2 PLS factors determined by LOOCV using the minimum residual validation variance value (Figure 59). The retained variables (87 variables) were the signals at the wavelengths around 301 - 307 nm and 486 - 565 nm (Figure 60). The first region, the wavelengths around 301 – 307 nm, was located between the absorption maxima of hydroxybenzoates and flavan-3-ols and the absorption maxima of hydroxycinnamates. And the latter region was possibly due to the visible absorption peak of anthocyanins. The variables at around 354 to 439 nm which represent to the degradable brown product of anthocyanins were excluded. The regression coefficients and the robustness of UVE-PLS1 model were shown in Figure 60 and summarized in Table 30, respectively.

From the validation results of the PLS1 and the UVE PLS1 models (Table 30), the RMSECV values were opposed with the RMSEP values i.e. the validation results of LOOCV were unrelated with those of test set validation. In details, the RMSECV of UVE-PLS1 model seemed to be less than that of PLS1 model but the RMSEP of UVE-PLS1 model seemed to be more than that of PLS1 model. The inconsistent results might be due to the method employed for the detection of uninformative variables, the uncertainty test function, as described earlier.

Both model were applied to predict of radical scavenging activity of external test samples, the prediction set (n = 13). The predicted values along with deviation as well as the measured values of radical scavenging activity of each prediction sample were shown in Table 31. The predicted values of both PLS1 and UVE-PLS1 models were not difference from the measured value (paired t-test, $p > 0.05$).

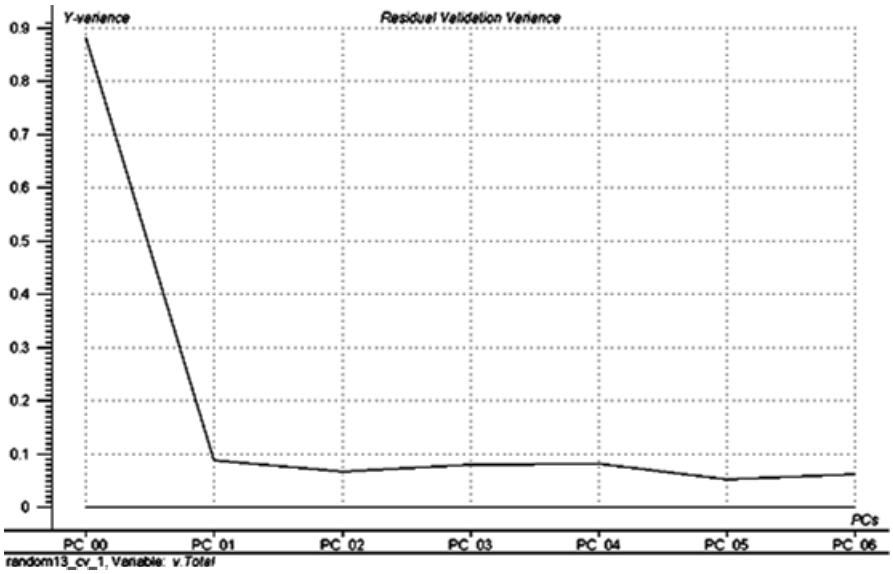

Figure 57 Residual variance of leave one out cross validation plotted as a function of PLS-factors of the PLS1 model built with all x-variables of UV-Vis spectrum (optimum number of PC = 2)

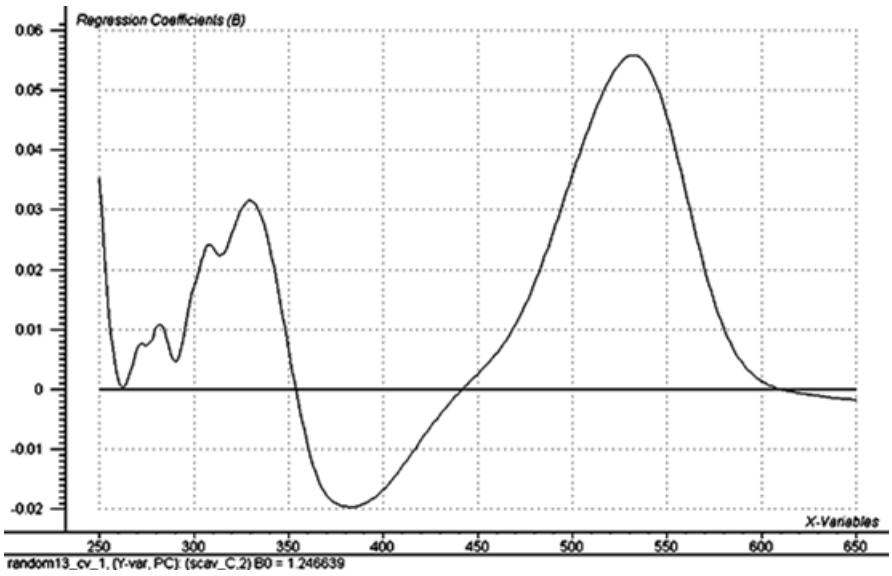

Figure 58 Regression coefficients of each variable of the PLS1 model built with all x-variables of UV-Vis spectrum (number of PC = 2, explained y calibration variance = 94.88%, offset = 1.246639)

Table 30 Summarize of model parameters and validation results of model using for prediction of radical scavenging activity by the UV-Vis spectrum

Model	Variables	PLS-factor[a]	RMSEC[b]	R (Calibration)[c]	RMSECV[d]	R (LOOCV)[e]	RMSEP[f]	R (Prediction set)[g]
PLS1_UV-Vis	401	2	0.2013	0.9740	0.2591	0.9567	0.2645	0.8645
UVE-PLS1_UV-Vis	87	2	0.1894	0.9771	0.2439	0.9617	0.2986	0.8191

[a] Number of optimum PLS-factors in model determined by leave one out cross validation (LOOCV)

[b] Root mean square error of calibration

[c] Correlation between measured value and predicted value of calibration

[d] Root mean square error of leave one out cross validation (LOOCV)

[e] Correlation between measured value and predicted value during leave one out cross validation (LOOCV)

[f] Root mean square error of prediction

[g] Correlation between measured value and predicted value of prediction

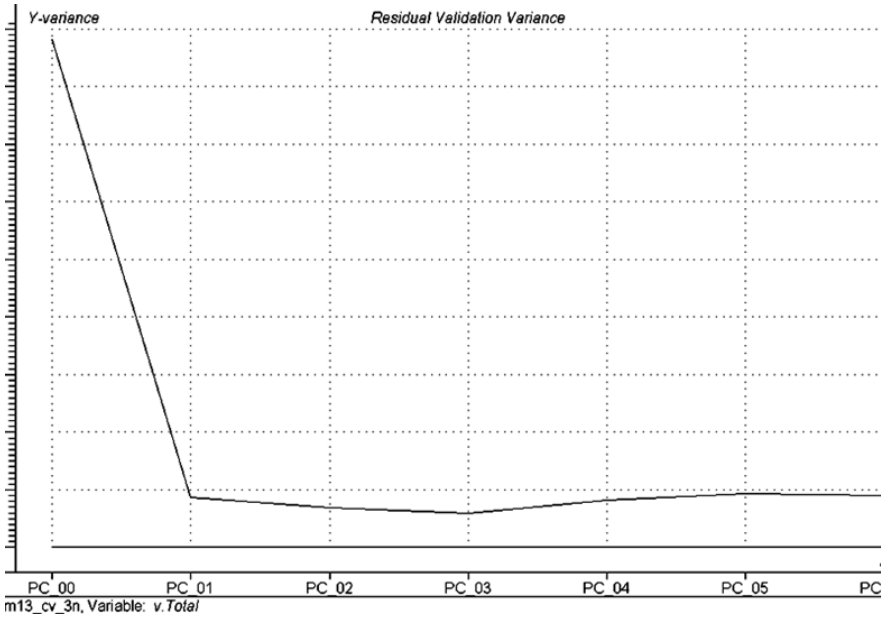

Figure 59 Residual variance of leave one out cross validation plotted as a function of PLS-factors of uninformative variable elimination PLS1 (UVE-PLS1) model built with x-variables of UV-Vis spectrum (optimum number of PC = 2)

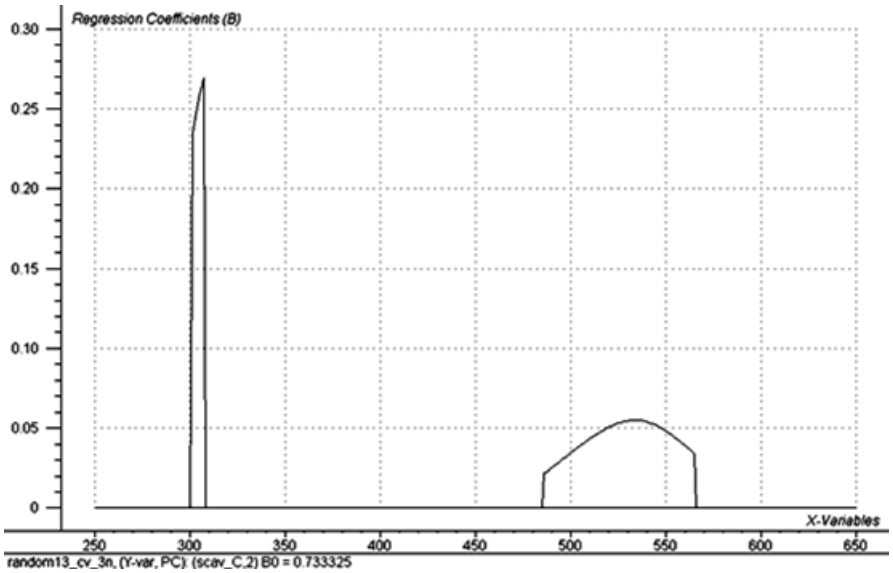

Figure 60 Regression coefficients of each variable of the model built with uninformative variable elimination PLS1 of x-variables of UV-Vis spectrum (number of PC = 2, explained y calibration variance = 94.30%, offset = 0.733325)

Table 31 The measured values (mean ± SD), predicted values and deviation of predicted values of radical scavenging activity (% w/w equivalence to ascorbic acid) predicted by the UV-Vis spectrum of the prediction set

Sample number	Measured value	PLS1		UVE-PLS1	
		Predicted	Deviation	Predicted	Deviation
08	5.43 ± 0.13	5.34	0.15	5.27	0.14
11	4.23 ± 0.15	3.99	0.15	3.89	0.18
14	4.51 ± 0.18	3.78	0.21	3.72	0.21
15	4.24 ± 0.14	4.04	0.20	3.89	0.20
18	4.31 ± 0.11	4.55	0.12	4.54	0.11
19	3.76 ± 0.06	4.12	0.13	4.09	0.18
21	3.59 ± 0.11	3.58	0.12	3.62	0.15
23	3.71 ± 0.06	3.86	0.17	3.94	0.21
25	3.81 ± 0.08	3.84	0.21	3.92	0.20
27	3.55 ± 0.12	3.62	0.15	3.70	0.21
29	4.16 ± 0.11	3.97	0.16	4.08	0.20
30	3.51 ± 0.07	3.37	0.14	3.39	0.15
33	3.79 ± 0.08	3.77	0.12	3.84	0.17

6.2.3 Overall results of the prediction of radical scavenging activity

The overall results demonstrated that the radical scavenging activity of roselle could be predicted by the data from the whole HPLC chromatogram, the AUC of HPLC chromatogram or the UV-Vis spectrum. From the RMSEP, the best model was the PLS1 model of HPLC chromatogram with 3 PLS factors, R = 0.9326 and RMSEP = 0.1910. However the best model would be the UVE-PLS1 model of HPLC chromatogram with 2 PLS, R = 0.9693 and RMSECV = 0.2187 if the RMSECV was regarded as a foremost criterion (Table 26, Table 28, Table 30). There were difference conclusions between using these two criterions i.e. RMSECV and RMSEP.

To make more precise comparison, the range of RMSEP of each model was calculated by bootstrapping technique. The 6 tested models were the PLS1_HPLC, UVE-PLS1_HPLC, PLS1_AUC, UVE-PLS1_AUC, PLS1_UV-Vis and UVE-PLS1_UV-Vis. Each tested model was fixed, then the simulation prediction set (n = 13) were repeatedly drawn with replacement from the original data of the prediction set (n = 13). These simulation prediction sets were independent in each model. The distribution of RMSEP for the type I error rate at 0.05 were estimated from 5000 bootstrap samples or 5000 collections of

prediction set. The lower bound and upper bound of RMSEP were the $RMSEP_{(125)}$ and $RMSEP_{(4875)}$, respectively. For enhancing the estimation accuracy, ten rounds of such bootstrap were repeated. The lower bound and upper bound of RMSEP of each model were shown in Table 32. For the PLS1_HPLC, the lower bounds of RMSEP, $RMSEP_{(125)}$, were 0.1178, 0.1189, 0.1198, 0.1192, 0.1198, 0.1170, 0.1214, 0.1201, 0.1155 and 0.1192 while the mean of these values was 0.1189. And the upper bounds of RMSEP, $RMSEP_{(4875)}$, were 0.2546, 0.2544, 0.2530, 0.2518, 0.2539, 0.2516, 0.2514, 0.2503, 0.2530 and 0.2531 while the mean of these values was 0.2527. For the other 5 models i.e. UVE-PLS1_HPLC, PLS1_AUC, UVE-PLS1_AUC, PLS1_UV-Vis and UVE-PLS1_UV-Vis, the range between the lower bound and the upper bound of RMSEP were 0.1648 - 0.2647, 0.1519 - 0.3447, 0.1518 - 0.3453, 0.1325 - 0.3935 and 0.1660 - 0.4318, respectively (Table 32). Among all 6 models, these 95% confidence intervals of RMSEP were partially united (Figure 61).

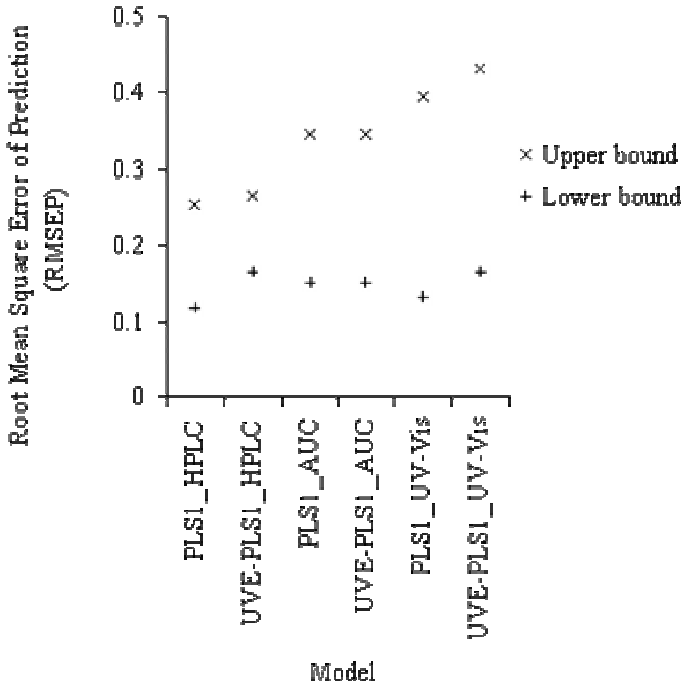

Figure 61 The lower and upper bound of the root mean square error of prediction (RMSEP) of each 6 model

The distribution of the simulated RMSEP of each model was also shown by boxplot in the Figure 62. The upper and lower edges of the box represent the third (Q_3) and the first quartile (Q_1), respectively. And a line located across this box shows the second quartile (Q_2) or the median value. The box length or the interquartile range (IQR) is

the range between Q_3 and Q_1. The upper and lower bars show the maximum and minimum limits of values that justified as normal values. These bars are calculated from Q_3 + 1.5(IQR) and Q_1 - 1.5(IQR), respectively. Cases with values between 1.5 and 3 box lengths from the upper or lower edge of the box are outliers. And cases with values more than 3 box lengths from the upper edge or less than 3 box lengths from the lower edge of the box are extremes. Among all 6 models, the distribution of the RMSEP of the UVE-PLS1_HPLC model was the narrowest. While those of the PLS1_UV-Vis and UVE-PLS1_UV-Vis models seemed to be the widest (Figure 62). Therefore the UVE-PLS1_HPLC model was the most robust, whereas the PLS1_UV-Vis and UVE-PLS1_UV-Vis models were the most instable. The best model seemed to be the PLS1_HPLC model since it gave the lowest median of RMSEPs from 5000 bootstapping samples (Figure 62).

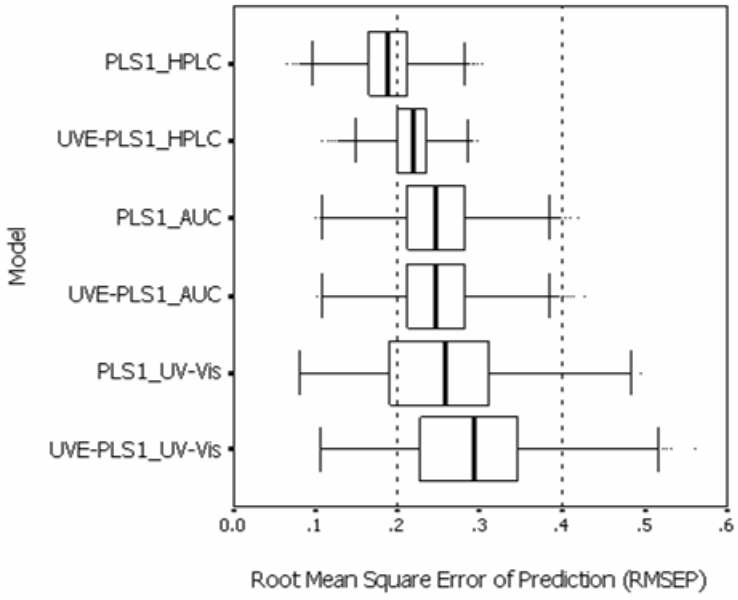

Figure 62 The boxplot of the root mean square error of prediction (RMSEP) of each 6 model

Table 32 The lower and upper bound of root mean square error of prediction (RMSEP) of each 6 model

Model	95% Confidence interval	1	2	3	4	5	6	7	8	9	10	Mean
PLS1_HPLC	Lower bound	0.1178	0.1189	0.1198	0.1192	0.1198	0.1170	0.1214	0.1201	0.1155	0.1192	0.1189
	Upper bound	0.2546	0.2544	0.2530	0.2518	0.2539	0.2516	0.2514	0.2503	0.2530	0.2531	0.2527
UVE-PLS1_HPLC	Lower bound	0.1645	0.1639	0.1647	0.1652	0.1661	0.1639	0.1659	0.1655	0.1636	0.1646	0.1648
	Upper bound	0.2652	0.2653	0.2644	0.265	0.2648	0.2647	0.2641	0.2648	0.2648	0.264	0.2647
PLS1_AUC	Lower bound	0.1507	0.153	0.1542	0.1527	0.1538	0.1486	0.1527	0.1518	0.1529	0.1485	0.1519
	Upper bound	0.3465	0.3451	0.3422	0.3451	0.3421	0.3429	0.3467	0.3472	0.3437	0.345	0.3447
UVE-PLS1_AUC	Lower bound	0.1510	0.1522	0.1508	0.1507	0.1517	0.1527	0.1507	0.1544	0.1521	0.1518	0.1518
	Upper bound	0.3452	0.3445	0.3438	0.3466	0.3434	0.3458	0.3465	0.3503	0.3434	0.3437	0.3453
PLS1_UV-Vis	Lower bound	0.1334	0.1332	0.1301	0.1321	0.1317	0.1316	0.1331	0.1339	0.1344	0.1320	0.1325
	Upper bound	0.3932	0.3960	0.3960	0.3911	0.3949	0.3937	0.3913	0.3932	0.3933	0.3926	0.3935
UVE-PLS1_UV-Vis	Lower bound	0.1671	0.1660	0.1660	0.1670	0.1631	0.1656	0.1633	0.1691	0.1674	0.1658	0.1660
	Upper bound	0.4336	0.4308	0.4323	0.4307	0.4318	0.4315	0.4325	0.4324	0.4313	0.4313	0.4318

7 Overall chemical quality of *H. sabdariffa* in Thailand

The overall chemical qualities of roselle cultivated in Thailand were studied in 35 roselle samples. The quantitative parameters i.e. total phenolics, total anthocyanins, organic acid, potassium and radical scavenging capacity in each sample were again shown in Table 33. The total phenolics content varied from 1.33 - 3.58 % w/w calculated as GAE and 1.13 - 3.10 % w/w calculated as protocatechuic acid equivalence. The total anthocyanins content ranged from 0.05 - 2.95 % w/w calculated as delphinidin-3-sambubioside equivalence. The acid content varied from 7.93 - 20.10 % w/w calculated as citric acid equivalence, while the potassium content varied from 1.32 - 3.13 % w/w. The radical scavenging activity ranged from 1.92 - 5.80 w/w calculated as ascorbic acid equivalence.

As described above, the tested samples (n = 35) had different characteristics and they could be classified into two major groups, the reddish (n = 17), and the brownish (n = 16) groups. The other two samples had distinct characteristics i.e. they had very small calyx therefore they were grouped in to another group, the small calyx group. The parameters of each group, were summarized as mean $\pm$ SD (Table 34). Analytical data that considered as outliers and extremes of each quantitative parameter by boxplot were excluded before calculation. Comparison between the reddish and the brownish groups, all of the quantitative parameters except for the potassium content, were significantly different ($p < 0.05$). The mean of those parameters i.e. total phenolics content, total anthocyanins content, organic acid content and radical scavenging activity of the reddish group were higher than those of the brownish group. The comparison among all three groups could not be performed, because the number of samples of the small calyx group was too low.

Table 33 Quantitative quality control in each roselle sample (mean ± SD)

Sample number	Total phenolics (GAE) (% w/w dried wt.)	Total phenolics (Protocatechuic acid equivalence) (% w/w dried wt.)	Total anthocyanins (Dp-3-sam equivalence) (% w/w dried wt.)	Organic acid (citric acid equivalence) (% w/w dried wt.)	Potassium[d] (% w/w dried wt.)	Radical scavenging activity (ascorbic acid equivalence) (% w/w)
01	1.84 ± 0.03[a]	1.58 ± 0.07[a]	0.51 ± 0.01	16.04 ± 0.02	1.77	2.67 ± 0.14[b]
02	2.64 ± 0.02	2.27 ±0.02	1.38 ± 0.01	15.78 ± 0.07	1.49	4.01 ± 0.17
03	2.79 ± 0.02	2.40 ± 0.02	1.29 ± 0.02	12.20 ± 0.09	1.81	4.15 ± 0.14
04	1.79 ± 0.01	1.53 ± 0.01	0.32 ± 0.00	20.10 ± 0.02[c]	1.48	2.36 ± 0.11[b, c]
05	1.33 ± 0.02[c]	1.13 ± 0.07[c]	0.11 ± 0.00	16.31 ± 0.24	1.93	1.92 ± 0.16[b, c]
06	3.39 ± 0.02	2.92 ± 0.02	2.16 ± 0.02	14.33 ± 0.05	1.50	5.06 ± 0.16[b]
07	3.07 ± 0.02	2.63 ± 0.02	1.78 ± 0.01	13.67 ± 0.18	2.45	4.69 ± 0.15
08	3.46 ± 0.01	2.97 ± 0.01	2.55 ± 0.01	14.96 ± 0.06	2.06	5.43 ± 0.13[b, c]
09	3.22 ± 0.03	2.80 ± 0.02	1.97 ± 0.01	13.74 ± 0.06	1.90	4.95 ± 0.15
10	3.57 ± 0.04	3.09 ± 0.07	2.95 ± 0.02	17.20 ± 0.03	2.05	5.80 ± 0.20[c]
11	2.52 ± 0.02	2.20 ± 0.01	1.32 ± 0.01	15.26 ± 0.04	1.75	4.23 ± 0.15
12	3.16 ± 0.01	2.75 ± 0.01	1.77 ± 0.02	15.40 ± 0.09	3.13[a]	4.90 ± 0.15
13	3.58 ± 0.01	3.10 ± 0.01	2.64 ± 0.01	15.11 ± 0.10	2.02	5.74 ± 0.19[b, c]
14	2.65 ± 0.02	2.30 ± 0.02	1.86 ± 0.01	7.93 ± 0.06[a]	2.17	4.51 ± 0.18
15	2.67 ± 0.02	2.33 ± 0.01	1.59 ± 0.01	14.32 ± 0.02	1.96	4.24 ± 0.14
16	2.56 ± 0.03	2.24 ± 0.03	1.04 ± 0.01	13.74 ± 0.02	2.22	4.02 ± 0.10
17	2.53 ± 0.01	2.26 ± 0.01	1.22 ± 0.02	14.02 ± 0.18	2.32	4.10 ± 0.12
18	3.11 ± 0.02	2.76 ± 0.02	1.83 ± 0.01	12.42 ± 0.10	2.33	4.31 ± 0.11
19	2.52 ± 0.01	2.25 ± 0.01	1.24 ± 0.01	15.32 ± 0.06	2.60	3.76 ± 0.06
20	2.36 ± 0.04	2.10 ± 0.03	0.49 ± 0.00	12.18 ± 0.17	1.59	3.32 ± 0.07
21	2.53 ± 0.01	2.24 ± 0.01	0.51 ± 0.01	10.80 ± 0.02	1.59	3.59 ± 0.11
22	2.39 ± 0.02	2.13 ± 0.02	0.67 ± 0.00	11.09 ± 0.04	1.59	3.69 ± 0.07
23	2.55 ± 0.04	2.26 ± 0.03	0.66 ± 0.00	11.12 ± 0.05	2.72	3.71 ± 0.06
24	2.09 ± 0.03[a]	1.86 ± 0.02	0.45 ± 0.01	13.74 ± 0.04	2.03	3.29 ± 0.21
25	2.46 ± 0.02	2.18 ± 0.01	0.58 ± 0.01	13.21 ± 0.04	1.49	3.81 ± 0.08
26	1.61 ± 0.02[a]	1.45 ± 0.02[a]	0.05 ± 0.00[a]	15.76 ± 0.06	1.86	2.68 ± 0.11[b]
27	2.39 ± 0.01	2.06 ± 0.01	0.47 ± 0.02	11.96 ± 0.04	1.32	3.55 ± 0.12
28	2.59 ± 0.04	2.23 ± 0.03	0.68 ± 0.01	11.75 ± 0.06	1.40	4.04 ± 0.12
29	2.64 ± 0.01	2.27 ± 0.01	0.67 ± 0.00	11.39 ± 0.08	1.39	4.16 ± 0.11
30	2.19 ± 0.01	1.90 ± 0.01	0.37 ± 0.00	11.69 ± 0.08	1.32	3.51 ± 0.07
31	2.39 ± 0.01	2.07 ± 0.01	0.65 ± 0.01	11.47 ± 0.04	2.24	3.98 ± 0.07
32	1.51 ± 0.01[a, c]	1.32 ± 0.01[a, c]	0.06 ± 0.00[a]	14.60 ± 0.02	2.54	2.84 ± 0.05[b]
33	2.32 ± 0.02	2.01 ± 0.01	0.62 ± 0.00	12.25 ± 0.06	2.62	3.79 ± 0.08
34	2.42 ± 0.04	2.09 ± 0.03	0.63 ± 0.00	11.95 ± 0.05	2.44	3.88 ± 0.06
35	3.43 ± 0.02	2.95 ± 0.02	2.03 ± 0.02	13.56 ± 0.15	2.67	5.55 ± 0.06[b, c]

[a] The outliers and extremes of each group

[b] The outliers and extremes of the reddish combined with the brownish groups (n = 33)

[c] The outliers and extremes of all samples (n = 35)

[d] SD could not be acquired

Table 34 Quantitative quality control of roselle samples in each group (mean ± SD)

Quantitative quality control	Reddish (n = 17)	Brownish (n = 16)	Small calyx (n = 2)	Reddish and Brownish (n = 33)	Total (n = 35)
Total phenolics (GAE) (% w/w dried wt.)	2.99 ± 0.40[a]	2.44 ± 0.13[a]	1.56 ± 0.33	2.64 ± 0.52	2.65 ± 0.50
Total phenolics (Protocatechuic acid equivalence) (% w/w dried wt.)	2.60 ± 0.33[a]	2.11 ± 0.13[a]	1.33 ± 0.28	2.30 ± 0.44	2.31 ± 0.43
Total anthocyanins (Dp-3-sam equivalence) (% w/w dried wt.)	1.80 ± 0.54[a]	0.57 ± 0.10[a]	0.22 ± 0.15	1.17 ± 0.77	1.12 ± 0.78
Organic acid (citric acid equivalence) (% w/w dried wt.)	14.44 ± 1.27[a]	12.56 ± 1.65[a]	18.20 ± 2.68	13.33 ± 1.96	13.42 ± 2.00
Potassium (% w/w dried wt.)	2.08 ± 0.35	1.87 ± 0.49	1.70 ± 0.32	2.01 ± 0.47	1.99 ± 0.47
Radical scavenging capacity (ascorbic acid equivalence) (% w/w)	4.67 ± 0.66[a]	3.53 ± 0.46[a]	2.14 ± 0.31	4.01 ± 0.44	3.91 ± 0.61

[a] Mean values between reddish and brownish groups are significantly different ($p < 0.05$)

CHAPTER V
CONCLUSIONS

As the basic information of roselle cultivated in Thailand, physical and chemical properties of the roselle from various sources of Thailand (n = 35) were characterized. The samples were classified into 3 subgroups (the reddish, n = 17; the brownish, n = 16; and the small calyx, n = 2). The reddish, the brownish and the small calyx sample were regarded as a higher grade, a lower grade and an atypical material, respectively. General quality control methods or physical characteristics including foreign matter, loss on drying, total ash and acid insoluble ash of the roselle in the first two groups were not different. But both the water extractive and the ethanol extractive values of the reddish group were higher than those of the brownish group. These might be due to the conversion of extractable red monomeric anthocyanins to non-extractable brown polymeric anthocyains in the brownish roselle.

According to the marker approach, the qualitative quality control of roselle was accomplished by TLC and HPLC technique. In TLC analysis, quinaldine red was used as a marker component, as described in the European Pharmacopoeia. In addition, two major anthocyanins of roselle i.e. delphinidin-3-sambubioside and cyanindin-3-sambubioside, isolated in laboratory, were also spotted on TLC to identify the relative Rf to the quinaldine red. The TLC chromatogram of typical roselle contained two red spots of the two major anthocyanins. Other spots might be found as summarized in Table 12. In the HPLC analysis, delphinidin-3-sambubioside was used as a marker component. The HPLC chromatogram of roselle contained 7 characteristics peaks. The retention time and area of each peak were shown in Table 15. The quantitative quality control was achieved by quantifying of four selected chemical component groups i.e. total phenolics, organic acid, potassium and total anthocyanins. To determine of total anthocyanin content in roselle, the pH-differential spectrophotometric method was modified and validated. Compared with the original pH-differential spectrophotometric method, the modified method using methyl orange as a standard showed acceptable validation results. Compared with HPLC method, an independent method, the analysis results of the developed method were not different from those of the HPLC method (paired t-test, p = 0.71). Therefore, to save the cost for the standard anthocyanins providing, this modified pH-differential spectrophotometry was suggested as a routine method for analysis of total anthocyanins. Overall chemical analysis except for the

analysis of potassium content showed that the chemical contents of the reddish and the brownish groups were significantly different ($p < 0.05$). Total phenolics content calculated as GAE and protocatechuic acid equivalence, organic acid content calculated as citric acid equivalence and total anthocyanins content calculated as delphinidin-3-sambubioside equivalence of the reddish group were higher than those of the brownish group. Therefore, these basic chemical contents were the rational indications of quality of roselle. On the other hand, the physical characteristics could provide not much information in the quality of the plant. The chemical analysis was the necessity in the quality control of roselle.

According to the pattern-based approach, the quality control of roselle was accomplished by HPLC fingerprint technique. The established HPLC fingerprint of roselle (Figure 17) could be applied with the critical value to classify roselle sample into reddish and non-reddish or qualified sample and unqualified sample, respectively. Whereas UV-Vis fingerprint and DRIFT fingerprint did not succeed in this purpose. The failure might be due to partial overlapping between these two groups as shown in the PCA score plots (Figure 19 and Figure 26).

For screening of antioxidant activity, one of the most prominent activities of roselle, an ability to scavenge stable DPPH radical was determined. Radical scavenging activity of the reddish and the brownish roselle were significantly different ($p < 0.05$) (Table 34). The models for prediction of radical scavenging activity were constructed from the chemical profiles of roselle for simultaneous identification of the plant and determination of radical scavenging activity. The best model was obtained from the PLS1_HPLC model with 3 PLS-factors since it gave the lowest median of RMSEPs from 5000 bootstapping samples (Figure 62). When uninformative variables had been excluded from the model, it could increase the robustness of the new model, the UVE-PLS1_HPLC model. However, it also increased the error of prediction. Balancing between the predictive ability and the robustness, the PLS1_HPLC model seemed to be the best choice. The error of prediction, the RMSEP, was equal to 0.1910, what corresponded to 4.58%. Compared with the errors of the analysis method, the pooled SD, 0.1869, what corresponded to about 4.48%, the model was satisfactory. Therefore, in the future, the HPLC chromatogram of sample could be applied to identify the plant and to predict its radical scavenging activity simultaneously.

REFERENCES

1 Ross IA. *Hibiscus sabdariffa*. In Medicinal Plants of The World, Volume I: Chemical Constituents, Traditional and Modern Medicinal Uses. 2 edition. Totowa, New Jersey: Humana Press; 2003: 267-75.

2 Boonkerd T, Songkhla BN, Thephuttee W. *Hibiscus sabdariffa* L. In: Siemonsma JS, Pileuk K editors. PROSEA : Plant Resources of South-East Asia 8 Vegetables. Bogor: Prosea Foundation; 1994: 178-80.

3 Bunyapraphatsara N, Chansrakaew W, Chayamarit K, Chokechaijaroenporn O, Chuokul W. *Hibiscus sabdariffa* Linn. In: Farnsworth NR, Bunyapraphatsara N editors. Thai Medicinal Plants Recommended for Primary Health Care System. Bangkok: Prachachon 1992: 163-6.

4 Haji Faraji M, Haji Tarkhani A. The effect of sour tea (*Hibiscus sabdariffa*) on essential hypertension. J Ethnopharmacol 1999; 65 (3): 231-6.

5 Herrera-Arellano A, Flores-Romero S, Chavez-Soto MA, Tortoriello J. Effectiveness and tolerability of a standardized extract from *Hibiscus sabdariffa* in patients with mild to moderate hypertension: a controlled and randomized clinical trial. Phytomedicine 2004; 11 (5): 375-82.

6 Market Survey: *Hibiscus sabdariffa*. Available at http://www.herbs.org/africa/hibiscus.html. Accessed December 12, 2006.

7 ภัสรา ชวประดิษฐ์. สมุนไพรไทย-ภูมิปัญญาไทย แผนยุทธศาสตร์การพัฒนาอุตสาหกรรมสมุนไพรกับบทบาทของกรมส่งเสริมการเกษตร. จดหมายข่าว ส่วนส่งเสริมการผลิตผัก ไม้ดอกไม้ประดับและสมุนไพร สำนักส่งเสริมและจัดการสินค้าเกษตร ปีที่ 3 ฉบับที่ 3 เดือน เมษยน 2548 Available at http://www2.doae.go.th/www/floriade/03%20year/03.doc. Accessed July 7, 2006.

8 Wong PK, Yusof S, Ghazali HM, Man YBC. Physico-chemical characteristics of roselle (*Hibiscus sabdariffa* L.). Nutrition & Food Science 2002; 32 (2): 68-73.

9 Chewonarin T, Kinouchi T, Kataoka K, Arimochi H, Kuwahara T, Vinitketkumnuen U, et al. Effects of roselle (*Hibiscus sabdariffa* Linn.), a Thai medicinal plant, on the mutagenicity of various known mutagens in *Salmonella typhimurium* and on formation of aberrant crypt foci induced by the colon carcinogens azoxymethane and 2-amino-1-methyl-6-phenylimidazo[4,5-b]pyridine in F344 rats. Food Chem Toxicol 1999; 37 (6): 591-601.

10 Hirunpanich V, Utaipat A, Morales NP, Bunyapraphatsara N, Sato H, Herunsale A, et al. Hypocholesterolemic and antioxidant effects of aqueous extracts from the dried calyx of *Hibiscus sabdariffa* L. in hypercholesterolemic rats. J Ethnopharmacol 2006; 103 (2): 252-60.

11 Tseng TH, Kao ES, Chu CY, Chou FP, Lin Wu HW, Wang CJ. Protective effects of dried flower extracts of *Hibiscus sabdariffa* L. against oxidative stress in rat primary hepatocytes. Food Chem Toxicol 1997; 35 (12): 1159-64.

12 Onyenekwe PC, Ajani EO, Ameh DA, Gamaniel KS. Antihypertensive effect of roselle (*Hibiscus sabdariffa*) calyx infusion in spontaneously hypertensive rats and a comparison of its toxicity with that in Wistar rats. Cell Biochem Funct 1999; 17 (3): 199-206.

13 Harold Woodall. Food Additive Status List. In: US Food and Drug Administration, Department of Health and Human Services, Center for Food Safety and applied Nutrition (CFSAN) Office of Food Additive Safety editors; 2006:88.

14 Anderson L, Briggs D, Cardini F, Chan MFC, Chan P, Chandra SS, et al. General Guidelines for Methodologies on Research and Evaluation of Traditional Medicine. Available at http://www.paho.org/Spanish/AD/THS/EV/PM-WHOTraditional-medicines-research-evaluation.pdf. Accessed September 3, 2008.

15 หน่วยบริการฐานข้อมูลสมุนไพร ณ สำนักงานข้อมูลสมุนไพร คณะเภสัชศาสตร์ มหาวิทยาลัยมหิดล. สมุนไพรที่ใช้ในงานสาธารณสุขมูลฐาน. Available at http://www.medplant.mahidol.ac.th/pubhealth/index.html. Accessed July 7, 2006.

16 Kinouchi T, Suaeyun R, Chewonarin T, Intiyot Y, Arimochi H, Kataoka K, et al. Chemopreventive effects of Thai medicinal plants on formation of azoxymethane-induced DNA adducts and aberrant crypt foci in the rat colon. Mutat Res-Fund Mol M 1997; 379 (1, Supplement 1): S 181.

17 Hirunpanich V, Utaipat A, Morales NP, Bunyapraphatsara N, Sato H, Herunsalee A, et al. Antioxidant effects of aqueous extracts from dried calyx of *Hibiscus sabdariffa* Linn. (Roselle) *in vitro* using rat low-density lipoprotein (LDL). Biol Pharm Bull 2005; 28 (3): 481-4.

18 Mok DKW, Chau FT. Chemical information of Chinese medicines: A challenge to chemist. Chemometr Intell Lab 2005; 82 (1-2): 210-7.

19 European Pharmacopoeia 4.4, 4 edition. Nordlingen: Druckerei C. H. Beck; 2001

20 Subcommittee on the Establishment of the Thai Herbal Pharmacopoeia. Thai Herbal Pharmacopoeia 2. In: Department of Medical Science, Bureau of Drug and Narcotic editors. Bangkok: Prachachon; 2000

21 Working groups in the Medical Policy, Pharmacology and Toxicology, Complex Drug Substances Coordinating Committees. Guidance for Industry Botanical Drug Products. In: U.S. Department of Health and Human Services, Food and Drug Administration, Center for Drug Evaluation and Research (CDER) editors. Rockville: US Food and Drug Administration (FDA). 2004

22 Committee for Medicinal Products for Human Use (CHMP), Committee for Medicinal Products for Veterinary Use (CVMP). Guideline on Quality of Herbal Medicinal Products/ Traditional Herbal Medicinal Products. Available at http://www.emea.europa.eu/pdfs/human/qwp/281900en.pdf. Accessed August 31, 2008.

23 Liang YZ, Xie P, Chan K. Quality control of herbal medicines (Review). J Chromatogr B 2004; 812 (1-2): 53-70.

24 Massart DL, Vandeginste BGM, Deming SN, Michotte Y, Kaufman L. Chemometrics: a textbook Amsterdam: Elsevier Science Publisher B.V.; 1988

25 Fang KT, Liang YZ, Yin XL, Chan K, Lu GH. Critical value determination on similarity of fingerprints. Chemometr Intell Lab 2006; 82 (1-2): 236-40.

26 van Nederkassel AM, Daszykowski M, Massart DL, Heyden YV. Prediction of total green tea antioxidant capacity from chromatograms by multivariate modeling. J Chromatogr A 2005; 1096 (1-2): 177-86.

27 Ji YB, Xu QS, Hu YZ, Heyden YV. Development, optimization and validation of a fingerprint of *Ginkgo biloba* extracts by high-performance liquid chromatography. J Chromatogr A 2005; 1066 (1-2): 97-104.

28 Roselle. In: European Directorate for the Quality of Medicines (EDQM),editor European Pharmacopoeia 4.4. 4 edition. Nordlingen: Druckerei C. H. Beck; 2001: 3520-1.

29 Subcommittee on the Establishment of the Thai Herbal Pharmacopoeia. Thai Herbal Pharmacopoeia 1, Bangkok: Prachachon; 1995

30 Ali BH, Wabel NA, Blunden G. Phytochemical, pharmacological and toxicological aspects of *Hibiscus sabdariffa* L.: A review. Phytother Res 2005; 19 (5): 369-75.

31 Duke JA. Handbook of Phytochemical Constituents of GRAS Herbs and other Economic Plants. Available at http://www.ars-grin.gov/duke/. 2007.

32 Tseng TH, Wang CJ, Kao ES, Chu HY. Hibiscus protocatechuic acid protects against oxidative damage induced by *tert*-butylhydroperoxide in rat primary hepatocytes. Chem Biol Interact 1996; 101 (2): 137-48.

33 Du CT, Francis FJ. Anthocyanins of Roselle *(Hibiscus sabdariffa* L.). J Food Sci 1973; 38: 810-2.

34 Chen SH, Huang TC, Ho CT, Tsai PJ. Extraction, analysis, and study on the volatiles in Roselle tea. J Agric Food Chem 1998; 46: 1101-5.

35 Glew RH, VanderJagt DJ, Lockett C, Grivetti LE, Smith GC, Pastuszyn A, et al. Amino acid, fatty acid, and mineral composition of 24 indigenous plants of Burkina Faso. J Food Compos Anal 1997; 10: 205-17.

36 Lin WL, Hsieh YJ, Chou FP, Wang CJ, Cheng MT, Tseng TH. Hibiscus protocatechuic acid inhibits lipopolysaccharide-induced rat hepatic damage. Arch Toxicol 2003; 77 (1): 42-7.

37 Lee MJ, Chou FP, Tseng TH, Hsieh MH, Lin MC, Wang CJ. Hibiscus protocatechuic acid or esculetin can inhibit oxidative LDL induced by either copper ion or nitric oxide donor. J Agric Food Chem 2002; 50: 2130-6.

38 Wang CJ, Wang JM, Lin WL, Chu CY, Chou FP, Tseng TH. Protective effect of Hibiscus anthocyanins against *tert*-butyl hydroperoxide-induced hepatic toxicity in rats. Food Chem Toxicol 2000; 38 (5): 411-6.

39 Chang YC, Huang KX, Huang AC, Ho YC, Wang CJ. Hibiscus anthocyanins-rich extract inhibited LDL oxidation and oxLDL-mediated macrophages apoptosis. Food Chem Toxicol 2006; 44 (7): 1015-23.

40 Lessing C, Liberti L, McElerney A, Swannick G, Tokelove S, Vandermey D. Roselle. In: DerMarderosian A, Beutler JA editors. The Review of Natural Products. 4 edition. St. Louis, Missouri: Facts and Comparisons part of Wolters Kluwer Health; 2005: 980-3.

41 เต็ม สมิตินันทน์. ชื่อพรรณไม้แห่งประเทศไทย เต็ม สมิตินันทน์ ฉบับแก้ไขเพิ่มเติม พ.ศ.2544. In: สำนักงานหอพรรณไม้ กรมอุทยานแห่งชาติ สัตว์ป่า และพันธุ์พืช; 2544

42 Morton J. Roselle *Hibiscus sabdariffa* L. Fruits of Warm Climates 1987. Available at http://www.hort.purdue.edu/newcrop/morton/roselle.html. Accessed September 4, 2008.

43 Engels G. Herb Profile: Hibiscus. In, HerbalGram; 2007:1-6.

44 Appell SD. Red Sorrel, *Hibiscus sabdariffa*—The Other "Cranberry". In, Plants & Gardens News; 2003

45 Duke JA. Ethnobotanical Uses *Hibiscus sabdariffa* (MALVACEAE). Available at http://www.ars-grin.gov/cgi-bin/duke/ethnobot.pl. Accessed September 10, 2008.

46 Leclerc H. Sida sabdariffa (*Hibiscus sabdariffa* L). Presse Med 1938; 46: 1060.

47 El-Saadany SS, Sitohy MZ, Labib SM, El-Massry RA. Biochemical dynamics and hypocholesterolemic action of *Hibiscus sabdariffa* (Karkade). Nahrung 1991; 35 (6): 567-76.

48 Liu CL, Wang JM, Chu CY, Cheng MT, Tseng TH. *In vivo* protective effect of protocatechuic acid on *tert*-butyl hydroperoxide-induced rat hepatotoxicity. Food Chem Toxicol 2002; 40 (5): 635-41.

49 Liu JY, Chen CC, Wang WH, Hsu JD, Yang MY, Wang CJ. The protective effects of *Hibiscus sabdariffa* extract on CCl_4-induced liver fibrosis in rats. Food Chem Toxicol 2006; 44 (3): 336-43.

50 Tseng TH, Hsu JD, Lo MH, Chu CY, Chou FP, Huang CL, et al. Inhibitory effect of Hibiscus protocatechuic acid on tumor promotion in mouse skin. Cancer Lett 1998; 126 (2): 199-207.

51 Wang CJ, inventor Universal Biotech Co.,Ltd., assignee. Use of the *Hibiscus sabdariffa* extract in the preparation of a medicament. (June 4, 2003). Patent No. EP1316312A1

52 Kirdpon S, Nakorn SN, Kirdpon W. Changes in urinary chemical composition in healthy volunteers after consuming roselle (*Hibiscus sabdariffa* Linn.) juice. J Med Assoc Thai 1994; 77 (6): 314-21.

53 Hansawasdi C, Kawabata J, Kasai T. Alpha-amylase inhibitors from roselle (*Hibiscus sabdariffa* Linn.) tea. Biosci Biotechnol Biochem 2000; 64 (5): 1041-3.

54 Dafallah AA, Al-Mustafa Z. Investigation of the anti-inflammatory activity of *Acacia nilotica* and *Hibiscus sabdariffa*. Am J Chin Med 1996; 24 (3-4): 263-9.

55 Elsheikh SH, Bashir AK, Suliman SM, Wassila ME. Toxicity of certain Sudanese plant extracts to cercariae and miracidia of *Schistosoma mansoni.* Int J Crude Drug Res 1990; 28 (4): 241-5.

56 Adetutu A, Odunola OA, Owoade OA, Adeleke OA, Amuda OS. Anticlastogenic effects of *Hibiscus sabdariffa* fruits against sodium arsenite-induced micronuclei formation in erythrocytes in mouse bone marrow. Phytother Res 2004; 18 (10): 862-4.

57 Yasukawa K, Yamaguchi A, Arita J, Sakurai S, Ikeda A, Takido M. Inhibitory effect of edible plant extraction on 12-*O*-tetradecanoylphorbol-13-acetate-induced ear oedema in mice. Phytother Res 1993; 7 (2): 185-9.

58 Aboutabl EA, Goneid MH, Soliman SN, Selim AA. Analysis of certain plant polysaccharides and study of their antihyperlipidemic activity. Al-Azhar J Pharm Sci 1999; 24: 187-95.

59 The use of medicinal herbs for the treatment of kidney stone in the urinary system. In: Mungmum V editor, Seminar on the development of drugs from medicinal plants (Abstract). 1982:117.

60 Duh PD, Yen GC. Antioxidative activity of three herbal water extracts. Food Chem 1997; 60 (4): 639-45.

61 Kho JM, Yeh DB, Pan BS. Rapid photometric assay evaluating antioxidative activity in edible plant material. J Agric Food Chem 1999; 47 (8): 3206-9.

62 Shayeb NMAE, Mabrouk SS. Utilisation of some edible and medicinal plants to inhibit aflatoxin formation. Nutr Rep Int 1984; 29 (2): 273-82.

63 Murakami A, Jiwajiinda S, Koshimizu K, Ohigashi H. screening for *in vitro* anti-tumor promoting activities of edible plants from Thailand. Cancer Lett 1995; 95 (1/2): 137-46.

64 May G, Willuhn G. Antiviral activity of aqueous extracts from medicinal plants in tissue cultures. Arzneim-Forsch 1978; 28 (1): 1-7.

65 El-Merzabani MM, El-Aaser AA, Attia MA, El-Duweini AK, Ghazal AM. screening system for Egyptian plants with potential anti-tumour activity. Planta Med 1979; 36: 150-5.

66 Ali M, Salih W, Humida A. An oestrogen-like activity of *Hibiscus sabdariffa*. Fitoterapia 1989; 60 (6): 547-8.

67 Cáceres A, Girón LM, Martínez AM. Diuretic activity of plants used for the treatment of urinary ailments in Guatemala. J Ethnopharmacol 1987; 19 (3): 233-45.

68 Zhung Y, Yeh J, Lin D, Yuan J, Zhou R, Wang P. Antihypertensive effect of *Hibiscus sabdariffa*. Yao Hsueh T'Ung Pao 1981; 16 (5): 60C.

69 Ali MB, Salih WM, Mohamed AH, Homeida AM. Investigation of the antispasmodic potential of *Hibiscus sabdariffa* calyces. J Ethnopharmacol 1991; 31 (2): 249-57.

70 Sharaf A. The pharmacological characteristics of *Hibiscus sabdariffa*. Planta Med 1962; 10: 48-52

71 Ali M, Mohamed A, Salih W, Homeida A. Effect on an aqueous extract of *Hibiscus sabdariffa* calyces on the gastrointestinal tract. Fitoterapia 1991; 62 (6): 475-9.

72 Haruna A. Cathartic activity of Soborado:the aqueous extract of calyx of *Hibiscus sabdariffa* L. Phytother Res 1997; 11 (4): 307-8.

73 Chevalier J. The dietetic use of the flowers of *Hibiscus sabdariffa*. Bull Sci Pharmacol 1937; 44: 195.

74 Takeda N, YasuiI Y. Identification of mutagenic substances in Roselle color, Elderberry color and Safflower yellow. Agr Biol Chem 1985; 49 (6): 1851-2.

75 Food Coloring Agents from Hibiscus Flowers. JAPAN (1981). Sanyo-Kokusaku Pulp Co Ltd., Patent no. Japan Kokai Tokkyo Koho-81 141,358

76 El-Mekkawy S, Meselhy M, Kusumoto I, Kadota S, Hattori M, Namba T. Inhibitory effects of Egyptian folk medicines on Human Immunodeficiency Virus (HIV) reverse transcriptase. Chem Pharm Bull 1995; 43 (4): 641-8.

77 Obiefuna P, Owolabi O, Adegunloye B, Obiefuna I, Sofola OA. The petal extract of *Hibiscus sabdariffa* produces relaxation of isolated rat aorta. Int J Pharmacog 1994; 32 (1): 69-74.

78 Owolabi O, Adegunloye B, Ajagbona O, Sofola O, Obiefuna P. Mechanism of relaxant effect mediated by an aqueous extract of *Hibiscus sabdariffa* petals in isolated rat aorta. Int J Pharmacog 1995; 33 (3): 210-4

79 Akindahunsi AA, Olaleye MT. Toxicological investigation of aqueous-methanolic extract of the calyces of *Hibiscus sabdariffa* L. J Ethnopharmacol 2003; 89 (1): 161-4.

80 Orisakwe OE, Husaini DC, Afonne OJ. Testicular effects of sub-chronic administration of *Hibiscus sabdariffa* calyx aqueous extract in rats. Reprod Toxicol 2004; 18 (2): 295-8.

81 Obayashi K, Iwamoto A, Masaki H. Evaluation of plant extracts on depigmentation effect in Cultured B 16 Melanoma Cells. J SCCJ 1996; 30 (2): 153-60.

82 Duke JA. Chemicals in: *Hibiscus sabdariffa* L. (Malvaceae) -- Acedera de Guinea (Sp.), Indian Sorrel, Jamaica Sorrel, Kharkadi, Malventee (Ger.), Red Sorrel, Rosa de Jamaica (Sp.), Rosella (Ger.), Roselle, Sereni (Sp.), Sorrel. Available at http://www.ars-grin.gov/cgi-bin/duke/farmacy2.pl. Accessed July 7, 2006.

83 Lin Y. The study of red pigments in Taiwan plants. Proc Natl Sci Counc Part I (Taiwan) 1975; 8: 33-137.

84 กองประชาสัมพันธ์ มทร.ธัญบุรี. เครื่องแกะเม็ดกระเจี๊ยบแดง.

85 กลุ่มงานพัฒนาวิชาการแพทย์แผนไทยและสมุนไพร สถาบันการแพทย์แผนไทย กรมพัฒนาการแพทย์แผนไทยและการแพทย์ทางเลือก. นวัตกรรมสมุนไพรไทย... ก้าวไกลสู่อุตสาหกรรม, ใน นวัตกรรมสมุนไพรไทย ก้าวไกลสู่อุตสาหกรรม. ห้องประชุม เค ยู โฮม มหาวิทยาลัยเกษตรศาสตร์ บางเขน กรุงเทพฯ: งานส่งเสริมภาพลักษณ์องค์กร สำนักงานนวัตกรรมแห่งชาติ; 2547:49-58.

86 Castañeda-Ovando A, Pacheco-Hernández MDL, Páez-Hernández ME, Rodríguez JA, Galán-Vidal CA. Chemical studies of anthocyanins: A review. Food Chem 2009; 113 (4): 859-71

87 Delgado-Vargas F, Paredes-Lopez O. Anthocyanins and Betalains. In Natural Colorants for Food and Nutraceutical Uses. Boca Raton: CRC Press 2003: 167-211.

88 Delgado-Vargas F, Paredes-Lopez O. Natural Colorants for Food and Nutraceutical Uses Boca Raton: CRC Press LLC; 2003: 327.

89 Jackman RL, Smith JL. Anthocyanins and Betalains. In: Hendry GAF, Houghton JD editors. Natural Food Colorants. New York: AVI; 1992: 183-241.

90 Francis FJ. Analysis of Anthocyanins. In: Markakis P,editor Anthocyanins as Food Colors. New York: Academic Press; 1982: 181-207.

91 Timberlake CF, Bridle P. The Anthocyanins. In: Harborne JB, Mabry TJ, Mabry H editors. The Flavonoids Part 1. San Francisco: Academic Press, Inc.; 1975: 215-64.

92 Petri G, Krawczyk U, Kéry Á. Spectrophotometric and chromatographic investigation of Bilberry anthocyanins for quantification purposes. Microchem J 1997; 55 (1): 12-23.

93 Soriano A, Pérez-Juan PM, Vicario A, González JM, Pérez-Coello MS. Determination of anthocyanins in red wine using a newly developed method based on Fourier transform infrared spectroscopy. Food Chem 2007; 104 (3): 1295-303.

94 Sáenz-López R, Fernández-Zurbano P, Tena MT. Development and validation of a capillary zone electrophoresis method for the quantitative determination of anthocyanins in wine. J Chromatogr A 2003; 990 (1-2): 247-58.

95 Mondello L, Cotroneo A, Errante G, Dugo G, Dugo P. Determination of anthocyanins in blood orange juices by HPLC analysis. J Pharm Biomed Anal 2000; 23 (1): 191-5.

96 de Ancos B, Ibanez E, Reglero G, Cano MP. Frozen storage effects on anthocyanins and volatile compounds of raspberry fruit. J Agric Food Chem 2000; 48 (3): 873-9.

97 Lee J, Durst RW, Wrolstad RE. Determination of total monomeric anthocyanin pigment content of fruit juices, beverages, natural colorants, and wines by the pH differential method: collaborative study. J AOAC Int 2005; 88 (5): 1269-78.

98 Mazza G, Cacace JE, Kay CD. Methods of analysis for anthocyanins in plants and biological fluids. J AOAC Int 2004; 87 (1): 129-45.

99 da Costa CT, Horton D, Margolis SA. Analysis of anthocyanins in foods by liquid chromatography, liquid chromatography-mass spectrometry and capillary electrophoresis. J Chromatogr A 2000; 881 (1-2): 403-10.

100 Lee J, Rennaker C, Wrolstad RE. Correlation of two anthocyanin quantification methods: HPLC and spectrophotometric methods. Food Chem 2008; 110 (3): 782-6.

101 Giusti MM, Wrolstad RE. Characterization and measurement of anthocyanins by UV-visible spectroscopy. Available at http://www.does.org/masterli/facsample.htm. Accessed July 7, 2003.

102 Zeng Z, Chau FT, Chan HY, Cheung CY, Lau TY, Wei S, et al. Recent advances in the compound-oriented and pattern-oriented approaches to the quality control of herbal medicines. Chinese medicine 2008; 3: 9.

103 Chan CO, Applications of chemometrics techniques on chromatographic and spectroscopic methods to advance chemical analysis of Radix Ligustici Chuanxiong, Radix Angelicae Sinensis, Cortex Phellodendri and other Chinese herbal medicines. Ph.D. Disserttation, The Hong Kong Polytechnic University, 2006.

104 Xie Y, Jiang ZH, Zhou H, Cai X, Wong YF, Liu ZQ, et al. Combinative method using HPLC quantitative and qualitative analyses for quality consistency assessment of a herbal medicinal preparation. J Pharm Biomed Anal 2007; 43 (1): 204-12.

105 Williamson EM. Synergy and other interactions in phytomedicines. Phytomedicine 2001; 8 (5): 401-9.

106 Nielsen NPV, Carstensen JM, Smedsgaard J. Aligning of single and multiple wavelength chromatographic profiles for chemometric data analysis using correlation optimised warping. J Chromatogr A 1998; 805 (1-2): 17-35.

107 Hopke PK. The evolution of chemometrics. Anal Chim Acta 2003; 500 (1-2): 365-77.

108 Brereton RG. Applied Chemometrics for Scientists. In: John Wiley & Sons 2007

109 Brereton RG. Chemometrics : Data Analysis for the Laboratory and Chemical Plant Wiltshire: Antony Rowe Ltd; 2003: 543.

110 CAMO-Process-AS, The Unscrambler Version 9.5. (Oslo, 2005): Multivariate data analysis.

111 Liyana-Pathirana C, Shahidi F. Optimization of extraction of phenolic compounds from wheat using response surface methodology. Food Chem 2005; 93 (1): 47-56.

112 Herrero M, Martín-Álvarez PJ, Señoráns FJ, Cifuentes A, Ibáñez E. Optimization of accelerated solvent extraction of antioxidants from Spirulina platensis microalga. Food Chem 2005; 93 (3): 417-23.

113 Ji YB, Alaerts G, Xu CJ, Hu YZ, Vander Heyden Y. Sequential uniform designs for fingerprints development of *Ginkgo biloba* extracts by capillary electrophoresis. J Chromatogr A 2006; 1128 (1-2): 273-81.

114 Araujo P. A new high performance liquid chromatography multifactor methodology for systematic and simultaneous optimisation of the gradient solvent system and the instrumental/ experimental variables. Trends Analyt Chem 2000; 19 (9): 524-9.

115 Gong F, Liang YZ, Xie PS, Chau FT. Information theory applied to chromatographic fingerprint of herbal medicine for quality control. J Chromatogr A 2003; 1002 (1-2): 25-40.

116 Wong JWH, free online SpecAlign Version 2.3. (2006): Windows-based software developed for the alignment of multiple mass spectra.

117 Li BY, Hu Y, Liang YZ, Xie PS, Du YP. Quality evaluation of fingerprints of herbal medicine with chromatographic data. Anal Chim Acta 2004; 514 (1): 69-77.

118 Kramer R. Chemometric Techniques for Quantitative Analysis. New York: Marcel Dekker; 1998: 203.

119 Beebe KR, Pell RJ, Seasholtz MB. Chemometrics: A practical guide. New York: John Wiley and Sons; 1998: 348.

120 Wold S, Sjöström M, Eriksson L. PLS-regression: a basic tool of chemometrics. Chemometr Intell Lab 2001; 58 (2): 109-30.

121 Pale E, Koiuda-Bonafos M, Nacro M. Characterisation and antioxidative scavenging activities of anthocyanes plants of Burkina Faso. Comptes Rendus Chimie 2004; 7 (10-11): 973-80.

122 Harborne JB. Phenolic Compounds. In Phytochemical Methods A guide to modern techniques of plant analysis. 3 edition. London: Chapman &Hall; 1998: 66-74.

123 Blank S, free trial Resampling Stats for Excel (Resampling Stats, Inc, Virginia, 2006).

124 Validation of analytical procedures.
Available at http://www.nihs.go.jp/drug/validation/q2bwww.html. Accessed August 23, 2005.

125 Waterman PG, Mole S. Extraction and Chemical Quantification. In Analysis of Phenolic Plant Metabolites. Oxford and Northampton Great Britain: Alden Press Limited; 1994: 66-103.

126 Plant Dry Ash/Acid Extraction for Ca, K, and Mg
Available at http://www.uga.edu/~sisbl/plantash.html. Accessed January 3, 2007.

127 Leong LP, Shui G. An investigation of antioxidant capacity of fruits in Singapore markets. Food Chem 2002; 76 (1): 69-75.

128 Tsai PJ, Ou ASM. Colour degradation of dried roselle during storage (Abstract). Food Science 1996; 23 (5): 629-40.

129 Tsai PJ, McIntosh J, Pearce P, Camden B, Jordan BR. Anthocyanin and antioxidant capacity in Roselle (*Hibiscus sabdariffa* L.) extract. Food Res Int 2002; 35 (4): 351-6.

130 Tsai PJ, Huang HP. Effect of polymerization on the antioxidant capacity of anthocyanins in Roselle. Food Res Int l 2004; 37 (4): 313-8.

131 Lu GH, Chan K, Liang YZ, Leung K, Chan CL, Jiang ZH, et al. Development of high-performance liquid chromatographic fingerprints for distinguishing Chinese Angelica from related Umbelliferae herbs. J Chromatogr A 2005; 1073 (1-2): 383-92.

132 Yang LW, Wu DH, Tang X, Peng W, Wang XR, Ma Y, et al. Fingerprint quality control of Tianjihuang by high-performance liquid chromatography–photodiode array detection. J Chromatogr A 2005; 1070 (1-2): 35-42.

133 Biopharmaceutics Coordinating Committee in the Center for Drug Evaluation and Research (CDER), Center for Veterinary Medicine (CVM) at the Food and Drug Administration. Guidance for Industry Bioanalytical Method Validation. Available at http://www.fda.gov/cder/guidance/4252fnl.pdf. Accessed September 4, 2008.

134 Wrolstad RE, Durst RW, Giusti MM, Rodriguez-Saona LE. Analysis of anthocyanins in nutraceuticals. In: Ho CT, Zheng QY editors. Quality management of nutraceuticals. Washington, DC: American Chemical Society; 2001: 42-62.

135 Liu H, Qiu N, Ding H, Yao R. Polyphenols contents and antioxidant capacity of 68 Chinese herbals suitable for medical or food uses. Food Res Int 2008; 41 (4): 363-70.

136 Soobrattee MA, Bahorun T, Neergheen VS, Googoolye K, Aruoma OI. Assessment of the content of phenolics and antioxidant actions of the Rubiaceae, Ebenaceae, Celastraceae, Erythroxylaceae and Sterculaceae families of Mauritian endemic plants. Toxicol in Vitro 2008; 22 (1): 45-56.

137 Atoui AK, Mansouri A, Boskou G, Kefalas P. Tea and herbal infusions: Their antioxidant activity and phenolic profile. Food Chem 2005; 89 (1): 27-36.

138 Prenesti E, Berto S, Daniele PG, Toso S. Antioxidant power quantification of decoction and cold infusions of *Hibiscus sabdariffa* flowers. Food Chem 2007; 100 (2): 433-8.

139 Suboh SM, Bilto YY, Aburjai TA. Protective effects of selected medicinal plants against protein degradation, lipid peroxidation and deformability loss of oxidatively stressed human erythrocytes. Phytother Res 2004; 18 (4): 280-4.

140 Tee PL, Yusof S, Mohamed S. Antioxidative properties of roselle (*Hibiscus sabdariffa* L.) in linoleic acid model system. Nutrition & Food Science 2002; 32 (1): 17-20.

141 Aruoma OI. Methodological considerations for characterizing potential antioxidant actions of bioactive components in plant foods. Mutat Res 2003; 523-524: 9-20.

142 Sánchez- Moreno C. Review: Methods used to evaluate the free radical scavenging activity in foods and biological systems. Food Sci Tech Int 2002; 8 (3): 121-37.

APPENDICES

APPENDIX A

Crude drugs of *Hibiscus sabdariffa* L.

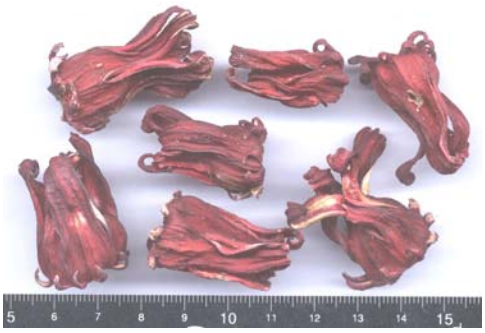
Sample 01


Sample 02


Sample 03


Sample 04


Sample 05

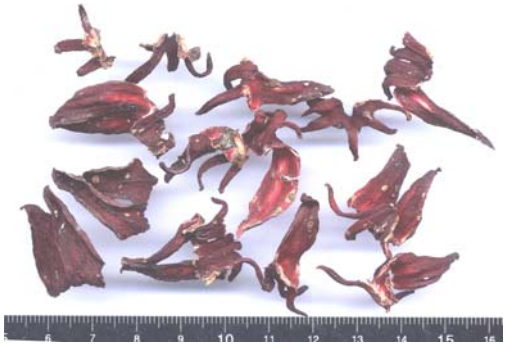
Sample 06


Sample 07

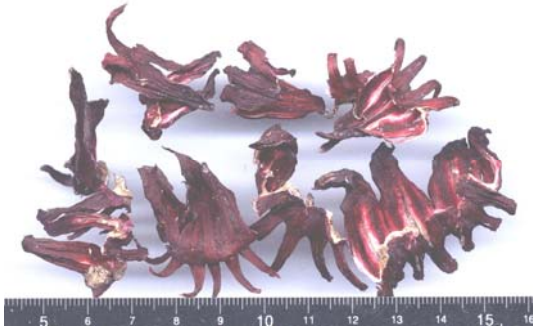
Sample 08

Figure 63 Crude drugs of *H. sabdariffa*

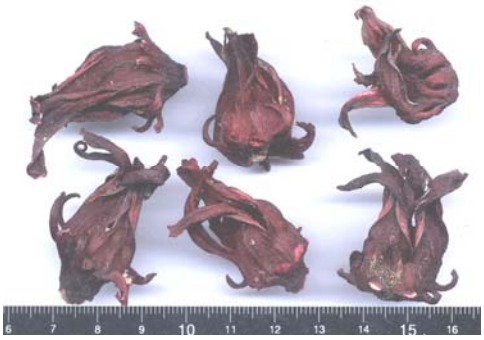
Sample 09

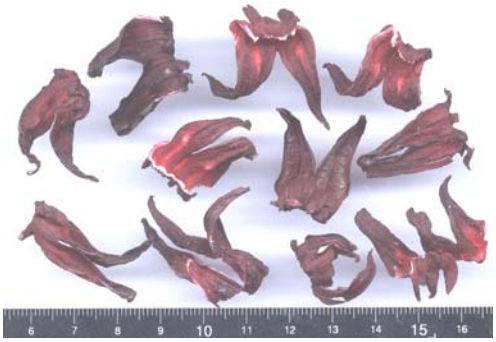
Sample 10


Sample 11


Sample 12

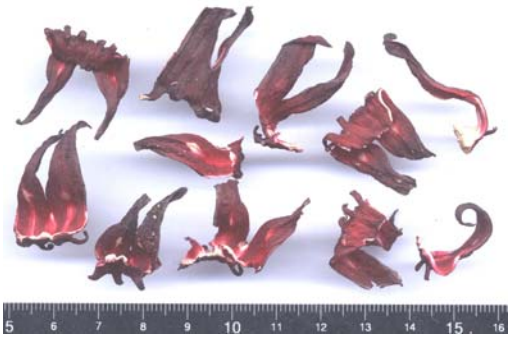
Sample 13

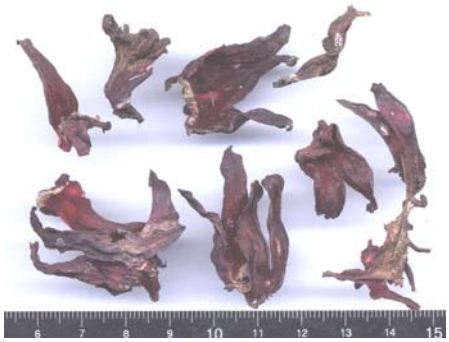
Sample 14

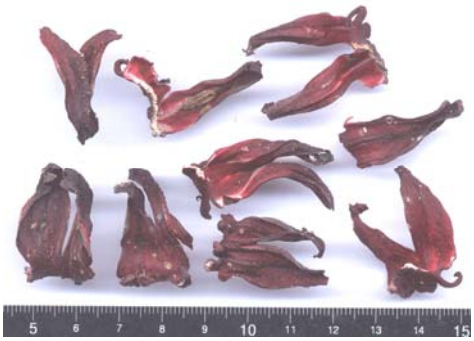
Sample 15


Sample 16

Figure 63 Crude drugs of *H. sabdariffa* (continued)

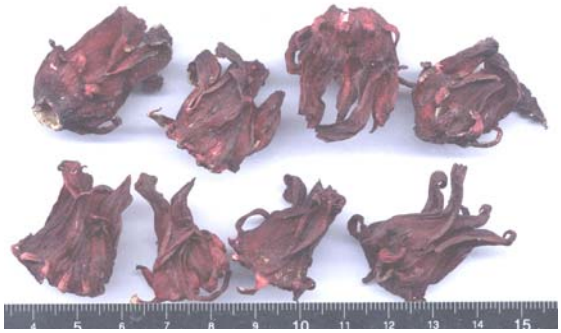
Sample 17


Sample 18


Sample 19


Sample 20


Sample 21


Sample 22


Sample 23


Sample 24

Figure 63 Crude drugs of *H. sabdariffa* (continued)


Sample 25


Sample 26


Sample 27


Sample 28

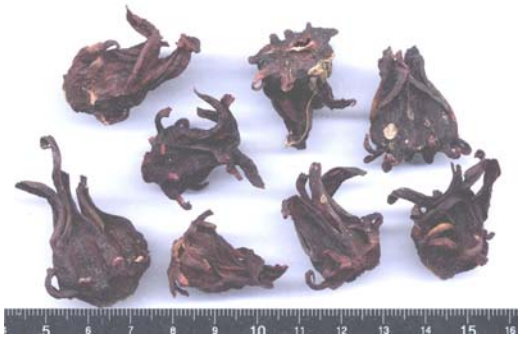
Sample 29


Sample 30


Sample 31


Sample 32

Figure 63 Crude drugs of *H. sabdariffa* (continued)

Sample 33

Sample 34

Sample 35

Figure 63 Crude drugs of *H. sabdariffa* (continued)

APPENDIX B

Reagents

Aluminium chloride test solution

Aluminium chloride, $AlCl_3 \cdot 6H_2O$ (5 g) was dissolved in sufficient methanol to make the solution of 100 ml.

Ferric chloride test solution

Ferric chloride, $FeCl_3 \cdot 6H_2O$ (9 g) was dissolved in sufficient water to make the solution of 100 ml.

2 M Hydrochloric acid

Hydrochloric acid, HCl (166 ml) was added to sufficient water to make the solution of 1,000 ml.

Lead acetate test solution

Lead acetate, $C_4H_6O_4Pb \cdot 3H_2O$ (9.5 g) was dissolved in sufficient water to make the solution of 100 ml.

0.025 M Potassium chloride buffer, pH 1.0

Potassium chloride, KCl, (1.86 g) was dissolved with distilled water (980 ml). The pH was measured and adjusted to 1.0 with conc. hydrochloric acid. The volume was adjusted to 1,000 ml with distilled water.

0.4 M Sodium acetate buffer, pH 4.5

Sodium acetate, $CH_3CO_2Na.3H_2O$, (54.43 g) was dissolved with distilled water (960 ml). The pH was measured and adjusted to 4.5 with conc. hydrochloric acid. The volume was adjusted to 1,000 ml with distilled water.

2 M Sodium hydroxide

Sodium hydroxide, NaOH (80 g) was dissolved in sufficient water to make the solution of 1,000 ml.

Dilute sulfuric acid

Sulfuric acid, H_2SO_4 (5 ml) was added to ice-cold methanol (95 ml)**.**

APPENDIX C

^{1}H NMR Spectra of the isolated anthocyanins of *H. sabdariffa* L.

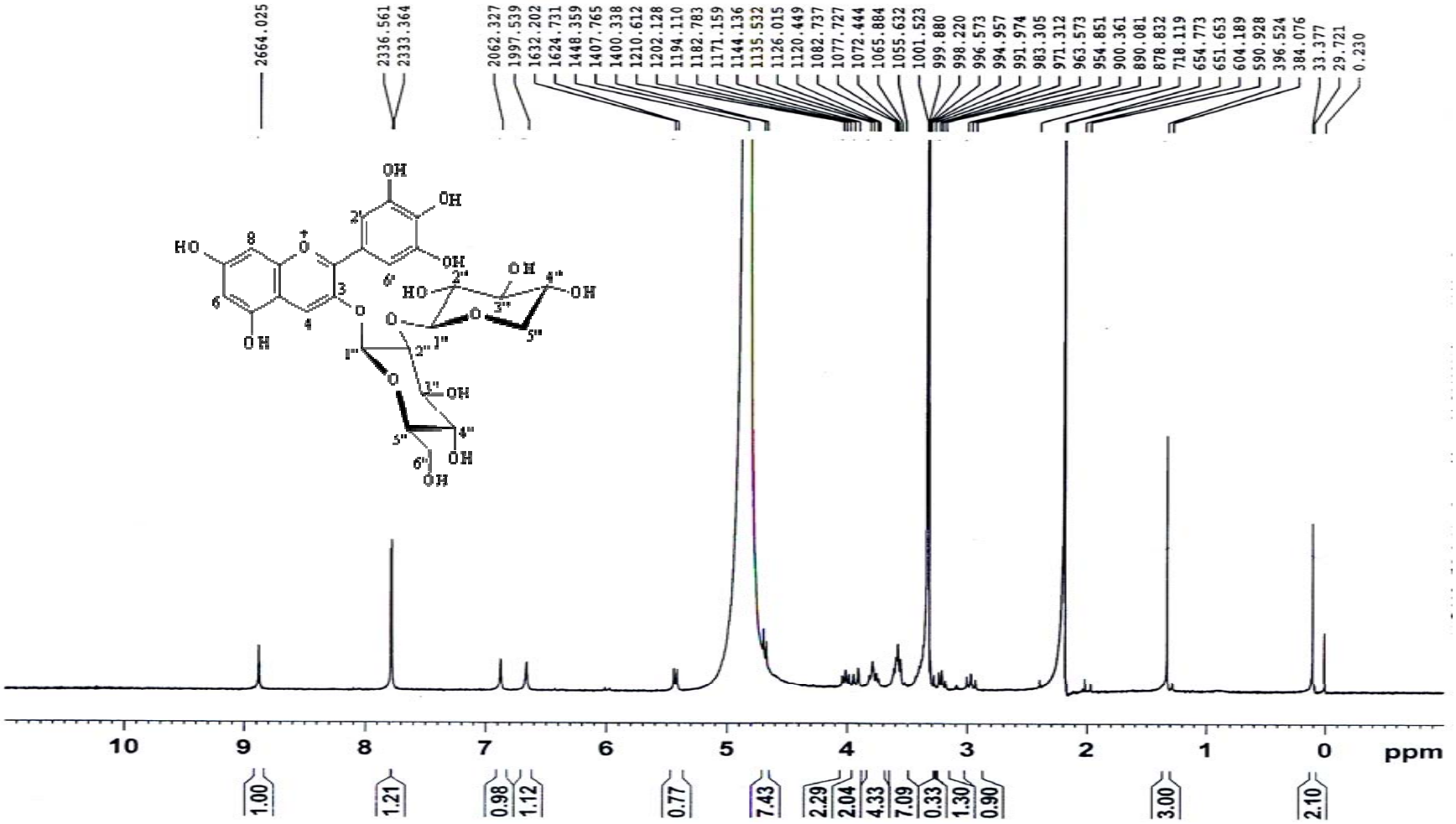

Figure 64 ^{1}H NMR spectrum of Compound I or delphinidin-3-sambubioside (300 MHz, CD_3OD:$CDCl_3$)

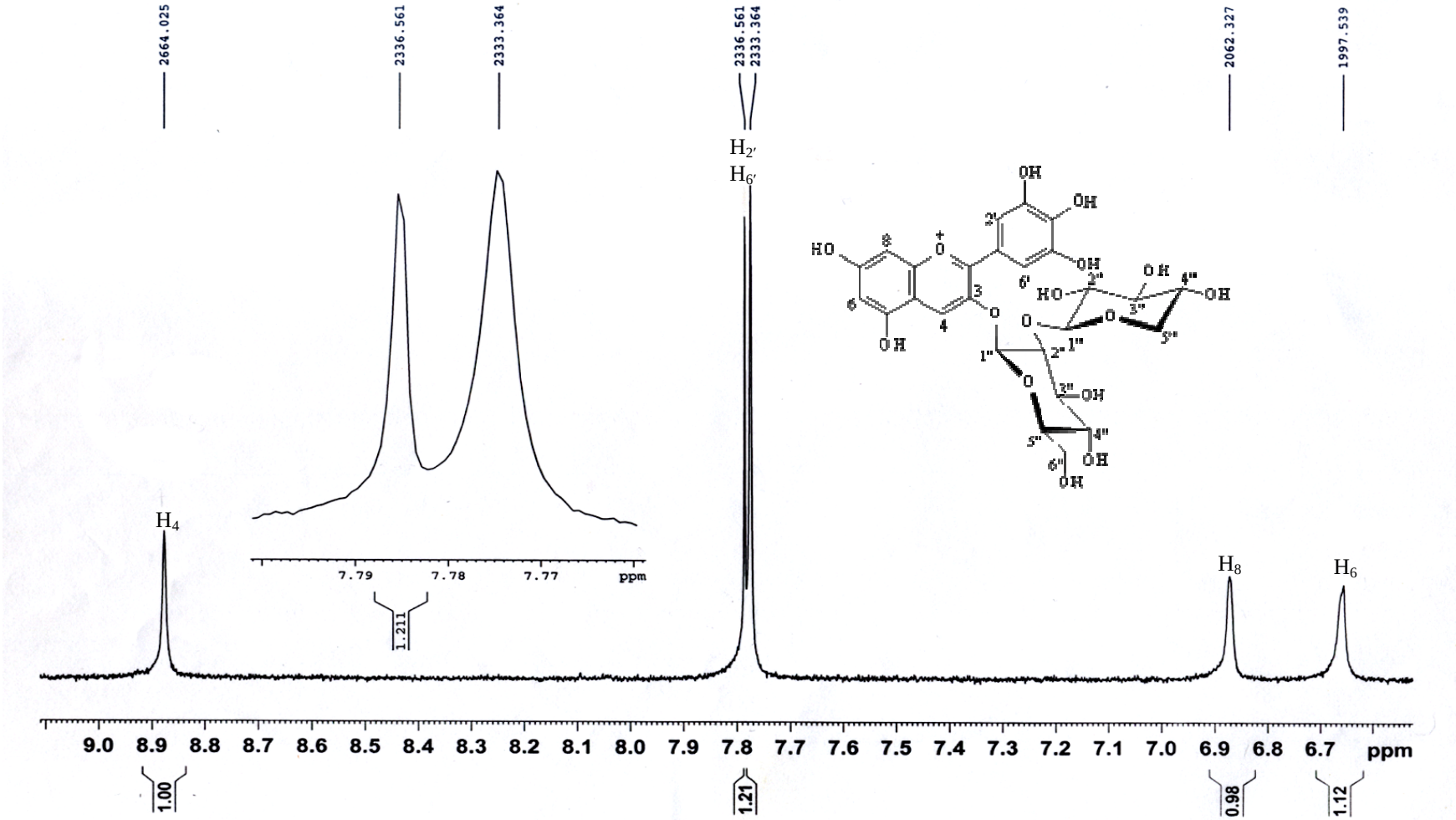

Figure 65 Expanded ^{1}H NMR spectrum of Compound I or delphinidin-3-sambubioside (300 MHz, CD_3OD:$CDCl_3$)

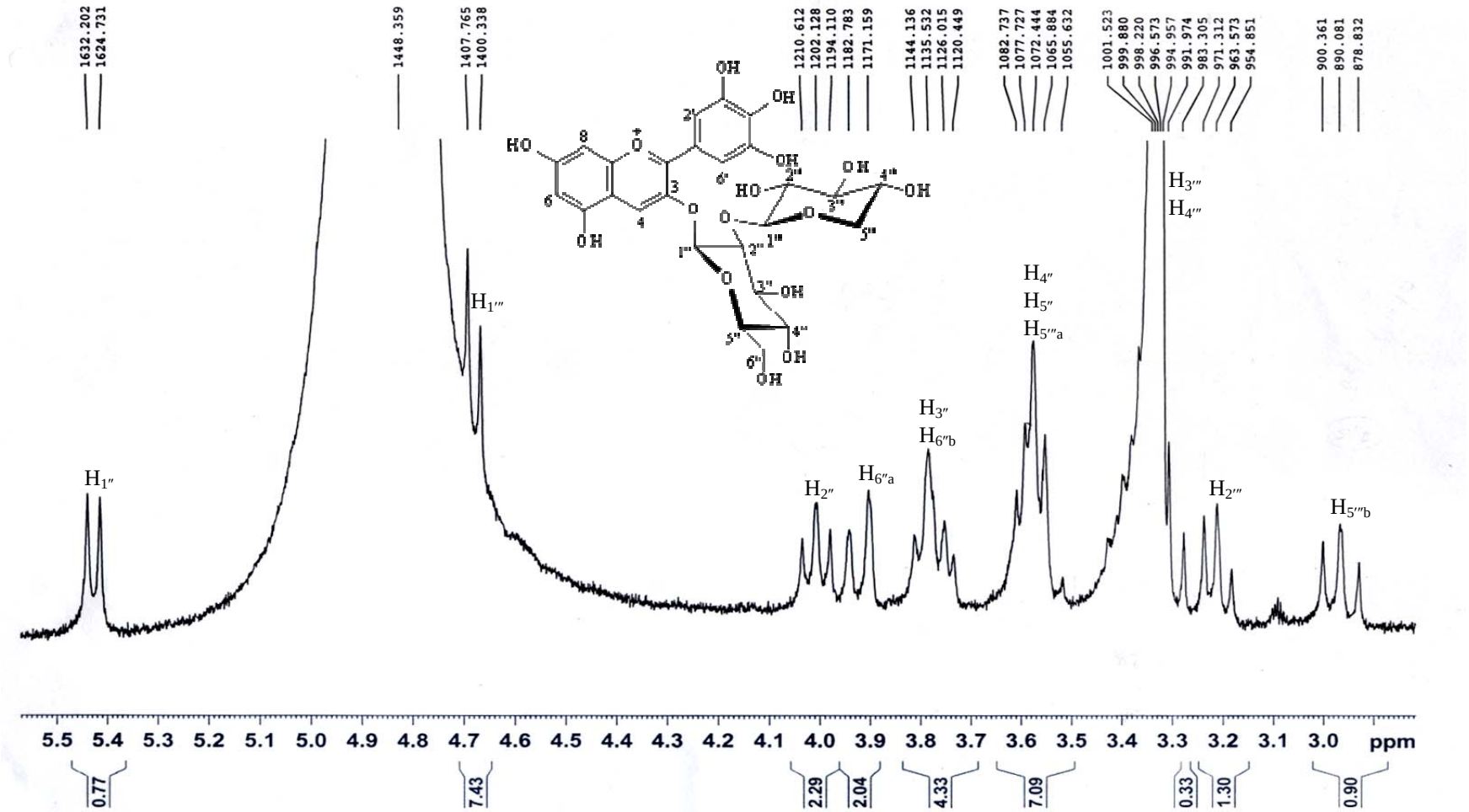

Figure 65 Expanded ^{1}H NMR spectrum of Compound I or delphinidin-3-sambubioside (300 MHz, CD_3OD:$CDCl_3$) (continued)

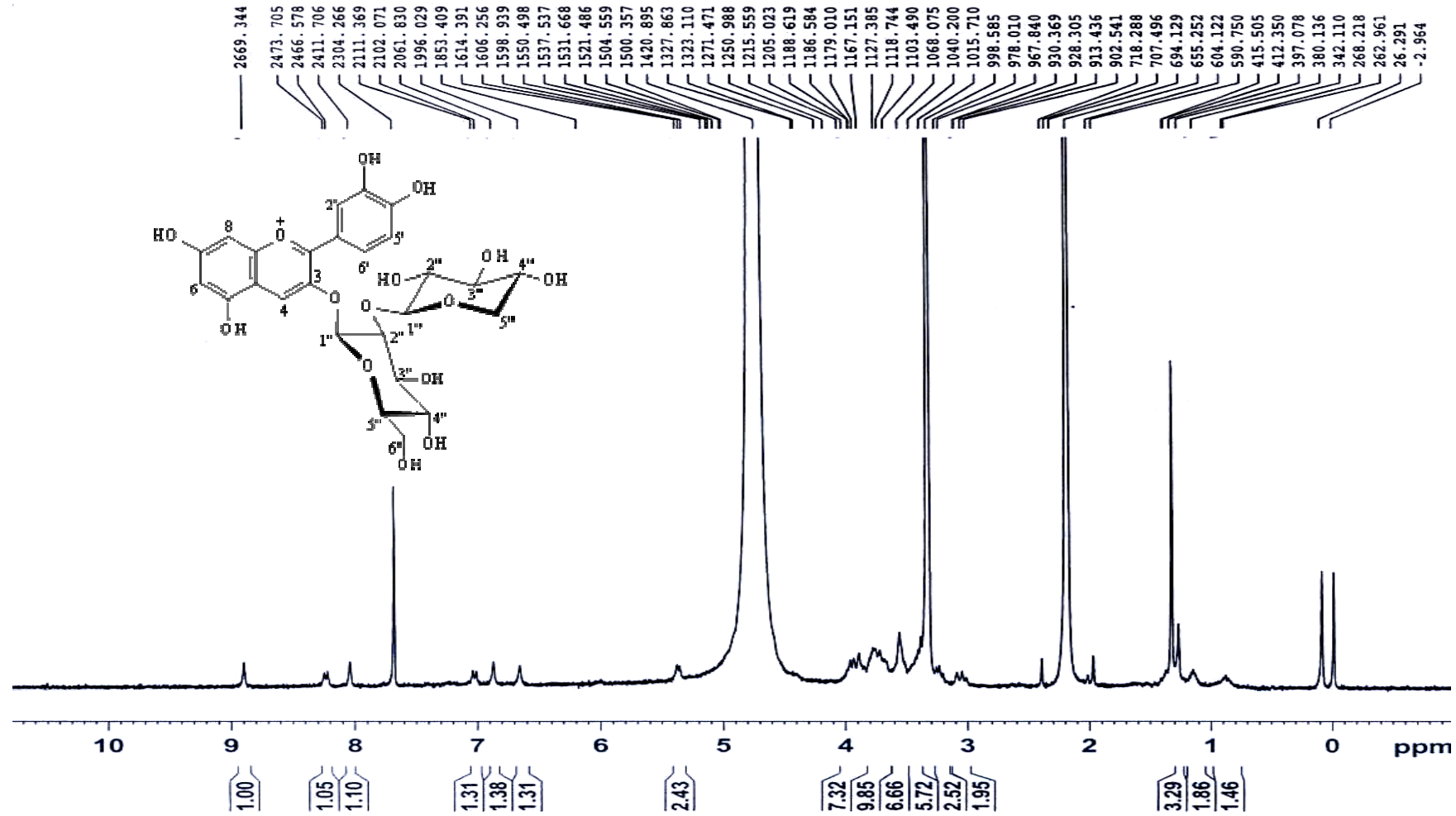

Figure 66 ^{1}H NMR spectrum of Compound II or cyanidin-3-sambubioside (300 MHz, CD_3OD:$CDCl_3$)

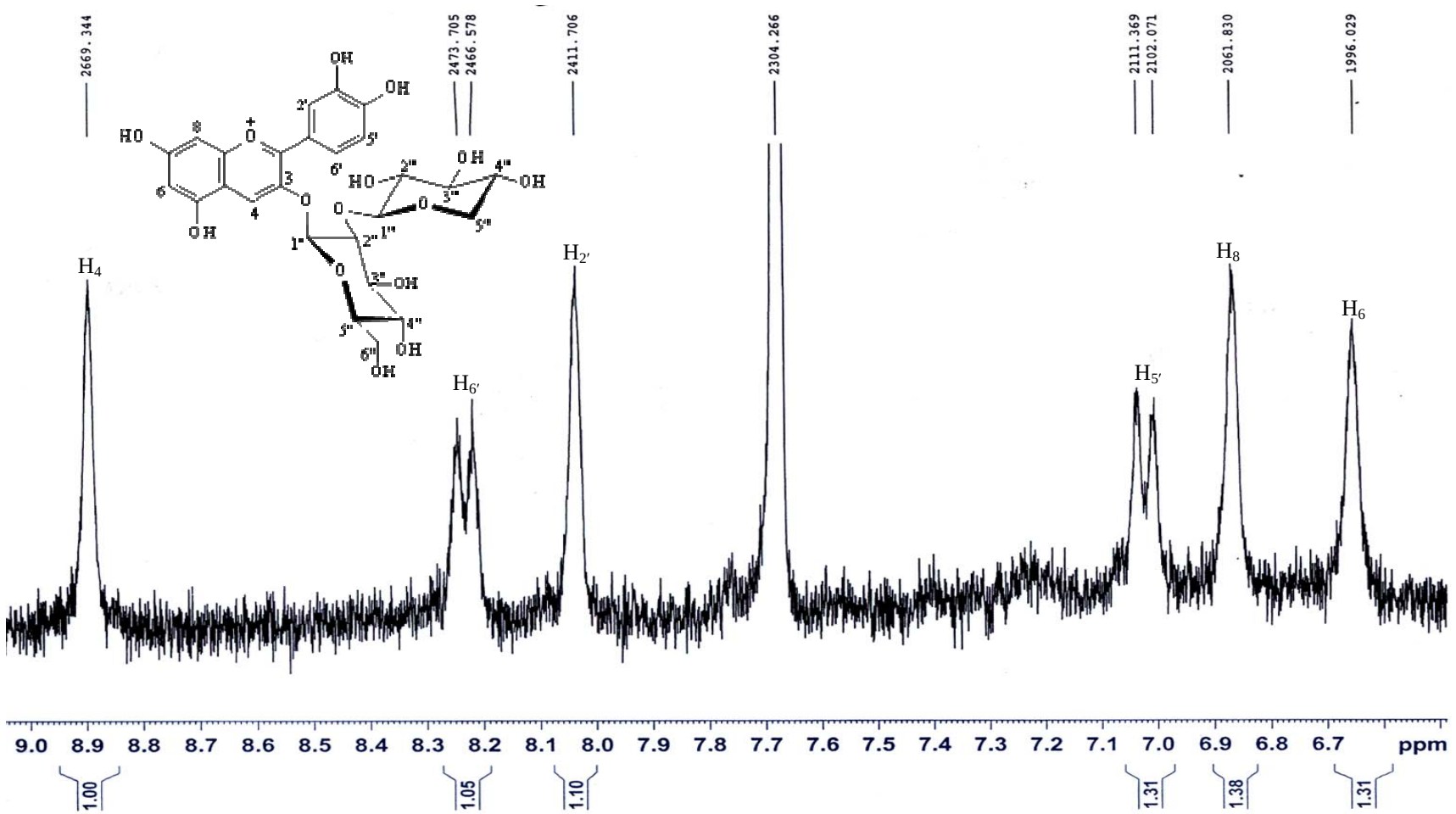

Figure 67 Expanded ^{1}H NMR spectrum of Compound II or cyanidin-3-sambubioside (300 MHz, CD_3OD:$CDCl_3$)

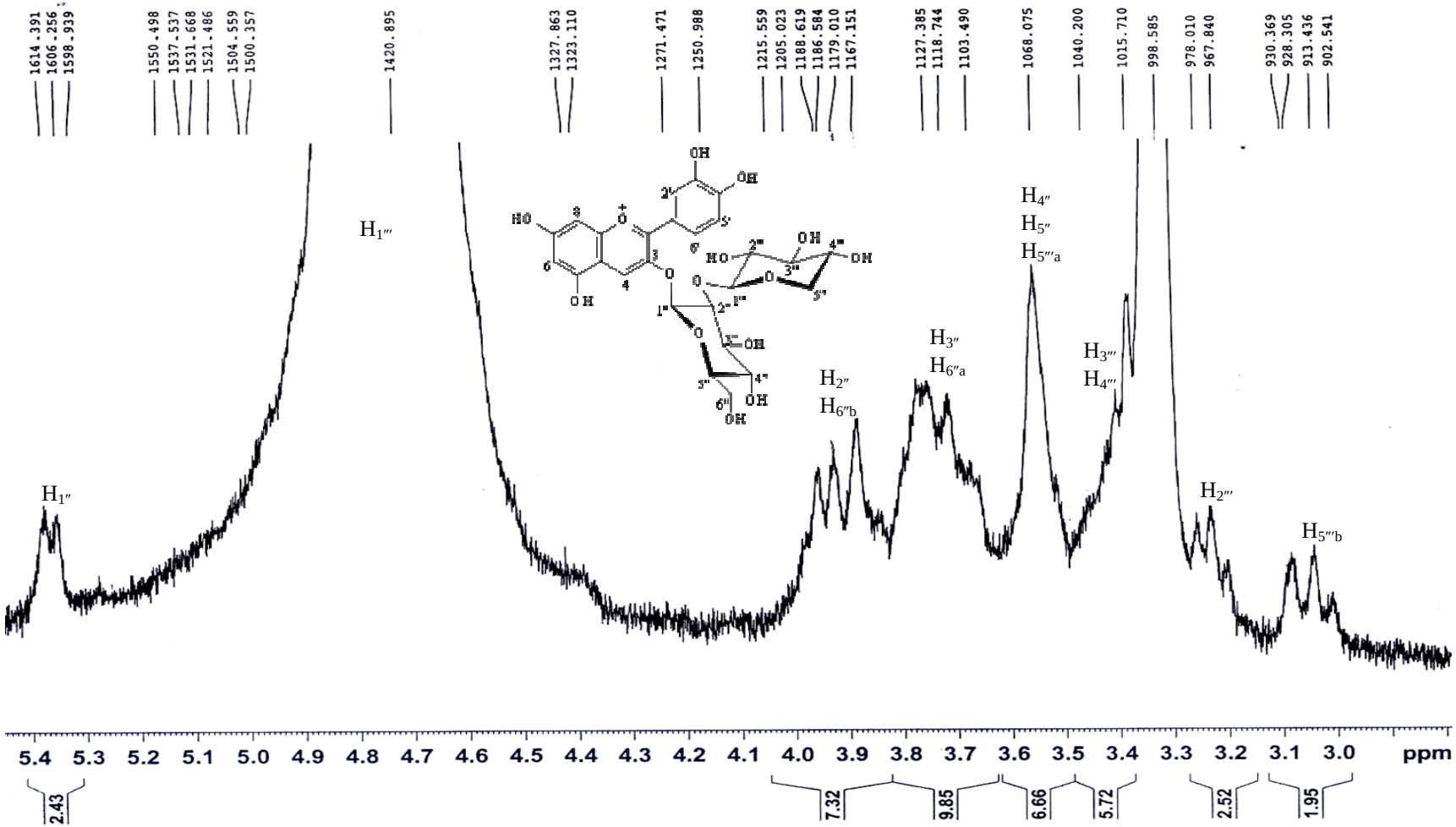

Figure 67 Expanded ^{1}H NMR spectrum of Compound II or cyanidin-3-sambubioside (300 MHz, CD_3OD:$CDCl_3$) (continued)

Biography

Name : Miss Tasamaporn Sukwattanasinit

Date of Birth : 13 August 1979

Place of Birth : Bangkok, Thailand

Home Address :

142 Ratniyom Rd., Tambon Song Phi Nong,
Amphoe Song Phi Nong, Suphan Buri 72110, Thailand

Education :

2001 Bachelor of Phamacy, Silpakorn University

Work :

2001-present Lecturer, Department of Pharmacognosy, Faculty of Pharmacy, Silpakorn University, Nakhon Pathom 73000, Thailand.

Publications :

1 Sukwattanasinit, T., Burana-osot, J. and Sotanaphun, U. Prediction of radical scavenging capacity of roselle (*Hibiscus sabdariffa*) using UV/VIS spectrophotometry and chemometric analysis. *The 8th NRCT-JSPS joint seminar: Innovative research in natural products for sustainable development*. 3-4 Febauary 2009. Bangkok, Thailand. pp.225-226.

2 Sukwattanasinit T, Burana-osot J, Sotanaphun U. Spectrophotometric method for quantitative determination of total anthocyanins and quality characteristics of roselle (*Hibiscus sabdariffa*). Planta Med 2007; 73 (14):1517-22.

3 Piyapolrungroj,N., Sotanaphun,U. and Sukwattanasinit,T. Inhibition of cytochrome P450 3A4 catalytic activity by *Hibiscus sabdariffa* L. methanol extract. *The 2nd AASP symposium and APEM conference 2005: Regional coorporation in pharmacy education, research and services*. 14-17 November 2005. Bangkok, Thailand, p.75.

4 Sukwattanasinit,T., Burana-osot,J. and Sotanaphun,U. Quantitative analysis of total anthocyanins in calyx of *Hibiscus sabdariffa* L. *The 2nd AASP symposium and APEM conference 2005: Regional coorporation in pharmacy education, research and services*. 14-17 November 2005. Bangkok, Thailand, p.165.

5 Sukwattanasinit, T. and Sotanaphun, U. Effect of solvent on extractive yield, total anthocyanin content and antioxidation of the extracts of *Hibiscus sabdariffa*. *The six JSPS-NRCT joint seminar : Recent advances in natural medicine research.* 2-4 Dec. 2003. Bangkok, Thailand, p.226.